MODELING AND CONSTRUCTION OF A COMPUTER CONTROLLED AIR
CONDITIONING SYSTEM

by

BRANDON S. FRINK

B.S., Kansas State University, 2005

A THESIS

submitted in partial fulfillment of the requirements for the degree

MASTER OF SCIENCE

Department of Mechanical and Nuclear Engineering
College of Engineering

KANSAS STATE UNIVERSITY
Manhattan, Kansas

2007

Approved by:

Major Professor
Warren N. White

Abstract

As energy efficient devices become more necessary, it is desired to increase the efficiency of air conditioning systems. Current systems use on/off control, where the unit primarily operates in the long lasting start up transients. A proposed solution is an air conditioning unit that runs continuously with active computer control implemented to maximize efficiency. The objective of this thesis is to develop a mathematical model for a specific air conditioning unit and to compare this model to measurements made on the specific unit. This model can then be used to develop a multi-input multi-output control law in the future.

In this thesis, a linearized moving interface lumped parameter model is presented, and the derivation verified with great detail. The model predicts transient perturbations from a steady state operating point. The air conditioner tested in this work required several modifications including the addition of sensors and controllers. A description of the system is provided. Methods used to determine all of the parameters for the model are given with explanation. The model is simulated with computer software and compared with experimental data. Simulations predict the final value of superheat and pressures in the evaporator and condenser well for step changes in the compressor speed and expansion valve opening.

Table of Contents

List of Figures

List of Tables

Nomenclature for the Evaporator

A: Cross-sectional area inside of tube

A_w: Cross-sectional area of tube wall

α_{ei1}:   Heat transfer coefficient on the inside of the two-phase region

α_{ei2}:   Heat transfer coefficient on the inside of the superheat region

α_{eo}:   Effective Heat transfer coefficient between tube wall and air

C_w: Thermal Capacitance of tube wall

D_i: Inside diameter of tube

D_o: Outside diameter of tube

γ_e: Void fraction in evaporator

h_{efg}:   Enthalpy of vaporization

h_{eL}:   Saturated liquid enthalpy

$h_{e,in}$:   Enthalpy at inlet of evaporator

$h_{e,out}$:   Enthalpy at outlet of evaporator

h_{ev}:   Saturated vapor enthalpy

h_{e2}:   Average enthalpy of superheat region

L_{e1}:   Length of two-phase region

L_{e2}:   Length of superheat region

L_{eT}:   Length of entire evaporator

$\dot{m}_{e,in}$:   Mass flow rate at inlet of evaporator

$\dot{m}_{e,int}$:   Mass flow rate at interface of the nodes

$\dot{m}_{e,out}$:   Mass flow rate at outlet of evaporator

P_e: Evaporator pressure

ρ_{eL}:   Saturated liquid density

ρ_{ev}:   Saturated vapor density

ρ_{e1}:   Average density in two-phase region

ρ_{e2}:   Average density in superheat region

ρ_w: Density of tube wall

T_{ew1}:   Temperature of two-phase region wall

T_{ew2}:   Temperature of superheat region wall

T_{er1}:   Temperature of two-phase region refrigerant

T_{er2}:   Temperature of superheat region refrigerant

T_{ea}:   Temperature of ambient air around evaporator

u: Velocity in the refrigerant for energy balances

u: Thermal energy in tube wall energy balances

v_e: Evaporator fan speed

$x_{e,in}$:   Quality at the inlet of the evaporator

In all cases an over bar indicates mean value.

Nomenclature for the Condenser

A: Cross-sectional area inside of tube

A_w: Cross-sectional area of tube wall

α_{ci1}:   Heat transfer coefficient on the inside of the superheat region

α_{ci2}:   Heat transfer coefficient on the inside of the two-phase region

α_{ci3}:   Heat transfer coefficient on the inside of subcool region

α_{co}:   Effective Heat transfer coefficient between tube wall and air

C_w: Thermal Capacitance of tube wall

D_i: Inside diameter of tube

D_o: Outside diameter of tube

γ_c: Void fraction in condenser

h_{cfg}:   Enthalpy of vaporization

h_{cL}:   Saturated liquid enthalpy

$h_{c,in}$:   Enthalpy at inlet of condenser

$h_{c,out}$:   Enthalpy at outlet of condenser

h_{cv}:   Saturated vapor enthalpy

h_{c1}:   Average enthalpy of superheat region

h_{c3}:   Average enthalpy of subcool region

L_{c1}:   Length of superheat region

L_{c2}:   Length of two-phase region

L_{c3}:   Length of subcool region

L_{cT}:   Length of entire condenser

$\dot{m}_{c,in}$:   Mass flow rate at inlet of condenser

$\dot{m}_{c,int1}$: Mass flow rate at interface of node 1 and node 2

$\dot{m}_{c,int2}$: Mass flow rate at interface of node 2 and node 3

$\dot{m}_{c,out}$: Mass flow rate at outlet of condenser

P_c: Condenser pressure

ρ_{cL}:   Saturated liquid density

ρ_{cv}:   Saturated vapor density

ρ_{c1}:   Average density in superheat region

ρ_{c2}:   Average density in two-phase region

ρ_{c3}:   Average density in subcool region

ρ_w: Density of tube wall

T_{cw1}:   Temperature of superheat region wall

T_{cw2}:   Temperature of two-phase region wall

T_{cw3}:   Temperature of subcool region wall

T_{cr1}:   Temperature of superheat region refrigerant

T_{cr2}:   Temperature of two-phase region refrigerant

T_{cr3}:   Temperature of subcool region refrigerant

u: Velocity in the refrigerant energy balances

u: Thermal energy in tube wall energy balances

v_c: Condenser fan speed

In all cases an over bar will indicate an averaged value

Acknowledgements

I would like to thank the members of my committee, Dr. Warren White, Dr. Terry Beck, and Dr. Steve Eckels. I thank you for the opportunity and all of the help. In addition, there is a long list of people who helped me with the experimental setup. I do not want to forget anybody, but I'm sure you know who you are.

CHAPTER 1 - Introduction

It is desired to develop a computer model of an air conditioning system to use to develop a control law. Active computer control could yield systems with higher energy efficiencies. The refrigerant system mathematical model should predict the dynamic transients of key system parameters. These include values that can be used to calculate the coefficient of performance as well as the superheat. It is important that the model be simple enough to develop a control law with, but still be accurate. This thesis presents a model proposed by He (1996) in further detail and tailored to a specific air conditioning system. It is a twelfth order linear state space set of equations. The model can be used to determine dynamic perturbations from a steady state operating point as a result of changes in system inputs. Inputs include: compressor speed, expansion valve setting, and both heat exchanger blower speeds.

Previous work to increase efficiency of HVAC systems includes controlling air flow throughout buildings, single input control, and multi-input multi-output (MIMO) control. Saboksayr (1995) presented a decentralized controller for multi-zone space heating and House (1995) optimized control of two-zone building with variable-air-volume air handlers. The work of Aprea (2004) varies the compressor speed with fuzzy control techniques. In Cerri (1994), the expansion valve is controlled for optimal performance. Jiang (2003) uses a Linear-Quadratic-Gaussian regulator for MIMO feedback control. The various papers by He discuss nonlinear models of the heat exchangers, a linear model of a refrigeration cycle, a reduced linear model, a low-order linear model, and LQG control. In He (1995), nonlinear control of the evaporator temperature is achieved with feedback linearization. Nonlinear observers are investigated in Cheng (2004 & 2006).

The Model Derivation Chapter of this thesis gives the form of the nonlinear heat exchanger equations as well as their linearized forms. Using linear equations for the expansion valve and compressor, the evaporator and condenser models are coupled to produce a linear model of the complete air conditioner. Appendices A, B, and C contain

the step-by-step derivation of all of the equations required for the model. The result of Chapter 2 is a symbolic set of state space equations. Chapter 4 presents numeric evaluations of parameters to complete the model for the particular air conditioner used in this project.

A great deal of work was required for the experimental setup. The Experimental Setup Chapter describes the setup and modifications made to the original system. This includes the refrigeration components and measurement hardware and software. Air flow meters were fabricated and calibrated as part of the setup.

A results chapter shows the comparison between computer simulated and measured data. Investigation of the values of some uncertain parameters is also done here. The thesis concludes with a critical discussion of the model and possible corrections for future consideration.

CHAPTER 2 - Lumped Parameter Modeling Equations

In this chapter the governing equations of the refrigeration loop are presented. The derivation follows the doctoral dissertation of He (1996). This thesis is intended to demonstrate the derivation more completely. In this moving interface lumped parameter model, the heat exchangers are broken up into nodes. The evaporator has two nodes; a two-phase saturation region and a single phase superheated gas region. The condenser has three nodes; a single phase superheated gas region, a two-phase saturation region, and a subcooled liquid region. Three equations are derived for each node. These equations represent mass and energy balances on the refrigerant and energy balances on the tube wall. The general approach for deriving the refrigerant equations starts with the differential forms. The conservation of mass or continuity equation applied to the refrigerant flow is

$$\frac{Dm}{Dt} = \frac{\partial \rho}{\partial t} + \frac{\partial \rho u}{\partial z} = 0 \, . \tag{2.1}$$

Conservation of energy in general can be expressed as

$\frac{\partial \rho (e + 0.5 \vec{u} \cdot \vec{u})}{\partial t} + \nabla \cdot [\rho \vec{u}(h + 0.5 \vec{u} \cdot \vec{u})] = -\nabla \cdot \vec{q} + \rho \vec{f} \cdot \vec{u} + \nabla \cdot (\tau \cdot \vec{u}) + \dot{Q}$, but is derived by

MacArthur (1989) for refrigerant flow in a cylindrical tube to be of the form

$$\frac{\partial}{\partial t}(\rho h - P) + \frac{\partial}{\partial z}(\rho u h) = \frac{4}{D_i} \alpha_i (T_w - T_r) \, . \tag{2.2}$$

The capital D's in the continuity equation represent a substantial derivative. Symbol definitions are given as D_i: inner diameter of tube, e: internal energy, f: body force vector, h: enthalpy, P: pressure, q: heat flux, $\dot{Q}$: heat generation rate, T_w: tube wall temperature, T_r: refrigerant temperature, u: velocity of the refrigerant, α_i: heat transfer coefficient between tube and refrigerant, ρ: density, and τ: shear stress tensor. The spatial length and time are given by z and t, respectively. In order to write the conservation of energy as equation (2.2) it must be assumed that the one-dimensional form is appropriate, spatial

variations of pressure are negligible, viscous dissipation is negligible, and axial conduction is negligible. MacArthur (1989) states that momentum equations are not required since the spatial variations of pressure and viscous dissipation are neglected.

The differential conservation equations are first integrated over the cross-sectional area of the tube, and then integrated along the length of the node. The conservation of mass equations from the evaporator nodes are combined to form one mass balance of the evaporator. Likewise, the three mass balances of the condenser are combined to form one equation for the condenser. The tube wall energy balances are derived starting with a conservation of energy equation expressed as

$$\frac{dE_{CV}}{dt} = \dot{Q} + \dot{E}_m .$$
(2.3)

where E_{CV} is the energy of the control volume, $\dot{Q}$ is the net heat transfer into or out of the control volume, and $\dot{E}_m$ is the energy transfer rate as a result of mass crossing the control volume boundary. This sets the time rate of change of energy equal to the sum of the main net energy rates. The main rates are considered to be from heat transfer and mass crossing the boundary, all other energy rates associated with the tube wall are assumed to be negligible.

The end result is five equations for the evaporator and seven equations for the condenser. These equations are first order nonlinear ordinary differential equations. Later in this chapter, these equations will be linearized and combined with equations for the expansion valve and compressor to form a linear model of the complete loop. Key assumptions used in the derivation are given in the following list. These are:

1. The heat exchangers are long, straight, thin walled tubes. The fins on the outside of the tube are assumed to create an effective heat transfer coefficient; therefore only the cylindrical shape of the tube is considered.
2. Conduction in the axial direction is considered negligible.
3. Average heat transfer coefficients can be used on each node.
4. Average refrigerant temperatures of nodes can be used in heat transfer equations.
5. Average tube wall temperatures can be used in heat transfer equations, and the temperature is constant throughout the thickness.

6. Pressure is constant throughout the length of both the evaporator and the condenser. Therefore, saturated properties are constant over the length.

7. Average lengths of nodes are used.

8. The cross-sectional area of the two-phase region can be split into two sections, liquid and vapor.

9. The mean void fraction is constant with time.

10. The heat flux on either side of the transition points of the two-phase regions are the same. This is not actually true due to the fact that the wall temperature of the real system is constant in the two-phase region and varying along the length of the single-phase region. This assumption is required for the system to be approximated as linear.

11. The density throughout the length of the subcool region of the condenser is the saturated liquid density.

These assumptions were used in the dissertation of He (1996). They result in a simplified model, which was shown to accurately predict transients associated with perturbations of system inputs. Various other assumptions are involved; they are pointed out as they are used in the derivations. Appendices A, B and C contain the in-depth derivation of the equations in this chapter.

A schematic of the major components is on page 6 in Figure 2-1. A pressure-enthalpy diagram illustrated in Figure 2-2 on page 6 shows the thermodynamic processes involved with the loop. As seen in the pressure-enthalpy diagram, the expansion valve is assumed to be a constant enthalpy process.
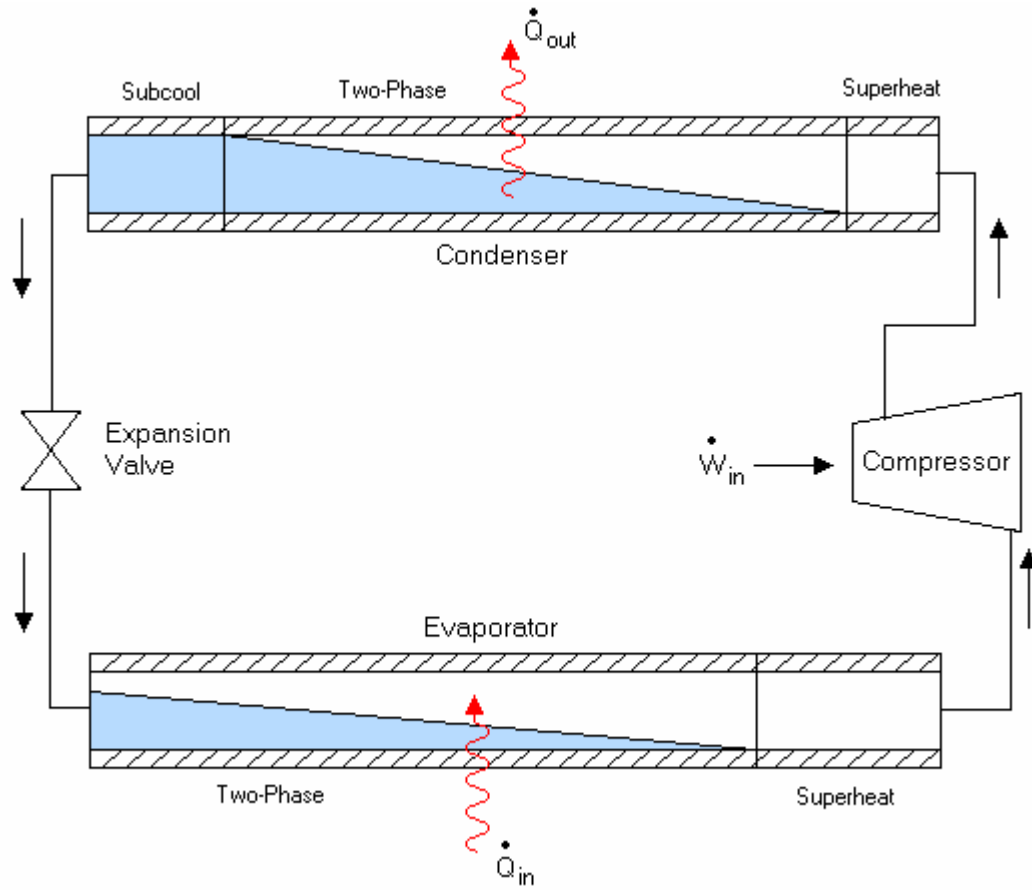
Figure 2-1 Refrigeration Loop Schematic
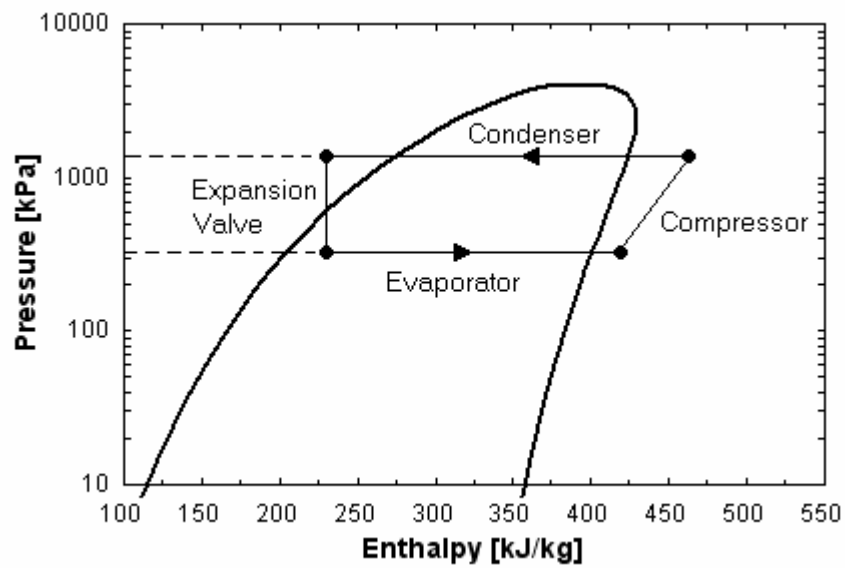
Figure 2-2 Pressure-Enthalpy Plot

Non-Linear Modeling Equations of the Evaporator

The evaporator is separated into two nodes for this derivation. Appendix A contains the complete derivations of the equations in this section. A schematic showing the key parameters of the evaporator is shown in Figure 2-3. Complete evaporator nomenclature is given on page ix.

α_{ei1} : Heat transfer coefficient on the inside of the two-phase region

α_{ei2} : Heat transfer coefficient on the inside of the superheat region

α_{eo} : Effective Heat transfer coefficient between tube wall and air

L_{e1} : Length of two-phase region

L_{e2} : Length of superheat region

$\dot{m}_{e,in}$: Mass flow rate at inlet of evaporator

$\dot{m}_{e,int}$: Mass flow rate at interface of the nodes

$\dot{m}_{e,out}$: Mass flow rate at outlet of evaporator

T_{ew1} : Temperature of two-phase region wall

T_{ew2} : Temperature of superheat region wall

T_{er1} : Temperature of two-phase region refrigerant

T_{er2} : Temperature of superheat region refrigerant

T_{ea} : Temperature of ambient air around evaporator

Figure 2-3 Evaporator Schematic

The control volumes for the two-phase and superheat regions are denoted by cv1 and cv2, respectively.

The conservation of mass equation for node one can be expressed as

$$AL_{e1}\frac{d\rho_{e1}}{dP_e}\frac{dP_e}{dt} + A(\rho_{e1} - \rho_{ev})\frac{dL_{e1}}{dt} = \dot{m}_{e,in} - \dot{m}_{e,\text{int}} , \tag{2.4}$$

and for node two as

$$AL_{e2}\frac{d\rho_{e2}}{dt} + A[\rho_{ev} - \rho_{e2}]\frac{dL_{e1}}{dt} + \dot{m}_{e,out} - \dot{m}_{e,\text{int}} = 0. \tag{2.5}$$

The overall mass balance equation of the evaporator is given as

$$A[\rho_{e1} - \rho_{e2}]\frac{dL_{e1}}{dt} + A\left[L_{e2}\frac{\partial\rho_{e2}}{\partial P_e} + L_{e1}\frac{d\rho_{e1}}{dP_e} \right]\frac{dP_e}{dt}$$
$$+ AL_{e2}\frac{\partial\rho_{e2}}{\partial h_{e,out}}\frac{dh_{e,out}}{dt} = \dot{m}_{e,in} - \dot{m}_{e,out} \tag{2.6}$$

The conservation of energy is derived to be

$$-A\left[(1-\bar{\gamma}_e)\rho_{eL}h_{efg}\right]\frac{dL_{e1}}{dt} + AL_{e1}\left[\rho_{e1}\frac{dh_{ev}}{dP_e} - (1-\bar{\gamma}_e)\frac{d\rho_{eL}h_{efg}}{dP_e} - 1 \right]\frac{dP_e}{dt} ,$$
$$= \dot{m}_{e,in}\left(h_{e,in} - h_{ev}\right) + L_{e1}\pi D_i\bar{\alpha}_{ei1}\left(\bar{T}_{ew1} - \bar{T}_{er1}\right) \tag{2.7}$$

and

$$-0.5A\rho_{e2}\left(h_{e,out} - h_{ev}\right)\frac{dL_{e1}}{dt} + AL_{e2}\left[0.5\rho_{e2}\frac{dh_{ev}}{dP_e} + 0.5\left(h_{e,out} - h_{ev}\right)\frac{\partial\rho_{e2}}{\partial P_e} - 1 \right]\frac{dP_e}{dt}$$
$$+ 0.5AL_{e2}\left[\rho_{e2} + \left(h_{e,out} - h_{ev}\right)\frac{\partial\rho_{e2}}{\partial h_{e,out}} \right]\frac{dh_{e,out}}{dt} \tag{2.8}$$
$$= L_{e2}\pi D_i\bar{\alpha}_{ei2}\left(\bar{T}_{ew2} - \bar{T}_{er2}\right) + \dot{m}_{e,out}\left(h_{ev} - h_{e,out}\right)$$

for the two-phase and superheat nodes, respectively.

The energy balances on the tube wall for node one and two respectively result in

$$(\rho CA)_w\left[\frac{d\bar{T}_{ew1}}{dt}\right] = \bar{\alpha}_{eo}\pi D_o\left(T_{ea} - \bar{T}_{ew1}\right) + \bar{\alpha}_{ei1}\pi D_i\left(\bar{T}_{er1} - \bar{T}_{ew1}\right), \tag{2.9}$$

and

$$(\rho CA)_w\left[\frac{d\bar{T}_{ew2}}{dt} + \frac{\left(\bar{T}_{ew1} - \bar{T}_{ew2}\right)}{L_{e2}}\frac{dL_{e1}}{dt}\right] = \bar{\alpha}_{eo}\pi D_o\left(T_{ea} - \bar{T}_{ew2}\right)$$
$$+ \bar{\alpha}_{ei2}\pi D_i\left(\bar{T}_{er2} - \bar{T}_{ew2}\right) \tag{2.10}$$

The average density in node one is defined to be

$$\rho_{e1} = (1-\bar{\gamma}_e)\rho_{eL} + \bar{\gamma}_e\rho_{ev}. \tag{2.11}$$

The average density of node two is a function of the evaporator pressure and the average enthalpy in node two, $h_{e2} = 0.5(h_{ev} + h_{e,out})$. Since the enthalpy of saturated vapor is a function of pressure the average density in node two can be expressed as $\rho_{e2} = \rho(P_e, h_{e,out})$. Similarly the average temperature is a thermodynamic function of the form $\overline{T}_{er2} = T(P_e, h_{e,out})$. More nomenclature is defined below.

A:	Cross-sectional area inside of tube	h_{eL}:	Saturated liquid enthalpy
A_w:	Cross-sectional area of tube wall	$h_{e,in}$:	Enthalpy at inlet of evaporator
C_w:	Thermal Capacitance of tube wall	$h_{e,out}$:	Enthalpy at outlet of evaporator
D_i:	Inside diameter of tube	h_{ev}:	Saturated vapor enthalpy
D_o:	Outside diameter of tube	P_e:	Evaporator pressure
γ_e:	Void fraction in evaporator	ρ_{eL}:	Saturated liquid density
h_{efg}:	Enthalpy of vaporization	ρ_{ev}:	Saturated vapor density
		ρ_w:	Density of tube wall

Non-Linear Modeling Equations of the Condenser

The condenser is divided into three nodes by phase. The first node is a superheat region, the second a two-phase region, and the third a subcool region. A diagram of the condenser's parameters is in Figure 2-4, and condenser nomenclature is given on page xi. For complete derivation of the modeling equations see Appendix B.
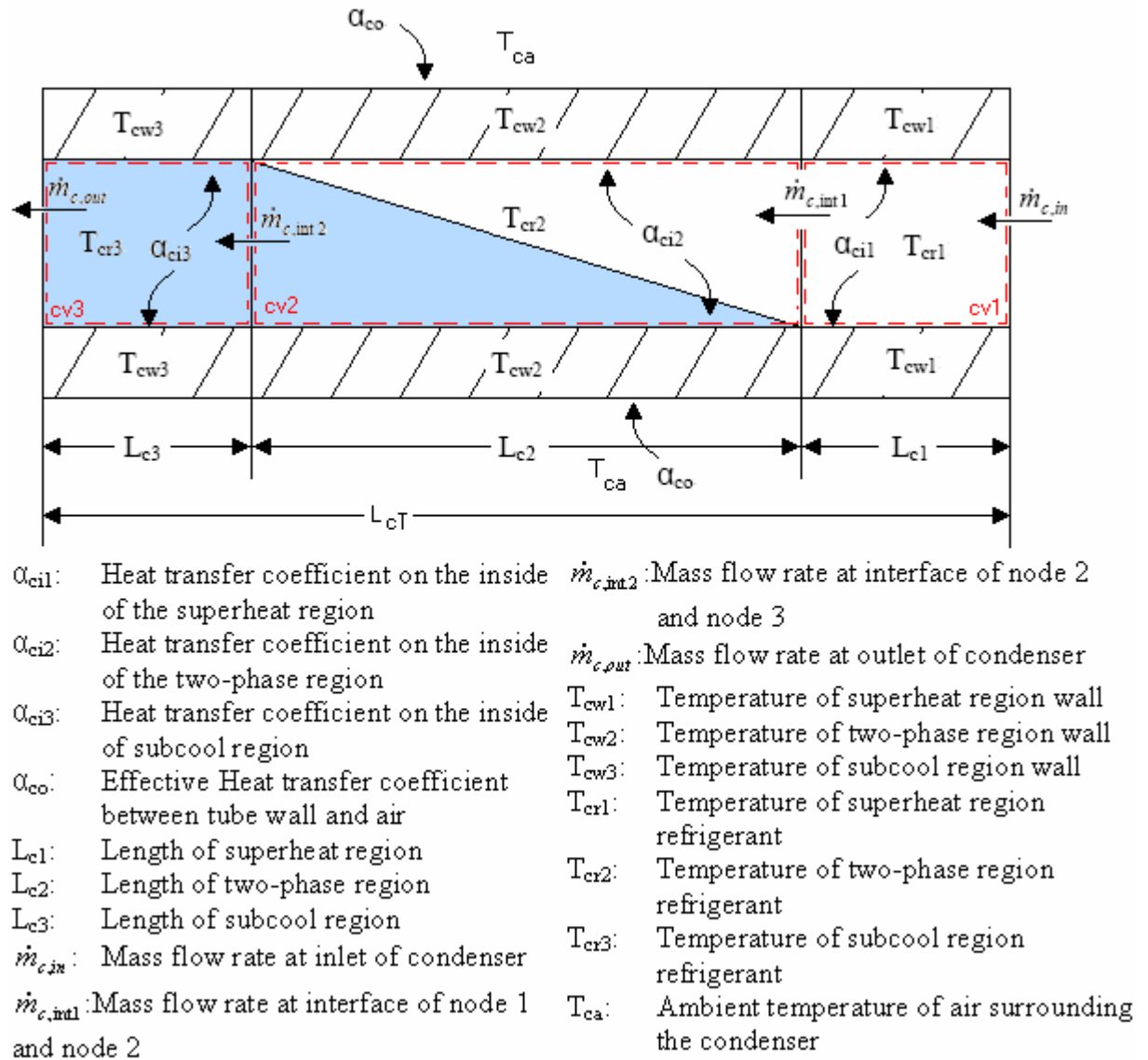
Figure 2-4 Condenser Schematic

α_{ci1}: Heat transfer coefficient on the inside of the superheat region

α_{ci2}: Heat transfer coefficient on the inside of the two-phase region

α_{ci3}: Heat transfer coefficient on the inside of subcool region

α_{co}: Effective Heat transfer coefficient between tube wall and air

L_{c1}: Length of superheat region

L_{c2}: Length of two-phase region

L_{c3}: Length of subcool region

$\dot{m}_{c,in}$: Mass flow rate at inlet of condenser

$\dot{m}_{c,int1}$: Mass flow rate at interface of node 1 and node 2

$\dot{m}_{c,int2}$: Mass flow rate at interface of node 2 and node 3

$\dot{m}_{c,out}$: Mass flow rate at outlet of condenser

T_{cw1}: Temperature of superheat region wall

T_{cw2}: Temperature of two-phase region wall

T_{cw3}: Temperature of subcool region wall

T_{cr1}: Temperature of superheat region refrigerant

T_{cr2}: Temperature of two-phase region refrigerant

T_{cr3}: Temperature of subcool region refrigerant

T_{ca}: Ambient temperature of air surrounding the condenser

The control volumes for the superheat, two-phase, and subcooled regions are denoted by cv1, cv2, and cv3, respectively.

The conservation of mass equation for node one, node two, and node three can be expressed as

$$AL_{c1}\frac{d\rho_{c1}}{dt} + A[\rho_{c1} - \rho_{cv}]\frac{dL_{c1}}{dt} = \dot{m}_{c,in} - \dot{m}_{c,int1}, \tag{2.12}$$

$$AL_{c2}\frac{d\rho_{c2}}{dt} + A[\rho_{c2} - \rho_{cL}]\frac{dL_{c2}}{dt} + A(\rho_{cv} - \rho_{cL})\frac{dL_{c1}}{dt} + \dot{m}_{c,int2} - \dot{m}_{c,int1} = 0, \tag{2.13}$$

and
$$\dot{m}_{c,int2} = \dot{m}_{c,out} + AL_{c3}\frac{d\rho_{cL}}{dt}, \tag{2.14}$$

respectively. The overall mass balance equation of the condenser is given as

$$A\left[L_{c3}\frac{d\rho_{cL}}{dP_c} + L_{c2}\frac{d\rho_{c2}}{dP_c} + L_{c1}\left(\frac{\partial\rho_{c1}}{\partial P_c} + \frac{\partial\rho_{c1}}{\partial h_{c1}}\frac{dh_{cv}}{dP_c}\right)\right]\frac{dP_c}{dt}$$
$$+ A[\rho_{c2} - \rho_{cL}]\frac{dL_{c2}}{dt} + A(\rho_{c1} - \rho_{cL})\frac{dL_{c1}}{dt} = \dot{m}_{c,in} - \dot{m}_{c,out} \tag{2.15}$$

The results from the conservation of energy on the refrigerant equations for node one, two, and three are given by

$$AL_{c1}\left[\rho_{c1}\frac{dh_{cv}}{dP_c} + 0.5(h_{c,in} - h_{cv})\left(\frac{\partial\rho_{c1}}{\partial P_c} + \frac{\partial\rho_{c1}}{\partial hc1}\frac{dh_{cv}}{dP_c}\right) - 1\right]\frac{dP_c}{dt}$$
$$+ 0.5A(h_{c,in} - h_{cv})\rho_{c1}\frac{dL_{c1}}{dt} = L_{c1}\pi D_i\bar{\alpha}_{ci1}\left(\bar{T}_{cw1} - \bar{T}_{cr1}\right) + (h_{c,in} - h_{cv})\dot{m}_{c,in} \tag{2.16}$$

$$A\rho_{cL}h_{cfg}\frac{dL_{c1}}{dt} + A\bar{\gamma}_c\rho_{cL}h_{cfg}\frac{dL_{c2}}{dt}$$
$$+ A\left\{L_{c2}\left[-(1-\bar{\gamma}_c)\frac{dh_{cfg}\rho_{cL}}{dP_c} + \rho_{c2}\frac{dh_{cv}}{dP_c} - 1\right] + L_{c3}(h_{cL} - h_{cv})\frac{d\rho_{cL}}{dP_c}\right\}\frac{dP_c}{dt} \tag{2.17}$$
$$= \dot{m}_{c,out}h_{cfg} + \pi L_{c2}D_i\bar{\alpha}_{ci2}\left(\bar{T}_{cw2} - \bar{T}_{cr2}\right)$$

and
$$0.5A\rho_{cL}[h_{cL} - h_{c,out}]\frac{dL_{c1}}{dt} + 0.5A\rho_{cL}[h_{cL} - h_{c,out}]\frac{dL_{c2}}{dt}$$
$$+ AL_{c3}\left[0.5(h_{c,out} - h_{cL})\frac{d\rho_{cL}}{dP_c} + 0.5\rho_{cL}\frac{dh_{cL}}{dP_c} - 1\right]\frac{dP_c}{dt} \tag{2.18}$$
$$+ 0.5AL_{c3}\rho_{cL}\frac{dh_{c,out}}{dt} = \dot{m}_{c,out}(h_{cL} - h_{c,out}) + \pi L_{c3}D_i\bar{\alpha}_{ci3}\left(\bar{T}_{cw3} - \bar{T}_{cr3}\right)$$

respectively.

The governing equations given by the conservation of energy on the tube walls can be written as

$$(\rho CA)_w \left[\frac{d\overline{T}_{cw1}}{dt} + \frac{(\overline{T}_{cw1} - \overline{T}_{cw2})}{L_{c1}} \frac{dL_{c1}}{dt} \right] = \overline{\alpha}_{co} \pi D_o (T_{ca} - \overline{T}_{cw1}),$$

$$+ \overline{\alpha}_{ci1} \pi D_i (\overline{T}_{cr1} - \overline{T}_{cw1}) \tag{2.19}$$

$$(\rho CA)_w \frac{d\overline{T}_{cw2}}{dt} = \overline{\alpha}_{co} \pi D_o (T_{ca} - \overline{T}_{cw2}) + \overline{\alpha}_{ci2} \pi D_i (\overline{T}_{cr2} - \overline{T}_{cw2}), \tag{2.20}$$

and
$$(\rho CA)_w \frac{d\overline{T}_{cw3}}{dt} + (\rho CA)_w \left[\frac{\overline{T}_{cw2} - \overline{T}_{cw3}}{L_{c3}} \right] \frac{dL_{c1}}{dt} + (\rho CA)_w \left[\frac{\overline{T}_{cw2} - \overline{T}_{cw3}}{L_{c3}} \right] \frac{dL_{c2}}{dt} \tag{2.21}$$

$$= \overline{\alpha}_{co} \pi D_o (T_{ca} - \overline{T}_{cw3}) + \overline{\alpha}_{ci3} \pi D_i (\overline{T}_{cr3} - \overline{T}_{cw3})$$

respectively. The average density in node two is defined to be

$$\rho_{c2} = (1 - \overline{\gamma}_c)\rho_{cL} + \overline{\gamma}_c \rho_{cv}. \tag{2.22}$$

The average density of node one is a function of the condenser pressure and the average enthalpy in the node one, $\rho_{c1} = \rho(P_c, h_{c1})$, where $h_{c1} = 0.5(h_{cv} + h_{c,in})$. More nomenclature is given below.

A:	Cross-sectional area inside of tube	h_{cL}:	Saturated liquid enthalpy
A_w:	Cross-sectional area of tube wall	$h_{c,in}$:	Enthalpy at inlet of condenser
C_w:	Thermal Capacitance of tube wall	$h_{c,out}$:	Enthalpy at outlet of condenser
D_i:	Inside diameter of tube	h_{cv}:	Saturated vapor enthalpy
D_o:	Outside diameter of tube	P_c:	Condenser pressure
γ_c:	Void fraction in condenser	ρ_{cL}:	Saturated liquid density
h_{cfg}:	Enthalpy of vaporization	ρ_{cv}:	Saturated vapor density
		ρ_w:	Density of tube wall

It is worth noting that the equations for the subcool region refrigerant mass, (2.14), and energy balance,(2.18), differ by an extra term from those derived by He (1996). The extra term is $AL_{c3} \frac{d\rho_{cL}}{dt}$ in (2.14) and $0.5AL_{c3}(h_{c,out} - h_{cL}) \frac{d\rho_{cL}}{dP_c} \frac{dP_c}{dt}$ in (2.18). The difference will also show up in the overall condenser mass balance, eq. (2.15), as $AL_{c3} \frac{d\rho_{cL}}{dP_c} \frac{dP_c}{dt}$. The refrigerant energy balance of node two, eq. (2.17), has the extra term $AL_{c3}(h_{cL} - h_{cv}) \frac{d\rho_{cL}}{dP_c} \frac{dP_c}{dt}$. It was determined that the equations derived in this thesis would be equivalent to the He (1996) equations if the time derivative of

saturated liquid density in the subcool region was set to zero. The effects of this difference are small, but it is retained to be consistent with the other modeling equations where this time derivative is not zero.

Linear Modeling Equations of the Refrigeration Loop

The model developed in this thesis is a linear model. It will be able to predict the small perturbations from an operating point. This is a reasonable way to model an air conditioner for computer control, provided the perturbations remain small. Most likely the conditions of the environment and the state properties of the refrigerant will not be changing by large amounts when the control is being applied, so the model will still be valid. A linear model allows for a simpler simulation, as well as a wider variety of possible control schemes.

To obtain a linear model of the refrigeration loop, linear equations of the heat exchangers are coupled by linear equations for the compressor and the expansion valve. Derivations of these equations and elements of the matrices are presented in Appendix C. The linear equations of the evaporator and the condenser can be expressed in matrix form by

$$D_e \delta \ \dot{x}_e = A'_e \delta \ x_e + B'_e \delta \ u_e \tag{2.23}$$

and
$$D_c \delta \ \dot{x}_c = A'_c \delta \ x_c + B'_c \delta \ u_c, \tag{2.24}$$

respectively.

The states and inputs of the evaporator are given as

$$x_e = \begin{bmatrix} L_{e1} & P_e & h_{e,out} & \overline{T}_{ew1} & \overline{T}_{ew2} \end{bmatrix}^T \text{ and } u_e = \begin{bmatrix} \dot{m}_{e,in} & h_{e,in} & \dot{m}_{e,out} & v_e \end{bmatrix}^T, \text{ where } v_e$$
is the evaporator blower setting.

The states and inputs of the condenser are given as

$$x_c = \begin{bmatrix} L_{c1} & L_{c2} & P_c & h_{c,out} & \overline{T}_{cw1} & \overline{T}_{cw2} & \overline{T}_{cw3} \end{bmatrix}^T \text{ and } u_c = \begin{bmatrix} \dot{m}_{c,in} & h_{c,in} & \dot{m}_{c,out} & v_c \end{bmatrix}^T,$$
where v_c is the condenser blower setting.

To model the compressor and expansion valve, equations are written for the change in enthalpy at the exit of the compressor, and the change in mass flow rate through each device. It is assumed that the enthalpy at the exit of the compressor is a function of the evaporator and condenser pressures as well as the inlet enthalpy. The

compressor exit enthalpy is assumed to be equal to the condenser inlet enthalpy and the compressor inlet enthalpy is assumed to be equal to the evaporator exit enthalpy. This leads to the equation $h_{c,in} = h(P_e, P_c, h_{e,out})$. The mass flow rate through each device is assumed to be a function of evaporator and condenser pressures and their respective control settings. Recognizing that the flow rate through the compressor is equal to the flow rate out of the evaporator and into the condenser, the mass flow rate through the compressor can be expressed in the following form $\dot{m}_{comp} = \dot{m}_{e,out} = \dot{m}_{c,in} = \dot{m}(P_e, P_c, u_{comp})$, where u_{comp} is the compressor setting. The mass flow rate out of the condenser and into the evaporator is the flow rate through the expansion valve, which can be written as $\dot{m}_{valve} = \dot{m}_{c,out} = \dot{m}_{e,in} = \dot{m}(P_e, P_c, u_{valve})$, where u_{valve} is the expansion valve setting. Taking the differentials of these equations results in the linear modeling equations of the compressor and expansion valve. The change in mass flow rate through the valve is expressed by

$$\delta \dot{m}_{valve} = \delta \dot{m}_{c,out} = \delta \dot{m}_{e,in} = k_{11}\delta P_e + k_{12}\delta P_c + k_{13}\delta u_{valve}. \tag{2.25}$$

The change in compressor outlet enthalpy and mass flow rate are given by

$$\delta h_{comp,out} = \delta h_{c,in} = k_{21}\delta P_e + k_{22}\delta P_c + k_{23}\delta h_{e,out}, \tag{2.26}$$

and $\qquad \delta \dot{m}_{comp} = \delta \dot{m}_{e,out} = \delta \dot{m}_{c,in} = k_{31}\delta P_e + k_{32}\delta P_c + k_{33}\delta u_{comp}, \tag{2.27}$

respectively. The k_{ij} coefficients are to be determined experimentally.

The equations for the evaporator and condenser can be written in terms of system state variables and inputs. This is done by replacing the inputs of the heat exchanger models with functions of the system states and inputs. The system state variables are the states of the evaporator and condenser and the inputs are compressor setting, expansion valve setting, evaporator blower setting, and condenser blower setting.

The complete linear model of the refrigeration loop in state space form is

$$\delta \dot{x} = \begin{bmatrix} A_{ee} & A_{ec} \\ A_{ce} & A_{cc} \end{bmatrix} \delta x + \begin{bmatrix} B_{ee} \\ B_{cc} \end{bmatrix} \delta u \tag{2.28}$$

where the system states and inputs are

$$\delta x = \begin{bmatrix} \delta x_e \\ \delta x_c \end{bmatrix} \text{ and } \delta u = \begin{bmatrix} \delta u_{comp} & \delta u_{valve} & \delta v_e & \delta v_c \end{bmatrix}^T.$$

With this set of state space modeling equations the transient responses of the air conditioner can be simulated. Chapter 4 discusses the determination of parameters required to simulate the system and Chapter 5 presents a comparison of simulated and measured results.

CHAPTER 3 - Experimental Setup

In this section the air conditioner and data acquisition used to develop the model are discussed in detail. This will include modifications of the original air conditioner design, hardware of the system, and measurements and controls applied to the system. The unit is a modified version of a Technovate air conditioning and refrigeration education system. It originally was a learning tool to observe, analyze, and change the characteristics of an air conditioner. The basic setup of the Technovate remains. It has been retrofitted to use R-134a. Changes were also made to allow for a variable speed compressor, heat exchanger blower speeds, and expansion valve opening. Sensors have been introduced to the system for computer measurements of pressures, refrigerant temperatures, air relative humidity and temperature, air flow rates across the heat exchangers, and flow rate of the refrigerant. A picture of the current setup is in Figure 3-1.

Figure 3-1 Picture of Setup

At the onset of the project the air conditioner had not been fully assembled, refurbished, tested, or wired for computer measurements and control. A great deal of time and effort went into refurbishing the looks of the unit, leak proofing the refrigerant lines, and eliminating noise from measurement signals. A few repairs and modifications were required in order to achieve the final design. Figure D-2 and D-3 on page 127 and 128 illustrate the layout of the initial and final design respectively. A list of parts is also given in Tables D.6 to D.8 starting on page 144.

System Description of Components

This section describes the experimental setup at its current state. The evaporator and condenser have the same geometry. Each are finned compact single route heat exchangers with twenty passes of ⅜" o.d. copper tubing. They have slots for glass sight tubes at the entry, middle, and exit. The middle tube allows for visualization of two-phase flow. The entry and exit glass tubes were replaced with copper tubes to avoid leaks. Wooden boxes with a Plexiglas front enclose the heat exchangers. Ducts at the top of the boxes connect to air flow meters. Blowers for the heat exchangers are turned by ¼ hp 230 VAC three phase motors. These motors are controlled by variable frequency drives. Ducts connect the blower output to the inlet of the heat exchangers. The ducting and boxes are sealed so that all the air flowing out of the blower goes through the air flow meter. The compressor is a belt driven single cylinder ¼ hp unit, driven by a ¾ hp 230 VAC three phase motor. The motor is powered by a variable frequency drive similar to the blower motor's drives. The system has the capability for using one of two expansion devices, a stepper motor expansion valve rated at ½ ton of cooling or a capillary tube. The size of the expansion valve opening is controlled with a temperature control board. This board drives the stepper motor in the expansion valve to a desired setting using a reference voltage supplied by the computer. All of the testing in this thesis utilized the stepper motor expansion valve.

The unit can run in a few different configurations. A flow reversing valve can change the direction of flow and switch the roles of the condenser and evaporator making the unit a heat pump. A set of check valves throughout the loop allow for this change in flow direction. Energizing and un-energizing the solenoid in this valve can be controlled

with a TTL signal from the computer. For the work done in this thesis, the valve was always set to run as an air conditioner. Flow can be directed through an accumulator at the exit of the evaporator; valves allow for bypassing this accumulator. The purpose of the accumulator is to collect liquid refrigerant to protect the compressor. It is specially designed to keep the refrigerant oil in circulation. During testing it was determined that the accumulator affected transient responses to changes in system inputs in ways not consistent with the current model development. Therefore, the system was always run bypassing the accumulator. The refrigerant accumulator at the exit of the condenser can be used to store refrigerant as well as add or remove refrigerant from the main circulation loop. It was not utilized in this work.

Modifications to Original Design

This section explains the modifications to obtain the current setup. The first and most important change was to upgrade the expansion devices. There are two possible expansion devices, a computer controlled expansion valve and a capillary tube. Initially, the goal was to operate the unit with the capillary tube and then get the expansion valve working. A blockage in the loop became a reoccurring issue when using the capillary tube. All of the components which were likely to clog up were replaced. This included the filter dryer, capillary tube, and strainers ahead of and behind the capillary tube. Also the solenoid valve used to close off the path to the capillary tube was replaced with a manual variable opening valve. Replacing the solenoid valve eliminated the ability to select the expansion device with a computer, but this was determined to be an unnecessary feature for the current work. A manual variable valve ahead of the capillary tube will allow for some adjustment of the flow rate; it was not utilized in this work.

The original design had a proportional solenoid valve as the variable expansion valve. This component failed because it had a maximum pressure difference of 345 kPa. The air conditioner requires a pressure difference on the order of 700 kPa. It also had VITON seals, which are not compatible with R-134a. A stepper motor expansion valve replaced this faulty component. This required additional plumbing, due to the different valve geometry. Changing the direction of the check valves around it was necessary, because the new expansion valve requires flow to go up through the device.

The refrigerant/oil separator and oil receiver at the exit of the evaporator were replaced by a suction line accumulator. Originally, the system had the capability of adding or removing oil from circulation. When the appropriate valves were open and flow went through the separator, oil would be removed from circulation. The separated oil could then be put in the oil receiver and if desired put into the sump of the compressor, which would eventually lead to the oil circulating through the loop again. A suitable fitting could not be found to connect the oil receiver to the compressor sump, so this oil separating feature could not be achieved. Instead, the suction line accumulator was added. This accumulator is designed for recirculation of oil while protecting the compressor from liquid.

Thermocouple probes replaced the bimetallic dial thermometers of the original setup. While visual verification of refrigerant temperature is important, it was deemed more important for the computer to have an accurate measure of refrigerant temperature.

Measurements and Controls

The system has measurements of refrigerant pressure, temperature, and flow rate. There are five pressure transducers; one at the inlet and exit of both heat exchangers and one at the exit of the compressor. Thermocouple probes are near each of the pressure transducers. Dial pressure gauges located at the inlet and exit of the heat exchangers give a visual verification that the computer measurements are reasonable. A V-cone Flowmeter is positioned at the exit of the compressor. This meter produces a pressure differential measured by the differential pressure transmitter. This pressure difference combined with the line pressure and temperature can be used to determine a mass flow rate. The meter was calibrated for gas, which is why it is located at the exit of the compressor. It is guaranteed that the state of the refrigerant at output of the compressor will be gas. Unfortunately, oil is also present in the flow and the flow meter never produced reliable measurements, likely because of the presence of oil. Communication with the manufacturer of the V-cone confirmed that oil would lead to inaccurate flow measurements.

Relative humidity and temperature sensors are located at the inlet and exit of each heat exchanger. Air flow meters are positioned at the exit of the two heat exchangers.

These meters were constructed and calibrated as part of this project, and will be discussed in a later section of this chapter. With these measurements the energy gained or lost by the air can be estimated.

Thermocouples attached to the tubes of the heat exchangers give a rough estimate of the tube wall temperature. The beads of the thermocouples were glued into place using epoxy. This results in some insulation between the tube and the air. The insulation lowers the local heat transfer; hence the temperature measured is too close to that of the refrigerant. These thermocouple measurements were taken by a ten channel Omega Digital Thermometer.

The system inputs include compressor speed, expansion valve setting, evaporator blower speed, and condenser blower speed. Variable frequency drives control the speeds of the three motors. They can either be controlled manually with the keypad or by a 0-10 VDC reference signal. The temperature control board uses a 0-10 VDC reference signal to control the valve opening. All of the signals are referenced with respect to the analog out ground on the screw terminal boards of the data acquisition system.

The manual or computer control switch plate allows the user to select the operation mode of each of the four components. When a switch is to the left the corresponding device will be controlled manually, computer control is required when the switches are to the right. In manual mode the operator uses the keypads of the variable frequency drives to control motor speeds. The fourth, bottom, switch is for the expansion valve and is a little different. In the left position the stepper motor expansion valve closes and the flow reversing valve solenoid is guaranteed not to be energized. In this configuration the flow will go through the capillary tube and the unit will be in air conditioning mode. When the switch is to the right the expansion valve opening is controlled by the reference signal from the computer, and the reversing valve can be controlled by a TTL signal.

The measurements and controls are implemented using National Instruments data acquisition hardware and software. The hardware includes two PCI-6024E DAQ cards coupled with two SC-2070 screw terminal boards. The screw terminal boards have a cold junction reference to be used with the thermocouples. The DAQ cards are installed in a PC with an AMD Athlon 902 Mhz processor, 512 MB RAM, and MS Windows XP

operating system. National Instruments LabVIEW 8 software processes, records, and displays the measurements.

Electrical Wiring

The entire unit is powered by 120 VAC single phase, i.e. wall outlets. Wiring diagrams are located in Appendix D starting on page 130. The air conditioner and computer are connected to grounded plug 1. The variable frequency drives for the blower motors are connected to grounded plug 2. These drives are a terrible source of noise, it was determined that powering them separately reduced noise in the measurements. These grounded plugs are then connected to extension cords that plug into wall outlets. The air conditioner's power from grounded plug 1 runs through the main switch, a watt meter, and to the power strip. The watt meter does not measure power used by the blower motors. It has a shunt so that it only measures half of the power used by the rest of the unit. A switch below the meter allows for selecting low and high scales. The power strip supplies the compressor speed controller, temperature control board, flow reversing solenoid, and DC power supply. The reversing valve was not used in this work so it was never plugged into the power strip.

With the 24 VDC from the power supply, a 24 to 5 VDC converter, and a 24 to ±12 VDC converter all of the sensors get their required supply voltage. Wiring of the sensors is fairly simple, power and ground wires run from the power bus to the device and signal wires are routed to the screw terminal board. All of the sensors' signals are referenced to their supply voltage's ground so only one wire needs to be routed to the screw terminal board from each sensor. Shielded wires were used in all cases to help eliminate the noise.

The three variable frequency drives and the temperature control board use reference inputs from the computer. Shielded wires carry the signal from the screw terminal board to the respective devices. It is important to note the location where the shielding is grounded. The blower motor frequency controllers require that the shielding be grounded only at the screw terminal board enclosure. Grounding the shielding at the drive will add excessive noise to the computer measurements. This is the opposite for the compressor motor speed controller; noise was less when the shielding was grounded at

the controller. To avoid unnecessary measurement noise, the blower motors need their frames to be grounded at their respective frequency drive which is then grounded at the wall outlet. The compressor motor frame should also be grounded at the motor controller. Electrical isolation between the mounting bolts of the frequency drives and the main electronics box is also required to avoid a ground loop. The proper grounding of the frequency drives enormously reduces the noise on computer measurements and is an absolute necessity.

A ground bar connected to a solid ground line provides a reference for the computer measurements and the sensors. The DC power supply, computer, screw terminal board enclosure, main electronics box, and copper refrigerant tubes are grounded at the ground bar. The pressure transducers require that their cases be grounded. These cases are connected to the refrigerant tubes, which makes them all electrically connected. To avoid ground loops, only the case of one pressure transducer is directly connected to the ground bar.

Most of the noise in the measurements is due to the variable frequency drives. The noise can be reduced greatly with proper grounding of the sensors, computer, frequency drives, motors, and shielding. The grounding and shielding was iteratively changed until the noise was acceptable. Appendix D wiring diagrams starting on page 130 illustrate the proper grounding of the system.

Software

Measurements and controls are implemented using LabVIEW 8 software. The software converts all of the sensor signal voltages to the proper measurement units, e.g. kPa for pressures. Several of the signals are filtered by the software. Measurements are plotted on charts and displayed numerically on the front panel, in addition they can be written to a file which is usable in MS Excel. Control signals for the four system inputs are also generated by the virtual instrument. The subcool and superheat are calculated and displayed continuously on the front panel. A picture of the front panel of the virtual instrument is in Figure 3-2 on page 23.
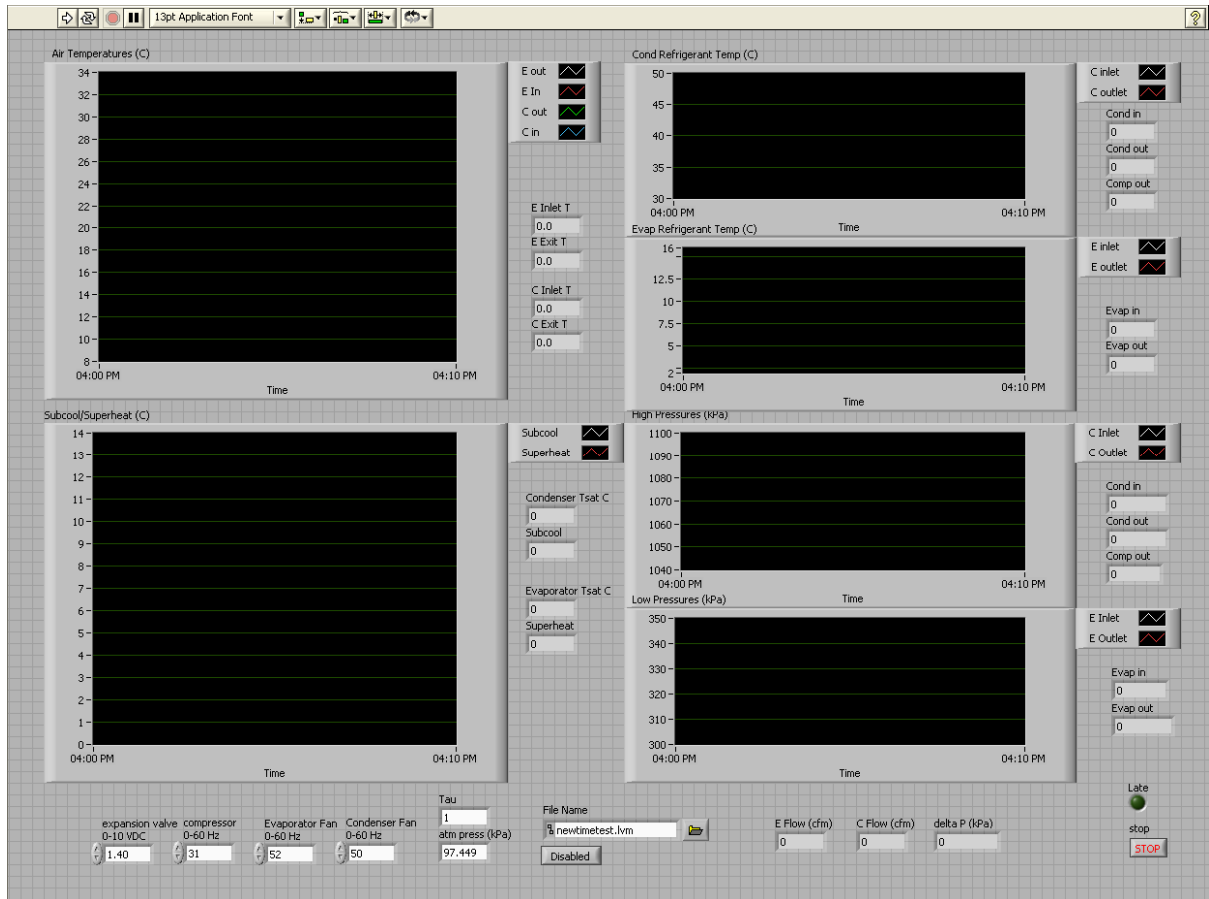
Figure 3-2 Front Panel of Virtual Instrument

All signals are displayed numerically. Temperatures are in degrees Celsius, pressures are absolute and in kPa, air flow rates are in cubic feet per minute. The output of the differential pressure transmitter is displayed in kPa. In order to calculate a mass flow rate from this pressure, a complex formula and thermodynamic tables must be used, therefore the mass flow rate was not calculated on the fly. The air temperatures, refrigerant pressures, refrigerant temperatures, subcool, and superheat are plotted versus time. Refrigerant temperature and pressure at the compressor exit were not plotted, because they were not variables that needed to be tracked while operating the unit. Waveform charts help to determine when the air conditioner is at a steady state operating point. A time span of ten or twenty minutes was commonly used. To save space, abbreviations of C or Cond, E or Evap, Comp denote measurements related to the condenser, evaporator, and compressor, respectively. Saturation temperature is abbreviated by Tsat. The four controls are in the bottom left corner. Motor speeds are input as the frequency that the variable frequency drives are desired to output. The

23

expansion valve setting is simply a 0-10 VDC input. Two additional inputs are tau, the

time constant for the software filters, and the atmospheric pressure used to calculated

total pressure from the gauge pressure measurements. A time constant of one second and

a nominal atmospheric pressure of 97.449 kPa (14.13 psi) were used in all instances.

This nominal atmospheric pressure was measured on a local barometer once and was

assumed not to vary significantly from day to day. Users can input a distinct file name

into the File Name box and use the enable/disable button for writing measurements to

files. A late light in the bottom right flashes when the virtual instruments did not finish

all tasks on time during the last loop iteration. The stop button shuts down the virtual

instrument.

All reference information for the virtual instrument is given in Appendix D.

Figures D-10 and D-11 starting on page 137 illustrate the block diagram of the virtual

instrument. All of the tasks are placed in a timed while loop that starts every 100 ms.

This time step was determined to be adequate for completing all of the tasks. Two DAQ

assistants, Board 1 and Board 2, take the measurements. The thermocouple signals are

taken in Board 2 and the rest are done in Board 1. Channel assignments, DAQ assistant

scales, and formula block equations are shown in Table D.3, D.4 and D.5 starting on page

136, respectively. An acquisition mode of one sample on demand was used in both

assistants. The board 1 signals are all reference single ended, meaning the voltage

measured on a channel is referenced to the computer's ground. Custom scales created in

the DAQ assistant convert voltages to measurement units in Board 1. The sub virtual

instrument (sub-vi) board_1_router.vi routes the measurements from Board 1 to be

displayed, written to a file, or filtered. Figure D-12 on page 139 shows the block

diagram.

Temperature signals are acquired in Board 2. The DAQ assistant outputs the

voltage from each thermocouple as well as the temperature measured by the cold junction

reference. The thermocouple channels are set to a differential terminal configuration and

the cold junction is a referenced single ended input on channel 0. The screw terminal

board where the thermocouples are connected is configured to output the cold junction

signal to channel 0. A custom scale converts the cold junction voltage to a temperature in

degrees Celsius. The thermocouple measurements are converted to milli-volts with a

custom scale. An offset voltage was added to each measurement. This is because the differential channels where shown to measure approximately 0.12 mV when the channels were shorted. This offset is enough to noticeably change temperature readings from a thermocouple. The temperature signals are sent to a sub-vi, temperature processing.vi, where they are converted to degrees Celsius and filtered. Figure D-17 on page 142 contains the block diagram of the sub-vi. To determine the refrigerant temperature from each thermocouple, the cold junction reference temperature is converted to a voltage, then added to the thermocouple voltage, and finally the sum is converted to a temperature in degrees Celsius. The conversions are done with third order polynomials. Both polynomials were curve fit to type K thermocouple reference table data over the range of -50 to +50 degrees Celsius.

Several of the measurements had enough noise that a filter was required. These signals include the pressures, refrigerant temperatures, differential pressure, and the air flow rates. The signals are filtered inside of the sub-vi's press processing.vi, flow processing.vi, and temperature processing.vi. Figures D-15 to D-17 starting on page 140 illustrate the block diagrams of these sub-vi's. In all cases the first order filter is of the form

$$V_{out} = \frac{1}{\tau}\int_0^t (V_{in} - V_{out})dt ,$$

which can be approximated by

$$V_{out}(t) = \frac{\Delta t}{2}(x(t) + x(t - \Delta t)) + V_{out}(t - \Delta t),$$

where the value of x is determined by

$$x(t) = \frac{1}{\tau}(V_{in}(t) - V_{out}(t - \Delta t)).$$

Time t is the current loop iteration and $t - \Delta t$ is the previous loop iteration. The time constant τ determines the cut off frequency of the filter, this time constant can be changed in the tau numeric input on the front panel. V_{in} is the raw signal and V_{out} is the filtered signal.

The program calculates the subcooling value of the condenser and superheat value of the evaporator using the exit pressures and temperatures of the heat exchangers. The

superheat is the exit temperature minus the evaporator saturation temperature and the subcooling is the condenser saturation temperature minus the exit temperature. These values help in determining when the air conditioner is operating at a good set point. By rule of thumb, five degrees Celsius of superheat is desired. The saturation temperatures are calculated in the sub-vi sat temps.vi, shown in Figure D-13 on page 139. It contains two formula blocks that use a polynomial for saturation temperature as a function of pressure. The polynomials were curve fit to saturation tables over the range of 685 to 1105 kPa for the condenser and 170 to 380 kPa for the evaporator.

The sub-vi file_writing.vi, depicted in Figure D-14 on page 140, writes the measurements to the user specified file name when the enable/disable button is enabled. For filtered signals, only the filtered values are written. Measurements are written once for every ten iterations, which is once per second. This is accomplished by finding the remainder of the current loop iteration number divided by ten. When the remainder is zero and the button is enabled the current measurements are written.

Motor speed and valve setting inputs are converted to a 0-10VDC value and sent to DAQ assistants to output the voltage to the controllers. The motor speed conversions are linear where 0 Hz corresponds to 0 VDC and 60 Hz to 10VDC. In the case of the valve setting no conversion is needed. The Valve and Comp assistant handles the expansion valve setting and the compressor motor while the Fans assistant controls the blower motor control signals. Each DAQ assistant is set for a generation mode of one sample on demand. Channel assignments are shown in Table D.3 on page 136.

Air Flow Rate Meters

In order to measure the flow rate of air through the heat exchangers two flow meters were constructed and calibrated. These meters are turbine meters that generate a frequency which is then converted to a voltage. The basic design is a propeller blade mounted inside of a six inch diameter tube with an infrared emitter upstream of the blade and a detector downstream. When the blade rotates it periodically breaks the path between the emitter and detector creating an on/off signal with a frequency proportional to the flow rate. A chip and surrounding circuit convert the generated frequency to a voltage.

The propeller blade is connected to a shaft that rotates on a bearing mounted on an axial fan casing. The casing is bolted to the six inch diameter PVC tube, and then silicone sealed to assure that all flow goes through the inside of the casing. A flow straightening mesh is upstream of the blade to achieve more accurate measurements. The setup is illustrated in the sketch in Figure 3-3.
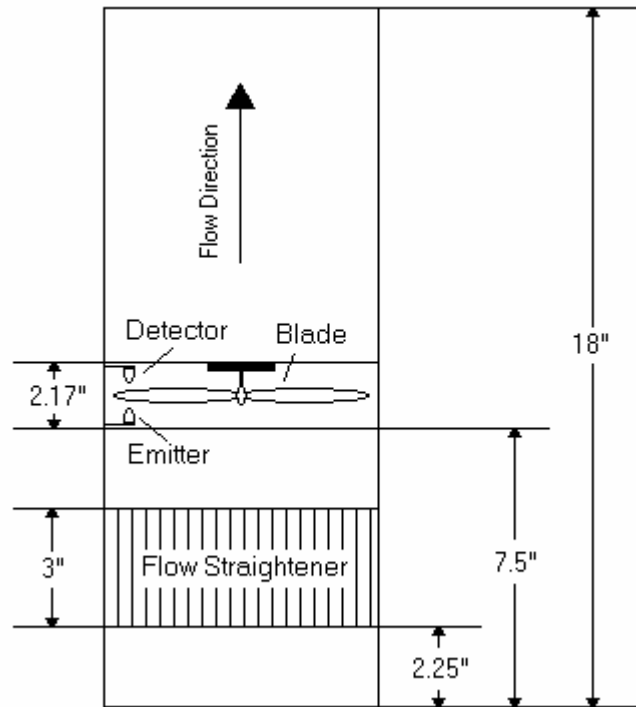
Figure 3-3 Air Flow Meter Sketch

To generate a frequency, the emitter/detector circuit is wired to output 5 VDC when the path is open and 0 VDC when the path is broken. This frequency is converted to a voltage by a frequency to voltage chip and surrounding circuit. The surrounding circuit was constructed as per the applications specification sheet for the chip. The chip used is a VFC32KP manufactured by Burr-Brown. A digital flip-flop was added to clean up the emitter/detector signal. This chip creates a discontinuous on/off signal that the frequency to voltage chip requires. The signal directly from the detector would not work. Also an op-amp was added to the output signal. Without the op-amp the output voltage would change without a change in flow rate when the variable frequency drives were turned on. There are also numerous bypass capacitors added to the supply voltages to filter out AC voltages due to the blower motor controllers' noise. It is important that the

27

shielding of the output signal wire be grounded at the screw terminal board and connected to the ground of the frequency to voltage converting circuit board. The output voltage will occasionally drop for no apparent reason without this special grounding. A wiring diagram is located in Appendix D on page 134.

Calibration of the meters was required to convert the output voltage into a flow rate. The meters were put in series with a calibrated vane anemometer. A set up of the calibration is shown in Figure 3-4, which is not to scale.
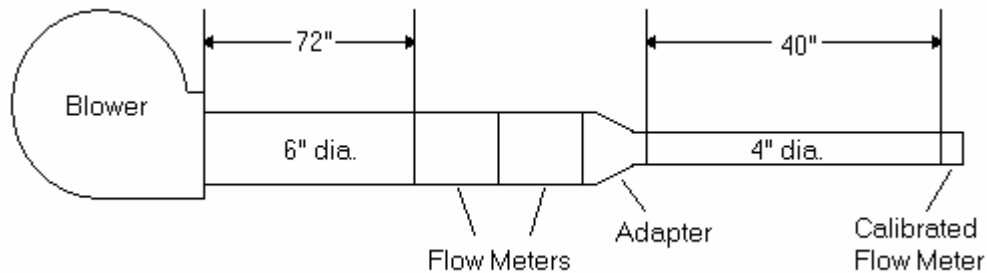
Figure 3-4 Air Flow Meter Calibration Setup

The voltage output of the meters and the measured flow rate were measured for several flow rates. Pressure measurements were taken ahead of and behind the flow meters, the pressure was never more than an inch of water different than atmospheric pressure in the room. Therefore, effects of pressure difference were ignored. To adjust the flow the inlet of the blower was covered by varying amounts. The output voltage was averaged over approximately fifteen seconds with a sample period of 100 ms for each data point. The output of the vane anemometer was read from its digital display as a magnitude of velocity. The magnitude of velocity was later converted to a volumetric flow rate for the calibration. This calibration was done over the range of 50 to 260 cubic feet per minute, the blower could not source any more flow than this. Although the meters will need to measure flow rates up to 340 cfm, the calibration was quite linear and should be okay for slightly higher flows. A plot of the calibration points and deviations are shown in Figure 3-5 on page 29. The meters are named after the heat exchanger that they will be used with. The total uncertainty was determined to be about two percent at 300 cfm. Results of the linear regression calibration and uncertainty analysis are located in Appendix D on page 146.
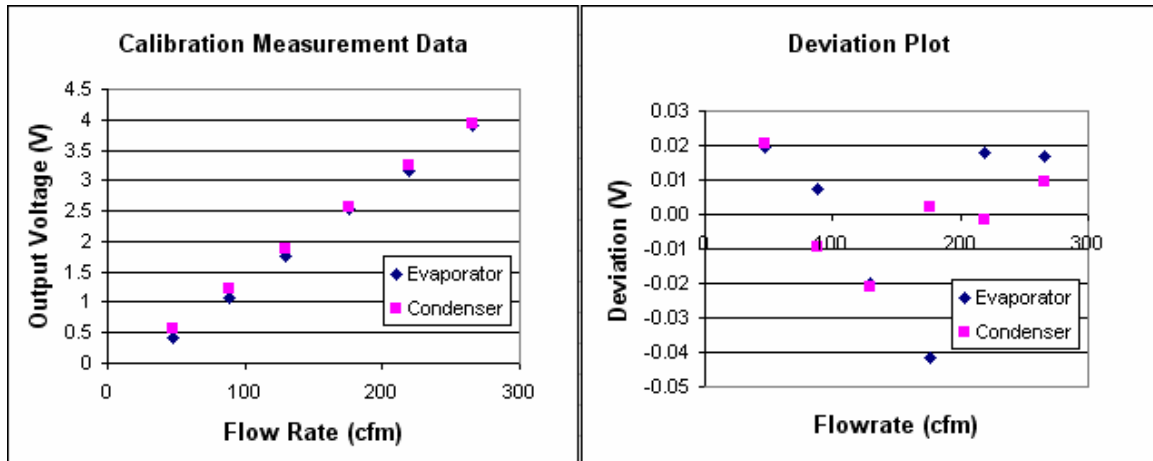
Figure 3-5 Calibration Plots

The deviations are the difference between the voltages calculated with the linear regression equation and the measured voltage. The equation for the evaporator curve fit is $V = 0.016F - 0.334$, and the condenser's is $V = 0.015F - 0.159$. The symbols V and F represent the voltage in Volts and flow rate in cubic feet per minute, respectively.

CHAPTER 4 - Determination of Modeling Parameters

Numerous parameters are needed to fill out the terms of the state space modeling equations. Throughout this thesis the term parameter will refer to quantities that appear directly in the linear modeling equations. This chapter will cover in detail determination of these parameters. The values are measured, calculated, evaluated from thermodynamic relationships, or determined experimentally. The parameters will be broken into three sections according to which set of heat exchanger matrices the numbers go into (i.e. mutual, evaporator, and condenser). Parameters in the mutual section appear in matrices for the evaporator and condenser. A complete listing of the parameters and their values is located in Appendix E starting on page147.

Mutual

Values that can be measured directly include the inside and outside diameter of the tubes and the total length of the heat exchangers. The total length was chosen to only include the finned tubes, because this is where most of the heat transfer takes place. Also, the model was derived based on the assumption of considering only these sections. The cross-sectional area inside of the tube can be determined from the inside diameter. Also, the cross-sectional area of the tube wall can be calculated based on the inside and outside diameters. The specific heat and density of tubes can be found in a table for the properties of copper.

There is no direct measurement of the refrigerant mass flow rate, since the oil affects the V-cone measurement. The mass flow rate must be backed out by an energy balance on the heat exchangers. The condenser should produce more reliable results, because there will not be a change in the humidity of the air. Equating the heat transfer of the air and refrigerant yields $\dot{m}_{air}c_{p,air}\left(T_{air,out}-T_{air,in}\right)=\dot{m}_{ref}\left(h_{c,in}-h_{c,out}\right)$.

Solving for the mass flow rate of the refrigerant, $\dot{m}_{ref}$,

$$\dot{m}_{ref} = \frac{\dot{m}_{air} c_{p,air} \left(T_{air,out} - T_{air,in} \right)}{\left(h_{c,in} - h_{c,out} \right)}.$$ (4.1)

The enthalpies will be discussed in the condenser section of this chapter. Inlet and exit air temperatures are measured values and represented symbolically as $T_{air,in}$ and $T_{air,out}$, respectively. The specific heat, $c_{p,air}$, can be found in a table. The average of inlet and exit temperatures was used for the specific heat value. Volumetric flow rate of air is measured and the mass flow rate, symbolically $\dot{m}_{air}$, is simply the density multiplied by the volumetric flow rate. The density of air at the average temperature was obtained from tables just as with the specific heat.

The coefficients of the linear expansion valve and compressor modeling equations, (2.25), (2.26), and (2.27), were determined experimentally. The testing procedure went as follows:

1. Start up the air conditioner and let it reach a steady state operating point.
2. Record data for about twenty minutes at the steady state.
3. Continue recording data and apply a step change to a single input, the valve opening or compressor speed.
4. Record data until the system reaches a new steady state.
5. Determine the change in mass flow rate, evaporator pressure, condenser pressure, condenser inlet enthalpy, and evaporator exit enthalpy.
6. This is done a sufficient number of times to perform a least squares fit, which is described in a later paragraph.

From the initial start up, the air conditioner was given forty minutes to reach its steady state. It is worth noting that steady state does not mean that all of the properties of the system are constant. Steady state will be characterized by the properties having a fairly constant average value over time. The properties will always oscillate. This is due to the nature of condensing and evaporating two-phase flow. The new steady state is defined as the point where the system states level out for the first time. Generally, the system will respond very deliberately to an input. Properties will follow a smooth path to their new values, often times including overshoot and damping. Then things will level

off for awhile. The usual time frame for leveling off is five to ten minutes. As time goes on the states will start roaming and oscillating. This roaming cannot be predicted by the model and therefore will not be considered. The plots in Figure 4-1 illustrate this phenomenon. They show the exact same response measurements over two different time frames.
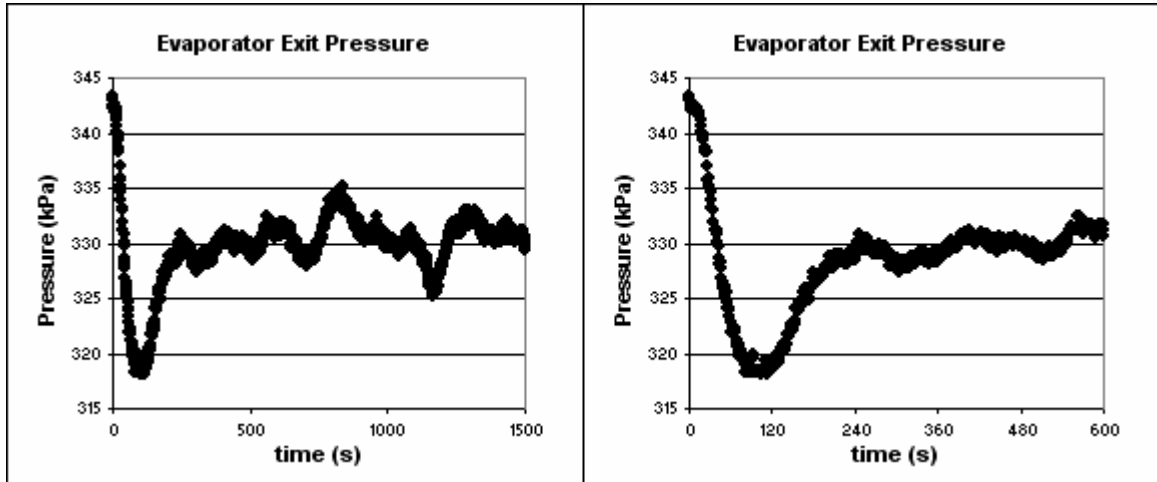
Figure 4-1 Long Term and Short Term Transient Responses

The changes were evaluated between the average values during the twenty minute steady state point and the average values during the initial stable point after the change in input. The second average period was between five minutes and ten minutes after the step change. At this point a least squares method can be used to determine the coefficients for equations (2.25), (2.26), and (2.27). A least squares fit was done for each equation separately using test results from both expansion valve and compressor initiated transients. All of the tests were done to increase the superheat. Initial testing that decreased the superheat often led to losing all superheat, which is bad for the compressor. Input step changes must be large enough to have measurable effects, but not so large that the system cannot be approximated as linear.

Several tests were done, but some of them were not used in the least squares fit. Occasionally tests results were not good because of changes in the room temperature, which has an influence on the refrigerant pressures due to the fact that pressure is a function of temperature in the two-phase regions. For instance, the condenser pressure can rise by twenty seven kPa for a one degree Celsius temperature increase. Similarly, in the evaporator the pressure rises by twelve kPa per degree Celsius. These changes are of

32

significance considering tests changed the pressure by at most fifty kPa in the condenser and twenty kPa in the evaporator. If a test's data did not fit well into the least squares solution, it would be discarded and the least squares repeated. Another factor was whether the solution for the coefficients produced a reasonable response in the computer simulation. The least squares fit was done with different sets of test data to produce the most accurate simulation. Results from the least squares analysis are located in Appendix E on page 152.

The steady state control settings for all of the tests presented in this thesis are given in Table 4.1.

Table 4.1 Steady State Control Settings

Control Settings	
Compressor	31 Hz
Expansion Valve	1.7 V
Evaporator Blower	52 Hz
Condenser Blower	50 Hz

Evaporator

The parameters that are directly measured are the ambient temperature of air at the inlet of the evaporator, the inlet and exit pressures of the refrigerant, and the exit temperature of the refrigerant. While the refrigerant pressure and temperature do not directly go into any of the matrix terms they are required to evaluate other parameters. An average of inlet and exit pressure will be used for the model.

Thermodynamic tables are used to find a number of the required parameters. Table 4.2 on page 34 lists these parameters as well as what values are required to determine them. Asterisks denote parameters that do not directly appear in the model. The density of saturated vapor, specific heat of node two, viscosity of node two, and thermal conductivity of node two are represented symbolically as ρ_{ev}, $c_{p,e2}$, μ_{e2}, k_{e2} respectively. The enthalpy of node two, h_{e2}, is the average of the outlet enthalpy and saturated vapor enthalpy.

Table 4.2 Evaporator Thermodynamic Tabulated Parameters

Thermodynamic Relation Parameters		
ρ_{eL} (P_e)	h_{ev} (P_e)	*μ_{e2} (P_e, h_{e2})
*ρ_{ev} (P_e)	T_{er1} (P_e)	*$c_{p,e2}$ (P_e, h_{e2})
*h_{eL} (P_e)	ρ_{e2} (P_e, h_{e2})	*k_{e2} (P_e, h_{e2})
h_{efg} (P_e)	T_{er2} (P_e, h_{e2})	$h_{e,out}$ (P_e, $T_{e,out}$)

The length of the saturation node is estimated from a heat transfer balance and can be calculated as

$$L_{e1} = \frac{\dot{m}(h_{ev} - h_{e,in})}{\overline{\alpha}_{ei1} D_i \pi (\overline{T}_{ew1} - \overline{T}_{er1})}. \tag{4.2}$$

The length of the superheat region, $L_{e2,}$ is found by

$$L_{e2} = \frac{\dot{m}(h_{e,out} - h_{ev})}{\overline{\alpha}_{ei2} D_i \pi (\overline{T}_{ew2} - \overline{T}_{er2})}, \tag{4.3}$$

and should be equal to the total length of the evaporator minus the length of node one.

The mean void fraction is determined using Zivi's model from

$$\overline{\gamma}_e = \frac{1}{1-C} + \frac{C \ln[C + (1-C)x_{e,in}]}{(1-C)^2 (1 - x_{e,in})}, \tag{4.4}$$

where $C = \left(\dfrac{\rho_{ev}}{\rho_{eL}}\right)^{\frac{2}{3}}$ and the inlet quality is $x_{e,in} = \dfrac{h_{e,in} - h_{eL}}{h_{ev} - h_{eL}}$. The form of equation

(4.4) was obtained from Wedekind (1978).

The inlet enthalpy is equal to the condenser exit enthalpy, which will be discussed in the condenser section of this chapter. An average density of node one will be defined as $\rho_{e1} = \rho_{eL}(1 - \overline{\gamma}_e) + \rho_{ev}\overline{\gamma}_e$, which is equation (2.11).

The average heat transfer coefficients on the inside of the tubes in the two-phase region and superheat region are determined by correlations. In the two-phase region, the models proposed by Shah (1982), Kandlikar (1897), Chaddock and Brunemann (1967), Gungor and Winterton (1986), Jung and Radermacher (1989), and Kattan et al. (1998) were used to determine average heat transfer coefficients. These calculations were achieved using software developed in a dissertation prepared by Kelly (2000). Table 4.3 on page 35 lists the results of the heat transfer coefficient analysis. The Kattan value was used for this thesis, it was near the average of the all models.

Table 4.3 Evaporating Average Heat Transfer Coefficients

Model	Average Heat Transfer Coefficient $\left(\dfrac{W}{m^2 K}\right)$
Shah	2206.6
Kandlikar	2483.2
Chaddock-Brunemann	2812.0
Kattan	2761.7
Gungor-Winterton	2901.1
Jung-Radermacher	2873.5

In the superheat region, the Dittus-Boelter equation for heating presented in Incropera (2002) is used. It is given by

$$\bar{\alpha}_{ei2} = 0.023 \left(\frac{k_{e2}}{D_i}\right) \text{Re}^{0.8} \, \text{Pr}^{0.4}, \tag{4.5}$$

where $\text{Re} = \dfrac{\dot{m} D_i}{A \mu_{e2}}$ and $\text{Pr} = \dfrac{\mu_{e2} c_{p,e2}}{k_{e2}}$.

An estimate of the average effective heat transfer coefficient between the outside of the tube wall and the air is found from

$$\bar{\alpha}_{eo} = \frac{\dot{m}(h_{ev} - h_{e,in})}{\pi D_i L_{e1} (T_{ea} - T_{ew1})}. \tag{4.6}$$

This equation is derived from rearranging an equation which equates the heat transfer from the air to the tube and the energy gained by the refrigerant in node one.

Measurements of the wall temperatures are taken, but they are not accurate as mentioned in Chapter 3. To find numbers for the wall temperatures an optimizing technique was used with the MS Excel Solver tool. This involved iteratively changing the wall temperatures, calculating the new node lengths, and determining the outside heat transfer coefficient in an effort to minimize the difference between the energy gained by the refrigerant and the convective heat transfer from the air to the tube wall in the superheat node. The energy balance in the two-phase node is automatically satisfied by equation (4.6). The length of node one was calculated as per equation (4.2), the length of node two was calculated with equation (4.3), and the outside heat transfer coefficient with equation (4.6).

The energy gained by the refrigerant was evaluated as the mass flow rate multiplied by the change in enthalpy across the node. The heat transfer from the air to the tube wall for node j is defined by

$$\dot{Q}_{j,air} = \overline{\alpha}_{eo} \pi D_i L_{ej} (T_{ea} - T_{ewj}).$$

This optimization was done using the solver tool in MS Excel. A constraint must be added so the solution makes physical sense; the sum of the length of the nodes must be equal to the total length of the evaporator. The spreadsheet used to accomplish this is given on page 150 in Table E.4.

Quite a few derivatives of properties go into the model. The majority of the slopes can be evaluated by curve fitting a line to a region of the property's function. The slopes were evaluated between pressures of 300 and 370 kPa and enthalpies of 401 and 406 kJ/kg. Saturation properties are strictly functions of pressure. The average density of node one, ρ_{e1}, will be a function of pressure because it is defined in terms of saturated densities. The mean void fraction is also a function of saturated densities and inlet quality as defined by equation (4.3). Quality was evaluated at each pressure using the saturation enthalpies and a constant value for the inlet enthalpy. The properties of the superheat region can be defined as functions of pressure and enthalpy. These properties were plotted holding either pressure or enthalpy constant to find the slope. The derivative of temperature with respect to enthalpy can be determined as the inverse of the specific heat, which is a function of the enthalpy and pressure. Table 4.4 lists the required derivatives. Asterisks denote parameters that do not directly appear in the model, but are required to find other values.

Table 4.4 Evaporator Model Derivatives

Derivatives	
$d(\rho_{e1})/dP_e$	$*dh_{efg}/dP_e$
$d(\rho_{eL}*h_{efg})/dP_e$	$(\partial T_{er2}/\partial P_e)_{he2}$
dh_{ev}/dP_e	$(\partial \rho_{e2}/\partial h_{e,out})_P$
dT_{er1}/dP_e	$(\partial \rho_{e2}/\partial P_e)_{he2}$
$*d\rho_{eL}/dP_e$	$dT_{er2}/dh_{e,out} = 1/c_{p,e2}$

The product rule was used to determine

$$\frac{d\left(\rho_{eL}h_{efg}\right)}{dP_e} = \rho_{eL}\frac{dh_{efg}}{dP_e} + h_{efg}\frac{d\rho_{eL}}{dP_e} \, .$$

Since the evaporator and condenser have the same geometry, the derivative of outside heat transfer coefficient with respect to volumetric air flow rate will be the same. The derivative of interest in the evaporator modeling equations is given by

$$\frac{\partial \overline{\alpha}_{eo}}{\partial v_e} = \frac{\partial \overline{\alpha}_{eo}}{\partial \dot{V}}\frac{\partial \dot{V}}{\partial v_e} \, ,$$

where $\dot{V}$ is the volumetric flow rate of air. It is assumed that the volumetric flow rate of air is the most important variable affecting the outside heat transfer coefficient and all other variables can be neglected.

The change in flow rate with respect to blower setting will be different for the evaporator and condenser due to the differences in ducting. It can be determined by changing the blower speed and recording the change in flow rate, and then dividing the change in flow rate by the change in blower speed setting. In order to determine how the outside heat transfer coefficient changes with flow rate, the coefficient must be calculated before and after a change in flow rate. Calculating the outside heat transfer coefficient was discussed earlier in this section and requires knowing many other parameters including the mass flow rate of refrigerant. The derivative is approximated in a manner similar to the change in flow rate with respect to blower setting.

Condenser

Direct measurements yield values for the refrigerant pressures, inlet temperature, and exit temperature. These values do not directly appear in the model, but are required for other calculations. An average of inlet and exit pressure will be used for the model. The ambient temperature of air entering the condenser is also measured.

Similar to the evaporator analysis many properties need to be found in thermodynamic relation tables. Table 4.5 on page 38 lists these parameters as well as the properties that determine them. The viscosity, specific heat, and thermal conductivity values are required for both of the single phase regions of the condenser. The table lists these values for the jth node as μ_{cj}, $c_{p,cj}$, and k_{cj}, respectively.

Table 4.5 Condenser Thermodynamic Tabulated Parameters

Thermodynamic Relation Parameters		
$\rho_{c1}(P_c, h_{c1})$	$h_{cv}\ (P_c)$	*$\mu_{cj}\ (P_c,\ h_{c,j})$
$\rho_{cL}\ (P_c)$	$h_{cL}\ (P_c)$	*$c_{p,cj}\ (P_c,\ h_{c,j})$
*$\rho_{cv}\ (P_c)$	$h_{cfg}\ (P_c)$	*$k_{cj}\ (P_c,\ h_{c,j})$
$h_{c,in}\ (P_c,\ T_{c,in})$	$T_{cr1}\ (P_c,\ h_{c1})$	
$h_{c,out}\ (P_c,\ T_{c,out})$	$T_{cr2}\ (P_c)$	

The length of the nodes is calculated similarly to the evaporator. The length of the superheat region is given as

$$L_{c1} = \frac{\dot{m}(h_{c,in} - h_{cv})}{\overline{\alpha}_{ci1} D_i \pi (\overline{T}_{cr1} - \overline{T}_{cw1})}.$$
(4.7)

The length of the two-phase region is

$$L_{c2} = \frac{\dot{m}(h_{cv} - h_{cL})}{\overline{\alpha}_{ci2} D_i \pi (\overline{T}_{cr2} - \overline{T}_{cw2})}.$$
(4.8)

The subcool region then has a length consisting of the rest of the condenser, but for the wall temperature optimization should be calculated as

$$L_{c3} = \frac{\dot{m}(h_{cL} - h_{c,out})}{\overline{\alpha}_{ci3} D_i \pi (\overline{T}_{cr3} - \overline{T}_{cw3})}.$$
(4.9)

As with the evaporator, the Zivi model is used to determine the mean void fraction from

$$\overline{\gamma}_c = \frac{1}{1-C} + \frac{C\ln(C)}{(1-C)^2},$$
(4.10)

where $C = \left(\dfrac{\rho_{ev}}{\rho_{eL}}\right)^{\frac{2}{3}}$. The form of equation (4.10) was obtained from Wedekind (1978).

With the mean void fraction the average density in the two-phase region will be defined as $\rho_{c2} = \rho_{cL}(1 - \overline{\gamma}_c) + \rho_{cv}\overline{\gamma}_c$, which is equation (2.22).

The enthalpy of node one, h_{c1}, is the average of the condenser inlet enthalpy and the saturated vapor enthalpy. Similarly, the enthalpy of node three is the average of the enthalpy at the start and end of the region.

An average temperature of the subcool region is given by

$$\overline{T}_{cr3} = \overline{T}_{cr2} + \frac{h_{c3} - h_{cL}}{c_{p,c3}} = \overline{T}_{cr2} + \frac{h_{c,out} - h_{cL}}{2c_{p,c3}} \; . \tag{4.11}$$

The Dittus-Boelter correlation equation for cooling from Incropera (2002) is used to determine the average heat transfer coefficients in the single phase regions.

These values are determined by

$$\overline{\alpha}_{ci1} = 0.023\left(\frac{k_{c1}}{D_i}\right)\mathrm{Re}_{c1}^{0.8}\,\mathrm{Pr}_{c1}^{0.3}\,, \tag{4.12}$$

$$\overline{\alpha}_{ci3} = 0.023\left(\frac{k_{c3}}{D_i}\right)\mathrm{Re}_{c3}^{0.8}\,\mathrm{Pr}_{c3}^{0.3}\,, \tag{4.13}$$

where $\mathrm{Re}_{cj} = \dfrac{\dot{m}D_i}{A\mu_{cj}}$ and $\mathrm{Pr}_{cj} = \dfrac{\mu_{cj}c_{p,cj}}{k_{cj}}$.

The software developed by Kelly (2000) was again used to determine the average heat transfer coefficient in the two-phase region. The models presented in Shah (1979), Traviss et al. (1972), and Cavallini and Zecchin (1974) are shown in Table 4.6. The value from the Traviss model was used for the simulation; this is the correlation that was used in He (1996).

Table 4.6 Condensing Average Heat Transfer Coefficients

Model	Average Heat Transfer Coefficient $\left(\dfrac{W}{m^2 K}\right)$
Shah	1635.1
Traviss	1795.5
Cavallini	1870.5

Similar to the evaporator parameter, the outside heat transfer coefficient is evaluated from the two-phase region wall to air heat balance as

$$\overline{\alpha}_{co} = \frac{\dot{m}(h_{cv} - h_{cL})}{\pi D_i L_{c2}(\overline{T}_{cw2} - T_{ca})} \; . \tag{4.14}$$

An optimization technique similar to the one described in the evaporator section was used to determine the wall temperatures, but this time two nodes must be considered, the superheat and subcool.

Many derivatives are required for the condenser matrices. Table 4.7 lists the required derivatives.

Table 4.7 Condenser Model Derivatives

Derivatives	
$d(h_{cv})/dP_c$	$(\partial(\rho_{c1})/\partial P_c)_{hc1}$
$d(h_{cL})/dP_c$	$(\partial(\rho_{c1})/\partial h_{c1})_P$
$d(\rho_{cL})/dP_c$	$(\partial(T_{cr1})/\partial P_c)_{hc1}$
$d(\rho_{c2})/dP_c$	$(\partial(T_{cr1})/\partial h_{c1})_P = 1/c_{p,c1}$
$d(\rho_{cL}*h_{cfg})/dP_c$	$(\partial(T_{cr3})/\partial P_c)_{hc,out}$
$*d(h_{cfg})/dP_c$	$(\partial(T_{cr3})/\partial h_{c,out})_P$
$d(T_{cr2})/dP_c$	

All but one of the derivatives were estimated by the slope of a line curve fit to a section of the data. Ranges of 950-1140 kPa and 420-425 kJ/kg were used for pressure and enthalpy plots, respectively. The saturated related variables can be plotted as a function of pressure. For the single phase region slopes, the enthalpy was held constant for derivatives with respect to pressure and vice versa for derivatives with respect to enthalpy. The derivative of the average two-phase region density with respect to pressure is evaluated similar to the evaporator. In order to plot the average temperature in the subcool region, equation (4.11) was used at each pressure value holding the value of the outlet enthalpy constant. A plot was not generated for T_{cr3} as a function of the outlet enthalpy, instead the slope was estimated as

$$\left(\frac{\partial T_{cr3}}{\partial h_{c,out}}\right)_{Pc} = \frac{T_{cr3}(P_c,h_{c,out}+\delta h)-T_{cr3}(P_c,h_{c,out}-\delta h)}{2\delta h} \text{ , where } \delta h \text{ is a small}$$

perturbation.

The derivative of the product of saturated liquid density and enthalpy of vaporization is found similarly to the evaporator counterpart.

A value for the change in outside heat transfer coefficient with respect to change in blower setting can be determined in the same way as with the evaporator. Since the derivative of the coefficient with respect to flow rate should be the same, the value from the evaporator can be used. The slope of air flow rate with respect to blower setting will be slightly different due to the variation in ducting of the heat exchangers.

CHAPTER 5 - Simulation Results and Comparison to Measured Data

This section will present plots of measured data and the simulated responses. In and effort to improve the model, some of the more uncertain terms will be varied to determine their effects. The values determined in Chapter 4 are substituted into the matrix elements from Chapter 2. A Matlab m-file constructs the required matrices. This results in the linear state equations used for simulation. The output equation is of the form

$$\delta y = C\,\delta x + D\,\delta u,$$

where

$$\delta y = \begin{bmatrix} \delta P_e & \delta P_c & \delta sh \end{bmatrix},$$

and

$$C = \begin{bmatrix} 0 & 1 & 0 & 0 & 0 & 0 & 0 & 0 & 0 & 0 & 0 & 0 \\ 0 & 0 & 0 & 0 & 0 & 0 & 0 & 1 & 0 & 0 & 0 & 0 \\ 0 & \dfrac{dT_{er1}}{dP_e} & \left(\dfrac{\partial T_{er2}}{\partial h_{e,out}}\right)_{Pe} & 0 & 0 & 0 & 0 & 0 & 0 & 0 & 0 & 0 \end{bmatrix}.$$

The D matrix is a zero matrix. The outputs are the changes in evaporator pressure, condenser pressure, and superheat. These are quantities that can be measured and are of interest.

The simulation is done with a Matlab Simulink model using a state space block and four step input blocks as seen in Figure 5-1.
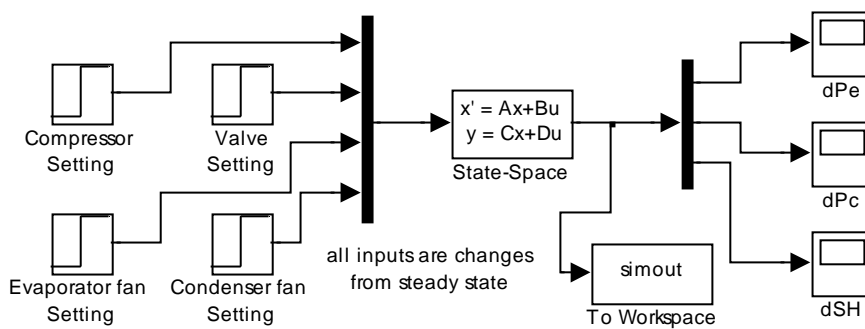
Figure 5-1 Simulink Block Diagram

Changes in the outputs are added to the initial absolute measured values to generate the plots in this section. In all cases the change in input occurs at time equal zero. The graphs show the exit pressure changes of the heat exchangers. Test measurements demonstrated that the general shape of the inlet and exit pressures were the same. The Figures 5-2 to 5-4 illustrate transient responses for step changes in valve opening with all other control inputs held constant. The sizes of the changes are indicated in the figure captions.
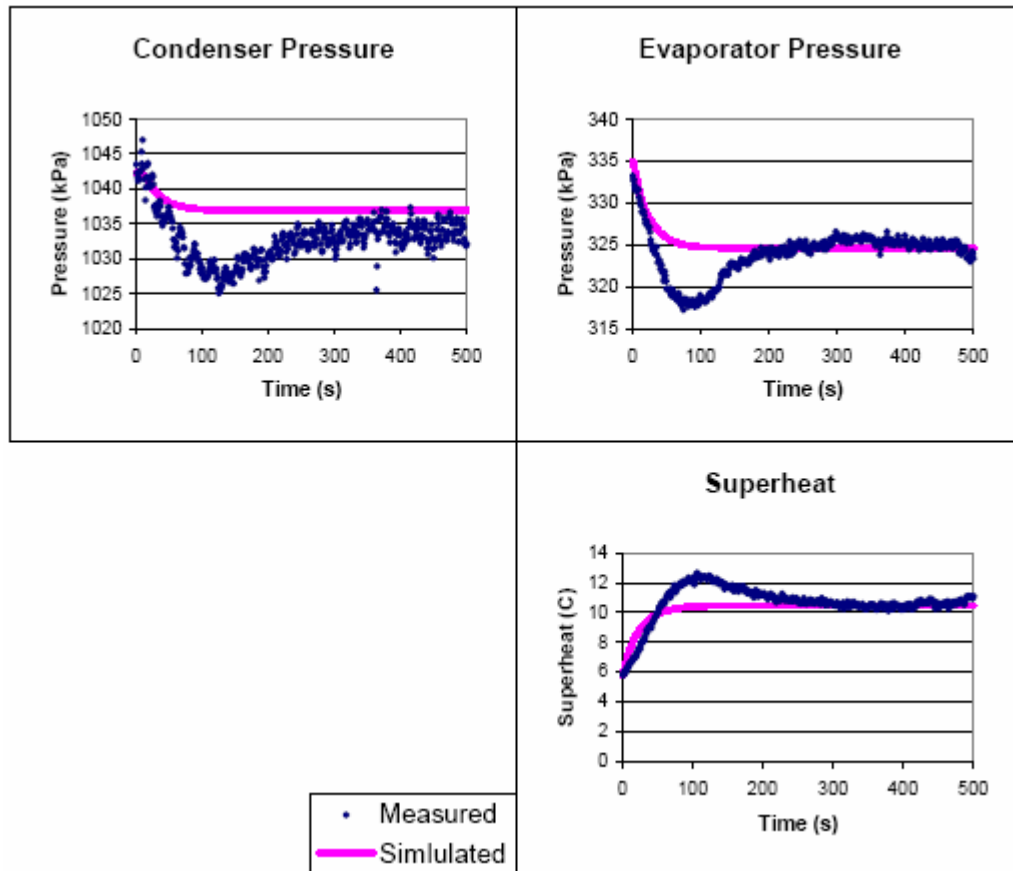
Figure 5-2 Response for Valve Setting Decreased by 0.2V
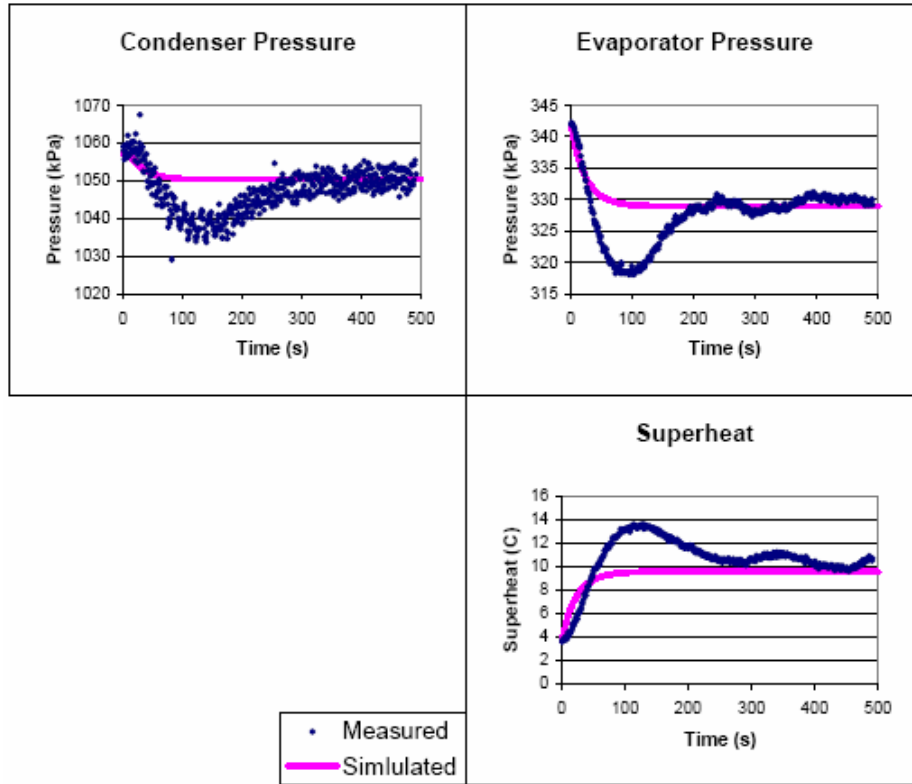
Figure 5-3 Response for Valve Setting Decreased by 0.25V
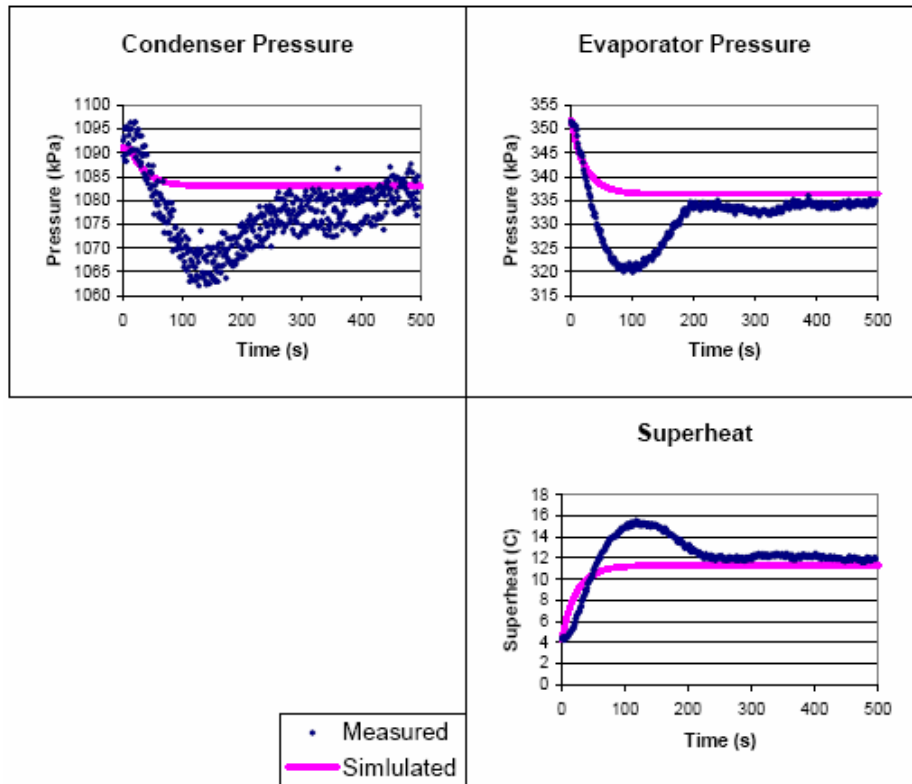
Figure 5-4 Response for Valve Setting Decreased by 0.3V

The model predicts the change in steady state values of these three quantities quite well. Time constants for the actual and simulated systems are not exactly consistent. In each case the initial upward slope is generally the same when comparing measurements and simulations. Although, the simulation tends to be a little faster. Measurements of the superheat have a time delay that the model lacks. The model obviously does not exhibit the overshoot present in the air conditioner. Measurements for each test appear to exhibit linear system responses.

The Figures 5-5 to 5-7 present results for compressor speed initiated transients with all other control inputs held constant. The size of the change is given in the caption.
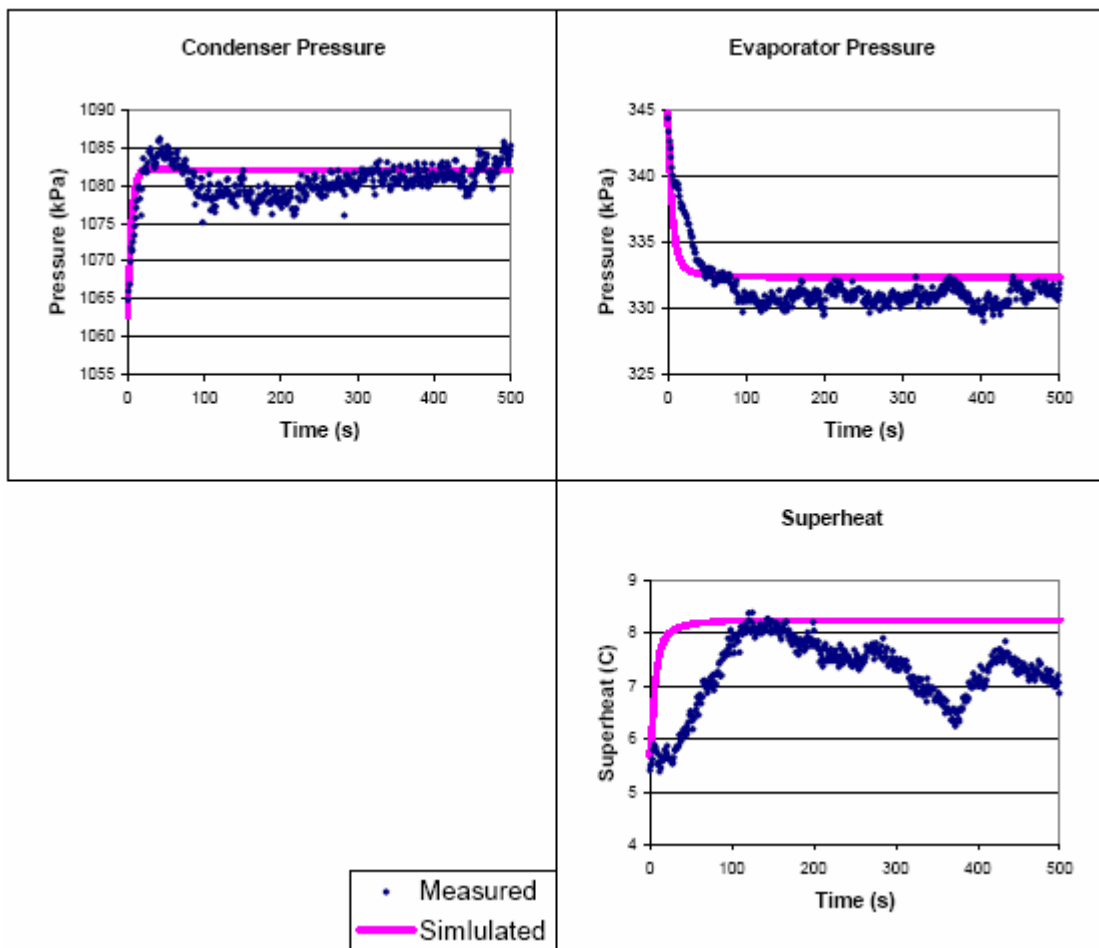
Figure 5-5 Response for Compressor Setting Increased by 2 Hz

44
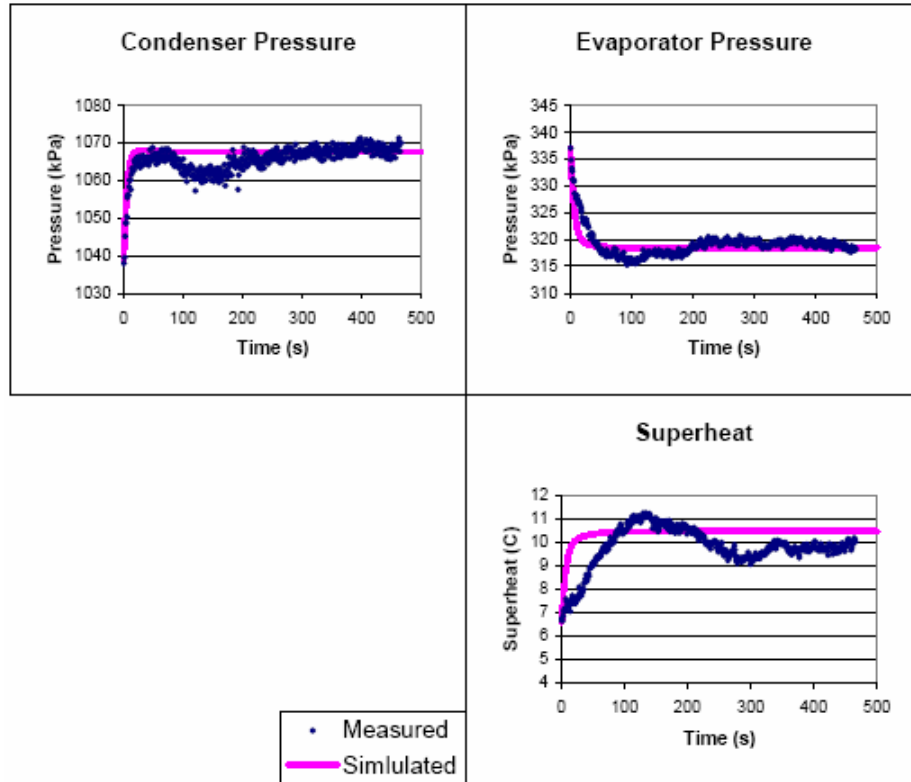
Figure 5-6 Response for Compressor Setting Increased by 3 Hz
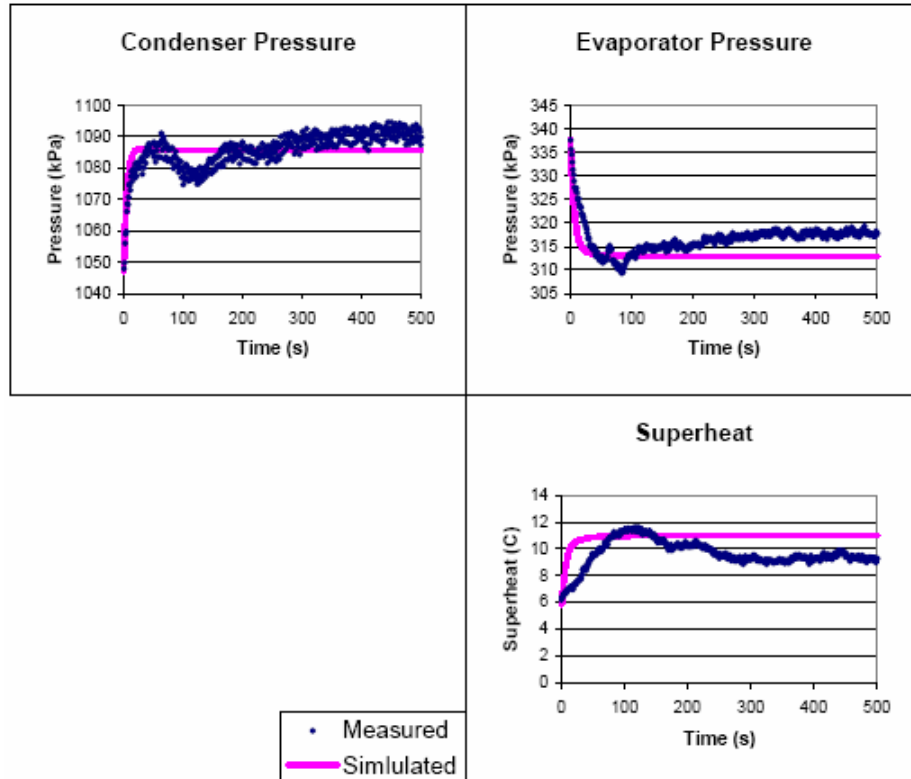
Figure 5-7 Response for Compressor Setting Increased by 4 Hz

45

The comparison for the compressor tests is similar to that of the expansion valve tests where the simulation is often too fast and misses transient shapes for overshoot and damping, but the final value is fairly reliable. The model shows a very fast response for the superheat which is not present in any of the actual tests. Again the measurement responses are representative of a linear system, comparing test to test.

Figures 5-8 and 5-9 contain the responses created by changes in blower speed setting with all other control inputs held constant.
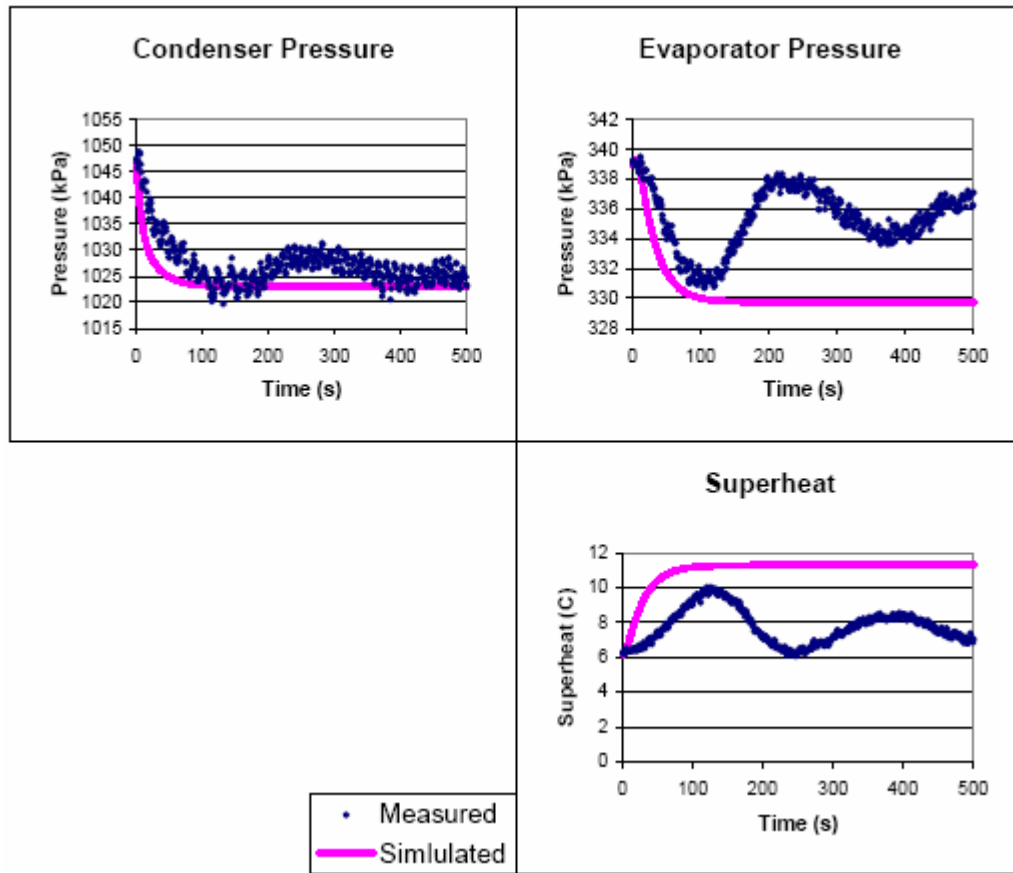
Figure 5-8 Response for Condenser Blower setting increased by 5 Hz

The condenser pressure simulation is the only one that is decently accurate. It is a little fast, but predicts the final value nicely. Simulated values follow the evaporator pressure to the peak value, but do not oscillate back to the correct final value. The superheat response is in the correct direction, not much else is good. Measurements of the evaporator pressure and superheat almost seem to go back to their original values, which is curious.

46
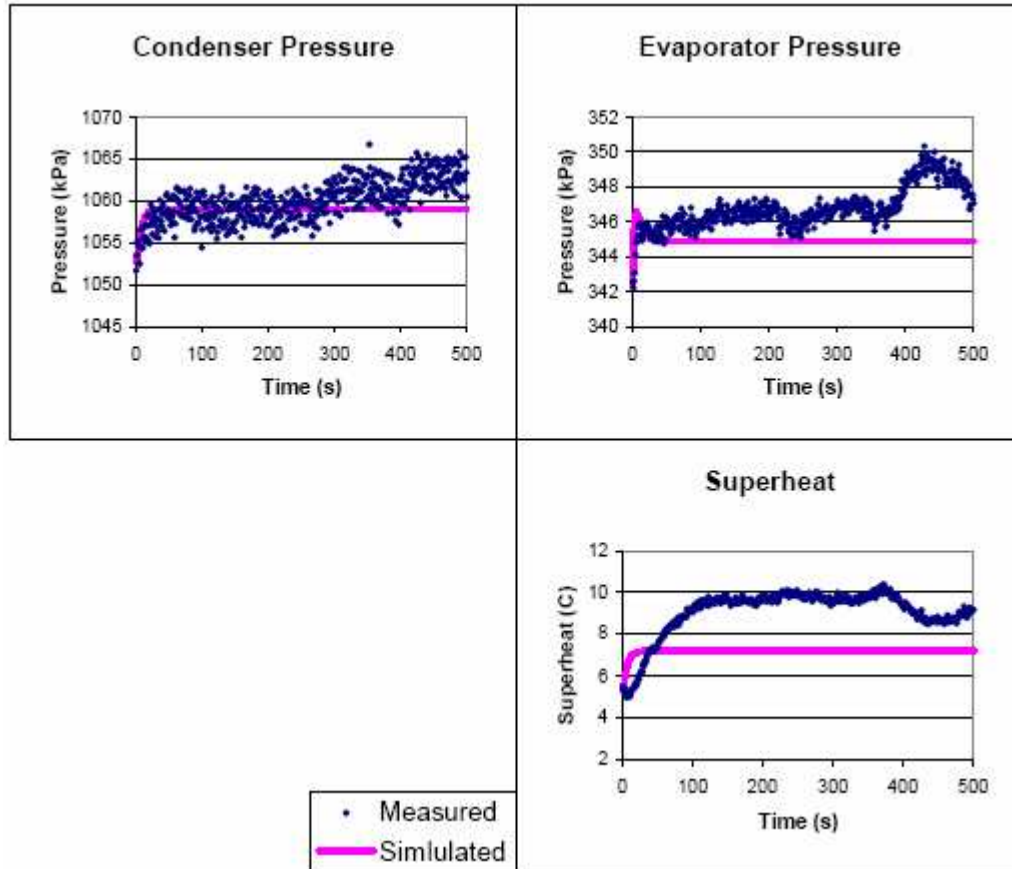
Figure 5-9 Response for Evaporator Blower setting increased by 8 Hz

As with the condenser blower test, the condenser pressure response is the best. The evaporator pressure is better, and the superheat is again only in the correct direction. Clearly the model has trouble with these blower initiated transients and investigation in this area is desired. Further testing of blower speed changes could not be accomplished due to equipment failure.

Modified Parameter Results

In the Determination of Modeling Parameters Chapter there were several values that had some uncertainty. In this section, the values of certain modeling parameters will be numerically altered from their calculated values, and the rest will remain constant. This creates a slightly different model to simulate and compare to the original model. Values will be made smaller and larger to determine if they can make the model response more like the measured data, or at least determine their effects. The main parameters that could be questioned include the mass flow rate of refrigerant, heat transfer coefficients,

47

tube wall temperatures, lengths of nodes, appropriate ambient temperatures, mean void fractions and the coefficients for the expansion valve and compressor equations. The term parameter is used here to indicate quantities that appear directly in the modeling equations.

The mass flow rate is solved for indirectly from a heat transfer balance equation between the air and the refrigerant. This requires measurements of air temperature, air flow rate, refrigerant temperatures, and refrigerant pressures. Combining all of the uncertainties from these measurements could result in an inaccurate value for the mass flow rate of the refrigerant. In addition, there are heat losses for the air that cannot be accurately quantified. Some of the heat will conduct from the exchanger tubes to the mounting brackets and then to the mounting board. Energy can also be lost through the box that encases the condenser. It is reasonable to assume that the mass flow rate may need to be altered to achieve an accurate model. To determine the effects of the mass flow rate on the model, the value used in the model will be varied, and then the modeling parameters it affects will be recalculated. These parameters include heat transfer coefficients, tube wall temperatures, and lengths of nodes. Table E.5 on page 151 lists the new values. The model will be reassembled with these new values. Figure 5-10 on page 49 illustrates the model simulations for step inputs of the valve and compressor setting. The valve input transients were initiated by a -0.2V change in input with all other control inputs constant, and the compressor input transients were initiated by a +2 Hz change with all other control inputs constant. The evaporator pressure and superheat are plotted, because they are of the most interest. These figures show the simulation results for the original model and the model with the mass flow rate modeling value adjusted by plus and minus ten percent. Varying the mass flow rate mostly affects the final value of the outputs. This does not help the model to better follow the actual system's transient shape.
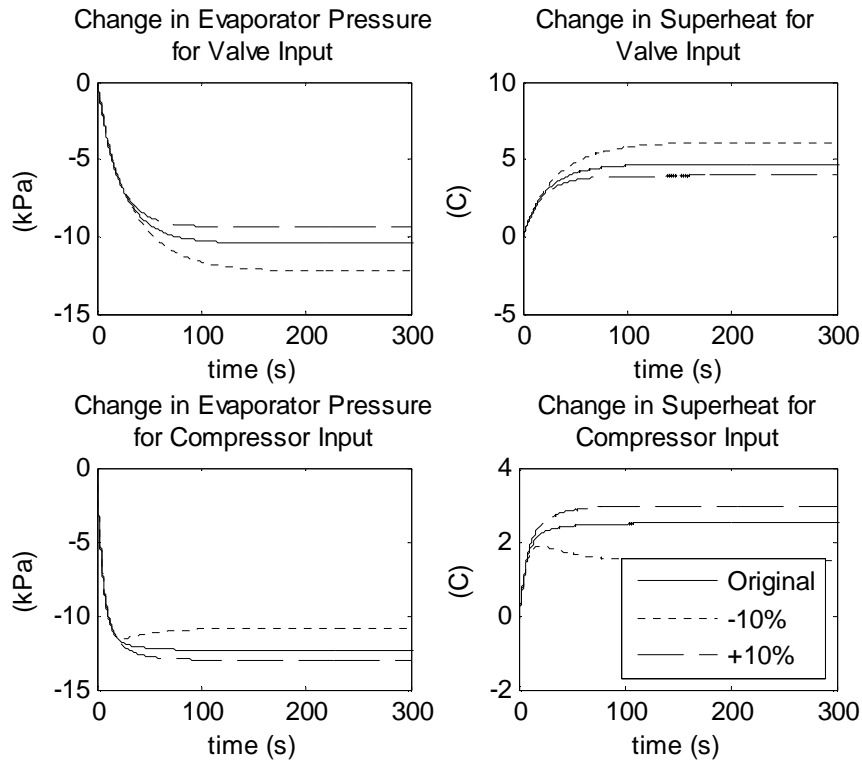
Figure 5-10 Simulated Responses with Adjusted Mass Flow Rate

The ambient temperature used in the model was that of the air just ahead of the heat exchangers. These temperatures are used for heat balance equations between the tube wall and the air. Since the air is changing temperature as it flows through the heat exchanger, the inlet temperature may not be the appropriate temperature to use. The ambient temperature could be approximated with a weighted average between the inlet and exit temperatures with the equation $T_{amb} = T_{in}(x) + T_{out}(1-x)$, where the value x represents the percentage of the inlet temperature present in the ambient temperature. Figure 5-11 on page 50 shows the changes in response for $x = 100\%$, 75%, and 50%. The same changes of inputs were used as with the modified mass flow rate plots. Both heat exchanger ambient temperatures are adjusted with the same x. The node lengths, wall temperatures, and outside heat transfer coefficients were recalculated. Table E.5 on page 151 lists the new values. These new values were used to create the modified model. As with the mass flow rate, the major effect is the final values. It also has a longer time constant for valve tests, but does not add any overshoot.

49
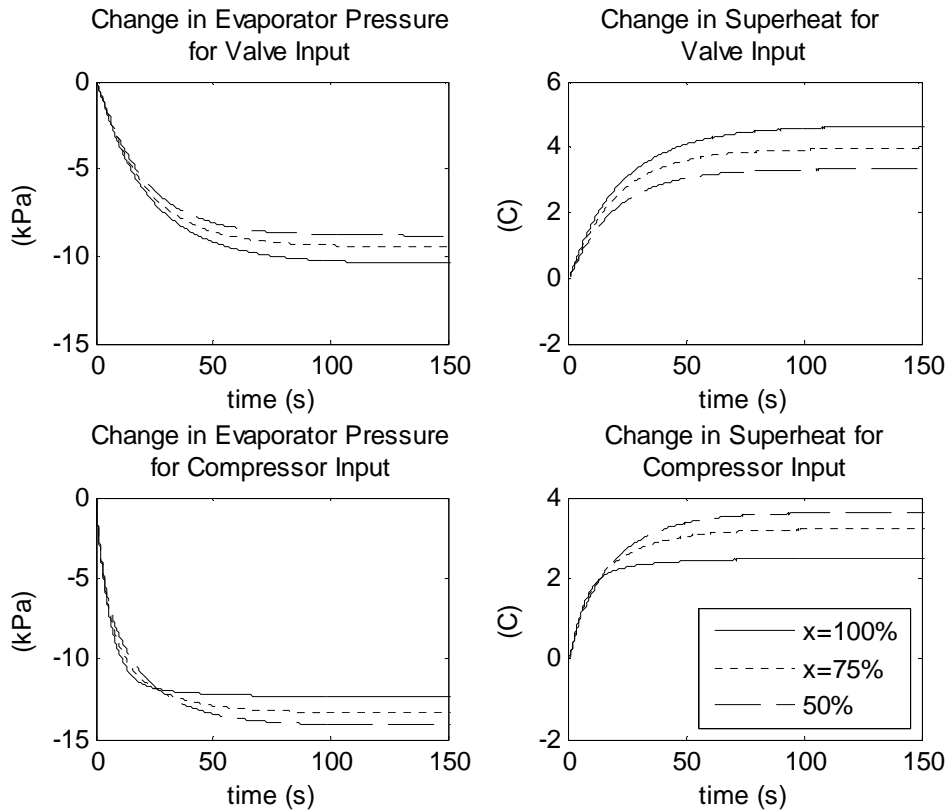
Figure 5-11 Simulated Responses with Adjusted Ambient Temperatures

The mean void fractions of the evaporator and condenser were estimated using the Zivi model. Various other models can be used to find different values for the mean void fraction. The effects of this parameter are therefore of interest. Figures 5-12 and 5-13 on pages 51 and 52 demonstrate the response for variations of the evaporator and condenser mean void fractions respectively. These plots show the responses of the original model as well as the modified models. The same changes of inputs were used as with the modified mass flow rate plots. The mean void fractions were increased and decreased by twenty percent, except for the evaporator. Only a three percent increase was reasonable here, since the mean void fraction is less than one.

The final values were invariant with changes in either mean void fraction. A three percent increase in the evaporator was too small to have any effect, and the decrease tended to make the pressure respond faster and the superheat slower. Overall, this did not make the model follow the measured data better. A higher mean void fraction in the condenser slowed the system down. Decreasing the condenser mean void fraction made the responses faster for the valve transients and added overshoot for the compressor

initiated transients. This overshoot is present in the measured data, so this adjustment
helps the model for compressor tests. Although, the system is still too fast, and the valve
response is no better.
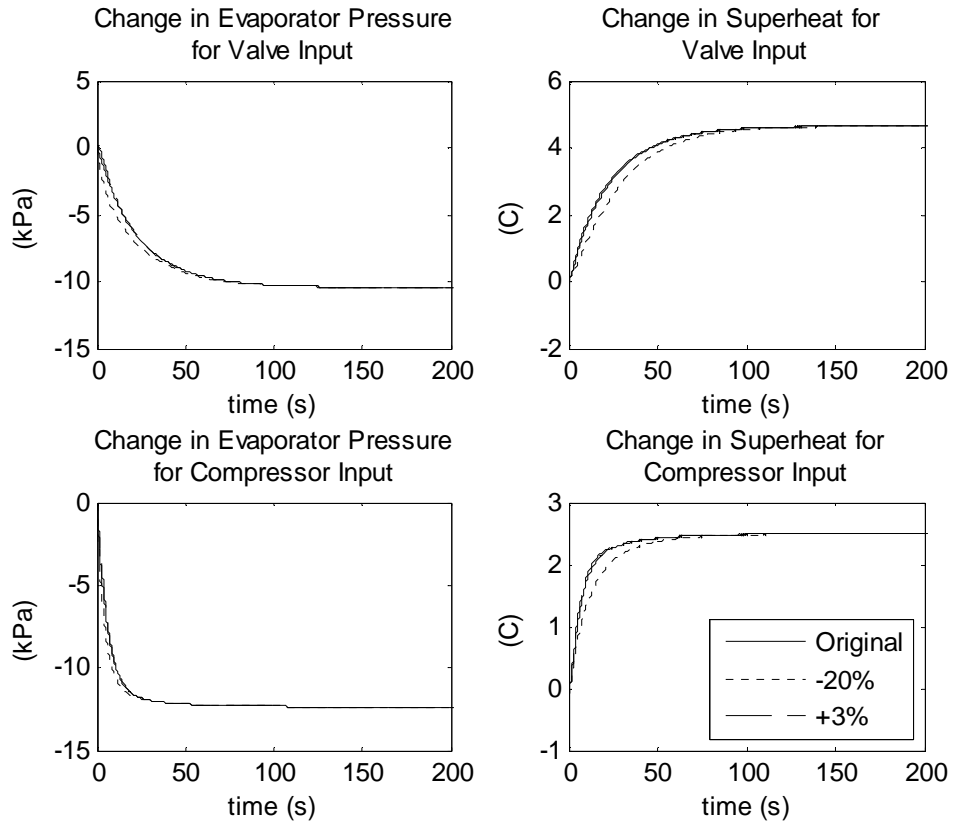
Figure 5-12 Simulate Responses with Adjusted Evaporator Mean Void Fraction
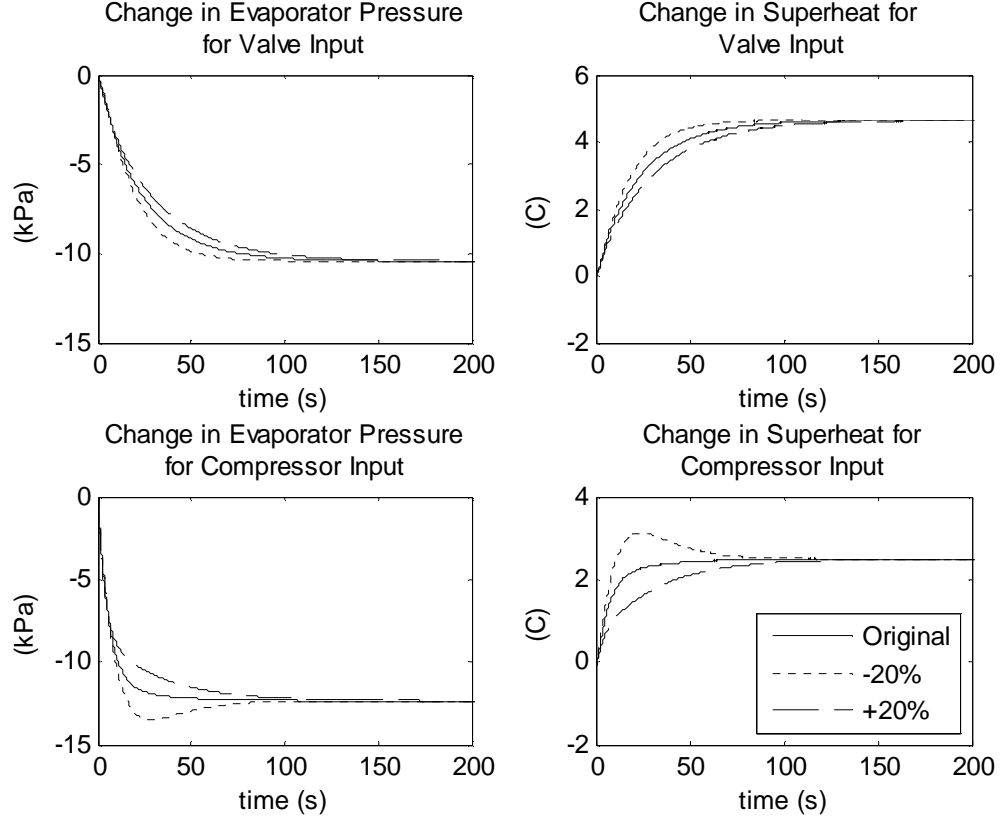
Figure 5-13 Simulated Responses with Adjusted Condenser Mean Void Fraction

The coefficients for the expansion valve and compressor modeling equations can also be questioned since they rely on measurements of mass flow rate. The mass flow rate through the valve can be expressed by the orifice equation

$$\dot{m}_{valve} = C_v A_v \sqrt{\rho_v (P_c - P_e)}, \tag{5.1}$$

where C_v is a valve coefficient, A_v is the valve opening area, and ρ_v is the density of the fluid flowing through the valve. This equation does not take into account the phase change, so it is not entirely accurate. Taking the differential of this equation assuming C_v and ρ_v are constant will result in equation (2.25), where

$$k_{11} = \frac{\partial \dot{m}_{valve}}{\partial P_e} = -C_v A_v \sqrt{\frac{\rho_v}{P_c - P_e}} = \frac{-\dot{m}_{valve}}{P_c - P_e},$$

$$k_{12} = \frac{\partial \dot{m}_{valve}}{\partial P_c} = C_v A_v \sqrt{\frac{\rho_v}{P_c - P_e}} = \frac{\dot{m}_{valve}}{P_c - P_e},$$

and
$$k_{13} = \frac{\partial \dot{m}_{valve}}{\partial u_{valve}} = C_v \sqrt{\rho_v (P_c - P_e)} = \frac{\dot{m}_{valve}}{u_{valve}}.$$

52

Rearranging equation (5.1) into a fraction equaling one and multiplying it by the intermediate derivative can be used to find the final form of these derivatives. This is assuming that the area of the valve opening can be expressed as $A_v = \dfrac{u_{valve}}{10} A_{max}$, where u_{valve} is between zero and ten Volts. The symbol A_{max} is the maximum valve opening area. Numerical values of the k_{ij} are determined by plugging in values measured during the steady state operation. In all of the partial derivatives that define the k_{ij} coefficients, all variables other than the one that the derivative is with respect to are held constant.

As presented by McQuiston (1994), the mass flow rate through the piston compressor can be written as

$$\dot{m}_{comp} = \omega V_c \rho_c \left(1 + C_c - C_c \left(\frac{P_c}{P_e} \right)^{\frac{1}{n}} \right). \tag{5.2}$$

The compressor rotation speed, volumetric displacement, clearance volume to displacement volume ratio, density, and polytropic coefficient are symbolically ω, V_c, ρ_c, C_c, and n, respectively.

Similar to the differentiation of the orifice equation, the coefficients in equation (2.27) can be shown to be:

$$k_{31} = \frac{\partial \dot{m}_{comp}}{\partial P_e} = \frac{1}{n} \omega V_c \rho_c C_c P_c (P_e)^{(1/n+1)} = \frac{P_c}{P_e^2} \left[\frac{\dot{m}_{comp} C_c \left(\frac{1}{n} \right) \left(\frac{P_c}{P_e} \right)^{\left(\frac{1}{n} - 1 \right)}}{1 + C_c - C_c \left(\frac{P_c}{P_e} \right)^{\frac{1}{n}}} \right],$$

$$k_{32} = \frac{\partial \dot{m}_{comp}}{\partial P_c} = -\frac{1}{n} \omega V_c \rho_c C_c (P_c)^{(1/n-1)} (P_e)^{(-1/n)} = \frac{-1}{P_e} \left[\frac{\dot{m}_{comp} C_c \left(\frac{1}{n} \right) \left(\frac{P_c}{P_e} \right)^{\left(\frac{1}{n} - 1 \right)}}{1 + C_c - C_c \left(\frac{P_c}{P_e} \right)^{\frac{1}{n}}} \right],$$

and
$$k_{33} = \frac{\partial \dot{m}_{comp}}{\partial u_{comp}} = V_c \rho_c \left(1 + C_c - C_c \left(\frac{P_c}{P_e} \right)^{\frac{1}{n}} \right) = \frac{\dot{m}_{comp}}{u_{comp}}.$$

This is assuming that V_c, ρ_c, C_c, and n are constants. Rearranging equation (5.2) into a fraction equaling one and multiplying it by the intermediate derivative can be used to find the final form of these derivatives. The clearance ratio is approximated as one tenth and the polytropic coefficient as the ratio of specific heat at constant pressure, c_p, over specific heat at constant volume, c_v. These specific heats are taken at the compressor inlet temperature and pressure. The rotation speed is assume to be $\omega = \omega_{max} \frac{u_{comp}}{60}$, where ω_{max} is the maximum rotation speed, and u_{comp} is between zero and sixty Hertz.

Using the definition of isentropic efficiency the enthalpy at the outlet of the compressor is $h_{comp,out} = \frac{h_{comp,out,s} - h_{comp,in}}{\eta_{comp}} + h_{comp,in}$. The subscripts *comp* and *s* denote the compressor and isentropic value respectively. The compressor isentropic efficiency is given by η_{comp}. Values for the coefficients of equation (2.26) are:

$$k_{21} = \frac{\partial h_{comp,out}}{\partial P_e} = \frac{1}{\eta_{comp}} \frac{\partial h_{comp,out,s}}{\partial P_e}, \quad k_{22} = \frac{\partial h_{comp,out}}{\partial P_c} = \frac{1}{\eta_{comp}} \frac{\partial h_{comp,out,s}}{\partial P_c},$$

and $k_{23} = \frac{1}{\eta_{comp}} \left(\frac{\partial h_{comp,out,s}}{\partial h_{comp,in}} - 1 \right) + 1$.

The isentropic efficiency can be estimated from the steady state operation measurements and thermodynamic tables and assumed to be constant. Perturbing the evaporator pressure, condenser pressure, and inlet enthalpy and determining the change in the isentropic outlet enthalpy yields an estimate of the partial derivatives. These values are found to be

$$\frac{\partial h_{comp,out,s}}{\partial P_e} = -0.13 \frac{kJ}{kg \cdot kPa}, \quad \frac{\partial h_{comp,out,s}}{\partial P_c} = 0.02 \frac{kJ}{kg \cdot kPa}, \quad \text{and} \quad \frac{\partial h_{comp,out,s}}{\partial h_{comp,in}} = 1.13.$$

Two alternate methods for determining the coefficients will be used, constrained least squares and analytical. For the constraints, the values and k_{11} and k_{12} will be constrained to be equal but opposite. The values of k_{31} and k_{32} will be forced to satisfy

the equation $\dfrac{k_{31}}{k_{32}} = -\dfrac{P_c}{P_e}$. These constraints come from the analytical solutions for the

coefficients. No constraint was added for the other values. Table 5.1 summarizes the

different sets of coefficients. The constrained and analytical values for k_{11} make more

intuitive sense. They are negative, which would indicate that as the evaporator pressure

increases the flow through the valve would decrease. Also, the constrained and analytical

values of k_{32} are negative. This indicates that an increased condenser pressure would

decrease flow through the compressor, which makes physical sense. The constrained and

analytical solutions are fairly similar for the mass flow rate equations. Most values are

near the same order of magnitude, excluding sign differences, for each of the solutions.

The value of k_{23} is very different for the least squares fit and analytical solutions, and

may require additional consideration.

Table 5.1 Sets of Valve and Compressor Coefficients

Expansion Valve and Compressor Coefficients			
	Original	Constrained	Analytical
k11	8.56E-06	-8.56E-06	-1.31E-05
k12	1.75E-05	8.56E-06	1.31E-05
k13	6.06E-04	1.70E-03	5.40E-03
k21	-7.42E-02	-7.42E-02	-1.67E-01
k22	1.72E-02	1.72E-02	2.56E-02
k23	3.25E-02	3.25E-02	1.1667
k31	2.30E-05	3.54E-05	6.74E-06
k32	1.20E-05	-1.18E-05	-2.25E-06
k33	1.43E-04	4.71E-04	2.95E-04

Figure 5-14 on page 56 plots the responses of the original model, a new model

using the constrained solutions, and a new model using analytical solutions. The

compressor is stepped up by two Hertz in the compressor input plots, and the valve

closed by 0.2 V in the valve input plots. In each case the control inputs not mentioned in

the plot titles are held constant.
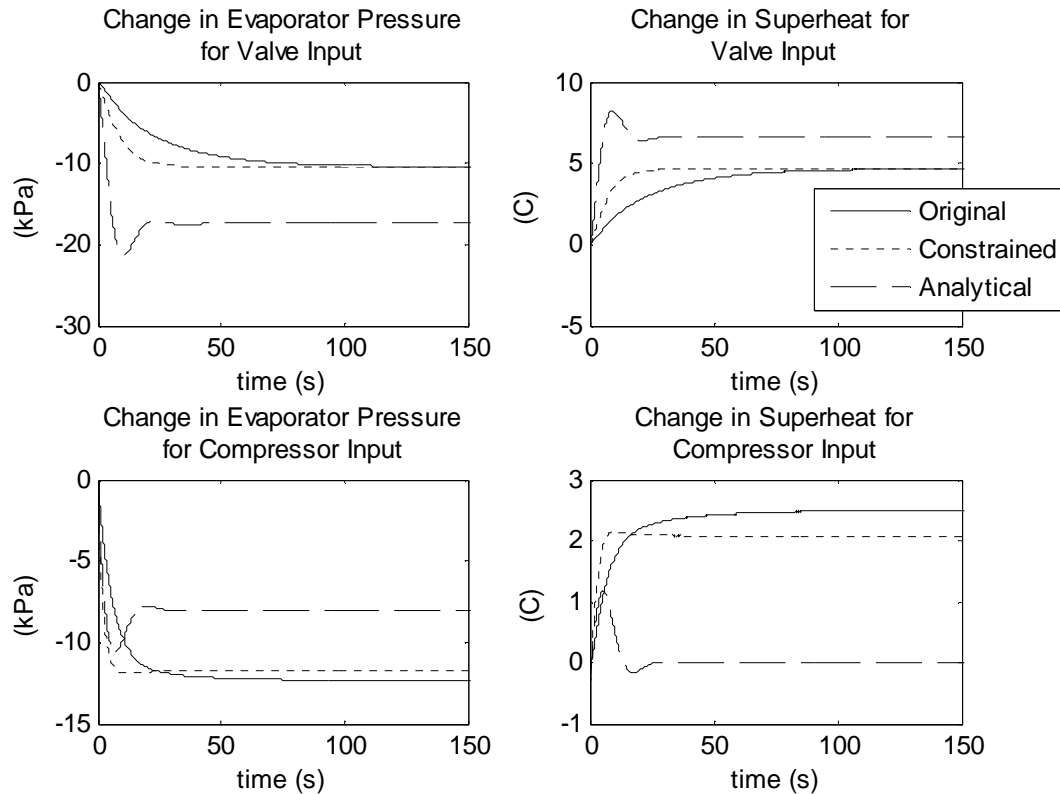
Figure 5-14 Responses with Adjusted Expansion Valve and Compressor Coefficients

The constrained and analytical solutions result in a system which is much faster. While the constrained system generally hits the correct final value the purely analytical set is not very accurate. Overshoot is added with the analytical solution, but its time constants and final values are poor.

Overall, the original model seems to be the most accurate. Some of the modifications will help a couple of features but never everything. The mass flow rate and ambient temperature variations primarily adjust final values, which is a strength of the original model. Modifying the evaporator mean void fraction does not have much effect, and the condenser fraction only helps in the compressor tests. The alternate expansion valve and compressor coefficients weaken the model, but can obviously have quite an effect. Constrained and analytical solutions contradict the data measured in tests. It makes physical sense that the mass flow rate through the valve decreases as the evaporator pressure increases, and the flow through the compressor decreases as condenser pressure increases. But, data from expansion valve tests suggest otherwise. This contradiction is most likely what leads to inaccurate final values.

56

CHAPTER 6 - Conclusions

This work has presented the lumped parameter nonlinear modeling equations for heat exchangers, and their detailed derivations. These equations were then linearized about an operating point and put in terms of the air conditioner's states and inputs. To accomplish this, linear modeling equations of the expansion valve and compressor replace heat exchanger inputs with system states and inputs. In order to determine values for parameters in the model, the air conditioner was modified, fixed, charged with refrigerant, leak proofed, and wired for measurements and controls. Several attempts at redesigning the loop were necessary to bring the air conditioner to proper operating conditions. Efforts were made to reduce noise in the measurements due to variable frequency drives for the blower motors. Air flow meters were also designed, constructed, and calibrated. Numerous tests were run and data was recorded to determine required parameters. This thesis provides detailed evaluations of the modeling parameters. The model was simulated with Matlab software and compared to experimental data. Some of the lesser known parameters were varied to determine their effects on the simulation. The original parameter values yielded the most accurate results. It predicts final value changes quite well and time constants decently. The transient dynamic shapes require improvement.

Critical Analysis of Model

The model requires many parameters which cannot easily be determined accurately. Individual adjustments of theses parameters did not improve the model, but better values for all of them combined should help. Measurements of mass flow rate are always challenging. In this case, the presence of oil in the lines compromises the V-cone Flowmeter. The refrigerant flow rate therefore had to be indirectly calculated with a heat transfer balance. This involves quite a few measurements as well as unquantifiable heat losses. More measurements increase the uncertainty. Perhaps measurements of the inlet and exit heat exchanger air temperatures were not as accurate as they should be. The

temperature was only measured in one spot on each side of the heat exchanger, so a better value for the bulk temperature may be possible. Small differences in temperature can have an impact on the calculations, due to the fact that the total temperature change across a heat exchanger is on the order of ten degrees Celsius. Higher quality air flow meters could also result in more accurate measurements. The oil may also affect the determination of thermodynamic properties such as enthalpies and densities. These properties were found in tables using pressure and temperature measurements. Inaccuracies in the flow rate will also manifest in the calculations of heat transfer coefficients, lengths of nodes, and tube wall temperatures.

There is always uncertainty when using correlations to determine heat transfer coefficients. Issues could arise with this. Although, the inside coefficients do not seem to have a large effect. A better determination of the tube wall to air heat transfer coefficient could help, instead of backing it out.

Measuring tube wall temperatures is a difficult task, and could not be accurately done in this work. Without a direct measurement of the wall temperatures, optimization was required to determine node lengths and outside heat transfer coefficients. With precise wall temperature measurements more confidence in the parameters calculated using these temperatures would exist. The lengths of nodes are also backed out of heat transfer equations, and cannot be determined directly.

The mean void fraction is another value that may need more improvement. The oil could create issues in the determination of the void fraction.

Better determination of the ambient temperatures surrounding the heat exchangers could be necessary.

The most questionable values are the coefficients of the linear expansion valve and compressor equations. The least squares fit used to find these values requires very accurate measurements of the refrigerant mass flow rate, which are probably not achieved using an indirect calculation. There did not seem to be a good solution for the coefficients in these equations. The differences between measured and calculated values of change in mass flow rate were quite similar for many different sets of coefficients. And, the model could be greatly affected with the alternate solutions. The counter intuitive signs of the k_{11} and k_{32} coefficients are curious. They most likely are a result of

the fact that during testing both the evaporator and condenser pressures decreased when the valve was closed slightly. This puts the tests used to determine the coefficients into question, which is troublesome. Due to nonlinearities, the coefficients must be found at the operating point of the air conditioner. This does not leave many alternatives. Certainly further investigation of these coefficients is desired.

Possible Solutions for a Better Model

A new refrigerant flow meter in addition to or replacing the current one should produce stronger measurements. Ideally, having two meters would heighten the confidence of the measurements. These measurements could also be used to check the validity of the mass flow rate calculated in this thesis. A different type of compressor or an oil separator will most likely be required. Hopefully, this would increase the accuracy of the current refrigerant flow meter. In addition, pure refrigerant would be circulating through the system making the tabulated thermodynamic properties truer. Perhaps, time delays occur do to the oil. With the current setup, the oil concentration is not controlled. This adds un-modeled features to the air conditioner. It is likely that changes in flow rate, especially with changed compressor speed, affect this concentration. Removing the oil from circulation definitely will not hurt, and will expectedly help. The compressor and its motor get quite hot when running for a long time. A method for cooling them is definitely worth consideration.

The tests were not run in an environmentally controlled chamber. Conditions could not be varied intentionally. Many times tests were compromised or steady state could not be reached due to changes in room temperature. Temperature changes of less than one degree Celsius affected pressures as much as changes in expansion valve setting. Testing in a more controlled environment would be desired.

The modeling equations may also need inspection. Too many or poor simplifications and assumptions could cause the model to miss the transient dynamics of the system. A better way to link the heat exchanger models into the complete model may be possible. This could include accurate determination of the expansion valve and compressor equation coefficients or possibly a different form for the equations.

References

Aprea, C., R. Mastrullo, and C. Renno. "Fuzzy Control of the Compressor Speed in a Refrigeration Plant*." International Journal of Refrigeration 27* (2004): 639-648.

Cavallini, A., and R. Zecchin. "A dimensionless correlation for flow boiling in forced convection condensation." In Vol III, *Heat Transfer 1974: Proceedings of the Fifth International Heat Transfer Conference Held in Tokyo 3-7 September 1974*: 309-313.

Cerri, G. and L. Battisti. "Valve Control for Optimum Performance in Compression Refrigeration Cycles." *Heat Recovery Systems & CHP* Vol. 14 No. 1 (1994): 61-66.

Chaddock, J. B., and H. Brunemann. "Forced convection boiling of refrigerants in horizontal tubes-Phase 3." Durham, NC: Duke University School of Engineering, (1967). HL-113.

Cheng, T. and H. Asada. "Nonlinear Observer Design for a Varying-Order Switched System with Application to Heat Exchangers." *Proceedings of the American Control Conference* Minneapolis, Minnesota June 14-16 2006: 2898-2903.

Cheng, T., X. He, and H. Asada. "Nonlinear Observer Design for Two-Phase Flow Heat Exchangers of Air Conditioning Systems." *Proceedings of the American Control Conference* Boston, Massachusetts June 30 – July 2 2004: 1534-1539.

Gungor, K. E., and R. H. S. Winterton. "A general correlation for flow boiling in tubes and annuli." *International Journal of Heat and Mass Transfer* 29 (1986): 351-358.

He, X. et al. "Multivariable Control of Vapor Compression Systems." *International Journal of Heating, Ventilating, Air-Conditioning, and Refrigerating Research.* Vol. 4 Issue 3 (1998): 205-230.

He, X. and H. Asada. "A New Feedback Linearization Approach to Advanced Control of Multi-Unit HVAC Systems." *Proceedings of the American Control Conference* Denver, Colorado June 4-6 2003: 2311-2316.

He, X. *Dynamic Modeling and Multivariable Control of Vapor Compression Cycles in Air Conditioning Systems.* Doctoral dissertation, Massachusetts Institute of Technology, 1996.

He, X., S. Liu, and H. Asada. "A Moving-Interface Model of Two-Phase Flow Heat Exchanger Dynamics for Control of Vapor Compression Cycle." *Heat Pump and Refrigeration Systems Design, Analysis and Applications* ASME Vol. 32 (1994): 69-75.

He, X., S. Liu, and H. Asada. "Modeling of Vapor Compression Cycles for Advances Controls in HVAC Systems." *Proceedings of the American Control Conference* Seattle, Washington June 1995: 3664-3668.

He, X., S. Liu, and H. Asada. "Modeling of Vapor Compression Cycles for Multivariable Feedback Control in HVAC Systems." *Journal of Dynamic Systems, Measurement, and Control.* Vol. 119 (1997): 183-191.

He, X., S. Liu, and H. Asada. "Multivariable Feedback Design for Regulating Vapor Compression Cycles." *Proceedings of the American Control Conference* Seattle, Washington June 1995: 4331-4335.

House, J. M. and T. F. Smith. "Optimal Control of Building and HVAC Systems." *Proceedings of the American Control Conference* Seattle, Washington June 1995: 4326-4330.

Incropera, F. P. and D. P. DeWitt. *Fundamentals of Heat and Mass Transfer,* 5th Edition John Wiley and Sons, 2002.

Jiang, J.H., R. Q. Zhu and X. Liu. "A Study of Control of Refrigeration Systems with LQG Method." *Proceedings of the International Congress of Cryogenics and Refrigeration* 2003: 673-677.

Jung, D. S., M. McLinden, R. Radermacher, and D. Didion. "A study of flow boiling heat transfer with refrigerant mixtures." *International Journal of Heat and Mass Transfer* 32 (1989): 1751-1764.

Kandlikar, S. S. "A general correlation for saturated two-phase flow and boiling heat transfer inside horizontal and vertical tubes." In *Boiling and Condensation in Heat Transfer Equipment*: ASME *Winter Annual Meeting held in Boston 13-18 December 1987*, 85 (1987): 9-19.

Kattan, N., Thome, J.R., and Favrat, D. "Flow boiling in horizontal tubes: Part 1 – Development of diabatic two-phase flow pattern map", ASME *Journal of Heat Transfer*, Vol 120. No. 1. (1998): 140-147.

Kattan, N., Thome, J.R., and Favrat, D. "Flow boiling in horizontal tubes: Part 2 –New heat transfer data for five refrigerants", ASME *Journal of Heat Transfer*, Vol 120. No. 1. (1998): 48-155.

Kattan, N., Thome, J.R., and Favrat, D. "Flow boiling in horizontal tubes: Part 3 – Development of a new heat transfer model based on flow pattern", ASME *Journal of Heat Transfer*, Vol 120. No. 1. (1998): 156-165.

Kelly, J. E. *Evaporation of Ammonia In Smooth And Enhanced Tubes With And Without Miscible Oil.* Doctoral dissertation, Kansas State University, 2000.

MacArthur, J. W. and E. W. Grald. E. W. "Unsteady Compressible Two-Phase Flow Model for Predicting Cyclic Heat Pump Performance and Comparison with Expermental Data." *International Journal of Refrigeration*, Vol 12 (1989): 29-41.

McQuiston, F. and Parker, J. *Heating, Ventilating, and Air Conditioning Design and Analysis,* 4th Edition John Wiley and Sons, 1994.

Saboksayr, S. H., R. V. Patel, and M. Zaheer-uddin. "Energy-Efficient Operation of HVAC Systems using Neural Network based Decentralized Controllers." *Proceedings of the American Control Conference Seattle, Washington* June 1995: 4321-4325.

Shah, M. M. "Chart correlation for saturated boiling heat transfer: equations and further study." ASHRAE *Transactions* 88 (1982): 66-86.

Shah. M. M. "A general correlation for heat transfer during film condensation inside pipes." *International Journal of Heat and Mass Transfer* 88 (1979): 185-196.

Traviss, D. P., W. M. Rohsenow, and A. B. Baron. "Forced convection condensation inside tubes: a heat transfer equation for condenser design." ASHRAE *Transactions* 79 (1972): 157-165.

Wedekind, G.L., B.L. Bhatt, and B.T. Beck. "A System Mean Void Fraction Model for Predicting Various Transient Phenomena Associated with Two-Phase Evaporating and Condensing Flows." *Int. J. Multiphase Flow*, Vol. 4 (1978): 97-114.

Zivi, S. M. "Estimation of steady-state steam void fraction by means of the vapor volumetric concentration in boiling, forced convection systems under oscillatory conditions." *Int. J. Heat Mass Transfer 9* (1964): 871-894.

Appendix A - Derivation of Evaporator Equations

Two-Phase Region

Mass Balance on the refrigerant in Two-Phase Region of the Evaporator

The control volume of interest is shown in Figure 2-3 as cv1.

$$\frac{Dm}{Dt} = \frac{\partial \rho}{\partial t} + \frac{\partial \rho u}{\partial z} = 0$$

Term 1: $\quad \dfrac{\partial \rho}{\partial t}$

Integrate over the cross-sectional area.

$$\int \frac{\partial \rho}{\partial t} dA$$

$$= \frac{\partial}{\partial t} \int \rho dA = \frac{\partial}{\partial t} \left[A \left(\rho_{eL} \frac{A_{eL}}{A} + \rho_{ev} \frac{A_{ev}}{A} \right) \right]$$

$$= \frac{\partial}{\partial t} \left[A (\rho_{eL} (1 - \gamma_e) + \rho_{ev} \gamma_e) \right]$$

A_{eL} is the cross-sectional area of saturated liquid, A_{ev} is the cross-sectional area

of saturated vapor and $\gamma_e \equiv \dfrac{A_{ev}}{A}$ and $(1 - \gamma_e) \equiv \dfrac{A_{eL}}{A}$

Integrate over the length.

$$\int_0^{Le1} \frac{\partial}{\partial t} \left[A (\rho_{eL} (1 - \gamma_e) + \rho_{ev} \gamma_e) \right] dz$$

Applying Leibniz' Rule

$$= \frac{d}{dt} \int_0^{Le1} \left[A (\rho_{eL} (1 - \gamma_e) + \rho_{ev} \gamma_e) \right] dz - \left[A (\rho_{eL} (1 - \gamma_e) + \rho_{ev} \gamma_e) \right]_{Le1} \frac{dL_{e1}}{dt}$$

$$+ \left[A (\rho_{eL} (1 - \gamma_e) + \rho_{ev} \gamma_e) \right]_0 \frac{d0}{dt}$$

$$= \frac{d}{dt} \int_0^{Le1} \left[A (\rho_{eL} (1 - \gamma_e) + \rho_{ev} \gamma_e) \right] dz - \left[A (\rho_{eL} (1 - 1) + \rho_{ev} \cdot 1) \right] \frac{dL_{e1}}{dt}$$

65

$$= \frac{d}{dt} \int_0^{Le1} [A(\rho_{eL}(1-\gamma_e) + \rho_{ev}\gamma_e)]dz - A\rho_{ev}\frac{dL_{e1}}{dt}$$

$$= \frac{d}{dt} L_{e1}\left(\frac{1}{L_{e1}}\right) \int_0^{Le1} [A(\rho_{eL}(1-\gamma_e) + \rho_{ev}\gamma_e)]dz - A\rho_{ev}\frac{dL_{e1}}{dt}$$

$$= \frac{d}{dt} L_{e1}[A(\rho_{eL}(1-\bar{\gamma}_e) + \rho_{ev}\bar{\gamma}_e)] - A\rho_{ev}\frac{dL_{e1}}{dt}$$

$$= A(1-\bar{\gamma}_e)\frac{dL_{e1}\rho_{eL}}{dt} + A\bar{\gamma}_e \frac{dL_{e1}\rho_{ev}}{dt} - A\rho_{ev}\frac{dL_{e1}}{dt}$$

$$= A(1-\bar{\gamma}_e)\left[L_{e1}\frac{d\rho_{eL}}{dt} + \rho_{eL}\frac{dL_{e1}}{dt}\right] + A\bar{\gamma}_e\left[L_{e1}\frac{d\rho_{ev}}{dt} + \rho_{ev}\frac{dL_{e1}}{dt}\right] - A\rho_{ev}\frac{dL_{e1}}{dt}$$

$$= AL_{e1}\left[\frac{d\rho_{eL}}{dt}(1-\bar{\gamma}_e) + \frac{d\rho_{ev}}{dt}\bar{\gamma}_e\right] + A[\rho_{eL}(1-\bar{\gamma}_e) + \rho_{ev}\bar{\gamma}_e]\frac{dL_{e1}}{dt} - A\rho_{ev}\frac{dL_{e1}}{dt}$$

$$= AL_{e1}\frac{d}{dt}[\rho_{eL}(1-\bar{\gamma}_e) + \rho_{ev}\bar{\gamma}_e] + A[\rho_{eL}(1-\bar{\gamma}_e) + \rho_{ev}\bar{\gamma}_e]\frac{dL_{e1}}{dt} - A\rho_{ev}\frac{dL_{e1}}{dt}$$

Using the definition of the average density in node 1, $\rho_{e1} = (1-\bar{\gamma}_e)\rho_{eL} + \bar{\gamma}_e\rho_{ev}$, simplify to:

$$\text{Term 1} = AL_{e1}\frac{d\rho_{e1}}{dt} + A(\rho_{e1} - \rho_{ev})\frac{dL_{e1}}{dt}$$

Term 2: $\qquad \dfrac{\partial \rho u}{\partial z}$

Integrate over the cross-sectional area.

$$\int \frac{\partial \rho u}{\partial z} dA$$

$$= \frac{\partial}{\partial z} \int \rho u dA = \frac{\partial}{\partial z}\left[A\left(\rho_{eL}u_{eL}\frac{A_{eL}}{A} + \rho_{ev}u_{ev}\frac{A_{ev}}{A}\right)\right]$$

$$= \frac{\partial}{\partial z}[A(\rho_{eL}u_{eL}(1-\gamma_e) + \rho_{ev}u_{ev}\gamma_e)]$$

Integrate over the length.

$$\int_0^{Le1} \frac{\partial}{\partial z}[A(\rho_{eL}u_{eL}(1-\gamma_e) + \rho_{ev}u_{ev}\gamma_e)]dz$$

$$= [A(\rho_{eL}u_{eL}(1-\gamma_e) + \rho_{ev}u_{ev}\gamma_e)]_{z=0}^{z=Le1}$$

$$= [A(\rho_{eL}u_{eL}(1-1) + \rho_{ev}u_{ev}(1))] - [A(\rho_{eL}u_{eL}(1-\gamma_e) + \rho_{ev}u_{ev}\gamma_e)]_{in}$$

$$= A\rho_{ev}u_{ev} - \left[A\left(\rho_{eL}u_{eL}\left(1-\gamma_e\right)+\rho_{ev}u_{ev}\gamma_e\right)\right]_{in}$$

$$= \dot{m}_{e,\text{int}} - \dot{m}_{eL,in} - \dot{m}_{ev,in}$$

Term 2 $= \dot{m}_{e,\text{int}} - \dot{m}_{e.in}$

Combining Term 1 and Term 2

$$AL_{e1}\frac{d\rho_{e1}}{dt} + A\left(\rho_{e1}-\rho_{ev}\right)\frac{dL_{e1}}{dt} + \dot{m}_{e,\text{int}} - \dot{m}_{e,in} = 0$$

$$AL_{e1}\frac{d\rho_{e1}}{dt} + A\left(\rho_{e1}-\rho_{ev}\right)\frac{dL_{e1}}{dt} = \dot{m}_{e,in} - \dot{m}_{e,\text{int}}$$

Since $\qquad \rho_{e1} = \rho_{e1}(P_e)$

$$\boxed{AL_{e1}\frac{d\rho_{e1}}{dP_e}\frac{dP_e}{dt} + A\left(\rho_{e1}-\rho_{ev}\right)\frac{dL_{e1}}{dt} = \dot{m}_{e,in} - \dot{m}_{e,\text{int}}} \qquad (2.4)$$

Energy Balance on Refrigerant in Two-Phase Region of the Evaporator

The control volume of interest is shown in Figure 2-3 as cv1.

$$\frac{\partial}{\partial t}(\rho h - P) + \frac{\partial}{\partial z}(\rho u h) = \frac{4}{D_i}\alpha_i(T_w - T_r)$$

Term 1: $\quad \frac{\partial}{\partial t}(\rho h - P)$

Integrate over the cross-sectional Area.

$$\int \frac{\partial}{\partial t}(\rho h - P)dA$$

$$= \frac{\partial}{\partial t}\int \rho h\, dA - \frac{\partial}{\partial t}\int P\, dA$$

$$= \frac{\partial}{\partial t} A\left[\rho_{eL}h_{eL}\frac{A_{eL}}{A} + \rho_{ev}h_{ev}\frac{A_{ev}}{A}\right] - A\frac{\partial P_e}{\partial t}$$

$$= \frac{\partial}{\partial t} A[\rho_{eL}h_{eL}(1-\gamma_e) + \rho_{ev}h_{ev}\gamma_e] - A\frac{\partial P_e}{\partial t}$$

$$= \frac{\partial}{\partial t} A[\rho_{eL}h_{eL}(1-\gamma_e) + \rho_{ev}h_{ev}\gamma_e - P_e]$$

Integrate over the length.

$$\int_0^{Le1} \frac{\partial}{\partial t} A[\rho_{eL}h_{eL}(1-\gamma_e) + \rho_{ev}h_{ev}\gamma_e - P_e]dz$$

Applying Leibniz' Rule

$$= A\frac{d}{dt}\int_0^{Le1}[\rho_{eL}h_{eL}(1-\gamma_e) + \rho_{ev}h_{ev}\gamma_e - P_e]dz + A[\rho_{eL}h_{eL}(1-\gamma_e) + \rho_{ev}h_{ev}\gamma_e - P_e]_{z=0}\frac{d0}{dt}$$

$$\quad - A[\rho_{eL}h_{eL}(1-\gamma_e) + \rho_{ev}h_{ev}\gamma_e - P_e]_{z=Le1}\frac{dL_{e1}}{dt}$$

$$= A\frac{d}{dt}\int_0^{Le1}[\rho_{eL}h_{eL}(1-\gamma_e) + \rho_{ev}h_{ev}\gamma_e - P_e]dz - A[\rho_{eL}h_{eL}(1-1) + \rho_{ev}h_{ev}\cdot 1 - P_e]\frac{dL_{e1}}{dt}$$

$$= A\frac{d}{dt}\int_0^{Le1}[\rho_{eL}h_{eL}(1-\gamma_e) + \rho_{ev}h_{ev}\gamma_e - P_e]dz - A\rho_{ev}h_{ev}\frac{dL_{e1}}{dt} + AP_e\frac{dL_{e1}}{dt}$$

$$= A\frac{d}{dt}L_{e1}\left(\frac{1}{L_{e1}}\right)\int_0^{Le1}[\rho_{eL}h_{eL}(1-\gamma_e) + \rho_{ev}h_{ev}\gamma_e - P_e]dz - A\rho_{ev}h_{ev}\frac{dL_{e1}}{dt} + AP_e\frac{dL_{e1}}{dt}$$

$$= A\frac{d}{dt}L_{e1}[\rho_{eL}h_{eL}(1-\bar{\gamma}_e) + \rho_{ev}h_{ev}\bar{\gamma}_e - P_e] - A\rho_{ev}h_{ev}\frac{dL_{e1}}{dt} + AP_e\frac{dL_{e1}}{dt}$$

$$= A(1-\bar{\gamma}_e)\frac{d}{dt}[L_{e1}\rho_{eL}h_{eL}] + A\bar{\gamma}_e\frac{d}{dt}[L_{e1}\rho_{ev}h_{ev}] - A\frac{dL_{e1}P_e}{dt} - A\rho_{ev}h_{ev}\frac{dL_{e1}}{dt} + AP_e\frac{dL_{e1}}{dt}$$

$$= A(1-\bar{\gamma}_e)\left[L_{e1}\frac{d\rho_{eL}h_{eL}}{dt} + \rho_{eL}h_{eL}\frac{dL_{e1}}{dt}\right] + A\bar{\gamma}_e\left[L_{e1}\frac{d\rho_{ev}h_{ev}}{dt} + \rho_{ev}h_{ev}\frac{dL_{e1}}{dt}\right]$$

$$- AL_{e1}\frac{dP_e}{dt} - AP_e\frac{dL_{e1}}{dt} - A\rho_{ev}h_{ev}\frac{dL_{e1}}{dt} + AP_e\frac{dL_{e1}}{dt}$$

$$= A[\rho_{eL}h_{eL}(1-\bar{\gamma}_e) + \rho_{ev}h_{ev}\bar{\gamma}_e - \rho_{ev}h_{ev}]\frac{dL_{e1}}{dt} + AL_{e1}\left[\frac{d\rho_{eL}h_{eL}}{dt}(1-\bar{\gamma}_e) + \frac{d\rho_{ev}h_{ev}}{dt}\bar{\gamma}_e\right]$$

$$- AL_{e1}\frac{dP_e}{dt}$$

Term 1 $= A(1-\bar{\gamma}_e)[\rho_{eL}h_{eL} - \rho_{ev}h_{ev}]\frac{dL_{e1}}{dt} + AL_{e1}\left[\frac{d\rho_{eL}h_{eL}}{dt}(1-\bar{\gamma}_e) + \frac{d\rho_{ev}h_{ev}}{dt}\bar{\gamma}_e - \frac{dP_e}{dt}\right]$

Term 2: $\dfrac{\partial}{\partial z}(\rho u h)$

Integrate over the cross-sectional area.

$$\int\frac{\partial}{\partial z}(\rho u h)dA = \frac{\partial}{\partial z}\int(\rho u h)dA$$

$$= \frac{\partial}{\partial z}A\left[\rho_{eL}u_{eL}h_{eL}\frac{A_{eL}}{A} + \rho_{ev}u_{ev}h_{ev}\frac{A_{ev}}{A}\right]$$

$$= \frac{\partial}{\partial z}A[\rho_{eL}u_{eL}h_{eL}(1-\gamma_e) + \rho_{ev}u_{ev}h_{ev}\gamma_e]$$

Integrate over the length.

$$\int_0^{Le1}\frac{\partial}{\partial z}A[\rho_{eL}u_{eL}h_{eL}(1-\gamma_e) + \rho_{ev}u_{ev}h_{ev}\gamma_e]dz$$

$$= A[\rho_{eL}u_{eL}h_{eL}(1-\gamma_e) + \rho_{ev}u_{ev}h_{ev}\gamma_e]_{z=0}^{z=Le1}$$

$$= A[\rho_{eL}u_{eL}h_{eL}(1-1) + \rho_{ev}u_{ev}h_{ev}(1)] - A[\rho_{eL}u_{eL}h_{eL}(1-\gamma_e) + \rho_{ev}u_{ev}h_{ev}\gamma_e]_{in}$$

$$= A\rho_{ev}u_{ev}h_{ev} - A[\rho_{eL}u_{eL}h_{eL}(1-\gamma_e) + \rho_{ev}u_{ev}h_{ev}\gamma_e]_{in}$$

$$= \dot{m}_{e,int}h_{ev} - [\dot{m}_{eL}h_{eL} + \dot{m}_{ev}h_{ev}]_{in}$$

Using the definition of quality $\qquad x_{e,in} = \dfrac{\dot{m}_{e,v}}{\dot{m}_{e,in}} = \dfrac{h_{e,in} - h_{eL}}{h_{ev} - h_{eL}}$

$$= \dot{m}_{e,int}h_{ev} - [(1-x_{e,in})\dot{m}_{e,in}h_{eL} + x_{e,in}\dot{m}_{e,in}h_{ev}]$$

$$= \dot{m}_{e,int}h_{ev} - \dot{m}_{e,in}[(1-x_{e,in})h_{eL} + x_{e,in}h_{ev}]$$

Term 2 $= \dot{m}_{e,int}h_{ev} - \dot{m}_{e,in}h_{e,in}$

Term 3: $\dfrac{4}{D_i}\alpha_i\left(T_w-T_r\right)$

Integrate over the cross-sectional Area.

$$\int \frac{4}{D_i}\alpha_i\left(T_{ew1}-T_{er1}\right)dA$$

$$=\frac{4}{D_i}\alpha_{ei1}\left(T_{ew1}-T_{er1}\right)A$$

$$=\frac{4}{D_i}\alpha_{ei1}\left(T_{ew1}-T_{er1}\right)\frac{\pi D_i^2}{4}$$

$$=\pi D_i\alpha_{ei1}\left(T_{ew1}-T_{er1}\right)$$

Integrate over the length.

$$\int\limits_{0}^{Le1}\pi D_i\alpha_{ei1}\left(T_{ew1}-T_{er1}\right)dz$$

$$=L_{e1}\left(\frac{1}{L_{e1}}\right)\int\limits_{0}^{Le1}\pi D_i\alpha_{ei1}\left(T_{ew1}-T_{er1}\right)dz$$

Term 3 $=L_{e1}\pi D_i\bar{\alpha}_{ei1}\left(\bar{T}_{ew1}-\bar{T}_{er1}\right)$

Combining Terms 1, 2, and 3

$$A\left[\rho_{eL}h_{eL}\left(1-\bar{\gamma}_e\right)+\rho_{ev}h_{ev}\bar{\gamma}_e\right]\frac{dL_{e1}}{dt}+AL_{e1}\left[\frac{d\rho_{eL}h_{eL}}{dt}\left(1-\bar{\gamma}_e\right)+\frac{d\rho_{ev}h_{ev}}{dt}\bar{\gamma}_e-\frac{dP_e}{dt}\right]$$

$$-A\rho_{ev}h_{ev}\frac{dL_{e1}}{dt}+\dot{m}_{e,\text{int}}h_{ev}-\dot{m}_{e,in}h_{e,in}=L_{e1}\pi D_i\bar{\alpha}_{ei1}\left(\bar{T}_{ew1}-\bar{T}_{er1}\right)$$

$$A\left[\rho_{eL}h_{eL}\left(1-\bar{\gamma}_e\right)+\rho_{ev}h_{ev}\bar{\gamma}_e-\rho_{ev}h_{ev}\right]\frac{dL_{e1}}{dt}+AL_{e1}\left[\frac{d\rho_{eL}h_{eL}}{dt}\left(1-\bar{\gamma}_e\right)+\frac{d\rho_{ev}h_{ev}}{dt}\bar{\gamma}_e-\frac{dP_e}{dt}\right]$$

$$=\dot{m}_{e,in}h_{e,in}-\dot{m}_{e,\text{int}}h_{ev}+L_{e1}\pi D_i\bar{\alpha}_{ei1}\left(\bar{T}_{ew1}-\bar{T}_{er1}\right)$$

$$A\left(1-\bar{\gamma}_e\right)\left[\rho_{eL}h_{eL}-\rho_{ev}h_{ev}\right]\frac{dL_{e1}}{dt}+AL_{e1}\left[\frac{d\rho_{eL}h_{eL}}{dt}\left(1-\bar{\gamma}_e\right)+\frac{d\rho_{ev}h_{ev}}{dt}\bar{\gamma}_e-\frac{dP_e}{dt}\right]$$

$$=\dot{m}_{ie,n}h_{e,in}-\dot{m}_{e,\text{int}}h_{ev}+L_{e1}\pi D_i\bar{\alpha}_{ei1}\left(\bar{T}_{ew1}-\bar{T}_{er1}\right)$$

From the mass balance equation (2.4) on node 1

$$-\dot{m}_{e,\text{int}}=-\dot{m}_{e,in}+AL_{e1}\frac{d\rho_{e1}}{dt}+A\left(\rho_{e1}-\rho_{ev}\right)\frac{dL_{e1}}{dt}$$

Substituting results of (2.4) into the energy balance equation

$$A(1-\bar{\gamma}_e)[\rho_{eL}h_{eL}-\rho_{ev}h_{ev}]\frac{dL_{e1}}{dt}+AL_{e1}\left[\frac{d\rho_{eL}h_{eL}}{dt}(1-\bar{\gamma}_e)+\frac{d\rho_{ev}h_{ev}}{dt}\bar{\gamma}_e-\frac{dP_e}{dt}\right]$$

$$=\dot{m}_{e,in}h_{e,in}+h_{ev}\left[-\dot{m}_{e,in}+AL_{e1}\frac{d\rho_{e1}}{dt}+A(\rho_{e1}-\rho_{ev})\frac{dL_{e1}}{dt}\right]+L_{e1}\pi D_i\bar{\alpha}_{ei1}(\bar{T}_{ew1}-\bar{T}_{er1})$$

$$A[(1-\bar{\gamma}_e)(\rho_{eL}h_{eL}-\rho_{ev}h_{ev})-(\rho_{e1}-\rho_{ev})h_{ev}]\frac{dL_{e1}}{dt}$$

$$+AL_{e1}\left[\frac{d\rho_{eL}h_{eL}}{dt}(1-\bar{\gamma}_e)+\frac{d\rho_{ev}h_{ev}}{dt}\bar{\gamma}_e-\frac{dP_e}{dt}-h_{ev}\frac{d\rho_{e1}}{dt}\right]$$

$$=\dot{m}_{e,in}(h_{e,in}-h_{ev})+L_{e1}\pi D_i\bar{\alpha}_{ei1}(\bar{T}_{ew1}-\bar{T}_{er1})$$

To further simplify this equation the two left hand side terms will be simplified separately as follows.

Term A: $\qquad A[(1-\bar{\gamma}_e)(\rho_{eL}h_{eL}-\rho_{ev}h_{ev})-(\rho_{e1}-\rho_{ev})h_{ev}]\frac{dL_{e1}}{dt}$

$$=A[(1-\bar{\gamma}_e)(\rho_{eL}h_{eL}-\rho_{ev}h_{ev})-(\rho_{eL}(1-\bar{\gamma}_e)+\rho_{ev}\bar{\gamma}_e-\rho_{ev})h_{ev}]\frac{dL_{e1}}{dt}$$

$$=A[(1-\bar{\gamma}_e)(\rho_{eL}h_{eL}-\rho_{ev}h_{ev})-(1-\bar{\gamma}_e)(\rho_{eL}-\rho_{ev})h_{ev}]\frac{dL_{e1}}{dt}$$

$$=A[(1-\bar{\gamma}_e)\rho_{eL}h_{eL}-(1-\bar{\gamma}_e)\rho_{eL}h_{ev}]\frac{dL_{e1}}{dt}$$

$$=A[(1-\bar{\gamma}_e)\rho_{eL}(h_{eL}-h_{ev})]\frac{dL_{e1}}{dt}$$

Using the definition of enthalpy of vaporization to simplify:

Term A $=-A[(1-\bar{\gamma}_e)\rho_{eL}h_{efg}]\dfrac{dL_{e1}}{dt}$

Term B:
$$AL_{e1}\left[\frac{d\rho_{eL}h_{eL}}{dt}(1-\bar{\gamma}_e)+\frac{d\rho_{ev}h_{ev}}{dt}\bar{\gamma}_e-\frac{dP_e}{dt}-h_{ev}\frac{d\rho_{e1}}{dt}\right]$$

$$=AL_{e1}\left[\frac{d\rho_{eL}h_{eL}}{dt}(1-\bar{\gamma}_e)+\frac{d\rho_{ev}h_{ev}}{dt}\bar{\gamma}_e-\frac{dP_e}{dt}-h_{ev}\frac{d\rho_{eL}(1-\bar{\gamma}_e)+\rho_{ev}\bar{\gamma}_e}{dt}\right]$$

$$=AL_{e1}\left[\begin{array}{l}\rho_{eL}\dfrac{dh_{eL}}{dt}(1-\bar{\gamma}_e)+h_{eL}\dfrac{d\rho_{eL}}{dt}(1-\bar{\gamma}_e)+\rho_{ev}\dfrac{dh_{ev}}{dt}\bar{\gamma}_e+h_{ev}\dfrac{d\rho_{ev}}{dt}\bar{\gamma}_e\\[2mm]-h_{ev}\dfrac{d\rho_{eL}(1-\bar{\gamma}_e)+\rho_{ev}\bar{\gamma}_e}{dt}-\dfrac{dP_e}{dt}\end{array}\right]$$

$$=AL_{e1}\left[\rho_{eL}\frac{dh_{eL}}{dt}(1-\bar{\gamma}_e)+h_{eL}\frac{d\rho_{eL}}{dt}(1-\bar{\gamma}_e)+\rho_{ev}\frac{dh_{ev}}{dt}\bar{\gamma}_e-h_{ev}\frac{d\rho_{eL}(1-\bar{\gamma}_e)}{dt}-\frac{dP_e}{dt}\right]$$

Using the definition of enthalpy of vaporization to replace h_{eL}

$$=AL_{e1}\left[\rho_{eL}\frac{dh_{eL}}{dt}(1-\bar{\gamma}_e)+(h_{ev}-h_{efg})\frac{d\rho_{eL}}{dt}(1-\bar{\gamma}_e)+\rho_{ev}\frac{dh_{ev}}{dt}\bar{\gamma}_e-h_{ev}\frac{d\rho_{eL}(1-\bar{\gamma}_e)}{dt}\right]$$

$$-AL_{e1}\frac{dP_e}{dt}$$

$$=AL_{e1}\left[\rho_{eL}\frac{dh_{ev}-h_{efg}}{dt}(1-\bar{\gamma}_e)-h_{efg}\frac{d\rho_{eL}}{dt}(1-\bar{\gamma}_e)+\rho_{ev}\frac{dh_{ev}}{dt}\bar{\gamma}_e-\frac{dP_e}{dt}\right]$$

$$=AL_{e1}\left[\rho_{e1}\frac{dh_{ev}}{dt}-\rho_{eL}\frac{dh_{efg}}{dt}(1-\bar{\gamma}_e)-h_{efg}\frac{d\rho_{eL}}{dt}(1-\bar{\gamma}_e)-\frac{dP_e}{dt}\right]$$

$$=AL_{e1}\left[\rho_{e1}\frac{dh_{ev}}{dt}-(1-\bar{\gamma}_e)\frac{d\rho_{eL}h_{efg}}{dt}-\frac{dP_e}{dt}\right]$$

Term B $=AL_{e1}\left[\rho_{e1}\dfrac{dh_{ev}}{dP_e}-(1-\bar{\gamma}_e)\dfrac{d\rho_{eL}h_{efg}}{dP_e}-1\right]\dfrac{dP_e}{dt}$

Putting terms A and B back together in energy balance equation

$$\boxed{\begin{array}{l}-A\big[(1-\bar{\gamma}_e)\rho_{eL}h_{efg}\big]\dfrac{dL_{e1}}{dt}+AL_{e1}\left[\rho_{e1}\dfrac{dh_{ev}}{dP_e}-(1-\bar{\gamma}_e)\dfrac{d\rho_{eL}h_{efg}}{dP_e}-1\right]\dfrac{dP_e}{dt}\\[3mm]=\dot{m}_{e,in}\big(h_{e,in}-h_{ev}\big)+L_{e1}\pi D_i\bar{\alpha}_{ei1}\big(\bar{T}_{ew1}-\bar{T}_{er1}\big)\end{array}}\qquad(2.7)$$

Energy Balance on the Tube Wall in Two-Phase Region of the Evaporator

$$\frac{dE_{CV}}{dt} = \dot{Q} + \dot{E}_m$$

$\dfrac{dE_{CV}}{dt}$ is the time rate of energy change in the control volume

$\dot{Q}$ is the net heat transfer rate of the control volume

$\dot{E}_m$ is the energy transfer rate as a result of mass crossing the control volume boundary

Figure A-1 illustrates the parameters involved with the derivation of the tube wall energy conservation equations. The positive Z direction corresponds to the direction of refrigerant flow. The length of the two-phase region is assumed to shorten while the superheat region lengthens. The velocity $\dfrac{dL_{e1}}{dt}$ is intentionally shown in the negative direction to illustrate that the two-phase region is getting shorter.
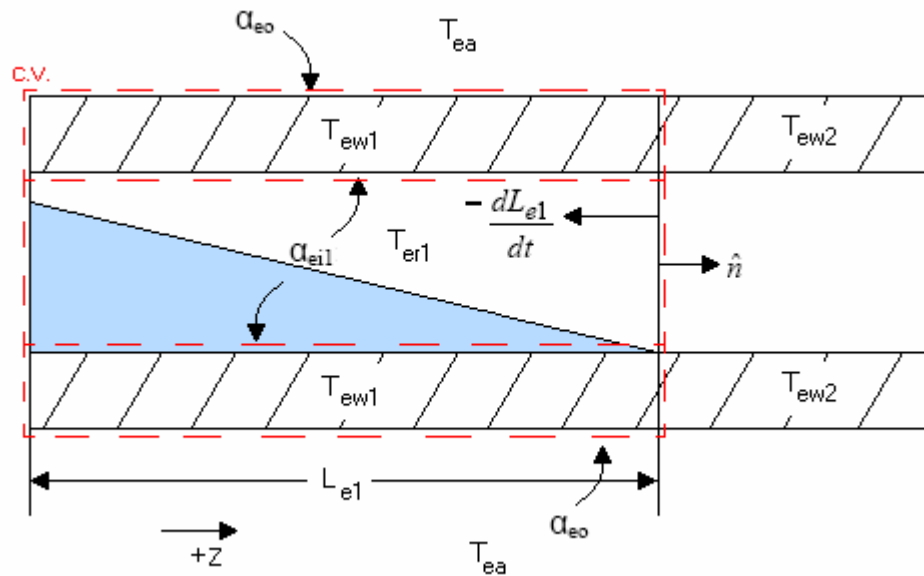
Figure A-1 Evaporator Two-Phase Wall Energy Balance Diagram

Term 1: $\dfrac{dE_{CV}}{dt}$

$$\frac{dE_{CV}}{dt} = \frac{d}{dt}\int_0^{Le1}(\rho CA)_w T_w\, dz$$

$$= (\rho CA)_w \frac{d}{dt}L_{e1}\left(\frac{1}{L_{e1}}\right)\int_0^{Le1}T_w\, dz$$

$$= (\rho CA)_w \frac{dL_{e1}\overline{T}_{ew1}}{dt}$$

$$\text{Term 1} = (\rho CA)_w\left[L_{e1}\frac{d\overline{T}_{ew1}}{dt} + \overline{T}_{ew1}\frac{dL_{e1}}{dt}\right]$$

Term 2: $\dot{Q}$

$$\text{Term 2} = \dot{Q} = \alpha_{eo}\pi D_o L_{e1}\left(T_{ea} - \overline{T}_{ew1}\right) + \overline{\alpha}_{ei1}\pi D_i L_{e1}\left(\overline{T}_{er1} - \overline{T}_{ew1}\right)$$

Term 3: $\dot{E}_m$

$$\dot{E}_m = -\int_{cs} u_w \rho_w\left(\vec{V} - \vec{V}_b\right)\bullet \hat{n}\, dA$$

$$= -\int_{cs} C_w T_w \rho_w\left(\vec{V} - \vec{V}_b\right)\bullet \hat{n}\, dA$$

$$= -(\rho CA)_w \overline{T}_{ew1}\left[0 - \left(-\frac{dL_{e1}}{dt}(-\hat{n})\right)\right]\bullet \hat{n} \qquad -\hat{n}\bullet\hat{n} = -1$$

$$\text{Term 3} = (\rho CA)_w \overline{T}_{ew1}\left(\frac{dL_{e1}}{dt}\right)$$

Combining Terms 1, 2, and 3

$$(\rho CA)_w\left[L_{e1}\frac{d\overline{T}_{ew1}}{dt} + \overline{T}_{ew1}\frac{dL_{e1}}{dt}\right] = \overline{\alpha}_{eo}\pi D_o L_{e1}\left(T_{ea} - \overline{T}_{ew1}\right) + \overline{\alpha}_{ei1}\pi D_i L_{e1}\left(\overline{T}_{er1} - \overline{T}_{ew1}\right)$$

$$+ (\rho CA)_w \overline{T}_{ew1}\left(\frac{dL_{e1}}{dt}\right)$$

$$(\rho CA)_w\left[L_{e1}\frac{d\overline{T}_{ew1}}{dt}\right] = \overline{\alpha}_{eo}\pi D_o L_{e1}\left(T_{ea} - \overline{T}_{ew1}\right) + \overline{\alpha}_{ei1}\pi D_i L_{e1}\left(\overline{T}_{er1} - \overline{T}_{ew1}\right)$$

$$\boxed{(\rho CA)_w\left[\frac{d\overline{T}_{ew1}}{dt}\right] = \overline{\alpha}_{eo}\pi D_o\left(T_{ea} - \overline{T}_{ew1}\right) + \overline{\alpha}_{ei1}\pi D_i\left(\overline{T}_{er1} - \overline{T}_{ew1}\right)} \qquad (2.9)$$

Superheat Region

Mass Balance on the Refrigerant in the Superheat Region of the Evaporator

The control volume of interest is shown in Figure 2-3 as cv2.

$$\frac{Dm}{Dt} = \frac{\partial \rho}{\partial t} + \frac{\partial \rho u}{\partial z} = 0$$

Term 1: $\dfrac{\partial \rho}{\partial t}$

Integrate over the cross-sectional area.

$$\int \frac{\partial \rho}{\partial t} dA = A \frac{\partial \rho}{\partial t}$$

Integrate over the length.

$$\int_{Le1}^{LeT} \left[A \frac{\partial \rho}{\partial t} \right] dz = A \int_{Le1}^{LeT} \frac{\partial \rho}{\partial t} dz$$

Applying Leibniz' Rule

$$= A \frac{d}{dt} \int_{Le1}^{LeT} \rho \, dz - A[\rho]_{LeT} \frac{dL_{eT}}{dt} + A[\rho]_{Le1} \frac{dL_{e1}}{dt}$$

$$= A \frac{d}{dt} L_{e2} \left(\frac{1}{L_{e2}} \right) \int_{Le1}^{LeT} \rho \, dz + A\rho_{ev} \frac{dL_{e1}}{dt}$$

$$= A \frac{dL_{e2} \rho_{e2}}{dt} + A\rho_{ev} \frac{dL_{e1}}{dt}$$

$$= AL_{e2} \frac{d\rho_{e2}}{dt} + A\rho_{e2} \frac{dL_{e2}}{dt} + A\rho_{ev} \frac{dL_{e1}}{dt}$$

Because the total length is fixed: $\quad \dfrac{d(L_{e1} + L_{e2})}{dt} = 0 \quad \Rightarrow \quad \dfrac{dL_{e2}}{dt} = -\dfrac{dL_{e1}}{dt}$

Replacing $\dfrac{dL_{e2}}{dt}$ with $-\dfrac{dL_{e1}}{dt}$

$$= AL_{e2} \frac{d\rho_{e2}}{dt} - A\rho_{e2} \frac{dL_{e1}}{dt} + A\rho_{ev} \frac{dL_{e1}}{dt}$$

Term 1 $= AL_{e2} \dfrac{d\rho_{e2}}{dt} + A[\rho_{ev} - \rho_{e2}] \dfrac{dL_{e1}}{dt}$

Term 2: $\dfrac{\partial \rho u}{\partial z}$

Integrate over the cross-sectional area.

$$\int \frac{\partial \rho u}{\partial z} dA$$

$$\frac{\partial}{\partial z} \int \rho u \, dA = A \frac{\partial \rho u}{\partial z}$$

Integrate over the length.

$$\int_{Le1}^{LeT} A \frac{\partial \rho u}{\partial z} dz = \left[A\rho u \right]_{z=Le1}^{z=LeT}$$

$$= \left[A\rho u \right]_{e,out} - \left[A\rho u \right]_{e,\text{int}}$$

$$\text{Term 2} = \dot{m}_{e,out} - \dot{m}_{e,\text{int}}$$

Combining Term 1 and Term 2

$$\boxed{AL_{e2} \frac{d\rho_{e2}}{dt} + A\left[\rho_{ev} - \rho_{e2} \right] \frac{dL_{e1}}{dt} + \dot{m}_{e,out} - \dot{m}_{e,\text{int}} = 0} \qquad (2.5)$$

Energy Balance on the Refrigerant in the Superheat Region of the Evaporator

The control volume of interest is shown in Figure 2-3 as cv2.

$$\frac{\partial}{\partial t}(\rho h - P) + \frac{\partial}{\partial z}(\rho u h) = \frac{4}{D_i}\alpha_i(T_w - T_r)$$

Term 1: $\quad \dfrac{\partial}{\partial t}(\rho h - P)$

Integrate over the cross-sectional Area.

$$\int \frac{\partial}{\partial t}(\rho h - P)dA$$

$$= \frac{\partial}{\partial t}\int (\rho h - P)dA$$

$$= \frac{\partial}{\partial t}A(\rho h - P_e)$$

Integrate over the length.

$$\int_{Le1}^{LeT} \frac{\partial}{\partial t}A(\rho h - P_e)dz$$

Applying Leibniz' Rule

$$= A\frac{d}{dt}\int_{Le1}^{LeT}(\rho h - P_e)dz + A[(\rho h - P_e)]_{z=Le1}\frac{dL_{e1}}{dt} - A[(\rho h - P_e)]_{z=LeT}\frac{dL_{eT}}{dt}$$

$$= A\frac{d}{dt}\int_{Le1}^{LeT}(\rho h - P_e)dz + A(\rho_{ev}h_{ev} - P_e)\frac{dL_{e1}}{dt}$$

$$= A\frac{d}{dt}L_{e2}\left(\frac{1}{L_{e2}}\right)\int_{Le1}^{LeT}(\rho h - P_e)dz + A(\rho_{ev}h_{ev} - P_e)\frac{dL_{e1}}{dt}$$

Assuming $\left(\dfrac{1}{L_{e2}}\right)\displaystyle\int_{Le1}^{LeT}\rho h dz = \rho_{e2}h_{e2}$

$$= A\frac{d}{dt}L_{e2}(\rho_{e2}h_{e2} - P_e) + A(\rho_{ev}h_{ev} - P_e)\frac{dL_{e1}}{dt}$$

$$= AL_{e2}\left[\frac{d\rho_{e2}h_{e2}}{dt} - \frac{dP_e}{dt}\right] + A[\rho_{e2}h_{e2} - P_e]\frac{dL_{e2}}{dt} + A(\rho_{ev}h_{ev} - P_e)\frac{dL_{e1}}{dt}$$

Substituting in $\dfrac{dL_{e2}}{dt} = -\dfrac{dL_{e1}}{dt}$

$$= AL_{e2}\left[\frac{d\rho_{e2}h_{e2}}{dt} - \frac{dP_e}{dt}\right] - A[\rho_{e2}h_{e2} - P_e]\frac{dL_{e1}}{dt} + A(\rho_{ev}h_{ev} - P_e)\frac{dL_{e1}}{dt}$$

$$= AL_{e2}\left[\frac{d\rho_{e2}h_{e2}}{dt} - \frac{dP_e}{dt}\right] + A(\rho_{ev}h_{ev} - \rho_{e2}h_{e2})\frac{dL_{e1}}{dt}$$

$$= AL_{e2}\left[\rho_{e2}\frac{dh_{e2}}{dt} + h_{e2}\frac{d\rho_{e2}}{dt} - \frac{dP_e}{dt}\right] + A(\rho_{ev}h_{ev} - \rho_{e2}h_{e2})\frac{dL_{e1}}{dt}$$

From Conservation of mass on superheat region, equation (2.5)

$$AL_{e2}\frac{d\rho_{e2}}{dt} + A[\rho_{ev} - \rho_{e2}]\frac{dL_{e1}}{dt} = \dot{m}_{e,\text{int}} - \dot{m}_{e,out}$$

$$AL_{e2}\frac{d\rho_{e2}}{dt} = \dot{m}_{e,\text{int}} - \dot{m}_{e,out} - A[\rho_{ev} - \rho_{e2}]\frac{dL_{e1}}{dt}$$

$$h_{e2}AL_{e2}\frac{d\rho_{e2}}{dt} = h_{e2}\dot{m}_{e,\text{int}} - h_{e2}\dot{m}_{e,out} - h_{e2}A[\rho_{ev} - \rho_{e2}]\frac{dL_{e1}}{dt}$$

Substituting this into Term 1

$$= AL_{e2}\left[\rho_{e2}\frac{dh_{e2}}{dt} - \frac{dP_e}{dt}\right] + h_{e2}\dot{m}_{e,\text{int}} - h_{e2}\dot{m}_{e,out} - h_{e2}A[\rho_{ev} - \rho_{e2}]\frac{dL_{e1}}{dt}$$

$$+ A(\rho_{ev}h_{ev} - \rho_{e2}h_{e2})\frac{dL_{e1}}{dt}$$

$$= AL_{e2}\left[\rho_{e2}\frac{dh_{e2}}{dt} - \frac{dP_e}{dt}\right] + h_{e2}\dot{m}_{e,\text{int}} - h_{e2}\dot{m}_{e,out} - h_{e2}A\rho_{ev}\frac{dL_{e1}}{dt} + A\rho_{ev}h_{ev}\frac{dL_{e1}}{dt}$$

$$= AL_{e2}\left[\rho_{e2}\frac{dh_{e2}}{dt} - \frac{dP_e}{dt}\right] + h_{e2}\dot{m}_{e,\text{int}} - h_{e2}\dot{m}_{e,out} + A\rho_{ev}(h_{ev} - h_{e2})\frac{dL_{e1}}{dt}$$

Defining $h_{e2} \equiv \dfrac{h_{ev} + h_{e,out}}{2}$

$$= AL_{e2}\left[0.5\rho_{e2}\frac{dh_{ev} + h_{e,out}}{dt} - \frac{dP_e}{dt}\right] + h_{e2}\dot{m}_{e,\text{int}} - h_{e2}\dot{m}_{e,out}$$

$$+ A\rho_{ev}(h_{ev} - 0.5h_{ev} - 0.5h_{e,out})\frac{dL_{e1}}{dt}$$

$$\text{Term 1} = AL_{e2}\left[0.5\rho_{e2}\frac{dh_{ev}}{dt} - \frac{dP_e}{dt}\right] + 0.5AL_{e2}\rho_{e2}\frac{dh_{e,out}}{dt} + h_{e2}\dot{m}_{e,\text{int}} - h_{e2}\dot{m}_{e,out}$$

$$+ 0.5A\rho_{ev}(h_{ev} - h_{e,out})\frac{dL_{e1}}{dt}$$

Term 2: $\dfrac{\partial}{\partial z}(\rho u h)$

Integrate over the cross-sectional area.

$$\int \frac{\partial}{\partial z}(\rho u h)dA = \frac{\partial}{\partial z}\int(\rho u h)dA$$

$$= \frac{\partial}{\partial z}A\rho u h$$

Integrate over the length.

$$\int_{Le1}^{Le}\frac{\partial}{\partial z}A\rho u h\,dz$$

$$= [A\rho u h]_{z=Le1}^{z=LeT}$$

Term 2 $= \dot{m}_{e,out}h_{e,out} - \dot{m}_{e,int}h_{ev}$

Term 3: $\dfrac{4}{D_i}\alpha_i(T_w - T_r)$

Integrate over the cross-sectional Area.

$$\int \frac{4}{D_i}\alpha_i(T_w - T_r)dA$$

$$= \frac{4}{D_i}\alpha_{ei2}(T_{ew2} - T_{er2})A$$

$$= \frac{4}{D_i}\alpha_{ei2}(T_{ew2} - T_{er2})\frac{\pi D_i^2}{4}$$

$$= \pi D_i\alpha_{ei2}(T_{ew2} - T_{er2})$$

Integrate over the length.

$$\int_{Le1}^{LeT}\pi D_i\alpha_{ei2}(T_{ew2} - T_{er2})dz$$

$$= L_{e2}\left(\frac{1}{L_{e2}}\right)\int_{Le1}^{LeT}\pi D_i\alpha_{ei2}(T_{ew2} - T_{er2})dz$$

Term3 $= L_{e2}\pi D_i\bar{\alpha}_{ei2}(\bar{T}_{ew2} - \bar{T}_{er2})$

Combining Terms 1, 2, and 3

$$AL_{e2}\left[0.5\rho_{e2}\frac{dh_{ev}}{dt}-\frac{dP_e}{dt}\right]+0.5AL_{e2}\rho_{e2}\frac{dh_{e,out}}{dt}+h_{e2}\dot{m}_{e,\mathrm{int}}-h_{e2}\dot{m}_{e,out}$$

$$+0.5A\rho_{ev}\left(h_{ev}-h_{e,out}\right)\frac{dL_{e1}}{dt}+\dot{m}_{e,out}h_{out}-\dot{m}_{e,\mathrm{int}}h_{ev}=L_{e2}\pi D_i\bar{\alpha}_{ei2}\left(\bar{T}_{ew2}-\bar{T}_{er2}\right)$$

$$AL_{e2}\left[0.5\rho_{e2}\frac{dh_{ev}}{dt}-\frac{dP_e}{dt}\right]+0.5AL_{e2}\rho_{e2}\frac{dh_{e,out}}{dt}+0.5A\rho_{ev}\left(h_{ev}-h_{e,out}\right)\frac{dL_{e1}}{dt}$$

$$+\dot{m}_{e,\mathrm{int}}\left(h_{e2}-h_{ev}\right)+\dot{m}_{e,out}\left(h_{e,out}-h_{e2}\right)=L_{e2}\pi D_i\bar{\alpha}_{ei2}\left(\bar{T}_{ew2}-\bar{T}_{er2}\right)$$

$$AL_{e2}\left[0.5\rho_{e2}\frac{dh_{ev}}{dt}-\frac{dP_e}{dt}\right]+0.5AL_{e2}\rho_{e2}\frac{dh_{e,out}}{dt}+0.5A\rho_{ev}\left(h_{ev}-h_{e,out}\right)\frac{dL_{e1}}{dt}$$

$$+\dot{m}_{e,\mathrm{int}}\left(0.5h_{ev}+0.5h_{e,out}-h_{ev}\right)+\dot{m}_{e,out}\left(h_{e,out}-0.5h_{ev}-0.5h_{e,out}\right)$$

$$=L_{e2}\pi D_i\bar{\alpha}_{ei2}\left(\bar{T}_{ew2}-\bar{T}_{er2}\right)$$

$$AL_{e2}\left[0.5\rho_{e2}\frac{dh_{ev}}{dt}-\frac{dP_e}{dt}\right]+0.5AL_{e2}\rho_{e2}\frac{dh_{e,out}}{dt}-0.5A\rho_{ev}\left(h_{e,out}-h_{ev}\right)\frac{dL_{e1}}{dt}$$

$$+0.5\dot{m}_{e,\mathrm{int}}\left(h_{e,out}-h_{ev}\right)+0.5\dot{m}_{e,out}\left(h_{e,out}-h_{ev}\right)=L_{e2}\pi D_i\bar{\alpha}_{ei2}\left(\bar{T}_{ew2}-\bar{T}_{er2}\right)$$

$$AL_{e2}\left[0.5\rho_{e2}\frac{dh_{ev}}{dt}-\frac{dP_e}{dt}\right]+0.5AL_{e2}\rho_{e2}\frac{dh_{e,out}}{dt}-0.5A\rho_{ev}\left(h_{e,out}-h_{ev}\right)\frac{dL_{e1}}{dt}$$

$$=-0.5\dot{m}_{e,\mathrm{int}}\left(h_{e,out}-h_{ev}\right)-0.5\dot{m}_{e,out}\left(h_{e,out}-h_{ev}\right)+L_{e2}\pi D_i\bar{\alpha}_{ei2}\left(\bar{T}_{ew2}-\bar{T}_{er2}\right)$$

From Mass Balance equation (2.5)

$$\dot{m}_{e,\mathrm{int}}=AL_{e2}\frac{d\rho_{e2}}{dt}+A[\rho_{ev}-\rho_{e2}]\frac{dL_{e1}}{dt}+\dot{m}_{e,out}$$

Substituting this into the Refrigerant Energy Balance

$$AL_{e2}\left[0.5\rho_{e2}\frac{dh_{ev}}{dt}-\frac{dP_e}{dt}\right]+0.5AL_{e2}\rho_{e2}\frac{dh_{e,out}}{dt}-0.5A\rho_{ev}\left(h_{e,out}-h_{ev}\right)\frac{dL_{e1}}{dt}$$

$$=L_{e2}\pi D_i\bar{\alpha}_{ei2}\left(\bar{T}_{ew2}-\bar{T}_{er2}\right)-0.5\left[AL_{e2}\frac{d\rho_{e2}}{dt}+A[\rho_{ev}-\rho_{e2}]\frac{dL_{e1}}{dt}+\dot{m}_{e,out}\right]\left(h_{e,out}-h_{ev}\right)$$

$$-0.5\dot{m}_{e,out}\left(h_{e,out}-h_{ev}\right)$$

$$AL_{e2}\left[0.5\rho_{e2}\frac{dh_{ev}}{dt}-\frac{dP_e}{dt}\right]+0.5AL_{e2}\rho_{e2}\frac{dh_{e,out}}{dt}-0.5A\rho_{ev}\left(h_{e,out}-h_{ev}\right)\frac{dL_{e1}}{dt}$$

$$=L_{e2}\pi D_i\bar{\alpha}_{ei2}\left(\bar{T}_{ew2}-\bar{T}_{er2}\right)-0.5\left[AL_{e2}\frac{d\rho_{e2}}{dt}+A[\rho_{ev}-\rho_{e2}]\frac{dL_{e1}}{dt}\right]\left(h_{e,out}-h_{ev}\right)$$

$$-\dot{m}_{e,out}\left(h_{e,out}-h_{ev}\right)$$

$$AL_{e2}\left[0.5\rho_{e2}\frac{dh_{ev}}{dt}-\frac{dP_e}{dt}\right]+0.5AL_{e2}\rho_{e2}\frac{dh_{e,out}}{dt}=L_{e2}\pi D_i\bar{\alpha}_{ei2}\left(\bar{T}_{ew2}-\bar{T}_{er2}\right)$$

$$-0.5\left[AL_{e2}\frac{d\rho_{e2}}{dt}-A\rho_{e2}\frac{dL_{e1}}{dt}\right]\left(h_{e,out}-h_{ev}\right)-\dot{m}_{e,out}\left(h_{e,out}-h_{ev}\right)$$

$$AL_{e2}\left[0.5\rho_{e2}\frac{dh_{ev}}{dt}-\frac{dP_e}{dt}\right]+0.5AL_{e2}\rho_{e2}\frac{dh_{e,out}}{dt}+0.5\left[AL_{e2}\frac{d\rho_{e2}}{dt}-A\rho_{e2}\frac{dL_{e1}}{dt}\right]\left(h_{e,out}-h_{ev}\right)$$

$$=L_{e2}\pi D_i\bar{\alpha}_{ei2}\left(\bar{T}_{ew2}-\bar{T}_{er2}\right)-\dot{m}_{e,out}\left(h_{e,out}-h_{ev}\right)$$

$$-0.5A\rho_{e2}\left(h_{e,out}-h_{ev}\right)\frac{dL_{e1}}{dt}+AL_{e2}\left[0.5\rho_{e2}\frac{dh_{ev}}{dt}+0.5\left(h_{e,out}-h_{ev}\right)\frac{d\rho_{e2}}{dt}-\frac{dP_e}{dt}\right]$$

$$+0.5AL_{e2}\rho_{e2}\frac{dh_{e,out}}{dt}=L_{e2}\pi D_i\bar{\alpha}_{ei2}\left(\bar{T}_{ew2}-\bar{T}_{er2}\right)-\dot{m}_{e,out}\left(h_{e,out}-h_{ev}\right)$$

Applying the chain rule assuming $\rho_{e2}=\rho_{e2}\left(h_{e,out},P_e\right)$

$$\frac{d\rho_{e2}}{dt}=\frac{\partial\rho_{e2}}{\partial h_{e,out}}\frac{dh_{e,out}}{dt}+\frac{\partial\rho_{e2}}{\partial P_e}\frac{dP_e}{dt}$$

Substitute this into the energy balance equation.

$$-0.5A\rho_{e2}\left(h_{e,out}-h_{ev}\right)\frac{dL_{e1}}{dt}+AL_{e2}\left[0.5\rho_{e2}\frac{dh_{ev}}{dt}+0.5\left(h_{e,out}-h_{ev}\right)\frac{\partial\rho_{e2}}{\partial P_e}\frac{dP_e}{dt}-\frac{dP_e}{dt}\right]$$

$$+0.5AL_{e2}\left[\rho_{e2}\frac{dh_{e,out}}{dt}+\left(h_{e,out}-h_{ev}\right)\frac{\partial\rho_{e2}}{\partial h_{e,out}}\frac{dh_{e,out}}{dt}\right]$$

$$=L_{e2}\pi D_i\bar{\alpha}_{ei2}\left(\bar{T}_{ew2}-\bar{T}_{er2}\right)-\dot{m}_{e,out}\left(h_{e,out}-h_{ev}\right)$$

$$\boxed{\begin{aligned}&-0.5A\rho_{e2}\left(h_{e,out}-h_{ev}\right)\frac{dL_{e1}}{dt}+AL_{e2}\left[0.5\rho_{e2}\frac{dh_{ev}}{dP_e}+0.5\left(h_{e,out}-h_{ev}\right)\frac{\partial\rho_{e2}}{\partial P_e}-1\right]\frac{dP_e}{dt}\\[2mm]&+0.5AL_{e2}\left[\rho_{e2}+\left(h_{e,out}-h_{ev}\right)\frac{\partial\rho_{e2}}{\partial h_{e,out}}\right]\frac{dh_{e,out}}{dt}\\[2mm]&=L_{e2}\pi D_i\bar{\alpha}_{ei2}\left(\bar{T}_{ew2}-\bar{T}_{er2}\right)+\dot{m}_{e,out}\left(h_{ev}-h_{e,out}\right)\end{aligned}}$$

$$(2.8)$$

Energy Balance on the Tube Wall in the Superheat Region of the Evaporator

$$\frac{dE_{CV}}{dt} = \dot{Q} + \dot{E}_m$$

This derivation is similar to that to the two-phase region. Again the two-phase region is shortening while the superheat region lengthens. Figure A-2 shows the parameters involved. The positive Z direction corresponds to the direction of refrigerant flow. The velocity $\frac{dL_{e1}}{dt}$ is intentionally shown in the negative direction to illustrate that the two-phase region is getting shorter.
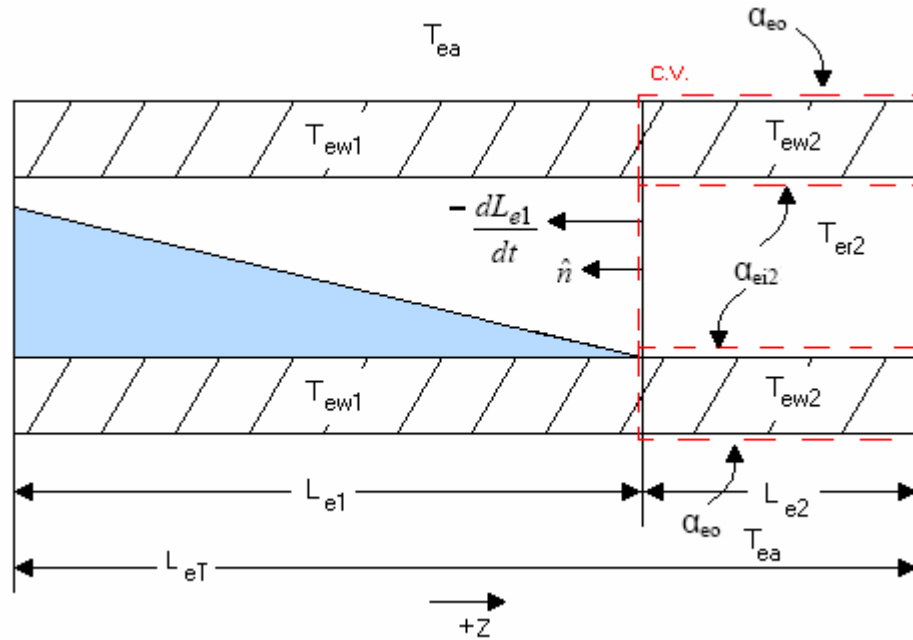
Figure A-2 Evaporator Superheat Wall Energy Balance Diagram

Term 1: $\dfrac{dE_{CV}}{dt}$

$$\frac{dE_{CV}}{dt} = \frac{d}{dt} \int_{Le1}^{LeT} (\rho C A)_w T_w dz$$

$$= (\rho C A)_w \frac{d}{dt} L_{e2} \left(\frac{1}{L_{e2}} \right) \int_{Le1}^{LeT} T_{ew2} dz$$

$$= (\rho C A)_w \frac{dL_{e2} \overline{T}_{ew2}}{dt}$$

$$= (\rho CA)_w \left[L_{e2} \frac{d\overline{T}_{ew2}}{dt} + \overline{T}_{ew2} \frac{dL_{e2}}{dt} \right]$$

Substituting $\quad \dfrac{dL_{e2}}{dt} = -\dfrac{dL_{e1}}{dt}$

Term 1 $= (\rho CA)_w \left[L_{e2} \dfrac{d\overline{T}_{ew2}}{dt} - \overline{T}_{ew2} \dfrac{dL_{e1}}{dt} \right]$

Term 2: $\qquad \dot{Q}$

Term 2 $= \dot{Q} = \overline{\alpha}_{eo} \pi D_o L_{e2} \left(T_{ea} - \overline{T}_{ew2} \right) + \overline{\alpha}_{ei2} \pi D_i L_{e2} \left(\overline{T}_{er2} - \overline{T}_{ew2} \right)$

Term 3: $\qquad \dot{E}_m$

$$\dot{E}_m = - \int_{cs} u_w \rho_w \left(\vec{V} - \vec{V}_b \right) \bullet \hat{n} dA$$

$$- \int_{cs} C_w T_w \rho_w \left(\vec{V} - \vec{V}_b \right) \bullet \hat{n} dA$$

$$- (\rho CA)_w \overline{T}_{ew1} \left[0 - \left(-\frac{dL_{e1}}{dt} \hat{n} \right) \right] \bullet \hat{n} \qquad \hat{n} \bullet \hat{n} = 1$$

Term 3 $= -(\rho CA)_w \overline{T}_{ew1} \left(\dfrac{dL_{e1}}{dt} \right)$

Combining terms 1, 2, and 3

$$(\rho CA)_w \left[L_{e2} \frac{d\overline{T}_{ew2}}{dt} - \overline{T}_{ew2} \frac{dL_{e1}}{dt} \right] = \overline{\alpha}_{eo} \pi D_o L_{e2} \left(T_{ea} - \overline{T}_{ew2} \right) + \overline{\alpha}_{ei2} \pi D_i L_{e2} \left(\overline{T}_{er2} - \overline{T}_{ew2} \right)$$

$$- (\rho CA)_w T_{ew1} \left(\frac{dL_{e1}}{dt} \right)$$

$$(\rho CA)_w \left[L_{e2} \frac{d\overline{T}_{ew2}}{dt} + \left(\overline{T}_{ew1} - \overline{T}_{ew2} \right) \frac{dL_{e1}}{dt} \right] = \overline{\alpha}_{eo} \pi D_o L_{e2} \left(T_{ea} - \overline{T}_{ew2} \right)$$

$$+ \overline{\alpha}_{ei2} \pi D_i L_{e2} \left(\overline{T}_{er2} - \overline{T}_{ew2} \right)$$

$$\boxed{\begin{aligned} (\rho CA)_w & \left[\frac{d\overline{T}_{ew2}}{dt} + \frac{\left(\overline{T}_{ew1} - \overline{T}_{ew2} \right)}{L_{e2}} \frac{dL_{e1}}{dt} \right] = \overline{\alpha}_{eo} \pi D_o \left(T_{ea} - \overline{T}_{ew2} \right) \\ & + \overline{\alpha}_{ei2} \pi D_i \left(\overline{T}_{er2} - \overline{T}_{ew2} \right) \end{aligned}} \qquad (2.10)$$

Overall Mass Balance of Evaporator

From mass balance on Two-Phase region, equation (2.4)

$$-\dot{m}_{e,int} = -\dot{m}_{e,in} + AL_{e1}\frac{d\rho_{e1}}{dP_e}\frac{dP_e}{dt} + A(\rho_{e1}-\rho_{ev})\frac{dL_{e1}}{dt}$$

From mass balance on the superheat region, equation (2.5)

$$AL_{e2}\frac{d\rho_{e2}}{dt} + A[\rho_{ev}-\rho_{e2}]\frac{dL_{e1}}{dt} + \dot{m}_{e,out} - \dot{m}_{e,int} = 0$$

Combining the two mass balances

$$AL_{e2}\frac{d\rho_{e2}}{dt} + A[\rho_{ev}-\rho_{e2}]\frac{dL_{e1}}{dt} + \dot{m}_{e,out} - \dot{m}_{e,in} + AL_{e1}\frac{d\rho_{e1}}{dP_e}\frac{dP_e}{dt} + A(\rho_{e1}-\rho_{ev})\frac{dL_{e1}}{dt} = 0$$

$$A[\rho_{e1}-\rho_{e2}]\frac{dL_{e1}}{dt} + A\left[L_{e2}\frac{d\rho_{e2}}{dt} + L_{e1}\frac{d\rho_{e1}}{dP_e}\frac{dP_e}{dt}\right] = \dot{m}_{e,in} - \dot{m}_{e,out}$$

Since $\rho_{e2} = \rho_{e2}(P_e, h_{e2})$ and $h_{e2} = h_{e2}(P_e, h_{e,out})$

$$\rho_{e2} = \rho_{e2}(P_e, h_{e,out})$$

Applying the chain rule $\dfrac{d\rho_{e2}}{dt} = \dfrac{\partial\rho_{e2}}{\partial h_{e,out}}\dfrac{dh_{e,out}}{dt} + \dfrac{\partial\rho_{e2}}{\partial P_e}\dfrac{dP_e}{dt}$

$$A[\rho_{e1}-\rho_{e2}]\frac{dL_{e1}}{dt} + A\left[L_{e2}\left(\frac{\partial\rho_{e2}}{\partial P_e}\frac{dP_e}{dt} + \frac{\partial\rho_{e2}}{\partial h_{e,out}}\frac{dh_{e,out}}{dt}\right) + L_{e1}\frac{d\rho_{e1}}{dP_e}\frac{dP_e}{dt}\right]$$

$$= \dot{m}_{e,in} - \dot{m}_{e,out}$$

$$\boxed{\begin{aligned} &A[\rho_{e1}-\rho_{e2}]\frac{dL_{e1}}{dt} + A\left[L_{e2}\frac{\partial\rho_{e2}}{\partial P_e} + L_{e1}\frac{d\rho_{e1}}{dP_e}\right]\frac{dP_e}{dt} + AL_{e2}\frac{\partial\rho_{e2}}{\partial h_{e,out}}\frac{dh_{e,out}}{dt} \\ &= \dot{m}_{e,in} - \dot{m}_{e,out} \end{aligned}} \qquad (2.6)$$

Appendix B - Derivation of Condenser Equations

Superheat Region

Mass Balance on Refrigerant in the Superheat Region of the Condenser

The control volume of interest is shown in Figure 2-4 as cv1.

$$\frac{Dm}{Dt} = \frac{\partial \rho}{\partial t} + \frac{\partial \rho u}{\partial z} = 0$$

Term 1: $\qquad \dfrac{\partial \rho}{\partial t}$

Integrate over the cross-sectional area.

$$\int \frac{\partial \rho}{\partial t} dA = A \frac{\partial \rho}{\partial t}$$

Integrate over the length.

$$\int_0^{Lc1} \left[A \frac{\partial \rho}{\partial t} \right] dz = A \int_0^{Lc1} \frac{\partial \rho}{\partial t} dz$$

Applying Leibniz' Rule

$$= A \frac{d}{dt} \int_0^{Lc1} \rho dz - A[\rho]_{Lc1} \frac{dL_{c1}}{dt} + A[\rho]_0 \frac{d0}{dt}$$

$$= A \frac{d}{dt} L_{c1} \left(\frac{1}{L_{c1}} \right) \int_0^{Lc1} \rho dz - A\rho_{cv} \frac{dL_{c1}}{dt}$$

Defining the average density in node 1 $\qquad \rho_{c1} \equiv \left(\frac{1}{L_{c1}} \right) \int_0^{Lc1} \rho dz$

$$= A \frac{dL_{c1}\rho_{c1}}{dt} - A\rho_{cv} \frac{dL_{c1}}{dt}$$

$$= A L_{c1} \frac{d\rho_{c1}}{dt} + A\rho_{c1} \frac{dL_{c1}}{dt} - A\rho_{cv} \frac{dL_{c1}}{dt}$$

Term 1 $= A L_{c1} \dfrac{d\rho_{c1}}{dt} + A[\rho_{c1} - \rho_{cv}] \dfrac{dL_{c1}}{dt}$

Term 2: $\dfrac{\partial \rho u}{\partial z}$

Integrate over the cross-sectional area.

$$\int \frac{\partial \rho u}{\partial z} dA$$

$$= \frac{\partial}{\partial z} \int \rho u dA = A \frac{\partial \rho u}{\partial z}$$

Integrate over the length.

$$\int_{Lc1}^{Lc} A \frac{\partial \rho u}{\partial z} dz = [A\rho u]_{z=0}^{z=Lc1}$$

$$= [A\rho u]_{Lc1} - [A\rho u]_0$$

Term 2 $= \dot{m}_{c,\text{int}1} - \dot{m}_{c,in}$

Combining Term 1 and Term 2

$$AL_{c1} \frac{d\rho_{c1}}{dt} + A[\rho_{c1} - \rho_{cv}] \frac{dL_{c1}}{dt} + \dot{m}_{c,\text{int}1} - \dot{m}_{c,in} = 0$$

$$\boxed{AL_{c1} \frac{d\rho_{c1}}{dt} + A[\rho_{c1} - \rho_{cv}] \frac{dL_{c1}}{dt} = \dot{m}_{c,in} - \dot{m}_{c,\text{int}1}} \qquad (2.12)$$

Energy Balance on the Refrigerant in the Superheat Region of the Condenser

The control volume of interest is shown in Figure 2-4 as cv1.

$$\frac{\partial}{\partial t}(\rho h - P) + \frac{\partial}{\partial z}(\rho u h) = \frac{4}{D_i}\alpha_i(T_w - T_r)$$

Term 1: $\quad \frac{\partial}{\partial t}(\rho h - P)$

Integrate over the cross-sectional Area.

$$\int \frac{\partial}{\partial t}(\rho h - P)dA$$

$$= \frac{\partial}{\partial t}\int(\rho h - P)dA$$

$$= \frac{\partial}{\partial t}A(\rho h - P_c)$$

Integrate over the length.

$$\int\limits_0^{Lc1} \frac{\partial}{\partial t}A(\rho h - P_c)dz$$

Applying Leibniz' Rule

$$= A\frac{d}{dt}\int\limits_0^{Lc1}(\rho h - P_c)dz + A[(\rho h - P_c)]_{z=0}\frac{d0}{dt} - A[(\rho h - P_c)]_{z=Lc1}\frac{dL_{c1}}{dt}$$

$$= A\frac{d}{dt}\int\limits_0^{Lc1}(\rho h - P_c)dz - A(\rho_{cv}h_{cv} - P_c)\frac{dL_{c1}}{dt}$$

$$= A\frac{d}{dt}L_{c1}\left(\frac{1}{L_{c1}}\right)\int\limits_0^{Lc1}(\rho h - P_c)dz - A(\rho_{cv}h_{cv} - P_c)\frac{dL_{c1}}{dt}$$

Defining the average enthalpy in node one $\quad h_{c1} \equiv \left(\frac{1}{L_{c1}}\right)\int\limits_0^{Lc1}hdz$

And, assuming the average of the product (ρh) equals the product of averages $\rho_{c1}h_{c1}$

$$= A\frac{d}{dt}L_{c1}(\rho_{c1}h_{c1} - P_c) - A(\rho_{cv}h_{cv} - P_c)\frac{dL_{c1}}{dt}$$

$$= AL_{c1}\left[\frac{d\rho_{c1}h_{c1}}{dt} - \frac{dP_c}{dt}\right] + A[\rho_{c1}h_{c1} - P_c]\frac{dL_{c1}}{dt} - A(\rho_{cv}h_{cv} - P_c)\frac{dL_{c1}}{dt}$$

$$= AL_{c1}\left[h_{c1}\frac{d\rho_{c1}}{dt} + \rho_{c1}\frac{dh_{c1}}{dt} - \frac{dP_c}{dt} \right] + A[\rho_{c1}h_{c1} - \rho_{cv}h_{cv}]\frac{dL_{c1}}{dt}$$

From conservation of mass on superheat region, equation (2.12)

$$AL_{c1}\frac{d\rho_{c1}}{dt} + A[\rho_{c1} - \rho_{cv}]\frac{dL_{c1}}{dt} = \dot{m}_{c,in} - \dot{m}_{c,int\,1}$$

$$AL_{c1}\frac{d\rho_{c1}}{dt} = \dot{m}_{c,in} - \dot{m}_{c,int\,1} - A[\rho_{c1} - \rho_{cv}]\frac{dL_{c1}}{dt}$$

$$h_{c1}AL_{c1}\frac{d\rho_{c1}}{dt} = h_{c1}\dot{m}_{c,in} - h_{c1}\dot{m}_{c,int\,1} - h_{c1}A[\rho_{c1} - \rho_{cv}]\frac{dL_{c1}}{dt}$$

Substituting this into term 1

$$= AL_{c1}\left[\rho_{c1}\frac{dh_{c1}}{dt} - \frac{dP_c}{dt} \right] + A[\rho_{c1}h_{c1} - \rho_{cv}h_{cv}]\frac{dL_{c1}}{dt} + h_{c1}\dot{m}_{c,in} - h_{c1}\dot{m}_{c,int\,1}$$

$$- h_{c1}A[\rho_{c1} - \rho_{cv}]\frac{dL_{c1}}{dt}$$

$$\text{Term 1} = AL_{c1}\left[\rho_{c1}\frac{dh_{c1}}{dt} - \frac{dP_c}{dt} \right] - A\rho_{cv}h_{cv}\frac{dL_{c1}}{dt} + h_{c1}\dot{m}_{c,in} - h_{c1}\dot{m}_{c,int\,1} + h_{c1}A\rho_{cv}\frac{dL_{c1}}{dt}$$

Term 2: $\dfrac{\partial}{\partial z}(\rho u h)$

Integrate over the cross-sectional area.

$$\int \frac{\partial}{\partial z}(\rho u h)dA = \frac{\partial}{\partial z}\int (\rho u h)dA$$

$$= \frac{\partial}{\partial z}A\rho u h$$

Integrate over the length.

$$\int_0^{Lc1} \frac{\partial}{\partial z}A\rho u h \, dz$$

$$= [A\rho u h]_{z=0}^{z=Lc1}$$

$$\text{Term 2} = \dot{m}_{c,int\,1}h_{cv} - \dot{m}_{c,in}h_{c,in}$$

Term 3: $\dfrac{4}{D_i}\alpha_i\left(T_w - Tr\right)$

Integrate over the cross-sectional Area.

$$\int \frac{4}{D_i}\alpha_i\left(T_w - T_r\right)dA$$

$$= \frac{4}{D_i}\alpha_{ci1}\left(T_{cw1} - T_{cr1}\right)A$$

$$= \frac{4}{D_i}\alpha_{ci1}\left(T_{cw1} - T_{cr1}\right)\frac{\pi D_i^2}{4}$$

$$= \pi D_i \alpha_{ci1}\left(T_{cw1} - T_{cr1}\right)$$

Integrate over the length.

$$\int_0^{Lc1} \pi D_i \alpha_{ci1}\left(T_{cw1} - T_{cr1}\right)dz$$

Term 3 $= L_{c1}\pi D_i \overline{\alpha}_{ci1}\left(\overline{T}_{cw1} - \overline{T}_{cr1}\right)$

Combining Terms 1, 2, and 3

$$AL_{c1}\left[\rho_{c1}\frac{dh_{c1}}{dt} - \frac{dP_c}{dt}\right] - A\rho_{cv}h_{cv}\frac{dL_{c1}}{dt} + h_{c1}\dot{m}_{c,in} - h_{c1}\dot{m}_{c,\mathrm{int}1} + h_{c1}A\rho_{cv}\frac{dL_{c1}}{dt}$$

$$+ \dot{m}_{c,\mathrm{int}1}h_{cv} - \dot{m}_{c,in}h_{c,in} = L_{c1}\pi D_i \overline{\alpha}_{ci1}\left(\overline{T}_{cw1} - \overline{T}_{cr1}\right)$$

Defining $h_{c1} \equiv \dfrac{h_{cv} + h_{c,in}}{2}$

$$AL_{c1}\left[\rho_{c1}\frac{dh_{c1}}{dt} - \frac{dP_c}{dt}\right] - A\rho_{cv}h_{cv}\frac{dL_{c1}}{dt} + \left(0.5h_{cv} + 0.5h_{c,in}\right)\dot{m}_{c,in} - \left(0.5h_{cv} + 0.5h_{c,in}\right)\dot{m}_{c,\mathrm{int}1}$$

$$+ h_{c1}A\rho_{cv}\frac{dL_{c1}}{dt} + \dot{m}_{c,\mathrm{int}1}h_{cv} - \dot{m}_{c,in}h_{c,in} = L_{c1}\pi D_i \overline{\alpha}_{ci1}\left(\overline{T}_{cw1} - \overline{T}_{cr1}\right)$$

$$AL_{c1}\left[\rho_{c1}\frac{dh_{c1}}{dt} - \frac{dP_c}{dt}\right] - A\rho_{cv}h_{cv}\frac{dL_{c1}}{dt} + \left(0.5h_{cv}\right)\dot{m}_{c,in} - \left(0.5h_{c,in}\right)\dot{m}_{c,\mathrm{int}1}$$

$$+ h_{c1}A\rho_{cv}\frac{dL_{c1}}{dt} + 0.5\dot{m}_{c,\mathrm{int}1}h_{cv} - 0.5\dot{m}_{c,in}h_{c,in} = L_{c1}\pi D_i \overline{\alpha}_{ci1}\left(\overline{T}_{cw1} - \overline{T}_{cr1}\right)$$

$$AL_{c1}\left[\rho_{c1}\frac{dh_{c1}}{dt} - \frac{dP_c}{dt}\right] - A\rho_{cv}h_{cv}\frac{dL_{c1}}{dt} + A\left(0.5h_{cv} + 0.5h_{c,in}\right)\rho_{cv}\frac{dL_{c1}}{dt} + 0.5\dot{m}_{c,\mathrm{int}1}\left(h_{cv} - h_{c,in}\right)$$

$$+ 0.5\dot{m}_{c,in}\left(h_{cv} - h_{c,in}\right) = L_{c1}\pi D_i \overline{\alpha}_{ci1}\left(\overline{T}_{cw1} - \overline{T}_{cr1}\right)$$

$$AL_{c1}\left[\rho_{c1}\frac{dh_{c1}}{dt}-\frac{dP_c}{dt}\right]-0.5A\big(h_{cv}-h_{c,in}\big)\rho_{cv}\frac{dL_{c1}}{dt}=L_{c1}\pi D_i\overline{\alpha}_{ci1}\big(\overline{T}_{cw1}-\overline{T}_{cr1}\big)$$
$$-0.5\big(h_{cv}-h_{c,in}\big)\big(\dot{m}_{c,int1}+\dot{m}_{c,in}\big)$$

From conservation of mass on superheat region, equation (2.12)

$$\dot{m}_{c,int1}=\dot{m}_{c,in}-AL_{c1}\frac{d\rho_{c1}}{dt}-A[\rho_{c1}-\rho_{cv}]\frac{dL_{c1}}{dt}$$

Substituting conservation of mass into term 1

$$AL_{c1}\left[\rho_{c1}\frac{dh_{c1}}{dt}-\frac{dP_c}{dt}\right]-0.5A\big(h_{cv}-h_{c,in}\big)\rho_{cv}\frac{dL_{c1}}{dt}=L_{c1}\pi D_i\overline{\alpha}_{ci1}\big(\overline{T}_{cw1}-\overline{T}_{cr1}\big)$$
$$-0.5\big(h_{cv}-h_{c,in}\big)\left(\dot{m}_{c,in}-AL_{c1}\frac{d\rho_{c1}}{dt}-A[\rho_{c1}-\rho_{cv}]\frac{dL_{c1}}{dt}+\dot{m}_{c,in}\right)$$

$$AL_{c1}\left[\rho_{c1}\frac{dh_{c1}}{dt}-\frac{dP_c}{dt}\right]-0.5A\big(h_{cv}-h_{c,in}\big)[\rho_{cv}+(\rho_{c1}-\rho_{cv})]\frac{dL_{c1}}{dt}-0.5AL_{c1}\big(h_{cv}-h_{c,in}\big)\frac{d\rho_{c1}}{dt}$$
$$=L_{c1}\pi D_i\overline{\alpha}_{ci1}\big(\overline{T}_{cw1}-\overline{T}_{cr1}\big)-\big(h_{cv}-h_{c,in}\big)\dot{m}_{c,in}$$
$$AL_{c1}\left[\rho_{c1}\frac{dh_{c1}}{dt}-\frac{dP_c}{dt}\right]+0.5A\big(h_{c,in}-h_{cv}\big)\rho_{c1}\frac{dL_{c1}}{dt}+0.5AL_{c1}\big(h_{c,in}-h_{cv}\big)\frac{d\rho_{c1}}{dt}$$
$$=L_{c1}\pi D_i\overline{\alpha}_{ci1}\big(\overline{T}_{cw1}-\overline{T}_{cr1}\big)+\big(h_{c,in}-h_{cv}\big)\dot{m}_{c,in}$$

Expanding the derivative of $\rho_{c1}=\rho(P_c,h_{c1})$ and assuming $\dfrac{dh_{c1}}{dt}=\dfrac{dh_{cv}}{dt}$

$$\frac{d\rho_{c1}}{dt}=\frac{\partial\rho_{c1}}{\partial P_c}\frac{dP_c}{dt}+\frac{\partial\rho_{c1}}{\partial hc1}\frac{dh_{c1}}{dt}$$
$$\frac{d\rho_{c1}}{dt}=\frac{\partial\rho_{c1}}{\partial P_c}\frac{dP_c}{dt}+\frac{\partial\rho_{c1}}{\partial h_{cv}}\frac{dh_{cv}}{dt}$$

Substituting these derivatives into the energy balance equation

$$AL_{c1}\left[\rho_{c1}\frac{dh_{cv}}{dt}-\frac{dP_c}{dt}\right]+0.5A\big(h_{c,in}-h_{cv}\big)\rho_{c1}\frac{dL_{c1}}{dt}$$
$$+0.5AL_{c1}\big(h_{c,in}-h_{cv}\big)\left(\frac{\partial\rho_{c1}}{\partial P_c}\frac{dP_c}{dt}+\frac{\partial\rho_{c1}}{\partial hc1}\frac{dh_{cv}}{dt}\right)=L_{c1}\pi D_i\overline{\alpha}_{ci1}\big(\overline{T}_{cw1}-\overline{T}_{cr1}\big)$$
$$+\big(h_{c,in}-h_{cv}\big)\dot{m}_{c,in}$$

$$AL_{c1}\left[\rho_{c1}\frac{dh_{cv}}{dt}-\frac{dP_c}{dt}+0.5\big(h_{c,in}-h_{cv}\big)\left(\frac{\partial\rho_{c1}}{\partial P_c}\frac{dP_c}{dt}+\frac{\partial\rho_{c1}}{\partial hc1}\frac{dh_{cv}}{dt}\right)\right]+0.5A\big(h_{c,in}-h_{cv}\big)\rho_{c1}\frac{dL_{c1}}{dt}$$

$$=L_{c1}\pi D_i\overline{\alpha}_{ci1}\big(\overline{T}_{cw1}-\overline{T}_{cr1}\big)+\big(h_{c,in}-h_{cv}\big)\dot{m}_{c,in}$$

Because $h_{cv}=h(P_c)$ the time derivative of h_{cv} can be written $\dfrac{dh_{cv}}{dt}=\dfrac{dh_{cv}}{dP_c}\dfrac{dP_c}{dt}$

$$AL_{c1}\left[\rho_{c1}\frac{dh_{cv}}{dP_c}+0.5\big(h_{c,in}-h_{cv}\big)\left(\frac{\partial\rho_{c1}}{\partial P_c}+\frac{\partial\rho_{c1}}{\partial hc1}\frac{dh_{cv}}{dP_c}\right)-1\right]\frac{dP_c}{dt}$$

$$+0.5A\big(h_{c,in}-h_{cv}\big)\rho_{c1}\frac{dL_{c1}}{dt}=L_{c1}\pi D_i\overline{\alpha}_{ci1}\big(\overline{T}_{cw1}-\overline{T}_{cr1}\big)+\big(h_{c,in}-h_{cv}\big)\dot{m}_{c,in}$$

$$(2.16)$$

Energy Balance on the Tube Wall in the Superheat Region of the Condenser

$$\frac{dE_{CV}}{dt}=\dot{Q}+\dot{E}_m$$

This derivation is similar the evaporator. The superheat region is assumed to be lengthening. FigureB-1 shows the parameters involved. The positive Z direction corresponds to the direction of refrigerant flow. Velocities are shown the direction that the derivation assumes.
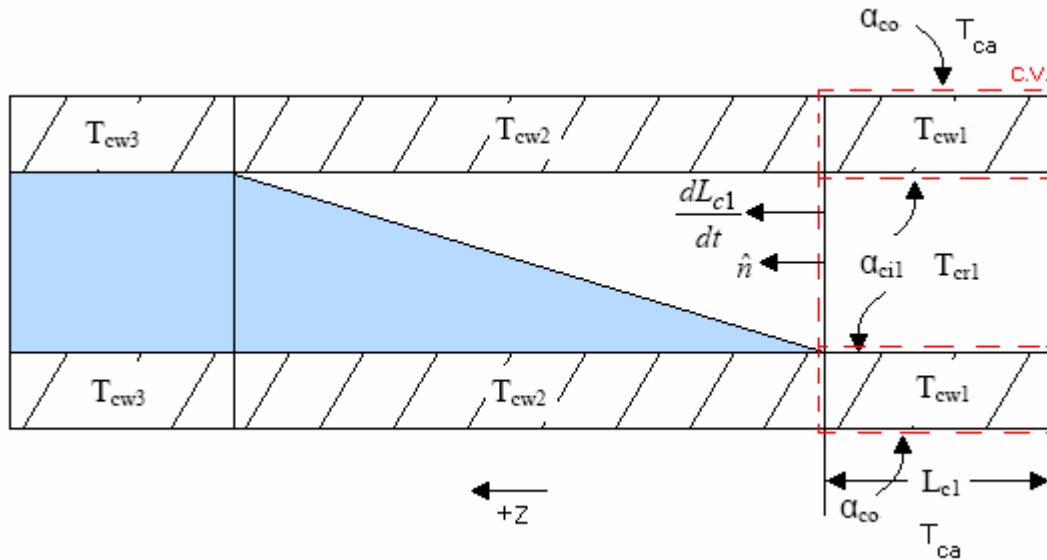
Figure B-1 Condenser Superheat Wall Energy Balance Diagram

Term 1: $\dfrac{dE_{CV}}{dt}$

$$\frac{dE_{CV}}{dt} = \frac{d}{dt}\int_0^{Lc1}(\rho CA)_w T_w \, dz$$

$$= (\rho CA)_w \frac{d}{dt} L_{c1}\left(\frac{1}{L_{c1}}\right)\int_0^{Lc1} T_{cw1} \, dz$$

$$= (\rho CA)_w \frac{dL_{c1}\overline{T}_{cw1}}{dt}$$

$$\text{Term 1} = (\rho CA)_w\left[L_{c1}\frac{d\overline{T}_{cw1}}{dt} + \overline{T}_{cw1}\frac{dL_{c1}}{dt}\right]$$

Term 2: $\dot{Q}$

$$\text{Term 2} = \dot{Q} = \overline{\alpha}_{co}\pi D_o L_{c1}\left(T_{ca} - \overline{T}_{cw1}\right) + \overline{\alpha}_{ci1}\pi D_i L_{c1}\left(\overline{T}_{cr1} - \overline{T}_{cw1}\right)$$

Term 3: $\dot{E}_m$

$$\dot{E}_m = -\int_{cs} u_w \rho_w\left(\vec{V} - \vec{V}_b\right)\bullet \hat{n}\,dA$$

$$= -\int_{cs} C_w T_w \rho_w\left(\vec{V} - \vec{V}_b\right)\bullet \hat{n}\,dA$$

$$= -(\rho CA)_w \overline{T}_{cw2}\left[0 - \left(\frac{dL_{c1}}{dt}\hat{n}\right)\right]\bullet \hat{n}$$

$$\text{Term 3} = (\rho CA)_w \overline{T}_{cw2}\left(\frac{dL_{c1}}{dt}\right)$$

Combining terms 1, 2, and 3

$$(\rho CA)_w\left[L_{c1}\frac{d\overline{T}_{cw1}}{dt} + \overline{T}_{cw1}\frac{dL_{c1}}{dt}\right] = \overline{\alpha}_{co}\pi D_o L_{c1}\left(T_{ca} - \overline{T}_{cw1}\right) + \overline{\alpha}_{ci1}\pi D_i L_{c1}\left(\overline{T}_{cr1} - \overline{T}_{cw1}\right)$$

$$+ (\rho CA)_w \overline{T}_{cw2}\left(\frac{dL_{c1}}{dt}\right)$$

$$(\rho CA)_w\left[L_{e2}\frac{d\overline{T}_{cw1}}{dt} + \left(\overline{T}_{cw1} - \overline{T}_{cw2}\right)\frac{dL_{c1}}{dt}\right] = \overline{\alpha}_{co}\pi D_o L_{c1}\left(T_{ca} - \overline{T}_{cw1}\right) + \overline{\alpha}_{ci1}\pi D_i L_{c1}\left(\overline{T}_{cr1} - \overline{T}_{cw1}\right)$$

$$\left(\rho CA\right)_w \left[\frac{d\overline{T}_{cw1}}{dt} + \frac{\left(\overline{T}_{cw1} - \overline{T}_{cw2}\right)}{L_{c1}} \frac{dL_{c1}}{dt} \right] = \overline{\alpha}_{co} \pi D_o \left(T_{ca} - \overline{T}_{cw1}\right) \qquad (2.19)$$
$$+ \overline{\alpha}_{ci1} \pi D_i \left(\overline{T}_{cr1} - \overline{T}_{cw1}\right)$$

Two-Phase Saturation Region

Mass Balance on Refrigerant in the Two-Phase Region of the Condenser

The control volume of interest is shown in Figure 2-4 as cv2.

$$\frac{Dm}{Dt} = \frac{\partial \rho}{\partial t} + \frac{\partial \rho u}{\partial z} = 0$$

Term 1: $\quad \dfrac{\partial \rho}{\partial t}$

Integrate over the cross-sectional area.

$$\int \frac{\partial \rho}{\partial t} dA$$

$$= \frac{\partial}{\partial t} \int \rho dA = \frac{\partial}{\partial t}\left[A\left(\rho_{cL} \frac{A_{cL}}{A} + \rho_{cv} \frac{A_{cv}}{A} \right) \right]$$

$$= \frac{\partial}{\partial t}\left[A(\rho_{cL}(1 - \gamma_c) + \rho_{cv}\gamma_c) \right]$$

Integrate over the length.

$$\int_{Lc1}^{Lc1+Lc2} \frac{\partial}{\partial t}\left[A(\rho_{cL}(1 - \gamma_c) + \rho_{cv}\gamma_c) \right] dz$$

Applying Leibniz' Rule

$$= \frac{d}{dt} \int_{Lc1}^{Lc1+Lc2} \left[A(\rho_{cL}(1 - \gamma_c) + \rho_{cv}\gamma_c) \right] dz + \left[A(\rho_{cL}(1 - \gamma_c) + \rho_{cv}\gamma_c) \right]_{Lc1} \frac{dL_{c1}}{dt}$$

$$- \left[A(\rho_{cL}(1 - \gamma_c) + \rho_{cv}\gamma_c) \right]_{Lc1+Lc2} \frac{d(L_{c1} + L_{c2})}{dt}$$

$$= \frac{d}{dt} \int_{Lc1}^{Lc1+Lc2} \left[A(\rho_{cL}(1 - \gamma_c) + \rho_{cv}\gamma_c) \right] dz + \left[A(\rho_{cL}(1 - 1) + \rho_{cv} \cdot 1)) \right] \frac{dL_{c1}}{dt}$$

$$- \left[A(\rho_{cL}(1 - 0) + \rho_{cv} \cdot 0) \right] \frac{d(L_{c1} + L_{c2})}{dt}$$

$$= \frac{d}{dt} L_{c2}\left(\frac{1}{L_{c2}} \right) \int_{Lc1}^{Lc1+Lc2} \left[A(\rho_{cL}(1 - \gamma_c) + \rho_{cv}\gamma_c) \right] dz + A\rho_{cv}\frac{dL_{c1}}{dt} - A\rho_{cL}\frac{d(L_{c1} + L_{c2})}{dt}$$

$$= \frac{d}{dt} L_{c2}\left[A(\rho_{cL}(1 - \bar{\gamma}_c) + \rho_{cv}\bar{\gamma}_c) \right] + A\rho_{cv}\frac{dL_{c1}}{dt} - A\rho_{cL}\frac{d(L_{c1} + L_{c2})}{dt}$$

$$= A(1 - \bar{\gamma}_c)\frac{dL_{c2}\rho_{cL}}{dt} + A\bar{\gamma}_c\frac{dL_{c2}\rho_{cv}}{dt} + A\rho_{cv}\frac{dL_{c1}}{dt} - A\rho_{cL}\frac{d(L_{c1} + L_{c2})}{dt}$$

$$= A(1-\bar{\gamma}_c)\left[L_{c2}\frac{d\rho_{cL}}{dt} + \rho_{cL}\frac{dL_{c2}}{dt}\right] + A\bar{\gamma}_c\left[L_{c2}\frac{d\rho_{cv}}{dt} + \rho_{cv}\frac{dL_{c2}}{dt}\right] + A\rho_{cv}\frac{dL_{c1}}{dt}$$

$$- A\rho_{cL}\frac{d(L_{c1}+L_{c2})}{dt}$$

$$= AL_{c2}\left[\frac{d\rho_{cL}}{dt}(1-\bar{\gamma}_c) + \frac{d\rho_{cv}}{dt}\bar{\gamma}_c\right] + A[\rho_{cL}(1-\bar{\gamma}_c) + \rho_{cv}\bar{\gamma}_c - \rho_{cL}]\frac{dL_{c2}}{dt} + A(\rho_{cv}-\rho_{cL})\frac{dL_{c1}}{dt}$$

Using the definition of average density in node two, $\rho_{c2} = \rho_{cL}(1-\bar{\gamma}_c) + \rho_{cv}\bar{\gamma}_c$

$$\text{Term 1} = AL_{c2}\frac{d\rho_{c2}}{dt} + A[\rho_{c2} - \rho_{cL}]\frac{dL_{c2}}{dt} + A(\rho_{cv}-\rho_{cL})\frac{dL_{c1}}{dt}$$

Term 2: $\quad \dfrac{\partial \rho u}{\partial z}$

Integrate over the cross-sectional area.

$$\int \frac{\partial \rho u}{\partial z} dA$$

$$= \frac{\partial}{\partial z}\int \rho u dA = \frac{\partial}{\partial z}\left[A\left(\rho_{cL}u_{cL}\frac{A_{cL}}{A} + \rho_{cv}u_{cv}\frac{A_{cv}}{A}\right)\right]$$

$$= \frac{\partial}{\partial z}[A(\rho_{cL}u_{cL}(1-\gamma_c) + \rho_{cv}u_{cv}\gamma_c)]$$

Integrate over the length.

$$\int_{Lc1}^{Lc1+Lc2} \frac{\partial}{\partial z}[A(\rho_{cL}u_{cL}(1-\gamma_c) + \rho_{cv}u_{cv}\gamma_c)]dz$$

$$= [A(\rho_{cL}u_{cL}(1-\gamma_c) + \rho_{cv}u_{cv}\gamma_c)]_{z=Lc1}^{z=Lc1+Lc2}$$

$$= [A(\rho_{cL}u_{cL}(1-0) + \rho_{cv}u_{cv}(0))] - [A(\rho_{cL}u_{cL}(1-1) + \rho_{cv}u_{cv}(1))]$$

$$= A\rho_{cL}u_{cL} - A\rho_{cv}u_{cv}$$

$\text{Term 3} = \dot{m}_{c,\text{int}2} - \dot{m}_{c,\text{int}1}$

Combining Term 1 and Term 2

$$\boxed{AL_{c2}\frac{d\rho_{c2}}{dt} + A[\rho_{c2} - \rho_{cL}]\frac{dL_{c2}}{dt} + A(\rho_{cv}-\rho_{cL})\frac{dL_{c1}}{dt} + \dot{m}_{c,\text{int}2} - \dot{m}_{c,\text{int}1} = 0}\,(2.13)$$

Energy Balance on the Refrigerant in the Two-Phase Region of the Condenser

The control volume of interest is shown in Figure 2-4 as cv2.

$$\frac{\partial}{\partial t}(\rho h - P) + \frac{\partial}{\partial z}(\rho u h) = \frac{4}{D_i}\alpha_i(T_w - Tr)$$

Term 1: $\quad \frac{\partial}{\partial t}(\rho h - P)$

Integrate over the cross-sectional Area.

$$\int \frac{\partial}{\partial t}(\rho h - P)dA$$

$$= \frac{\partial}{\partial t}\int \rho h \, dA - \frac{\partial}{\partial t}\int P \, dA$$

$$= \frac{\partial}{\partial t}A\left[\rho_{cL}h_{cL}\frac{A_{cL}}{A} + \rho_{cv}h_{cv}\frac{A_{cv}}{A}\right] - A\frac{\partial P_c}{\partial t}$$

$$= \frac{\partial}{\partial t}A[\rho_{cL}h_{cL}(1-\gamma_c) + \rho_{cv}h_{cv}\gamma_c] - A\frac{\partial P_c}{\partial t}$$

$$= \frac{\partial}{\partial t}A[\rho_{cL}h_{cL}(1-\gamma_c) + \rho_{cv}h_{cv}\gamma_c - P_c]$$

Integrate over the length.

$$\int_{Lc1}^{Lc1+Lc2}\frac{\partial}{\partial t}A[\rho_{cL}h_{cL}(1-\gamma_c) + \rho_{cv}h_{cv}\gamma_c - P_c]dz$$

Applying Leibniz' Rule

$$= A\frac{d}{dt}\int_{Lc1}^{Lc1+Lc2}[\rho_{cL}h_{cL}(1-\gamma_c) + \rho_{cv}h_{cv}\gamma_c - P_c]dz + A[\rho_{cL}h_{cL}(1-\gamma_c) + \rho_{cv}h_{cv}\gamma_c - P_c]_{z=Lc1}\frac{dL_{c1}}{dt}$$

$$-A[\rho_{cL}h_{cL}(1-\gamma_c) + \rho_{cv}h_{cv}\gamma_c - P_c]_{z=Lc1+Lc2}\frac{d(L_{c1}+L_{c2})}{dt}$$

$$= A\frac{d}{dt}\int_{Lc1}^{Lc1+Lc2}[\rho_{cL}h_{cL}(1-\gamma_c) + \rho_{cv}h_{cv}\gamma_c - P_c]dz + A[\rho_{cL}h_{cL}(1-1) + \rho_{cv}h_{cv}\cdot1 - P_c]\frac{dL_{c1}}{dt}$$

$$-A[\rho_{cL}h_{cL}(1-0) + \rho_{cv}h_{cv}\cdot0 - P_c]\frac{d(L_{c1}+L_{c2})}{dt}$$

$$= A\frac{d}{dt}L_{c2}\left(\frac{1}{L_{c2}}\right)\int_{Lc1}^{Lc1+Lc2}[\rho_{cL}h_{cL}(1-\gamma_c) + \rho_{cv}h_{cv}\gamma_c - P_c]dz + A[\rho_{cv}h_{cv} - P_c]\frac{dL_{c1}}{dt}$$

$$-A[\rho_{cL}h_{cL} - P_c]\frac{d(L_{c1}+L_{c2})}{dt}$$

$$= A\frac{d}{dt}L_{c2}[\rho_{cL}h_{cL}(1-\bar{\gamma}_c)+\rho_{cv}h_{cv}\bar{\gamma}_c - P_c] + A[\rho_{cv}h_{cv} - P_c]\frac{dL_{c1}}{dt} - A[\rho_{cL}h_{cL} - P_c]\frac{d(L_{c1}+L_{c2})}{dt}$$

$$= A(1-\bar{\gamma}_c)\frac{d}{dt}[L_{c2}\rho_{cL}h_{cL}] + A\bar{\gamma}_c\frac{d}{dt}[L_{c2}\rho_{cv}h_{cv}] - A\frac{dL_{c2}P_c}{dt} + A[\rho_{cv}h_{cv} - P_c]\frac{dL_{c1}}{dt}$$
$$- A[\rho_{cL}h_{cL}]\frac{d(L_{c1}+L_{c2})}{dt} + AP_c\frac{d(L_{c1}+L_{c2})}{dt}$$

$$= A(1-\bar{\gamma}_c)\frac{d}{dt}[L_{c2}\rho_{cL}h_{cL}] + A\bar{\gamma}_c\frac{d}{dt}[L_{c2}\rho_{cv}h_{cv}] - AP_c\frac{dL_{c2}}{dt} - AL_{c2}\frac{dP_c}{dt}$$
$$+ A[\rho_{cv}h_{cv} - P_c]\frac{dL_{c1}}{dt} - A[\rho_{cL}h_{cL}]\frac{d(L_{c1}+L_{c2})}{dt} + AP_c\frac{d(L_{c1}+L_{c2})}{dt}$$

$$= A(1-\bar{\gamma}_c)\frac{d}{dt}[L_{c2}\rho_{cL}h_{cL}] + A\bar{\gamma}_c\frac{d}{dt}[L_{c2}\rho_{cv}h_{cv}] - AL_{c2}\frac{dP_c}{dt} + A\rho_{cv}h_{cv}\frac{dL_{c1}}{dt}$$
$$- A[\rho_{cL}h_{cL}]\frac{d(L_{c1}+L_{c2})}{dt}$$

$$= A(1-\bar{\gamma}_c)\rho_{cL}h_{cL}\frac{dL_{c2}}{dt} + AL_{c2}(1-\bar{\gamma}_c)\frac{d\rho_{cL}h_{cL}}{dt} + AL_{c2}\bar{\gamma}_c\frac{d\rho_{cv}h_{cv}}{dt} + A\bar{\gamma}_c\rho_{cv}h_{cv}\frac{dL_{c2}}{dt}$$
$$- AL_{c2}\frac{dP_c}{dt} + A\rho_{cv}h_{cv}\frac{dL_{c1}}{dt} - A[\rho_{cL}h_{cL}]\frac{d(L_{c1}+L_{c2})}{dt}$$

$$= A[(1-\bar{\gamma}_c)\rho_{cL}h_{cL} + \bar{\gamma}_c\rho_{cv}h_{cv} - \rho_{cL}h_{cL}]\frac{dL_{c2}}{dt} + A(\rho_{cv}h_{cv} - \rho_{cL}h_{cL})\frac{dL_{c1}}{dt}$$
$$+ AL_{c2}\left[(1-\bar{\gamma}_c)\frac{d\rho_{cL}h_{cL}}{dt} + \bar{\gamma}_c\frac{d\rho_{cv}h_{cv}}{dt} - \frac{dP_c}{dt}\right]$$

$$\text{Term 1} = A\bar{\gamma}_c[\rho_{cv}h_{cv} - \rho_{cL}h_{cL}]\frac{dL_{c2}}{dt} + A(\rho_{cv}h_{cv} - \rho_{cL}h_{cL})\frac{dL_{c1}}{dt}$$
$$+ AL_{c2}\left[(1-\bar{\gamma}_c)\frac{d\rho_{cL}h_{cL}}{dt} + \bar{\gamma}_c\frac{d\rho_{cv}h_{cv}}{dt} - \frac{dP_c}{dt}\right]$$

Term 2: $\frac{\partial}{\partial z}(\rho u h)$

Integrate over the cross-sectional area.

$$\int\frac{\partial}{\partial z}(\rho u h)dA = \frac{\partial}{\partial z}\int(\rho u h)dA$$
$$= \frac{\partial}{\partial z}A\left[\rho_{cL}u_{cL}h_{cL}\frac{A_{cL}}{A} + \rho_{cv}u_{cv}h_{cv}\frac{A_{cv}}{A}\right]$$
$$= \frac{\partial}{\partial z}A[\rho_{cL}u_{cL}h_{cL}(1-\gamma_c) + \rho_{cv}u_{cv}h_{cv}\gamma_c]$$

Integrate over the length.

$$\int_{Lc1}^{Lc1+Lc2} \frac{\partial}{\partial z} A\left[\rho_{cL}u_{cL}h_{cL}(1-\gamma_c)+\rho_{cv}u_{cv}h_{cv}\gamma_c\right]dz$$

$$= A\left[\rho_{cL}u_{cL}h_{cL}(1-\gamma_c)+\rho_{cv}u_{cv}h_{cv}\gamma_c\right]_{z=Lc1}^{z=Lc1+Lc2}$$

$$= A\left[\rho_{cL}u_{cL}h_{cL}(1-0)+\rho_{cv}u_{cv}h_{cv}\cdot 0\right]-A\left[\rho_{cL}u_{cL}h_{cL}(1-1)+\rho_{cv}u_{cv}h_{cv}\cdot 1\right]$$

$$= A\rho_{cL}u_{cL}h_{cL}-A\rho_{cv}u_{cv}h_{cv}$$

Term 2 $= \dot{m}_{c,\text{int }2}h_{cL}-\dot{m}_{c,\text{int }1}h_{cv}$

Term 3: $\qquad \dfrac{4}{D_i}\alpha_i(T_w-T_r)$

Integrate over the cross-sectional Area.

$$\int \frac{4}{D_i}\alpha_i(T_{cw2}-T_{cr2})dA$$

$$= \frac{4}{D_i}\alpha_{ci2}(T_{cw2}-T_{cr2})A$$

$$= \frac{4}{D_i}\alpha_{ci2}(T_{cw2}-T_{cr2})\frac{\pi D_i^2}{4}$$

$$= \pi D_i\alpha_{ci2}(T_{cw2}-T_{cr2})$$

Integrate over the length.

$$\int_{Lc1}^{Lc1+Lc2} \pi D_i\alpha_{ci2}(T_{cw2}-T_{cr2})dz$$

Term 3 $= \pi L_{c2}D_i\overline{\alpha}_{ci2}\left(\overline{T}_{cw2}-\overline{T}_{cr2}\right)$

Combining Terms 1, 2, and 3

$$A\overline{\gamma}_c\left[\rho_{cv}h_{cv}-\rho_{cL}h_{cL}\right]\frac{dL_{c2}}{dt}+A(\rho_{cv}h_{cv}-\rho_{cL}h_{cL})\frac{dL_{c1}}{dt}+\dot{m}_{c,\text{int }2}h_{cL}-\dot{m}_{c,\text{int }1}h_{cv}$$

$$+AL_{c2}\left[(1-\overline{\gamma}_c)\frac{d\rho_{cL}h_{cL}}{dt}+\overline{\gamma}_c\frac{d\rho_{cv}h_{cv}}{dt}-\frac{dP_c}{dt}\right]=\pi L_{c2}D_i\overline{\alpha}_{ci2}\left(\overline{T}_{cw2}-\overline{T}_{cr2}\right)$$

From mass balance on two phase region, equation (2.13)

$$\dot{m}_{c,\text{int }1}=AL_{c2}\frac{d\rho_{c2}}{dt}+A\left[\rho_{c2}-\rho_{cL}\right]\frac{dL_{c2}}{dt}+A(\rho_{cv}-\rho_{cL})\frac{dL_{c1}}{dt}+\dot{m}_{c,\text{int }2}$$

From mass balance on subcool region, equation (2.14)

$$\dot{m}_{c,\text{int }2} = \dot{m}_{c,out} + AL_{c3}\frac{d\rho_{cL}}{dt}$$

Substituting the mass balance results into the energy balance equation

$$A\bar{\gamma}_c[\rho_{cv}h_{cv} - \rho_{cL}h_{cL}]\frac{dL_{c2}}{dt} + A(\rho_{cv}h_{cv} - \rho_{cL}h_{cL})\frac{dL_{c1}}{dt} + AL_{c2}\left[(1-\bar{\gamma}_c)\frac{d\rho_{cL}h_{cL}}{dt} + \bar{\gamma}_c\frac{d\rho_{cv}h_{cv}}{dt} - \frac{dP_c}{dt}\right]$$

$$+ \left(\dot{m}_{c,out} + AL_{c3}\frac{d\rho_{cL}}{dt}\right)h_{cL} - \left(\begin{array}{c} AL_{c2}\dfrac{d\rho_{c2}}{dt} + A[\rho_{c2} - \rho_{cL}]\dfrac{dL_{c2}}{dt} \\[2mm] + A(\rho_{cv} - \rho_{cL})\dfrac{dL_{c1}}{dt} + \dot{m}_{c,out} + AL_{c3}\dfrac{d\rho_{cL}}{dt} \end{array}\right)h_{cv}$$

$$= \pi L_{c2}D_i\bar{\alpha}_{ci2}\left(\bar{T}_{cw2} - \bar{T}_{cr2}\right)$$

$$A[\bar{\gamma}_c(\rho_{cv}h_{cv} - \rho_{cL}h_{cL}) - (\rho_{c2} - \rho_{cL})h_{cv}]\frac{dL_{c2}}{dt} + A[\rho_{cv}h_{cv} - \rho_{cL}h_{cL} - (\rho_{cv} - \rho_{cL})h_{cv}]\frac{dL_{c1}}{dt}$$

$$+ AL_{c2}\left[(1-\bar{\gamma}_c)\frac{d\rho_{cL}h_{cL}}{dt} + \bar{\gamma}_c\frac{d\rho_{cv}h_{cv}}{dt} - \frac{dP_c}{dt} - h_{cv}\frac{d\rho_{c2}}{dt}\right] + AL_{c3}(h_{cL} - h_{cv})\frac{d\rho_{cL}}{dt}$$

$$+ \dot{m}_{c,out}(h_{cL} - h_{cv}) = \pi L_{c2}D_i\bar{\alpha}_{ci2}\left(\bar{T}_{cw2} - \bar{T}_{cr2}\right)$$

To further simplify the equation the first and third terms of the left hand side will simplified separately as follows.

Term A: $\qquad A[\bar{\gamma}_c(\rho_{cv}h_{cv} - \rho_{cL}h_{cL}) - (\rho_{c2} - \rho_{cL})h_{cv}]\dfrac{dL_{c2}}{dt}$

$$= A[\bar{\gamma}_c(\rho_{cv}h_{cv} - \rho_{cL}h_{cL}) - \rho_{c2}h_{cv} + \rho_{cL}h_{cv}]\frac{dL_{c2}}{dt}$$

$$= A[\bar{\gamma}_c(\rho_{cv}h_{cv} - \rho_{cL}h_{cL}) - (1-\bar{\gamma}_c)\rho_{cL}h_{cv} - \bar{\gamma}_c\rho_{cv}h_{cv} + \rho_{cL}h_{cv}]\frac{dL_{c2}}{dt}$$

$$= A\bar{\gamma}_c[\rho_{cL}h_{cv} - \rho_{cL}h_{cL}]\frac{dL_{c2}}{dt}$$

Term A $= A\bar{\gamma}_c\rho_{cL}[h_{cv} - h_{cL}]\dfrac{dL_{c2}}{dt}$

Term B: $\qquad AL_{c2}\left[(1-\bar{\gamma}_c)\dfrac{d\rho_{cL}h_{cL}}{dt}+\bar{\gamma}_c\,\dfrac{d\rho_{cv}h_{cv}}{dt}-\dfrac{dP_c}{dt}-h_{cv}\dfrac{d\rho_{c2}}{dt}\right]$

$$= AL_{c2}\left[\begin{array}{l}(1-\bar{\gamma}_c)h_{cL}\dfrac{d\rho_{cL}}{dt}+(1-\bar{\gamma}_c)\rho_{cL}\dfrac{dh_{cL}}{dt}+\bar{\gamma}_ch_{cv}\dfrac{d\rho_{cv}}{dt}+\bar{\gamma}_c\rho_{cv}\dfrac{dh_{cv}}{dt}-\dfrac{dP_c}{dt}\\[2mm] -\,h_{cv}\dfrac{d(1-\bar{\gamma}_c)\rho_{cL}+\bar{\gamma}_c\rho_{cv}}{dt}\end{array}\right]$$

$$= AL_{c2}\left[\begin{array}{l}(1-\bar{\gamma}_c)h_{cL}\dfrac{d\rho_{cL}}{dt}+(1-\bar{\gamma}_c)\rho_{cL}\dfrac{dh_{cL}}{dt}+\bar{\gamma}_ch_{cv}\dfrac{d\rho_{cv}}{dt}+\bar{\gamma}_c\rho_{cv}\dfrac{dh_{cv}}{dt}-\dfrac{dP_c}{dt}\\[2mm] -\,h_{cv}(1-\bar{\gamma}_c)\dfrac{d\rho_{cL}}{dt}-h_{cv}\bar{\gamma}_c\dfrac{d\rho_{cv}}{dt}\end{array}\right]$$

$$= AL_{c2}\left[(1-\bar{\gamma}_c)h_{cL}\dfrac{d\rho_{cL}}{dt}+(1-\bar{\gamma}_c)\rho_{cL}\dfrac{dh_{cL}}{dt}+\bar{\gamma}_c\rho_{cv}\dfrac{dh_{cv}}{dt}-\dfrac{dP_c}{dt}-h_{cv}(1-\bar{\gamma}_c)\dfrac{d\rho_{cL}}{dt}\right]$$

Using the definition of enthalpy of vaporization, $h_{cL}=h_{cv}-h_{cfg}$, to replace h_{cL}

$$= AL_{c2}\left[\begin{array}{l}(1-\bar{\gamma}_c)(h_{cv}-h_{cfg})\dfrac{d\rho_{cL}}{dt}+(1-\bar{\gamma}_c)\rho_{cL}\dfrac{d(h_{cv}-h_{cfg})}{dt}+\bar{\gamma}_c\rho_{cv}\dfrac{dh_{cv}}{dt}-\dfrac{dP_c}{dt}\\[2mm] -\,h_{cv}(1-\bar{\gamma}_c)\dfrac{d\rho_{cL}}{dt}\end{array}\right]$$

$$= AL_{c2}\left[-h_{cfg}(1-\bar{\gamma}_c)\dfrac{d\rho_{cL}}{dt}+(1-\bar{\gamma}_c)\rho_{cL}\dfrac{d(h_{cv}-h_{cfg})}{dt}+\bar{\gamma}_c\rho_{cv}\dfrac{dh_{cv}}{dt}-\dfrac{dP_c}{dt}\right]$$

$$= AL_{c2}\left[-(1-\bar{\gamma}_c)\left(h_{cfg}\dfrac{d\rho_{cL}}{dt}+\rho_{cL}\dfrac{dh_{cfg}}{dt}\right)+((1-\bar{\gamma}_c)\rho_{cL}+\bar{\gamma}_c\rho_{cv})\dfrac{dh_{cv}}{dt}-\dfrac{dP_c}{dt}\right]$$

Term B $= AL_{c2}\left[-(1-\bar{\gamma}_c)\dfrac{dh_{cfg}\rho_{cL}}{dt}+\rho_{c2}\dfrac{dh_{cv}}{dt}-\dfrac{dP_c}{dt}\right]$

Putting terms back together in energy balance equation.

$$A\bar{\gamma}_c[\rho_{cL}h_{cv}-\rho_{cL}h_{cL}]\dfrac{dL_{c2}}{dt}+AL_{c2}\left[-(1-\bar{\gamma}_c)\dfrac{dh_{cfg}\rho_{cL}}{dt}+\rho_{c2}\dfrac{dh_{cv}}{dt}-\dfrac{dP_c}{dt}\right]$$

$$+A\rho_{cL}[h_{cv}-h_{cL}]\dfrac{dL_{c1}}{dt}+AL_{c3}(h_{cL}-h_{cv})\dfrac{d\rho_{cL}}{dt}+\dot{m}_{c,out}(h_{cL}-h_{cv})$$

$$=\pi L_{c2}D_i\bar{\alpha}_{ci2}(\bar{T}_{cw2}-\bar{T}_{cr2})$$

$$A\rho_{cL}[h_{cv} - h_{cL}]\frac{dL_{c1}}{dt} + A\bar{\gamma}_c\rho_{cL}[h_{cv} - h_{cL}]\frac{dL_{c2}}{dt}$$

$$+ AL_{c2}\left[-(1-\bar{\gamma}_c)\frac{dh_{cfg}\rho_{cL}}{dt} + \rho_{c2}\frac{dh_{cv}}{dt} - \frac{dP_c}{dt}\right] + AL_{c3}(h_{cL} - h_{cv})\frac{d\rho_{cL}}{dt}$$

$$= \dot{m}_{c,out}(h_{cv} - h_{cL}) + \pi L_{c2}D_i\bar{\alpha}_{ci2}(\bar{T}_{cw2} - \bar{T}_{cr2})$$

Using the definition of enthalpy of vaporization to substitute for $h_{cv} - h_{cL}$

$$A\rho_{cL}h_{cfg}\frac{dL_{c1}}{dt} + A\bar{\gamma}_c\rho_{cL}h_{cfg}\frac{dL_{c2}}{dt} + AL_{c2}\left[-(1-\bar{\gamma}_c)\frac{dh_{cfg}\rho_{cL}}{dt} + \rho_{c2}\frac{dh_{cv}}{dt} - \frac{dP_c}{dt}\right]$$

$$+ AL_{c3}(h_{cL} - h_{cv})\frac{d\rho_{cL}}{dt} = \dot{m}_{c,out}h_{cfg} + \pi L_{c2}D_i\bar{\alpha}_{ci2}(\bar{T}_{cw2} - \bar{T}_{cr2})$$

$$\boxed{\begin{aligned} &A\rho_{cL}h_{cfg}\frac{dL_{c1}}{dt} + A\bar{\gamma}_c\rho_{cL}h_{cfg}\frac{dL_{c2}}{dt} \\ &+ A\left\{L_{c2}\left[-(1-\bar{\gamma}_c)\frac{dh_{cfg}\rho_{cL}}{dP_c} + \rho_{c2}\frac{dh_{cv}}{dP_c} - 1\right] + L_{c3}(h_{cL} - h_{cv})\frac{d\rho_{cL}}{dP_c}\right\}\frac{dP_c}{dt} \\ &= \dot{m}_{c,out}h_{cfg} + \pi L_{c2}D_i\bar{\alpha}_{ci2}(\bar{T}_{cw2} - \bar{T}_{cr2}) \end{aligned}} \quad (2.17)$$

Energy Balance on the Tube Wall in the Two-Phase Region of the Condenser

$$\frac{dE_{CV}}{dt} = \dot{Q} + \dot{E}_m$$

This derivation is similar the evaporator. The superheat region is assumed to be lengthening, while the subcooled region is getting shorter. Figure B-2 shows the parameters involved. The positive Z direction corresponds to the direction of refrigerant flow. Velocities are shown the direction that the derivation assumes.
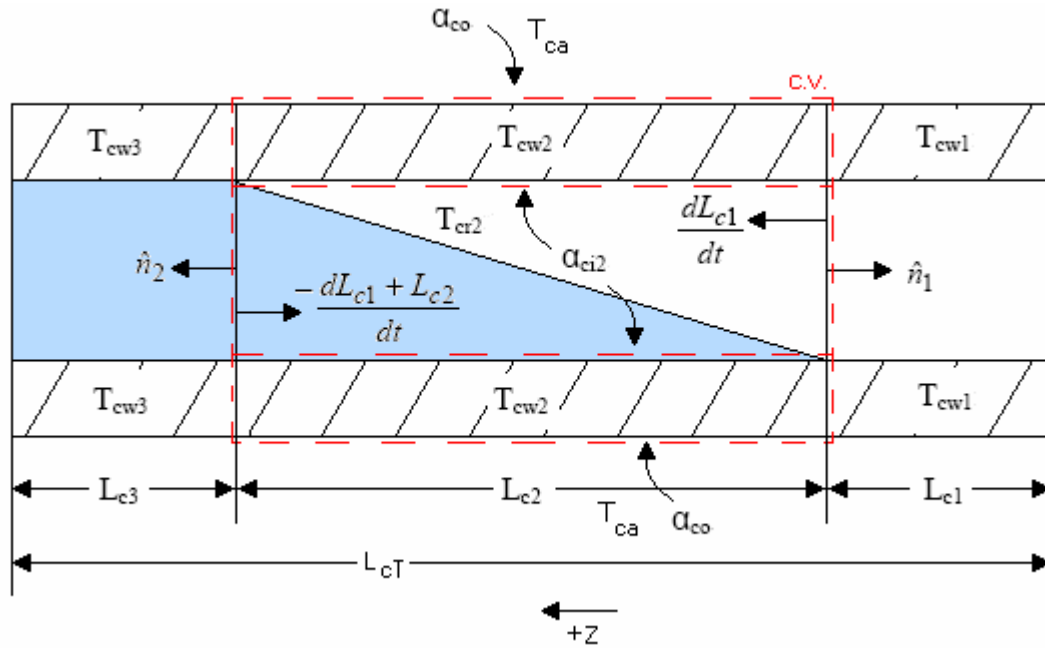
Figure B-2 Condenser Two–Phase Region Wall Energy Balance Diagram

Term 1: $\dfrac{dE_{CV}}{dt}$

$$\frac{dE_{CV}}{dt} = \frac{d}{dt}\int_{Lc1}^{Lc1+Lc2}(\rho CA)_w T_w dz$$

$$= (\rho CA)_w \frac{d}{dt}L_{c2}\left(\frac{1}{L_{c2}}\right)\int_{Lc1}^{Lc1+Lc2}T_w dz$$

$$= (\rho CA)_w \frac{dL_{c2}\overline{T}_{cw2}}{dt}$$

$$\text{Term 1} = (\rho CA)_w\left[L_{c2}\frac{d\overline{T}_{cw2}}{dt} + \overline{T}_{cw2}\frac{dL_{c2}}{dt}\right]$$

Term 2: $\dot{Q}$

Term 2 $= \dot{Q} = \overline{\alpha}_{co}\pi D_o L_{c2}\left(T_{ca} - \overline{T}_{cw2}\right) + \overline{\alpha}_{ci2}\pi D_i L_{c2}\left(\overline{T}_{cr2} - \overline{T}_{cw2}\right)$

Term 3: $\dot{E}_m$

$$\dot{E}_m = -\int_{cs} u_w \rho_w \left(\vec{V} - \vec{V}_b\right) \bullet \hat{n} dA$$

$$= -\int_{cs} C_w T_w \rho_w \left(\vec{V} - \vec{V}_b\right) \bullet \hat{n} dA$$

$$= -(\rho CA)_w \overline{T}_{cw2}\left[0 - \left(\frac{dL_{c1}}{dt}(-\hat{n}_1)\right)\right] \bullet \hat{n}_1 - (\rho CA)_w \overline{T}_{cw2}\left[0 - \left(-\frac{d(L_{c1} + L_{c2})}{dt}(-\hat{n}_2)\right)\right] \bullet \hat{n}_2$$

$$= -(\rho CA)_w \overline{T}_{cw2}\frac{dL_{c1}}{dt} + (\rho CA)_w \overline{T}_{cw2}\frac{dL_{c1}}{dt} + (\rho CA)_w \overline{T}_{cw2}\frac{dL_{c2}}{dt}$$

Term 3 $= (\rho CA)_w \overline{T}_{cw2}\dfrac{dL_{c2}}{dt}$

Combining Terms 1, 2, and 3

$$(\rho CA)_w \left[L_{c2}\frac{d\overline{T}_{cw2}}{dt} + \overline{T}_{cw2}\frac{dL_{c2}}{dt}\right] = \overline{\alpha}_{co}\pi D_o L_{c2}\left(T_{ca} - \overline{T}_{cw2}\right) + \overline{\alpha}_{ci2}\pi D_i L_{c2}\left(\overline{T}_{cr2} - \overline{T}_{cw2}\right)$$

$$+ (\rho CA)_w \overline{T}_{cw2}\frac{dL_{c2}}{dt}$$

$$(\rho CA)_w L_{c2}\frac{d\overline{T}_{cw2}}{dt} = \overline{\alpha}_{co}\pi D_o L_{c2}\left(T_{ca} - \overline{T}_{cw2}\right) + \overline{\alpha}_{ci2}\pi D_i L_{c2}\left(\overline{T}_{cr2} - \overline{T}_{cw2}\right)$$

$$\boxed{(\rho CA)_w \frac{d\overline{T}_{cw2}}{dt} = \overline{\alpha}_{co}\pi D_o\left(T_{ca} - \overline{T}_{cw2}\right) + \overline{\alpha}_{ci2}\pi D_i\left(\overline{T}_{cr2} - \overline{T}_{cw2}\right)} \qquad (2.20)$$

Subcool Region

Mass Balance on Refrigerant in the Subcool Region of the Condenser

The control volume of interest is shown in Figure 2-4 as cv3.

$$\frac{Dm}{Dt} = \frac{\partial \rho}{\partial t} + \frac{\partial \rho u}{\partial z} = 0$$

Term 1: $\quad \dfrac{\partial \rho}{\partial t}$

Integrate over the cross-sectional area

$$\int \frac{\partial \rho}{\partial t} dA = A \frac{\partial \rho}{\partial t}$$

Integrate over the length

$$\int\limits_{Lc1+Lc2}^{LcT} A \frac{\partial \rho}{\partial t} dz = A \int\limits_{Lc1+Lc2}^{LcT} \frac{\partial \rho}{\partial t} dz$$

Applying Leibniz' Rule

$$= A \frac{d}{dt} \int\limits_{Lc1+Lc2}^{LcT} \rho \, dz + A[\rho]_{z=Lc1+Lc2} \frac{d(L_{c1}+L_{c2})}{dt} - A[\rho]_{z=LcT} \frac{dL_{cT}}{dt}$$

$$= A \frac{d}{dt} \int\limits_{Lc1+Lc2}^{LcT} \rho \, dz + A\rho_{cL} \frac{dL_{c1}+L_{c2}}{dt}$$

Assuming that the density is the density of saturated liquid throughout the subcool region

$$= A \frac{dL_{c3}\rho_{cL}}{dt} + A\rho_{cL} \frac{d(L_{c1}+L_{c2})}{dt}$$

$$= AL_{c3} \frac{d\rho_{cL}}{dt} + A\rho_{cL} \frac{dL_{c3}}{dt} + A\rho_{cL} \frac{d(L_{c1}+L_{c2})}{dt}$$

$$= AL_{c3} \frac{d\rho_{cL}}{dt} + A\rho_{cL} \frac{d(L_{c1}+L_{c2}+L_{c3})}{dt}$$

$$= AL_{c3} \frac{d\rho_{cL}}{dt} + A\rho_{cL} \frac{dL_{cT}}{dt}$$

$$\text{Term 1} = AL_{c3} \frac{d\rho_{cL}}{dt}$$

Term 2: $\quad \dfrac{\partial \rho u}{\partial z}$

Integrate over the cross-sectional area.

$$\int \frac{\partial \rho u}{\partial z} dA$$

$$\frac{\partial}{\partial z} \int \rho u \, dA = \frac{\partial}{\partial z} A \rho u$$

Integrate over the length.

$$\int\limits_{Lc1+Lc2}^{LcT} \frac{\partial}{\partial z} A \rho \, dz$$

$$= \left[A \rho u \right]_{z=Lc1+Lc2}^{z=LcT}$$

Term $2 = \dot{m}_{c,out} - \dot{m}_{c,\mathrm{int}\,2}$

Combining Term 1 and Term 2

$$AL_{c3} \frac{d\rho_{cL}}{dt} + \dot{m}_{c,out} - \dot{m}_{c,\mathrm{int}\,2} = 0$$

$$\boxed{\dot{m}_{c,\mathrm{int}\,2} = \dot{m}_{c,out} + AL_{c3} \frac{d\rho_{cL}}{dt}} \tag{2.14}$$

Energy Balance on the Refrigerant in the Subcool Region of the Condenser

The control volume of interest is shown in Figure 2-4 as cv3.

$$\frac{\partial}{\partial t}(\rho h - P) + \frac{\partial}{\partial z}(\rho u h) = \frac{4}{D_i}\alpha_i(T_w - Tr)$$

Term 1: $\quad \frac{\partial}{\partial t}(\rho h - P)$

Integrate over the cross-sectional Area.

$$\int \frac{\partial}{\partial t}(\rho h - P)dA$$

$$= \frac{\partial}{\partial t}\int(\rho h - P)dA$$

$$= \frac{\partial}{\partial t}(\rho h - P_c)$$

Integrate over the length.

$$\int_{Lc1+Lc2}^{LcT} \frac{\partial}{\partial t}A(\rho h - P_c)dz$$

Applying Leibniz' Rule

$$= A\frac{d}{dt}\int_{Lc1+Lc2}^{LcT}(\rho h - P_c)dz + A(\rho h - P_c)_{z=Lc1+Lc2}\frac{d(L_{c1}+L)_{c2}}{dt} - A(\rho h - P_c)_{z=LcT}\frac{dL_{cT}}{dt}$$

$$= A\frac{d}{dt}L_{c3}\left(\frac{1}{L_{c3}}\right)_{Lc1+Lc2}^{LcT}\int(\rho h - P_c)dz + A(\rho_{cL}h_{cL} - P_c)\frac{d(L_{c1}+L_{c2})}{dt}$$

The density is assumed to be ρ_{cL} throughout the region

$$= A\frac{d}{dt}L_{c3}(\rho_{cL}h_{c3} - P_c) + A(\rho_{cL}h_{cL} - P_c)\frac{d(L_{c1}+L_{c2})}{dt}$$

$$= A\rho_{cL}h_{c3}\frac{dL_{c3}}{dt} + AL_{c3}\frac{d\rho_{cL}h_{c3}}{dt} - AP_c\frac{dL_{c3}}{dt} - AL_{c3}\frac{dP_c}{dt} + A(\rho_{cL}h_{cL} - P_c)\frac{d(L_{c1}+L_{c2})}{dt}$$

Using the fact that the length of the condenser is constant $\quad \dfrac{dL_{c3}}{dt} = -\dfrac{d(L_{c1}+L_{c2})}{dt}$

$$= -A\rho_{cL}h_{c3}\frac{d(L_{c1}+L_{c2})}{dt} + AL_{c3}\frac{d\rho_{cL}h_{c3}}{dt} + AP_c\frac{d(L_{c1}+L_{c2})}{dt} - AL_{c3}\frac{dP_c}{dt}$$

$$+ A(\rho_{cL}h_{cL} - P_c)\frac{d(L_{c1}+L_{c2})}{dt}$$

106

$$= -A\rho_{cL}h_{c3}\frac{d(L_{c1} + L_{c2})}{dt} + AL_{c3}\frac{d\rho_{cL}h_{c3}}{dt} - AL_{c3}\frac{dP_c}{dt} + A(\rho_{cL}h_{cL})\frac{d(L_{c1} + L_{c2})}{dt}$$

$$\text{Term 1} = A\rho_{cL}[h_{cL} - h_{c3}]\frac{d(L_{c1} + L_{c2})}{dt} + AL_{c3}\frac{d\rho_{cL}h_{c3}}{dt} - AL_{c3}\frac{dP_c}{dt}$$

Term 2: $\dfrac{\partial}{\partial z}(\rho u h)$

Integrate over the cross-sectional area.

$$\int \frac{\partial}{\partial z}(\rho u h)dA = \frac{\partial}{\partial z}\int (\rho u h)dA$$

$$= \frac{\partial}{\partial z}A(\rho u h)$$

Integrate over the length.

$$\int_{Lc1+Lc2}^{LcT} \frac{\partial}{\partial z}A(\rho u h)dz$$

$$= [A\rho u h]_{z=Lc1+Lc2}^{z=LcT}$$

$$\text{Term 2} = \dot{m}_{c,out}h_{c,out} - \dot{m}_{c,\text{int }2}h_{cL}$$

Term 3: $\quad \dfrac{4}{D_i}\alpha_i(T_w - T_r)$

Integrate over the cross-sectional Area.

$$\int \frac{4}{D_i}\alpha_i(T_{cw3} - T_{cr3})dA$$

$$= \frac{4}{D_i}\alpha_{ci3}(T_{cw3} - T_{cr3})A$$

$$= \frac{4}{D_i}\alpha_{ci3}(T_{cw3} - T_{cr3})\frac{\pi D_i^2}{4}$$

$$= \pi D_i\alpha_{ci3}(T_{cw3} - T_{cr3})$$

Integrate over the length.

$$\int_{Lc1+Lc2}^{LcT} \pi\alpha_{ci3}(T_{cw3} - T_{cr3})dz$$

$$\text{Term 3} = \pi L_{c3}D_i\bar{\alpha}_{ci3}(\bar{T}_{cw3} - \bar{T}_{cr3})$$

Combining Terms 1, 2, and 3

$$A\rho_{cL}[h_{cL} - \rho_{c3}h_{c3}]\frac{d(L_{c1} + L_{c2})}{dt} + AL_{c3}\frac{d\rho_L h_{c3}}{dt} - AL_{c3}\frac{dP_c}{dt} + \dot{m}_{c,out}h_{c,out} - \dot{m}_{c,\text{int }2}h_{cL}$$

$$= \pi L_{c3}D_i\overline{\alpha}_{ci3}\left(\overline{T}_{cw3} - \overline{T}_{cr3}\right)$$

From mass balance on subcool region, equation (2.14)

$$\dot{m}_{c,\text{int }2} = \dot{m}_{c,out} + AL_{c3}\frac{d\rho_{cL}}{dt}$$

Substituting this into the energy balance equation

$$A\rho_{cL}[h_{cL} - \rho_{c3}h_{c3}]\frac{d(L_{c1} + L_{c2})}{dt} + AL_{c3}\frac{d\rho_{cL}h_{c3}}{dt} - AL_{c3}\frac{dP_c}{dt} + \dot{m}_{c,out}h_{c,out} - \dot{m}_{c,out}h_{cL}$$

$$- AL_{c3}h_{cL}\frac{d\rho_{cL}}{dt} = \pi L_{c3}D_i\overline{\alpha}_{ci3}\left(\overline{T}_{cw3} - \overline{T}_{cr3}\right)$$

$$A\rho_{cL}[h_{cL} - \rho_{c3}h_{c3}]\frac{d(L_{c1} + L_{c2})}{dt} + AL_{c3}\frac{d\rho_{cL}h_{c3}}{dt} - AL_{c3}h_{cL}\frac{d\rho_{cL}}{dt} - AL_{c3}\frac{dP_c}{dt}$$

$$= \dot{m}_{c,out}\left(h_{cL} - h_{c,out}\right) + \pi L_{c3}D_i\overline{\alpha}_{ci3}\left(\overline{T}_{cw3} - \overline{T}_{cr3}\right)$$

$$A\rho_{cL}[h_{cL} - \rho_{c3}h_{c3}]\frac{d(L_{c1} + L_{c2})}{dt} + AL_{c3}h_{c3}\frac{d\rho_{cL}}{dt} + AL_{c3}\rho_{cL}\frac{dh_{c3}}{dt} - AL_{c3}h_{cL}\frac{d\rho_{cL}}{dt}$$

$$- AL_{c3}\frac{dP_c}{dt} = \dot{m}_{c,out}\left(h_{cL} - h_{c,out}\right) + \pi L_{c3}D_i\overline{\alpha}_{ci3}\left(\overline{T}_{cw3} - \overline{T}_{cr3}\right)$$

Defining $h_{c3} = \dfrac{h_{cL} + h_{c,out}}{2}$

$$A\rho_{cL}[h_{cL} - h_{c3}]\frac{d(L_{c1} + L_{c2})}{dt} + 0.5AL_{c3}\left(h_{cL} + h_{c,out}\right)\frac{d\rho_{cL}}{dt} + AL_{c3}\rho_{cL}\frac{dh_{c3}}{dt}$$

$$- AL_{c3}h_{cL}\frac{d\rho_{cL}}{dt} - AL_{c3}\frac{dP_c}{dt} = \dot{m}_{c,out}\left(h_{cL} - h_{c,out}\right) + \pi L_{c3}D_i\overline{\alpha}_{ci3}\left(\overline{T}_{cw3} - \overline{T}_{cr3}\right)$$

$$A\rho_{cL}[h_{cL} - h_{c3}]\frac{d(L_{c1} + L_{c2})}{dt} + 0.5AL_{c3}\left(h_{c,out} - h_{cL}\right)\frac{d\rho_{cL}}{dt} + AL_{c3}\rho_{cL}\frac{dh_{c3}}{dt}$$

$$- AL_{c3}\frac{dP_c}{dt} = \dot{m}_{c,out}\left(h_{cL} - h_{c,out}\right) + \pi L_{c3}D_i\overline{\alpha}_{ci3}\left(\overline{T}_{cw3} - \overline{T}_{cr3}\right)$$

$$A\rho_{cL}[h_{cL} - h_{c3}]\frac{d(L_{c1} + L_{c2})}{dt} + 0.5AL_{c3}\left(h_{c,out} - h_{cL}\right)\frac{d\rho_{cL}}{dt} + 0.5AL_{c3}\rho_{cL}\frac{dh_{cL}}{dt}$$

$$+ 0.5AL_{c3}\rho_{cL}\frac{dh_{c,out}}{dt} - AL_{c3}\frac{dP_c}{dt} = \dot{m}_{c,out}\left(h_{cL} - h_{c,out}\right) + \pi L_{c3}D_i\overline{\alpha}_{ci3}\left(\overline{T}_{cw3} - \overline{T}_{cr3}\right)$$

$$A\rho_{cL}[h_{cL}-h_{c3}]\frac{d(L_{c1}+L_{c2})}{dt}+AL_{c3}\left[0.5(h_{c,out}-h_{cL})\frac{d\rho_{cL}}{dP_c}+0.5\rho_{cL}\frac{dh_{cL}}{dP_c}-1\right]\frac{dP_c}{dt}$$

$$+0.5AL_{c3}\rho_{cL}\frac{dh_{c,out}}{dt}=\dot{m}_{c,out}(h_{cL}-h_{c,out})+\pi L_{c3}D_i\overline{\alpha}_{ci3}(\overline{T}_{cw3}-\overline{T}_{cr3})$$

$$A\rho_{cL}[h_{cL}-0.5h_{cL}-0.5h_{c,out}]\frac{d(L_{c1}+L_{c2})}{dt}+0.5AL_{c3}\rho_{cL}\frac{dh_{c,out}}{dt}$$

$$+AL_{c3}\left[0.5(h_{c,out}-h_{cL})\frac{d\rho_{cL}}{dP_c}+0.5\rho_{cL}\frac{dh_{cL}}{dP_c}-1\right]\frac{dP_c}{dt}$$

$$=\dot{m}_{c,out}(h_{cL}-h_{c,out})+\pi L_{c3}D_i\overline{\alpha}_{ci3}(\overline{T}_{cw3}-\overline{T}_{cr3})$$

$$0.5A\rho_{cL}[h_{cL}-h_{c,out}]\frac{d(L_{c1}+L_{c2})}{dt}+AL_{c3}\left[0.5(h_{c,out}-h_{cL})\frac{d\rho_{cL}}{dP_c}+0.5\rho_{cL}\frac{dh_{cL}}{dP_c}-1\right]\frac{dP_c}{dt}$$

$$+0.5AL_{c3}\rho_{cL}\frac{dh_{c,out}}{dt}=\dot{m}_{c,out}(h_{cL}-h_{c,out})+\pi L_{c3}D_i\overline{\alpha}_{ci3}(\overline{T}_{cw3}-\overline{T}_{cr3})$$

$$\boxed{\begin{aligned}&0.5A\rho_{cL}[h_{cL}-h_{c,out}]\frac{dL_{c1}}{dt}+0.5A\rho_{cL}[h_{cL}-h_{c,out}]\frac{dL_{c2}}{dt}\\&+AL_{c3}\left[0.5(h_{c,out}-h_{cL})\frac{d\rho_{cL}}{dP_c}+0.5\rho_{cL}\frac{dh_{cL}}{dP_c}-1\right]\frac{dP_c}{dt}\\&+0.5AL_{c3}\rho_{cL}\frac{dh_{c,out}}{dt}=\dot{m}_{c,out}(h_{cL}-h_{c,out})+\pi L_{c3}D_i\overline{\alpha}_{ci3}(\overline{T}_{cw3}-\overline{T}_{cr3})\end{aligned}}$$

(2.18)

Energy Balance on the Tube Wall in the Subcool Region of the Condenser

$$\frac{dE_{CV}}{dt} = \dot{Q} + \dot{E}_m$$

This derivation is similar the evaporator. The subcool region is assumed to be getting shorter. FigureB-3 shows the parameters involved. The positive Z direction corresponds to the direction of refrigerant flow. The velocity of the boundary is shown in the direction that the derivation assumes.
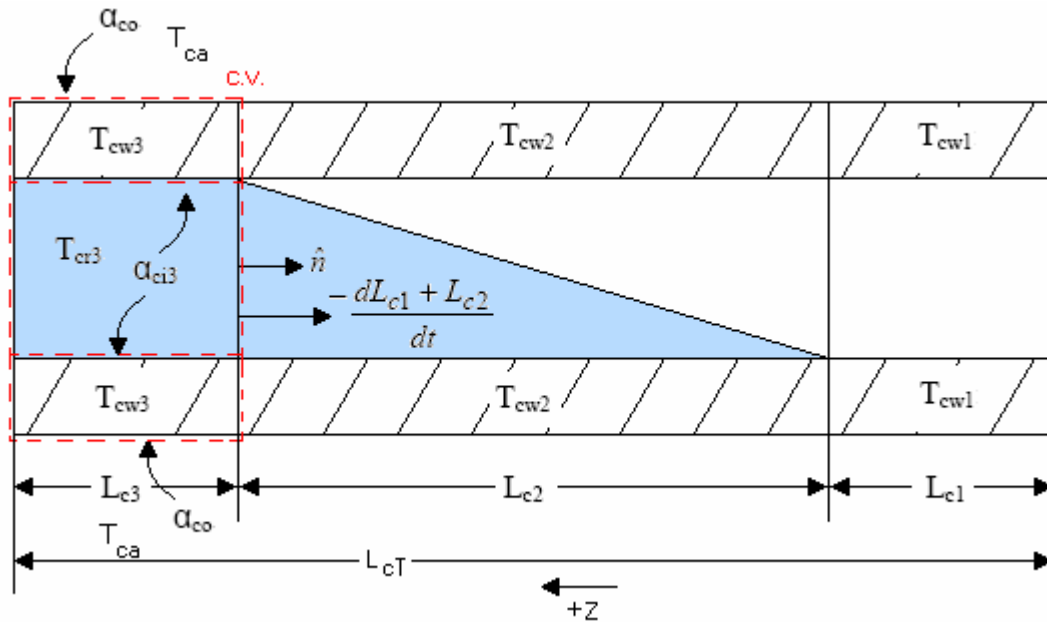
Figure B-3 Condenser Subcool Region Wall Energy Balance Diagram

Term 1: $\dfrac{dE_{CV}}{dt}$

$$\frac{dE_{CV}}{dt} = \frac{d}{dt}\int_{Lc1+Lc2}^{LcT}(\rho CA)_w T_w dz$$

$$= (\rho CA)_w \frac{d}{dt}L_{c3}\left(\frac{1}{L_{c3}}\right)\int_{Lc1+Lc2}^{LcT} T_w dz$$

$$= (\rho CA)_w \frac{dL_{c3}\overline{T}_{cw3}}{dt}$$

$$\text{Term 1} = (\rho CA)_w\left[L_{c3}\frac{d\overline{T}_{cw3}}{dt} + \overline{T}_{cw3}\frac{dL_{c3}}{dt}\right]$$

Term 2: $\dot{Q}$

Term 2 $= \dot{Q} = \overline{\alpha}_{co}\pi D_o L_{c3}\left(T_{ca} - \overline{T}_{cw3}\right) + \overline{\alpha}_{ci3}\pi D_i L_{c3}\left(\overline{T}_{cr3} - \overline{T}_{cw3}\right)$

Term 3: $\dot{E}_m$

$$\dot{E}_m = -\int_{cs} u_w \rho_w \left(\vec{V} - \vec{V}_b\right)\bullet \hat{n}dA$$

$$= -\int_{cs} C_w T_w \rho_w \left(\vec{V} - \vec{V}_b\right)\bullet \hat{n}dA$$

$$= -(\rho CA)_w \overline{T}_{cw2}\left[0 - \left(-\frac{d(L_{c1} + L_{c2})}{dt}\hat{n}\right)\right]\bullet \hat{n}$$

Term 3 $= -(\rho CA)_w \overline{T}_{cw2}\dfrac{d(L_{c1} + L_{c2})}{dt}$

Combining Terms 1, 2, and 3

$$(\rho CA)_w\left[L_{c3}\frac{d\overline{T}_{cw3}}{dt} + \overline{T}_{cw3}\frac{dL_{c3}}{dt}\right] = \overline{\alpha}_{co}\pi D_o L_{c3}\left(T_{ca} - \overline{T}_{cw3}\right) + \overline{\alpha}_{ci3}\pi D_i L_{c3}\left(\overline{T}_{cr3} - \overline{T}_{cw3}\right)$$

$$- (\rho CA)_w \overline{T}_{cw2}\frac{d(L_{c1} + L_{c2})}{dt}$$

Using the fact that the length of the condenser is constant $\dfrac{dL_{c3}}{dt} = -\dfrac{d(L_{c1} + L_{c2})}{dt}$

$$(\rho CA)_w L_{c3}\frac{d\overline{T}_{cw3}}{dt} - (\rho CA)_w \overline{T}_{cw3}\frac{d(L_{c1} + L_{c2})}{dt} = \overline{\alpha}_{co}\pi D_o L_{c3}\left(T_{ca} - \overline{T}_{cw3}\right)$$

$$+ \overline{\alpha}_{ci3}\pi D_i L_{c3}\left(\overline{T}_{cr3} - \overline{T}_{cw3}\right) - (\rho CA)_w \overline{T}_{cw2}\frac{d(L_{c1} + L_{c2})}{dt}$$

$$(\rho CA)_w L_{c3}\frac{d\overline{T}_{cw3}}{dt} + (\rho CA)_w\left[\overline{T}_{cw2} - \overline{T}_{cw3}\right]\frac{d(L_{c1} + L)_{c2}}{dt} = \overline{\alpha}_{co}\pi D_o L_{c3}\left(T_{ca} - \overline{T}_{cw3}\right)$$

$$+ \overline{\alpha}_{ci3}\pi D_i L_{c3}\left(\overline{T}_{cr3} - \overline{T}_{cw3}\right)$$

$$\boxed{\begin{aligned}(\rho CA)_w \frac{d\overline{T}_{cw3}}{dt} + (\rho CA)_w\left[\frac{\overline{T}_{cw2} - \overline{T}_{cw3}}{L_{c3}}\right]\frac{dL_{c1}}{dt} + (\rho CA)_w\left[\frac{\overline{T}_{cw2} - \overline{T}_{cw3}}{L_{c3}}\right]\frac{dL_{c2}}{dt} \\ = \overline{\alpha}_{co}\pi D_o\left(T_{ca} - \overline{T}_{cw3}\right) + \overline{\alpha}_{ci3}\pi D_i\left(\overline{T}_{cr3} - \overline{T}_{cw3}\right)\end{aligned}} \quad (2.21)$$

111

Overall Mass Balance of Condenser

From superheat region mass balance, equation (2.12)

$$\dot{m}_{c,\text{int}1} = \dot{m}_{c,in} - AL_{c1}\frac{d\rho_{c1}}{dt} - A[\rho_{c1} - \rho_{cv}]\frac{dL_{c1}}{dt}$$

From two-phase region mass balance, equation (2.13)

$$AL_{c2}\frac{d\rho_{c2}}{dt} + A[\rho_{c2} - \rho_{cL}]\frac{dL_{c2}}{dt} + A(\rho_{cv} - \rho_{cL})\frac{dL_{c1}}{dt} + \dot{m}_{c,\text{int}2} - \dot{m}_{c,\text{int}1} = 0$$

From subcool region mass balance, equation (2.14)

$$\dot{m}_{c,\text{int}2} = AL_{c3}\frac{d\rho_{cL}}{dt} + \dot{m}_{c,out}$$

Plugging results from the two single phase regions into the two-phase mass balance

$$AL_{c2}\frac{d\rho_{c2}}{dt} + A[\rho_{c2} - \rho_{cL}]\frac{dL_{c2}}{dt} + A(\rho_{cv} - \rho_{cL})\frac{dL_{c1}}{dt} + \dot{m}_{c,out} + AL_{c3}\frac{d\rho_{cL}}{dt} - \dot{m}_{c,in}$$

$$+ AL_{c1}\frac{d\rho_{c1}}{dt} + A[\rho_{c1} - \rho_{cv}]\frac{dL_{c1}}{dt} = 0$$

$$AL_{c2}\frac{d\rho_{c2}}{dt} + A[\rho_{c2} - \rho_{cL}]\frac{dL_{c2}}{dt} + A(\rho_{c1} - \rho_{cL})\frac{dL_{c1}}{dt} + AL_{c1}\frac{d\rho_{c1}}{dt} + AL_{c3}\frac{d\rho_{cL}}{dt} = \dot{m}_{c,in} - \dot{m}_{c,out}$$

If $\rho_{c1} = \rho(P_c, h_{c1})$ and assuming $\dfrac{dh_{c1}}{dt} = \dfrac{dh_{cv}}{dt}$, using the chain rule

$$\frac{d\rho_{c1}}{dt} = \frac{\partial\rho_{c1}}{\partial P_c}\frac{dP_c}{dt} + \frac{\partial\rho_{c1}}{\partial h_{c1}}\frac{dh_{cv}}{dt}.$$

Plugging this in to the mass balance equation

$$AL_{c2}\frac{d\rho_{c2}}{dt} + A[\rho_{c2} - \rho_{cL}]\frac{dL_{c2}}{dt} + A(\rho_{c1} - \rho_{cL})\frac{dL_{c1}}{dt} + AL_{c1}\left(\frac{\partial\rho_{c1}}{\partial P_c}\frac{dP_c}{dt} + \frac{\partial\rho_{c1}}{\partial h_{c1}}\frac{dh_{cv}}{dt}\right)$$

$$+ AL_{c3}\frac{d\rho_{cL}}{dt} = \dot{m}_{c,in} - \dot{m}_{c,out}$$

$$\boxed{A\left[L_{c3}\frac{d\rho_{cL}}{dP_c} + L_{c2}\frac{d\rho_{c2}}{dP_c} + L_{c1}\left(\frac{\partial\rho_{c1}}{\partial P_c} + \frac{\partial\rho_{c1}}{\partial h_{c1}}\frac{dh_{cv}}{dP_c}\right)\right]\frac{dP_c}{dt} + A[\rho_{c2} - \rho_{cL}]\frac{dL_{c2}}{dt}} \\ \boxed{+ A(\rho_{c1} - \rho_{cL})\frac{dL_{c1}}{dt} = \dot{m}_{c,in} - \dot{m}_{c,out}}$$
(2.15)

Appendix C - Derivation of Linear Modeling Equations

Evaporator Equations

Nonlinear equations with the left hand side expanded

from equation (2.7)

$$-A\left[(1-\bar{\gamma}_e)\rho_{eL}h_{efg}\right]\frac{dL_{e1}}{dt} + AL_{e1}\left[\rho_{e1}\frac{dh_{ev}}{dP_e} - (1-\bar{\gamma}_e)\frac{d\rho_{eL}h_{efg}}{dP_e} - \beta\right]\frac{dP_e}{dt} = f_{e1}$$

from equation (2.8)

$$-0.5A\rho_{e2}\left(h_{e,out} - h_{ev}\right)\frac{dL_{e1}}{dt} + AL_{e2}\left[0.5\rho_{e2}\frac{dh_{ev}}{dP_e} + 0.5(h_{e,out} - h_{ev})\frac{\partial\rho_{e2}}{\partial P_e} - \beta\right]\frac{dP_e}{dt}$$

$$+ 0.5AL_{e2}\left[\rho_{e2} + (h_{e,out} - h_{ev})\frac{\partial\rho_{e2}}{\partial h_{e,out}}\right]\frac{dh_{e,out}}{dt} = f_{e2}$$

from equation (2.6)

$$A[\rho_{e1} - \rho_{e2}]\frac{dL_{e1}}{dt} + A\left[L_{e2}\frac{\partial\rho_{e2}}{\partial P_e} + L_{e1}\frac{d\rho_{e1}}{dP_e}\right]\frac{dP_e}{dt} + AL_{e2}\frac{\partial\rho_{e2}}{\partial h_{e,out}}\frac{dh_{e,out}}{dt} = f_{e3}$$

from equation (2.9)

$$(\rho CA)_w\left[\frac{d\bar{T}_{ew1}}{dt}\right] = f_{e4}$$

from equation (2.10)

$$(\rho CA)_w\left[\frac{d\bar{T}_{ew2}}{dt} + \frac{(\bar{T}_{ew1} - \bar{T}_{ew2})}{L_{e2}}\frac{dL_{e1}}{dt}\right] = f_{e5}$$

The right hand sides of the nonlinear equations expanded

$$f_{e1} = \dot{m}_{e,in}\left(h_{e,in} - h_{ev}\right) + L_{e1}\pi D_i\bar{\alpha}_{ei1}\left(\bar{T}_{ew1} - \bar{T}_{er1}\right) \qquad \text{from equation (2.7)}$$

$$f_{e2} = L_{e2}\pi D_i\bar{\alpha}_{ei2}\left(\bar{T}_{ew2} - \bar{T}_{er2}\right) + \dot{m}_{e,out}\left(h_{ev} - h_{e,out}\right) \qquad \text{from equation (2.8)}$$

$$f_{e3} = \dot{m}_{e,in} - \dot{m}_{e,out} \qquad \text{from equation (2.6)}$$

$$f_{e4} = \bar{\alpha}_{eo}\pi D_o\left(T_{ea} - \bar{T}_{ew1}\right) + \bar{\alpha}_{ei1}\pi D_i\left(\bar{T}_{er1} - \bar{T}_{ew1}\right) \qquad \text{from equation (2.9)}$$

113

$$f_{e5} = \bar{\alpha}_{eo}\pi D_o\left(T_{ea} - \bar{T}_{ew2}\right) + \bar{\alpha}_{ei2}\pi D_i\left(\bar{T}_{er2} - \bar{T}_{ew2}\right) \qquad \text{from equation (2.10)}$$

States and inputs

$$x_e = \begin{bmatrix} L_{e1} & P_e & h_{e,out} & \bar{T}_{ew1} & \bar{T}_{ew2} \end{bmatrix}^T \qquad u_e = \begin{bmatrix} \dot{m}_{e,in} & h_{e,in} & \dot{m}_{e,out} & v_e \end{bmatrix}^T$$

Linearize f_{e1}

$$\delta f_{e1} = \pi D_i\bar{\alpha}_{ei1}\left(\bar{T}_{ew1} - T_{er1}\right)\delta L_{e1} + \left[-\dot{m}_{e,in}\frac{\partial h_{ev}}{\partial P_e} - L_{e1}\pi D_i\bar{\alpha}_{ei1}\frac{\partial T_{er1}}{\partial P_e}\right]\delta P_e + L_{e1}\pi D_i\bar{\alpha}_{ei1}\delta\bar{T}_{ew1}$$

$$+ \left(h_{e,in} - h_{ev}\right)\delta\dot{m}_{e,in} + \dot{m}_{e,in}\delta h_{e,in}$$

Linearize f_{e2}

$$\delta f_{e2} = \pi D_i\bar{\alpha}_{ei2}\left(\bar{T}_{ew2} - \bar{T}_{er2}\right)\frac{\partial L_{e2}}{\partial L_{e1}}\delta L_{e1} + \left[\dot{m}_{e,out}\frac{\partial h_{ev}}{\partial P_e} - L_{e2}\pi D_i\bar{\alpha}_{ei2}\frac{\partial\bar{T}_{er2}}{\partial P_e}\right]\delta P_e$$

$$+ \left[-\dot{m}_{e,out} - L_{e2}\pi D_i\bar{\alpha}_{ei2}\frac{\partial\bar{T}_{er2}}{\partial h_{e,out}}\right]\delta h_{e,out} + L_{e2}\pi D_i\bar{\alpha}_{ei2}\delta\bar{T}_{ew2} + \left(h_{ev} - h_{e,out}\right)\delta\dot{m}_{e,out}$$

Using the total length constraint

$$L_{e2} = L_{eT} - L_{e1} \qquad \frac{\partial L_{e2}}{\partial L_{e1}} = -1$$

Substituting this in

$$\delta f_{e2} = -\pi D_i\bar{\alpha}_{ei2}\left(\bar{T}_{ew2} - \bar{T}_{er2}\right)\delta L_{e1} + \left[\dot{m}_{e,out}\frac{\partial h_{ev}}{\partial P_e} - L_{e2}\pi D_i\bar{\alpha}_{ei2}\frac{\partial\bar{T}_{er2}}{\partial P_e}\right]\delta P_e$$

$$+ \left[-\dot{m}_{e,out} - L_{e2}\pi D_i\bar{\alpha}_{ei2}\frac{\partial\bar{T}_{er2}}{\partial h_{e,out}}\right]\delta h_{e,out} + L_{e2}\pi D_i\bar{\alpha}_{ei2}\delta\bar{T}_{ew2} + \left(h_{ev} - h_{e,out}\right)\delta\dot{m}_{e,out}$$

Linearize f_{e3}

$$\delta f_{e3} = \delta\dot{m}_{e,in} - \delta\dot{m}_{e,out}$$

Linearize f_{e4}

$$\delta f_{e4} = \left(\bar{\alpha}_{ei1}\pi D_i\frac{\partial T_{er1}}{\partial P_e}\right)\delta P_e + \left[-\bar{\alpha}_{ei1}\pi D_i - \bar{\alpha}_{eo}\pi D_o\right]\delta\bar{T}_{ew1} + \left[\pi D_o\left(T_{ea} - \bar{T}_{ew1}\right)\frac{\partial\bar{\alpha}_{eo}}{\partial v_e}\right]\delta v_e$$

Linearize f_{e5}

$$\delta f_{e5} = \left(\bar{\alpha}_{ei2}\pi D_i\frac{\partial\bar{T}_{er2}}{\partial P_e}\right)\delta P_e + \left(\bar{\alpha}_{ei2}\pi D_i\frac{\partial\bar{T}_{er2}}{\partial h_{e,out}}\right)\delta h_{e,out} + \left[-\bar{\alpha}_{ei2}\pi D_i - \bar{\alpha}_{eo}\pi D_o\right]\delta\bar{T}_{ew2}$$

$$+ \left[\pi D_o\left(T_{ea} - \bar{T}_{ew2}\right)\frac{\partial\bar{\alpha}_{eo}}{\partial v_e}\right]\delta v_e$$

Putting the equations into matrix form

$$D_e \dot{x}_e = f_e = \begin{bmatrix} f_{e1} \\ f_{e2} \\ f_{e3} \\ f_{e4} \\ f_{e5} \end{bmatrix}$$

Linearize the previous equation

$$D_e \left(\dot{x}_e + \delta \ \dot{x}_e \right) = f_e + A'_e \delta \ x_e + B'_e \delta \ u_e$$

$$\boxed{D_e \delta \ \dot{x}_e = A'_e \delta \ x_e + B'_e \delta \ u_e}$$ (2.23)

$$A'_e = \begin{bmatrix} a_{11}^E & a_{12}^E & 0 & a_{14}^E & 0 \\ a_{21}^E & a_{22}^E & a_{23}^E & 0 & a_{25}^E \\ 0 & 0 & 0 & 0 & 0 \\ 0 & a_{42}^E & 0 & a_{44}^E & 0 \\ 0 & a_{52}^E & a_{53}^E & 0 & a_{55}^E \end{bmatrix} \quad B'_e = \begin{bmatrix} b_{11}^E & b_{12}^E & 0 & 0 \\ 0 & 0 & b_{23}^E & 0 \\ 1 & 0 & -1 & 0 \\ 0 & 0 & 0 & b_{44}^E \\ 0 & 0 & 0 & b_{54}^E \end{bmatrix}$$

$$D_e = \begin{bmatrix} d_{11}^E & d_{12}^E & 0 & 0 & 0 \\ d_{21}^E & d_{22}^E & d_{23}^E & 0 & 0 \\ d_{31}^E & d_{32}^E & d_{33}^E & 0 & 0 \\ 0 & 0 & 0 & d_{44}^E & 0 \\ d_{51}^E & 0 & 0 & 0 & d_{55}^E \end{bmatrix}$$

Condenser Equations

Nonlinear equations with the left hand sides expanded

from equation (2.16)

$$AL_{c1}\left[\rho_{c1}\frac{dh_{cv}}{dP_c}+0.5\left(h_{c,in}-h_{cv}\right)\left(\frac{\partial\rho_{c1}}{\partial P_c}+\frac{\partial\rho_{c1}}{\partial hc1}\frac{dh_{cv}}{dP_c}\right)-\beta\right]\frac{dP_c}{dt}+0.5A\left(h_{c,in}-h_{cv}\right)\rho_{c1}\frac{dL_{c1}}{dt}=f_{c1}$$

from equation (2.17)

$$A\rho_{cL}h_{cfg}\frac{dL_{c1}}{dt}+A\bar{\gamma}_c\rho_{cL}h_{cfg}\frac{dL_{c2}}{dt}$$

$$+A\left\{L_{c2}\left[-\left(1-\bar{\gamma}_c\right)\frac{dh_{cfg}\,\rho_{cL}}{dP_c}+\rho_{c2}\frac{dh_{cv}}{dP_c}-\beta\right]+L_{c3}\left(h_{cL}-h_{cv}\right)\frac{d\rho_{cL}}{dP_c}\right\}\frac{dP_c}{dt}=f_{c2}$$

from equation (2.18)

$$0.5A\rho_{cL}\left[h_{cL}-h_{c,out}\right]\frac{dL_{c1}}{dt}+0.5A\rho_{cL}\left[h_{cL}-h_{c,out}\right]\frac{dL_{c2}}{dt}$$

$$+AL_{c3}\left[0.5\left(h_{c,out}-h_{cL}\right)\frac{d\rho_{cL}}{dP_c}+0.5\rho_{cL}\frac{dh_{cL}}{dP_c}-\beta\right]\frac{dP_c}{dt}+0.5AL_{c3}\rho_{cL}\frac{dh_{c,out}}{dt}=f_{c3}$$

from equation (2.15)

$$A\left[L_{c3}\frac{d\rho_{cL}}{dP_c}+L_{c2}\frac{d\rho_{c2}}{dP_c}+L_{c1}\left(\frac{\partial\rho_{c1}}{\partial P_c}+\frac{\partial\rho_{c1}}{\partial h_{c1}}\frac{dh_{cv}}{dP_c}\right)\right]\frac{dP_c}{dt}+A\left[\rho_{c2}-\rho_{cL}\right]\frac{dL_{c2}}{dt}+A\left(\rho_{c1}-\rho_{cL}\right)\frac{dL_{c1}}{dt}=f_{c4}$$

from equation (2.19)

$$\left(\rho CA\right)_w\left[\frac{d\bar{T}_{cw1}}{dt}+\frac{\left(\bar{T}_{cw1}-\bar{T}_{cw2}\right)}{L_{c1}}\frac{dL_{c1}}{dt}\right]=f_{c5}$$

from equation (2.20)

$$\left(\rho CA\right)_w\frac{d\bar{T}_{cw2}}{dt}=f_{c6}$$

from equation (2.21)

$$\left(\rho CA\right)_w\frac{d\bar{T}_{cw3}}{dt}+\left(\rho CA\right)_w\left[\frac{\bar{T}_{cw2}-\bar{T}_{cw3}}{L_{c3}}\right]\frac{dL_{c1}+L_{c2}}{dt}=f_{c7}$$

The right hand sides of the nonlinear equations expanded

$$f_{c1}=L_{c1}\pi D_i\bar{\alpha}_{ci1}\left(\bar{T}_{cw1}-\bar{T}_{cr1}\right)+\left(h_{c,in}-h_{cv}\right)\dot{m}_{c,in}\qquad\text{from equation (2.16)}$$

$$f_{c2}=\dot{m}_{c,out}h_{cfg}+\pi L_{c2}D_i\bar{\alpha}_{ci2}\left(\bar{T}_{cw2}-T_{cr2}\right)\qquad\text{from equation (2.17)}$$

$$f_{c3} = \dot{m}_{c,out}\left(h_{cL} - h_{c,out}\right) + \pi L_{c3} D_i \bar{\alpha}_{ci3}\left(\bar{T}_{cw3} - \bar{T}_{cr3}\right)$$ from equation (2.18)

$$f_{c4} = \dot{m}_{c,in} - \dot{m}_{c,out}$$ from equation (2.15)

$$f_{c5} = \bar{\alpha}_{co}\pi D_o\left(T_{ca} - \bar{T}_{cw1}\right) + \bar{\alpha}_{ci1}\pi D_i\left(\bar{T}_{cr1} - \bar{T}_{cw1}\right)$$ from equation (2.19)

$$f_{c6} = \bar{\alpha}_{co}\pi D_o\left(T_{ca} - \bar{T}_{cw2}\right) + \bar{\alpha}_{ci2}\pi D_i\left(T_{cr2} - \bar{T}_{cw2}\right)$$ from equation (2.20)

$$f_{c7} = \bar{\alpha}_{co}\pi D_o\left(T_{ca} - \bar{T}_{cw3}\right) + \bar{\alpha}_{ci3}\pi D_i\left(\bar{T}_{cr3} - \bar{T}_{cw3}\right)$$ from equation (2.21)

States and inputs

$$x_c = \begin{bmatrix} L_{c1} & L_{c2} & P_c & h_{c,out} & \bar{T}_{cw1} & \bar{T}_{cw2} & \bar{T}_{cw3} \end{bmatrix}^T \qquad u_c = \begin{bmatrix} \dot{m}_{c,in} & h_{c,in} & \dot{m}_{c,out} & v_c \end{bmatrix}^T$$

Linearize f_{c1}

$$\delta f_{c1} = \pi D_i \bar{\alpha}_{ci1}\left(\bar{T}_{cw1} - \bar{T}_{cr1}\right)\delta L_{c1} + \left[-\dot{m}_{c,in}\frac{\partial h_{cv}}{\partial P_c} - L_{c1}\pi D_i \bar{\alpha}_{ci1}\left(\frac{\partial \bar{T}_{cr1}}{\partial P_c} + \frac{\partial \bar{T}_{cr1}}{\partial h_{c1}}\frac{\partial h_{cv}}{\partial P_c}\right)\right]\delta P_c$$

$$+ L_{c1}\pi D_i \bar{\alpha}_{ci1}\delta \bar{T}_{cw1} + \left(h_{c,in} - h_{cv}\right)\delta \dot{m}_{c,in} + \dot{m}_{c,in}\delta h_{c,in}$$

This is assuming $\delta h_{c,in} = \dfrac{\partial h_{cv}}{\partial P_c}\delta P_c$ and $\dfrac{\partial \bar{T}_{cr1}}{\partial h_{c,in}} = \dfrac{\partial \bar{T}_{cr1}}{\partial h_{c1}}$

Linearize f_{c2}

$$\delta f_{c2} = \pi D_i \bar{\alpha}_{ci2}\left(\bar{T}_{cw2} - T_{cr2}\right)\delta L_{c2} + \left[\dot{m}_{c,out}\frac{\partial h_{cfg}}{\partial P_c} - \pi L_{c2} D_i \bar{\alpha}_{ci2}\frac{\partial T_{cr2}}{\partial P_c}\right]\delta P_c$$

$$+ \pi L_{c2} D_i \bar{\alpha}_{ci2}\delta \bar{T}_{cw2} + h_{cfg}\delta \dot{m}_{c,out}$$

Linearize f_{c3}

$$\delta f_{c3} = D_i \bar{\alpha}_{ci3}\pi\left(\bar{T}_{cw3} - \bar{T}_{cr3}\right)\left(\frac{\partial L_{c3}}{\partial L_{c1}}\delta L_{c1} + \frac{\partial L_{c3}}{\partial L_{c2}}\delta L_{c2}\right) + \left[\dot{m}_{c,out}\frac{\partial h_{cL}}{\partial P_c} - \pi L_{c3} D_i \bar{\alpha}_{ci3}\frac{\partial \bar{T}_{cr3}}{\partial P_c}\right]\delta P_c$$

$$+ \left[-\dot{m}_{c,out} - \pi L_{c3} D_i \bar{\alpha}_{ci3}\frac{\partial \bar{T}_{cr3}}{\partial h_{c,out}}\right]\delta h_{c,out} + \pi L_{c3} D_i \bar{\alpha}_{ci3}\delta \bar{T}_{cw3} + \left(h_{cL} - h_{c,out}\right)\delta \dot{m}_{c,out}$$

Using the total length contraint

$$L_{c3} = L_{cT} - \left(L_{c1} + L_{c2}\right) \qquad \frac{\partial L_{c3}}{\partial L_{c1}} = \frac{\partial L_{c3}}{\partial L_{c2}} = -1$$

117

Plugging this in

$$\delta f_{c3} = D_i \overline{\alpha}_{ci3} \pi \left(\overline{T}_{cw3} - \overline{T}_{cr3} \right) \left(- \delta L_{c1} - \delta L_{c2} \right) + \left[\dot{m}_{c,out} \frac{\partial h_{cL}}{\partial P_c} - \pi L_{c3} D_i \overline{\alpha}_{ci3} \frac{\partial \overline{T}_{cr3}}{\partial P_c} \right] \delta P_c$$

$$+ \left[- \dot{m}_{c,out} - \pi L_{c3} D_i \overline{\alpha}_{ci3} \frac{\partial \overline{T}_{cr3}}{\partial h_{c,out}} \right] \delta h_{c,out} + \pi L_{c3} D_i \overline{\alpha}_{ci3} \delta \overline{T}_{cw3} + \left(h_{cL} - h_{c,out} \right) \delta \dot{m}_{c,out}$$

Linearize f_{c4}

$$\delta f_{c4} = \delta \dot{m}_{c,in} - \delta \dot{m}_{c,out}$$

Linearize f_{c5}

$$\delta f_{c5} = \overline{\alpha}_{ci1} \pi D_i \left(\frac{\partial \overline{T}_{cr1}}{\partial P_c} + \frac{\partial \overline{T}_{cr1}}{\partial h_{c1}} \frac{\partial h_{c1}}{\partial P_c} \right) \delta P_c + \left[- \overline{\alpha}_{ci1} \pi D_i - \overline{\alpha}_{co} \pi D_o \right] \delta \overline{T}_{cw1} + \pi D_o \left(T_{ca} - \overline{T}_{cw1} \right) \frac{\partial \overline{\alpha}_{co}}{\partial v_c} \delta v_c$$

This is assuming $\delta h_{c,in} = \frac{\partial h_{cv}}{\partial P_c} \delta P_c$ and $\frac{\partial \overline{T}_{cr1}}{\partial h_{c,in}} = \frac{\partial \overline{T}_{cr1}}{\partial h_{c1}}$

Linearize f_{c6}

$$\delta f_{c6} = \overline{\alpha}_{ci2} \pi D_i \frac{\partial T_{cr2}}{\partial P_c} \delta P_c + \left[- \overline{\alpha}_{ci2} \pi D_i - \overline{\alpha}_{co} \pi D_o \right] \delta \overline{T}_{cw2} + \pi D_o \left(T_{ca} - \overline{T}_{cw2} \right) \frac{\partial \overline{\alpha}_{co}}{\partial v_c} \delta v_c$$

Linearize f_{c7}

$$\delta f_{c7} = \overline{\alpha}_{ci3} \pi D_i \frac{\partial \overline{T}_{cr3}}{\partial P_c} \delta P_c + \overline{\alpha}_{ci3} \pi D_i \frac{\partial \overline{T}_{cr3}}{\partial h_{c,out}} \delta h_{c,out} + \left[- \overline{\alpha}_{ci3} \pi D_i - \overline{\alpha}_{co} \pi D_o \right] \delta \overline{T}_{cw3}$$

$$+ \pi D_o \left(T_{ca} - \overline{T}_{cw3} \right) \frac{\partial \overline{\alpha}_{co}}{\partial v_c} \delta v_c$$

Putting the equations into matrix form

$$D_c \dot{x}_c = f_c = \begin{bmatrix} f_{c1} & f_{c2} & f_{c3} & f_{c4} & f_{c5} & f_{c6} & f_{c7} \end{bmatrix}^T$$

Linearize the previous equation

$$D_c \left(\dot{x}_c + \delta \dot{x}_c \right) = f_c + A'_c \delta x_c + B'_c \delta u_c$$

$$\boxed{D_c \delta \dot{x}_c = A'_c \delta x_c + B'_c \delta u_c} \qquad (2.24)$$

118

$$
A'_c = \begin{bmatrix}
a_{11}^C & 0 & a_{13}^C & 0 & a_{15}^C & 0 & 0 \\
0 & a_{22}^C & a_{23}^C & 0 & 0 & a_{26}^C & 0 \\
a_{31}^C & a_{32}^C & a_{33}^C & a_{34}^C & 0 & 0 & a_{37}^C \\
0 & 0 & 0 & 0 & 0 & 0 & 0 \\
0 & 0 & a_{53}^C & 0 & a_{55}^C & 0 & 0 \\
0 & 0 & a_{63}^C & 0 & 0 & a_{66}^C & 0 \\
0 & 0 & a_{73}^C & a_{74}^C & 0 & 0 & a_{77}^C
\end{bmatrix}
\qquad
B'_c = \begin{bmatrix}
b_{11}^C & b_{12}^C & 0 & 0 \\
0 & 0 & b_{23}^C & 0 \\
0 & 0 & b_{33}^C & 0 \\
1 & 0 & -1 & 0 \\
0 & 0 & 0 & b_{54}^C \\
0 & 0 & 0 & b_{64}^C \\
0 & 0 & 0 & b_{74}^C
\end{bmatrix}
$$

$$
D_c = \begin{bmatrix}
d_{11}^C & 0 & d_{13}^C & 0 & 0 & 0 & 0 \\
d_{21}^C & d_{22}^C & d_{23}^C & 0 & 0 & 0 & 0 \\
d_{31}^C & d_{32}^C & d_{33}^C & d_{34}^C & 0 & 0 & 0 \\
d_{41}^C & d_{42}^C & d_{43}^C & 0 & 0 & 0 & 0 \\
d_{51}^C & 0 & 0 & 0 & d_{55}^C & 0 & 0 \\
0 & 0 & 0 & 0 & 0 & d_{66}^C & 0 \\
d_{71}^C & d_{72}^C & 0 & 0 & 0 & 0 & d_{77}^C
\end{bmatrix}
$$

Complete Model

Fold δf_{e1} into complete model using $\quad \delta \dot{m}_{e,in} = \delta \dot{m}_{valve} = k_{11}\delta P_e + k_{12}\delta P_c + k_{13}\delta u_{valve}$

$$\delta h_{e,in} = \delta h_{c,out}$$

$$\delta f_{e1} = a_{11}^E \delta L_{e1} + a_{12}^E \delta P_e + a_{14}^E \delta T_{ew1} + b_{11}^E \delta \dot{m}_{e,in} + b_{12}^E \delta h_{e,in}$$

$$\delta f_{e1} = a_{11}^E \delta L_{e1} + a_{12}^E \delta P_e + a_{14}^E \delta T_{ew1} + b_{11}^E \left(k_{11}\delta P_e + k_{12}\delta P_c + k_{13}\delta u_{valve}\right) + b_{12}^E \delta h_{c,out}$$

$$\delta f_{e1} = a_{11}^E \delta L_{e1} + \left(a_{12}^E + b_{11}^E k_{11}\right)\delta P_e + a_{14}^E \delta T_{ew1} + b_{11}^E k_{12}\delta P_c + b_{11}^E k_{13}\delta u_{valve} + b_{12}^E \delta h_{c,out}$$

Fold δf_{e2} into complete model using $\quad \delta \dot{m}_{e,out} = \delta \dot{m}_{comp} = k_{31}\delta P_e + k_{32}\delta P_c + k_{33}\delta u_{comp}$

$$\delta f_{e2} = a_{21}^E \delta L_{e1} + a_{22}^E \delta P_e + a_{23}^E \delta h_{e,out} + a_{25}^E \delta \overline{T}_{ew2} + b_{23}^E \delta \dot{m}_{e,out}$$

$$\delta f_{e2} = a_{21}^E \delta L_{e1} + a_{22}^E \delta P_e + a_{23}^E \delta h_{e,out} + a_{25}^E \delta \overline{T}_{ew2} + b_{23}^E \left(k_{31}\delta P_e + k_{32}\delta P_c + k_{33}\delta u_{comp}\right)$$

$$\delta f_{e2} = a_{21}^E \delta L_{e1} + \left(a_{22}^E + b_{23}^E k_{31}\right)\delta P_e + a_{23}^E \delta h_{e,out} + a_{25}^E \delta \overline{T}_{ew2} + b_{23}^E k_{32}\delta P_c + b_{23}^E k_{33}\delta u_{comp}$$

Fold δf_{e3} into complete model using $\quad \delta \dot{m}_{e,out} = \delta \dot{m}_{comp} = k_{31}\delta P_e + k_{32}\delta P_c + k_{33}\delta u_{comp}$

$$\delta \dot{m}_{e,in} = \delta \dot{m}_{valve} = k_{11}\delta P_e + k_{12}\delta P_c + k_{13}\delta u_{valve}$$

$$\delta f_{e3} = \delta \dot{m}_{e,in} - \delta \dot{m}_{e,out}$$

$$\delta f_{e3} = k_{11}\delta P_e + k_{12}\delta P_c + k_{13}\delta u_{valve} - k_{31}\delta P_e - k_{32}\delta P_c - k_{33}\delta u_{comp}$$

$$\delta f_{e3} = \left(k_{11} - k_{31}\right)\delta P_e + \left(k_{12} - k_{32}\right)\delta P_c + k_{13}\delta u_{valve} - k_{33}\delta u_{comp}$$

δf_{e4} and δf_{e5} require no modifications for complete model

$$\delta f_{e4} = a_{42}^E \delta P_e + a_{44}^E \delta \overline{T}_{ew1} + b_{44}^E \delta v_e$$

$$\delta f_{e5} = a_{52}^E \delta P_e + a_{53}^E \delta h_{e,out} + a_{55}^E \delta \overline{T}_{ew2} + b_{54}^E \delta v_e$$

Fold δf_{c1} into complete model using $\quad \delta \dot{m}_{c,in} = \delta \dot{m}_{comp} = k_{31}\delta P_e + k_{32}\delta P_c + k_{33}\delta u_{comp}$

$$\delta h_{c,in} = k_{21}\delta P_e + k_{22}\delta P_c + k_{23}\delta h_{e,out}$$

$$\delta f_{c1} = a_{11}^C \delta L_{c1} + a_{13}^C \delta P_c + a_{15}^C \delta \bar{T}_{cw1} + b_{11}^C \delta \dot{m}_{c,in} + b_{12}^C \delta h_{c,in}$$

$$\delta f_{c1} = a_{11}^C \delta L_{c1} + a_{13}^C \delta P_c + a_{15}^C \delta \bar{T}_{cw1} + b_{11}^C \left(k_{31}\delta P_e + k_{32}\delta P_c + k_{33}\delta u_{comp}\right)$$
$$+ b_{12}^C \left(k_{21}\delta P_e + k_{22}\delta P_c + k_{23}\delta h_{e,out}\right)$$

$$\delta f_{c1} = a_{11}^C \delta L_{c1} + \left(a_{13}^C + b_{11}^C k_{32} + b_{12}^C k_{22}\right)\delta P_c + a_{15}^C \delta \bar{T}_{cw1} + b_{11}^C k_{33}\delta u_{comp}$$
$$+ b_{12}^C k_{23}\delta h_{e,out} + \left(b_{11}^C k_{31} + b_{12}^C k_{21}\right)\delta P_e$$

Fold δf_{c2} into complete model using $\quad \delta \dot{m}_{c,out} = \delta \dot{m}_{valve} = k_{11}\delta P_e + k_{12}\delta P_c + k_{13}\delta u_{valve}$

$$\delta f_{c2} = a_{22}^C \delta L_{c2} + a_{23}^C \delta P_c + a_{26}^C \delta \bar{T}_{cw2} + b_{23}^C \delta \dot{m}_{c,out}$$

$$\delta f_{c2} = a_{22}^C \delta L_{c2} + a_{23}^C \delta P_c + a_{26}^C \delta \bar{T}_{cw2} + b_{23}^C (k_{11}\delta P_e + k_{12}\delta P_c + k_{13}\delta u_{valve})$$

$$\delta f_{c2} = a_{22}^C \delta L_{c2} + \left(a_{23}^C + b_{23}^C k_{12}\right)\delta P_c + a_{26}^C \delta \bar{T}_{cw2} + b_{23}^C k_{13}\delta u_{valve} + b_{23}^C k_{11}\delta P_e$$

Fold δf_{c3} into complete model using $\quad \delta \dot{m}_{c,out} = \delta \dot{m}_{valve} = k_{11}\delta P_e + k_{12}\delta P_c + k_{13}\delta u_{valve}$

$$\delta f_{c3} = a_{31}^C \delta L_{c1} + a_{32}^C \delta L_{c2} + a_{33}^C \delta P_c + a_{34}^C \delta h_{c,out} + a_{37}^C \delta \bar{T}_{cw3} + b_{33}^C \delta \dot{m}_{c,out}$$

$$\delta f_{c3} = a_{31}^C \delta L_{c1} + a_{32}^C \delta L_{c2} + a_{33}^C \delta P_c + a_{34}^C \delta h_{c,out} + a_{37}^C \delta \bar{T}_{cw3}$$
$$+ b_{33}^C (k_{11}\delta P_e + k_{12}\delta P_c + k_{13}\delta u_{valve})$$

$$\delta f_{c3} = a_{31}^C \delta L_{c1} + a_{32}^C \delta L_{c2} + \left(a_{33}^C + b_{33}^C k_{12}\right)\delta P_c + a_{34}^C \delta h_{c,out} + a_{37}^C \delta \bar{T}_{cw3} + b_{33}^C k_{13}\delta u_{valve} + b_{33}^C k_{11}\delta P_e$$

Fold δf_{c3} into complete model using $\quad \delta \dot{m}_{c,out} = \delta \dot{m}_{valve} = k_{11}\delta P_e + k_{12}\delta P_c + k_{13}\delta u_{valve}$

$$\delta \dot{m}_{c,in} = \delta \dot{m}_{comp} = k_{31}\delta P_e + k_{32}\delta P_c + k_{33}\delta u_{comp}$$

$$\delta f_{c4} = \delta \dot{m}_{c,in} - \delta \dot{m}_{c,out}$$

$$\delta f_{c4} = k_{31}\delta P_e + k_{32}\delta P_c + k_{33}\delta u_{comp} - k_{11}\delta P_e - k_{12}\delta P_c - k_{13}\delta u_{valve}$$

$$\delta f_{c4} = (k_{31} - k_{11})\delta P_e + (k_{32} - k_{12})\delta P_c + k_{33}\delta u_{comp} - k_{13}\delta u_{valve}$$

δf_{c5}, δf_{c6} and δf_{e7} require no modifications for complete model

$$\delta f_{c5} = a_{53}^C \delta P_c + a_{55}^C \delta \overline{T}_{cw1} + b_{54}^C \delta v_c$$

$$\delta f_{c6} = a_{63}^C \delta P_c + a_{66}^C \delta \overline{T}_{cw2} + b_{64}^C \delta v_c$$

$$\delta f_{c7} = a_{73}^C \delta P_c + a_{74}^C \delta h_{c,out} + a_{77}^C \delta \overline{T}_{cw3} + b_{74}^C \delta v_c$$

Express the linear model of the evaporator in terms of the evaporator and condenser states and system inputs in matrix form

$$D_e \delta \dot{x}_e = A_e \delta x_e + B'_e \delta u_e = A'_{ee} \delta x_e + A'_{ec} \delta x_c + B'_e \delta u$$

$$D_e \delta \dot{x}_e = A'_{ee} \delta x_e + A'_{ec} \delta x_c + B'_{ee} \delta u$$

$$\delta \dot{x}_e = D_e^{-1} A'_{ee} \delta x_e + D_e^{-1} A'_{ec} \delta x_c + D_e^{-1} B'_{ee} \delta u$$

$$\delta \dot{x}_e = A_{ee} \delta x_e + A_{ec} \delta x_c + B_{ee} \delta u$$

Express the linear model of the condenser in terms of the evaporator and condenser states and system inputs in matrix form

$$D_c \delta \dot{x}_c = A'_c \delta x_c + B'_c \delta u_c = A'_{cc} \delta x_c + A'_{ce} \delta x_e + B'_{cc} \delta u$$

$$D_c \delta \dot{x}_c = A'_{cc} \delta x_c + A'_{ce} \delta x_e + B'_{cc} \delta u$$

$$\delta \dot{x}_c = D_c^{-1} A'_{cc} \delta x_c + D_c^{-1} A'_{ce} \delta x_e + D_c^{-1} B'_{cc} \delta u$$

$$\delta \dot{x}_c = A_{cc} \delta x_c + A_{ce} \delta x_e + B_{cc} \delta u$$

System states and inputs

$$\delta x = \begin{bmatrix} \delta x_e \\ \delta x_c \end{bmatrix} \qquad \delta u = \begin{bmatrix} \delta u_{comp} & \delta u_{valve} & \delta v_e & \delta v_c \end{bmatrix}^T$$

System linear modeling equations

$$\delta \dot{x} = \begin{bmatrix} A_{ee} & A_{ec} \\ A_{ce} & A_{cc} \end{bmatrix} \delta x + \begin{bmatrix} B_{ee} \\ B_{cc} \end{bmatrix} \delta u \tag{2.28}$$

$$A'_{cc} = \begin{bmatrix} a_{11}^C & 0 & \left(a_{13}^C + b_{11}^C k_{32} + b_{12}^C k_{22}\right) & 0 & a_{15}^C & 0 & 0 \\ 0 & a_{22}^C & \left(a_{23}^C + b_{23}^C k_{12}\right) & 0 & 0 & a_{26}^C & 0 \\ a_{31}^C & a_{32}^C & \left(a_{33}^C + b_{33}^C k_{12}\right) & a_{34}^C & 0 & 0 & a_{37}^C \\ 0 & 0 & \left(k_{32} - k_{12}\right) & 0 & 0 & 0 & 0 \\ 0 & 0 & a_{53}^C & 0 & a_{55}^C & 0 & 0 \\ 0 & 0 & a_{63}^C & 0 & 0 & a_{66}^C & 0 \\ 0 & 0 & a_{73}^C & a_{74}^C & 0 & 0 & a_{77}^C \end{bmatrix}$$

$$A'_{ce} = \begin{bmatrix} 0 & \left(b_{11}^C k_{31} + b_{12}^C k_{21}\right) & b_{12}^C k_{23} & 0 & 0 \\ 0 & b_{23}^C k_{11} & 0 & 0 & 0 \\ 0 & b_{33}^C k_{11} & 0 & 0 & 0 \\ 0 & \left(k_{31} - k_{11}\right) & 0 & 0 & 0 \\ 0 & 0 & 0 & 0 & 0 \\ 0 & 0 & 0 & 0 & 0 \\ 0 & 0 & 0 & 0 & 0 \end{bmatrix}$$

$$A'_{ee} = \begin{bmatrix} a_{11}^E & \left(a_{12}^E + b_{11}^E k_{11}\right) & 0 & a_{14}^E & 0 \\ a_{21}^E & \left(a_{22}^E + b_{23}^E k_{31}\right) & a_{23}^E & 0 & a_{25}^E \\ 0 & \left(k_{11} - k_{31}\right) & 0 & 0 & 0 \\ 0 & a_{42}^E & 0 & a_{44}^E & 0 \\ 0 & a_{52}^E & a_{53}^E & 0 & a_{55}^E \end{bmatrix}$$

$$A'_{ec} = \begin{bmatrix} 0 & 0 & b_{11}^E k_{12} & b_{12}^E & 0 & 0 & 0 \\ 0 & 0 & b_{23}^E k_{32} & 0 & 0 & 0 & 0 \\ 0 & 0 & \left(k_{12} - k_{32}\right) & 0 & 0 & 0 & 0 \\ 0 & 0 & 0 & 0 & 0 & 0 & 0 \\ 0 & 0 & 0 & 0 & 0 & 0 & 0 \end{bmatrix}$$

$$B'_{cc} = \begin{bmatrix} b_{11}^C k_{33} & 0 & 0 & 0 \\ 0 & b_{23}^C k_{13} & 0 & 0 \\ 0 & b_{33}^C k_{13} & 0 & 0 \\ k_{33} & -k_{13} & 0 & 0 \\ 0 & 0 & 0 & b_{54}^C \\ 0 & 0 & 0 & b_{64}^C \\ 0 & 0 & 0 & b_{74}^C \end{bmatrix} \qquad B'_{ee} = \begin{bmatrix} 0 & b_{11}^E k_{13} & 0 & 0 \\ b_{23}^E k_{33} & 0 & 0 & 0 \\ -k_{33} & k_{13} & 0 & 0 \\ 0 & 0 & b_{44}^E & 0 \\ 0 & 0 & b_{54}^E & 0 \end{bmatrix}$$

Evaporator Matrix Elements

$$a_{11}^E = \pi D_i \bar{\alpha}_{ei1} \left(\bar{T}_{ew1} - T_{er1} \right)$$

$$a_{12}^E = \left[-\dot{m}_{e,in} \frac{\partial h_{ev}}{\partial P_e} - L_{e1} \pi D_i \bar{\alpha}_{ei1} \frac{\partial T_{er1}}{\partial P_e} \right]$$

$$a_{14}^E = L_{e1} \pi D_i \bar{\alpha}_{ei1}$$

$$a_{21}^E = -\pi D_i \bar{\alpha}_{ei2} \left(\bar{T}_{ew2} - \bar{T}_{er2} \right)$$

$$a_{22}^E = \left[\dot{m}_{e,out} \frac{\partial h_{ev}}{\partial P_e} - L_{e2} \pi D_i \bar{\alpha}_{ei2} \frac{\partial \bar{T}_{er2}}{\partial P_e} \right]$$

$$a_{23}^E = -\left[\dot{m}_{e,out} + L_{e2} \pi D_i \bar{\alpha}_{ei2} \frac{\partial \bar{T}_{er2}}{\partial h_{e,out}} \right]$$

$$a_{25}^E = L_{e2} \pi D_i \bar{\alpha}_{ei2}$$

$$a_{42}^E = \left(\bar{\alpha}_{ei1} \pi D_i \frac{\partial T_{er1}}{\partial P_e} \right)$$

$$a_{44}^E = -\left[\bar{\alpha}_{ei1} \pi D_i + \bar{\alpha}_{eo} \pi D_o \right]$$

$$a_{52}^E = \left(\bar{\alpha}_{ei2} \pi D_i \frac{\partial \bar{T}_{er2}}{\partial P_e} \right)$$

$$a_{53}^E = \left(\bar{\alpha}_{ei2} \pi D_i \frac{\partial \bar{T}_{er2}}{\partial h_{e,out}} \right)$$

$$a_{55}^E = -\left[\bar{\alpha}_{ei2} \pi D_i + \bar{\alpha}_{eo} \pi D_o \right]$$

$$b_{11}^E = \left(h_{e,in} - h_{ev} \right)$$

$$b_{12}^E = \dot{m}_{e,in}$$

$$b_{23}^E = \left(h_{ev} - h_{e,out} \right)$$

$$b_{44}^E = \left[\pi D_o \left(T_{ea} - \bar{T}_{ew1} \right) \frac{\partial \bar{\alpha}_{eo}}{\partial v_e} \right]$$

$$b_{54}^E = \left[\pi D_o \left(T_{ea} - \bar{T}_{ew2} \right) \frac{\partial \bar{\alpha}_{eo}}{\partial v_e} \right]$$

$$d_{11}^E = -A \left[\left(1 - \bar{\gamma}_e \right) \rho_{eL} h_{efg} \right]$$

$$d_{12}^E = A L_{e1} \left[\rho_{e1} \frac{dh_{ev}}{dP_e} - \left(1 - \bar{\gamma}_e \right) \frac{d\rho_{eL} h_{efg}}{dP_e} - 1 \right]$$

$$d_{21}^E = -0.5 A \rho_{e2} \left(h_{e,out} - h_{ev} \right)$$

$$d_{22}^E = A L_{e2} \left[\begin{array}{l} 0.5 \rho_{e2} \dfrac{dh_{ev}}{dP_e} \\[2mm] + 0.5 \left(h_{e,out} - h_{ev} \right) \dfrac{\partial \rho_{e2}}{\partial P_e} - 1 \end{array} \right]$$

$$d_{23}^E = 0.5 A L_{e2} \left[\rho_{e2} + \left(h_{e,out} - h_{ev} \right) \frac{\partial \rho_{e2}}{\partial h_{e,out}} \right]$$

$$d_{31}^E = A \left[\rho_{e1} - \rho_{e2} \right]$$

$$d_{32}^E = A \left[L_{e2} \frac{\partial \rho_{e2}}{\partial P_e} + L_{e1} \frac{d\rho_{e1}}{dP_e} \right]$$

$$d_{33}^E = A L_{e2} \frac{\partial \rho_{e2}}{\partial h_{e,out}}$$

$$d_{44}^E = \left(\rho C A \right)_w$$

$$d_{51}^E = \left(\rho C A \right)_w \frac{\left(\bar{T}_{ew1} - \bar{T}_{ew2} \right)}{L_{e2}}$$

$$d_{55}^E = \left(\rho C A \right)_w$$

Condenser Matrix Elements

$$a_{11}^C = \pi D_i \overline{\alpha}_{ci1} \left(\overline{T}_{cw1} - \overline{T}_{cr1} \right)$$

$$a_{13}^C = - \begin{bmatrix} \dot{m}_{c,in} \dfrac{\partial h_{cv}}{\partial P_c} \\ + L_{c1} \pi D_i \overline{\alpha}_{ci1} \left(\dfrac{\partial \overline{T}_{cr1}}{\partial P_c} + \dfrac{\partial \overline{T}_{cr1}}{\partial h_{c1}} \dfrac{\partial h_{cv}}{\partial P_c} \right) \end{bmatrix}$$

$$a_{15}^C = L_{c1} \pi D_i \overline{\alpha}_{ci1}$$

$$a_{22}^C = \pi D_i \overline{\alpha}_{ci2} \left(\overline{T}_{cw2} - T_{cr2} \right)$$

$$a_{23}^C = \left[\dot{m}_{c,out} \dfrac{\partial h_{cfg}}{\partial P_c} - \pi L_{c2} D_i \overline{\alpha}_{ci2} \dfrac{\partial T_{cr2}}{\partial P_c} \right]$$

$$a_{26}^C = \pi L_{c2} D_i \overline{\alpha}_{ci2}$$

$$a_{31}^C = -D_i \overline{\alpha}_{ci3} \pi \left(\overline{T}_{cw3} - \overline{T}_{cr3} \right)$$

$$a_{32}^C = -D_i \overline{\alpha}_{ci3} \pi \left(\overline{T}_{cw3} - \overline{T}_{cr3} \right)$$

$$a_{33}^C = \left[\dot{m}_{c,out} \dfrac{\partial h_{cL}}{\partial P_c} - \pi L_{c3} D_i \overline{\alpha}_{ci3} \dfrac{\partial \overline{T}_{cr3}}{\partial P_c} \right]$$

$$a_{34}^C = - \left[\dot{m}_{c,out} + \pi L_{c3} D_i \overline{\alpha}_{ci3} \dfrac{\partial \overline{T}_{cr3}}{\partial h_{c,out}} \right]$$

$$a_{37}^C = \pi L_{c3} D_i \overline{\alpha}_{ci3}$$

$$a_{53}^C = \overline{\alpha}_{ci1} \pi D_i \left(\dfrac{\partial \overline{T}_{cr1}}{\partial P_c} + \dfrac{\partial \overline{T}_{cr1}}{\partial h_{c1}} \dfrac{\partial h_{cv}}{\partial P_c} \right)$$

$$a_{55}^C = - \left[\overline{\alpha}_{ci1} \pi D_i + \overline{\alpha}_{co} \pi D_o \right]$$

$$a_{63}^C = \overline{\alpha}_{ci2} \pi D_i \dfrac{\partial T_{cr2}}{\partial P_c}$$

$$a_{66}^C = - \left[\overline{\alpha}_{ci2} \pi D_i + \overline{\alpha}_{co} \pi D_o \right]$$

$$a_{73}^C = \overline{\alpha}_{ci3} \pi D_i \dfrac{\partial \overline{T}_{cr3}}{\partial P_c}$$

$$a_{74}^C = \overline{\alpha}_{ci3} \pi D_i \dfrac{\partial \overline{T}_{cr3}}{\partial h_{c,out}}$$

$$a_{77}^C = - \left[\overline{\alpha}_{ci3} \pi D_i + \overline{\alpha}_{co} \pi D_o \right]$$

$$b_{11}^C = \left(h_{c,in} - h_{cv} \right)$$

$$b_{12}^C = \dot{m}_{c,in}$$

$$b_{23}^C = h_{cfg}$$

$$b_{33}^C = \left(h_{cL} - h_{c,out} \right)$$

$$b_{54}^C = \pi D_o \left(T_{ca} - \overline{T}_{cw1} \right) \dfrac{\partial \overline{\alpha}_{co}}{\partial v_c}$$

$$b_{64}^C = \pi D_o \left(T_{ca} - \overline{T}_{cw2} \right) \dfrac{\partial \overline{\alpha}_{co}}{\partial v_c}$$

$$b_{74}^C = \pi D_o \left(T_{ca} - \overline{T}_{cw3} \right) \dfrac{\partial \overline{\alpha}_{co}}{\partial v_c}$$

$$d_{11}^C = 0.5A(h_{c,in} - h_{cv})\rho_{c1}$$

$$d_{13}^C = AL_{c1}\left[\rho_{c1}\frac{dh_{cv}}{dP_c} + 0.5(h_{c,in} - h_{cv})\left(\frac{\partial\rho_{c1}}{\partial P_c} + \frac{\partial\rho_{c1}}{\partial hc1}\frac{dh_{cv}}{dP_c}\right) - 1\right]$$

$$d_{21}^C = A\rho_{cL}h_{cfg}$$

$$d_{22}^C = A\bar{\gamma}_c\rho_{cL}h_{cfg}$$

$$d_{23}^C = A\left\{L_{c2}\left[-(1-\bar{\gamma}_c)\frac{dh_{cfg}\,\rho_{cL}}{dP_c} + \rho_{c2}\frac{dh_{cv}}{dP_c} - 1\right] + L_{c3}(h_{cL} - h_{cv})\frac{d\rho_{cL}}{dP_c}\right\}$$

$$d_{31}^C = 0.5A\rho_{cL}\left[h_{cL} - h_{c,out}\right]$$

$$d_{32}^C = 0.5A\rho_{cL}\left[h_{cL} - h_{c,out}\right]$$

$$d_{33}^C = AL_{c3}\left[0.5(h_{c,out} - h_{cL})\frac{d\rho_{cL}}{dP_c} + 0.5\rho_{cL}\frac{dh_{cL}}{dP_c} - 1\right]$$

$$d_{34}^C = 0.5AL_{c3}\rho_{cL}$$

$$d_{41}^C = A(\rho_{c1} - \rho_{cL})$$

$$d_{42}^C = A[\rho_{c2} - \rho_{cL}]$$

$$d_{43}^C = A\left[L_{c3}\frac{d\rho_{cL}}{dP_c} + L_{c2}\frac{d\rho_{c2}}{dP_c} + L_{c1}\left(\frac{\partial\rho_{c1}}{\partial P_c} + \frac{\partial\rho_{c1}}{\partial h_{c1}}\frac{dh_{cv}}{dP_c}\right)\right]$$

$$d_{51}^C = (\rho CA)_w\frac{(\overline{T}_{cw1} - \overline{T}_{cw2})}{L_{c1}}$$

$$d_{55}^C = (\rho CA)_w$$

$$d_{66}^C = (\rho CA)_w$$

$$d_{71}^C = (\rho CA)_w\left[\frac{\overline{T}_{cw2} - \overline{T}_{cw3}}{L_{c3}}\right]$$

$$d_{72}^C = (\rho CA)_w\left[\frac{\overline{T}_{cw2} - \overline{T}_{cw3}}{L_{c3}}\right]$$

$$d_{77}^C = (\rho CA)_w$$

Appendix D - Experimental Setup References

System Diagrams
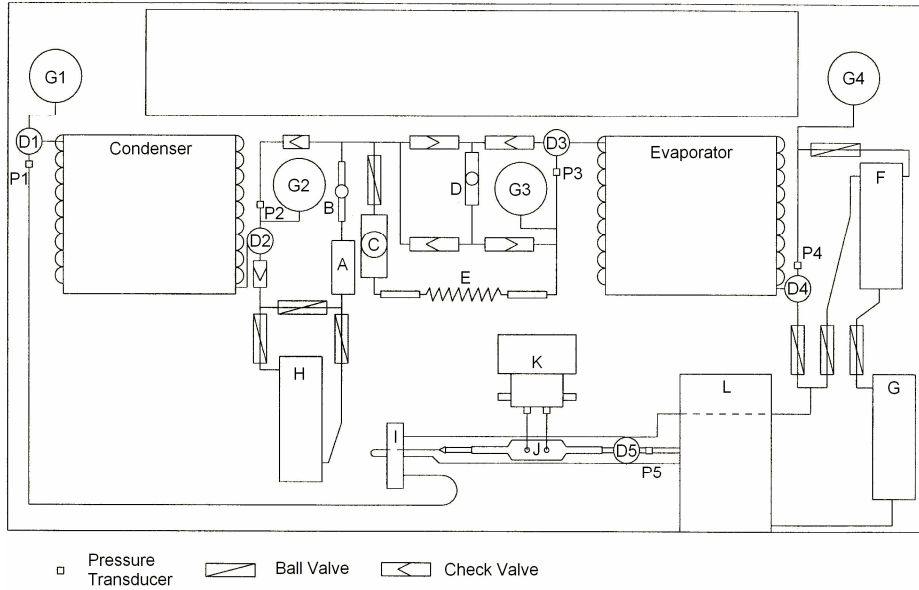
Figure D-1 Original Design Diagram
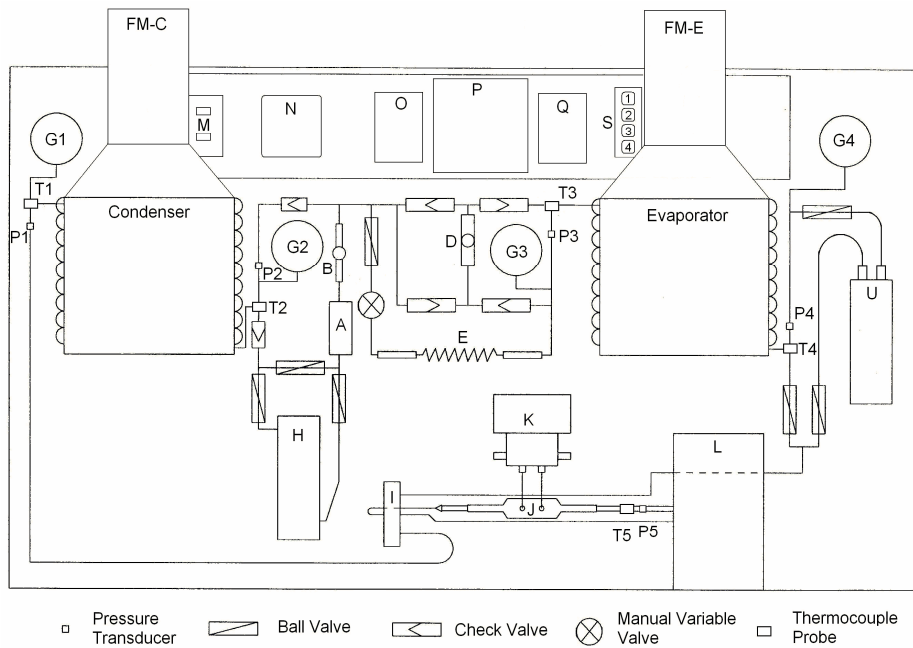
Figure D-2 Final Design Diagram (Front)

(See Table D.1 for key to diagrams)
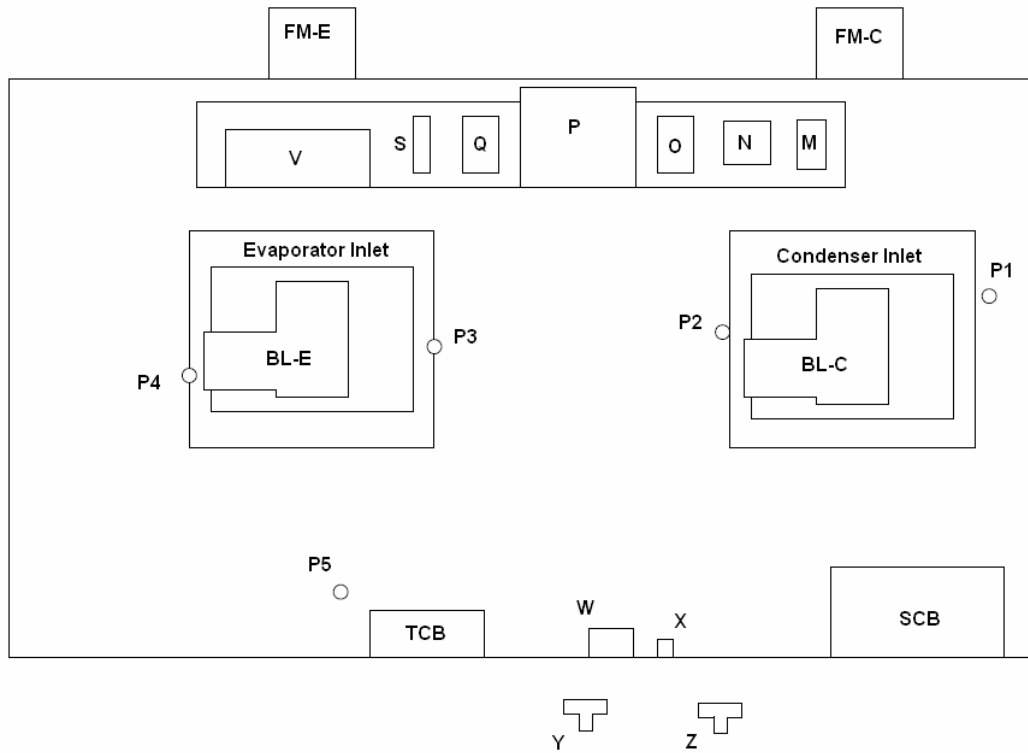
Figure D-3 Final Design Diagram (Back)

(See Table D.1 for key diagrams)

Table D.1 Key to Diagrams

A	Filter/Dryer	G3	Pressure Gauge 3	S-1	Switch, Condenser Blower Motor Control
B	Moisture/Liquid Sight Glass	G4	Pressure Gauge 4	S-2	Switch, Evaporator Blower Motor Control
BL-C	Blower/Motor Assembly, Condenser	H	Receiver, Refrigerant	S-3	Switch, Compressor Motor Control
BL-E	Blower/Motor Assembly, Evaporator	I	Reversing Valve	S-4	Switch, Expansion Valve
C	Solenoid Valve	J	V cone Flowmeter	TCB	Temperature Control Board
D	Expansion Valve	K	Differential Pressure Transmitter	T1	Thermocouple Probe 1
D1	Dial Thermometer 1	L	Compressor	T2	Thermocouple Probe 2
D2	Dial Thermometer 2	M	Main Switch	T3	Thermocouple Probe 3
D3	Dial Thermometer 3	N	Watt Meter	T4	Thermocouple Probe 4
D4	Dial Thermometer 4	O	Condenser Blower Motor Variable Frequency Drive	T5	Thermocouple Probe 5
D5	Dial Thermometer 5	P	Compressor Motor Variable Frequency Drive	U	Suction Line Accumulator
E	Capillary Tube	P1	Pressure Transducer 1	V	24 VDC Power Supply
F	Separator, Oil/Refrigerant	P2	Pressure Transducer 2	W	Power Strip, 6 outlet
FM-E	Air Flowmeter, Evaporator	P3	Pressure Transducer 3	X	Ground Bar
FM-C	Air Flowmeter, Condenser	P4	Pressure Transducer 4	Y	Grounded Plug 2 (3 outlet)
G	Reciever, Oil	P5	Pressure Transducer 5	Z	Grounded Plug 1 (3 outlet)
G1	Pressure Gauge 1	Q	Evaporator Blower Motor Variable Frequency Drive		
G2	Pressure Gauge 2	SCB	Screw Terminal Board		
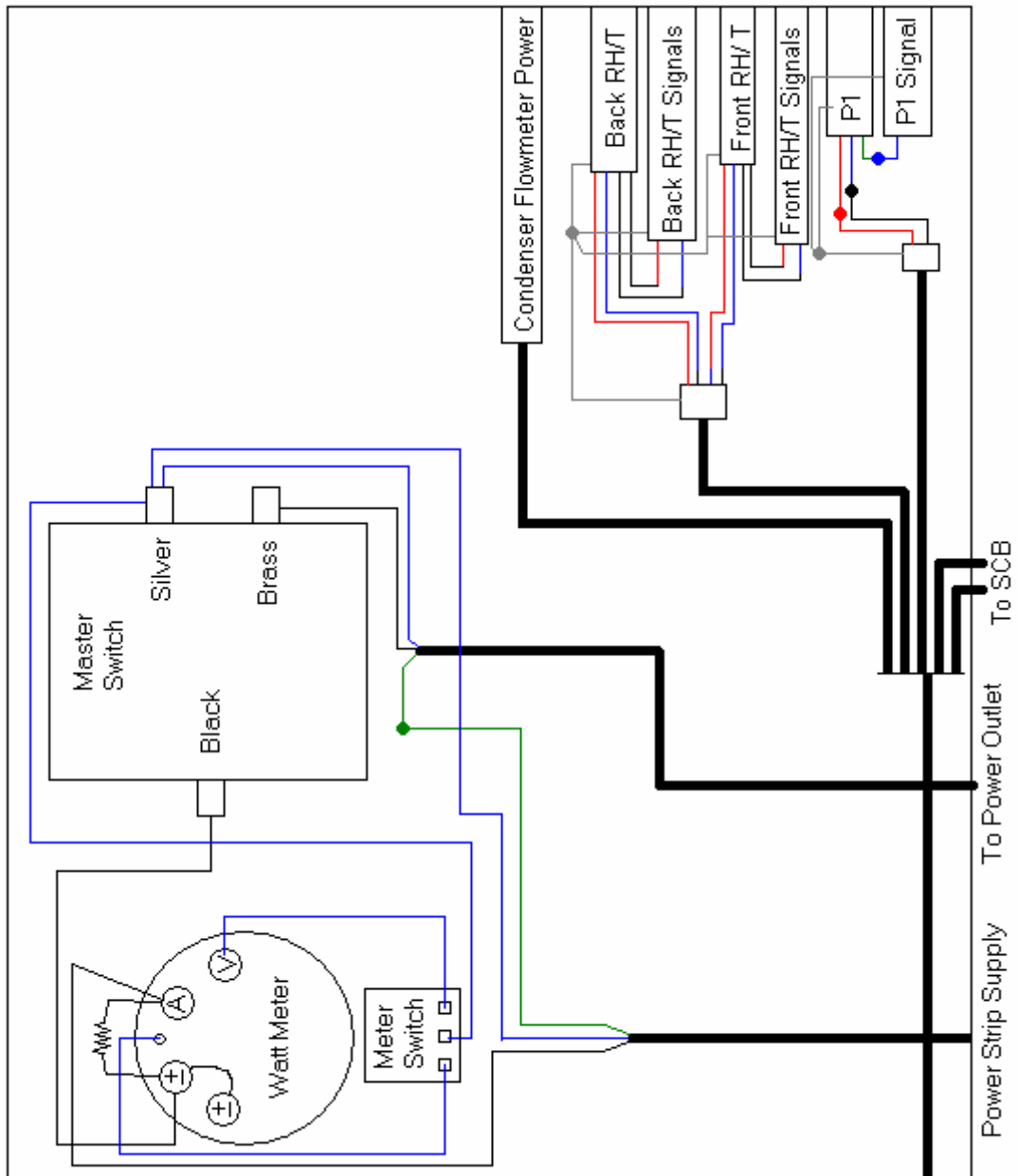
Wiring Diagrams

Figure D-4 Main Box Wiring Diagram (Right)
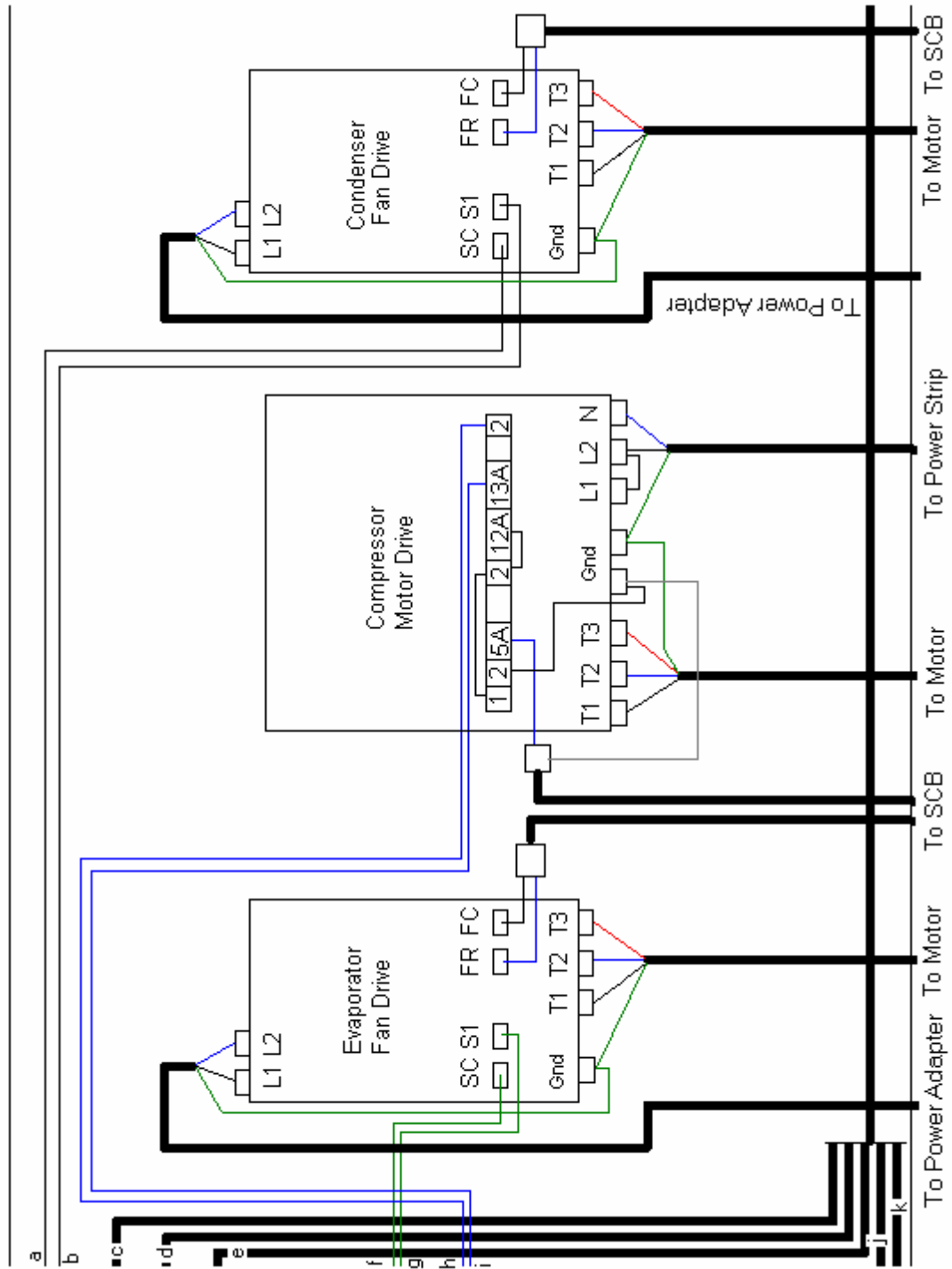
Figure D-5 Main Box Wiring Diagram (Center)
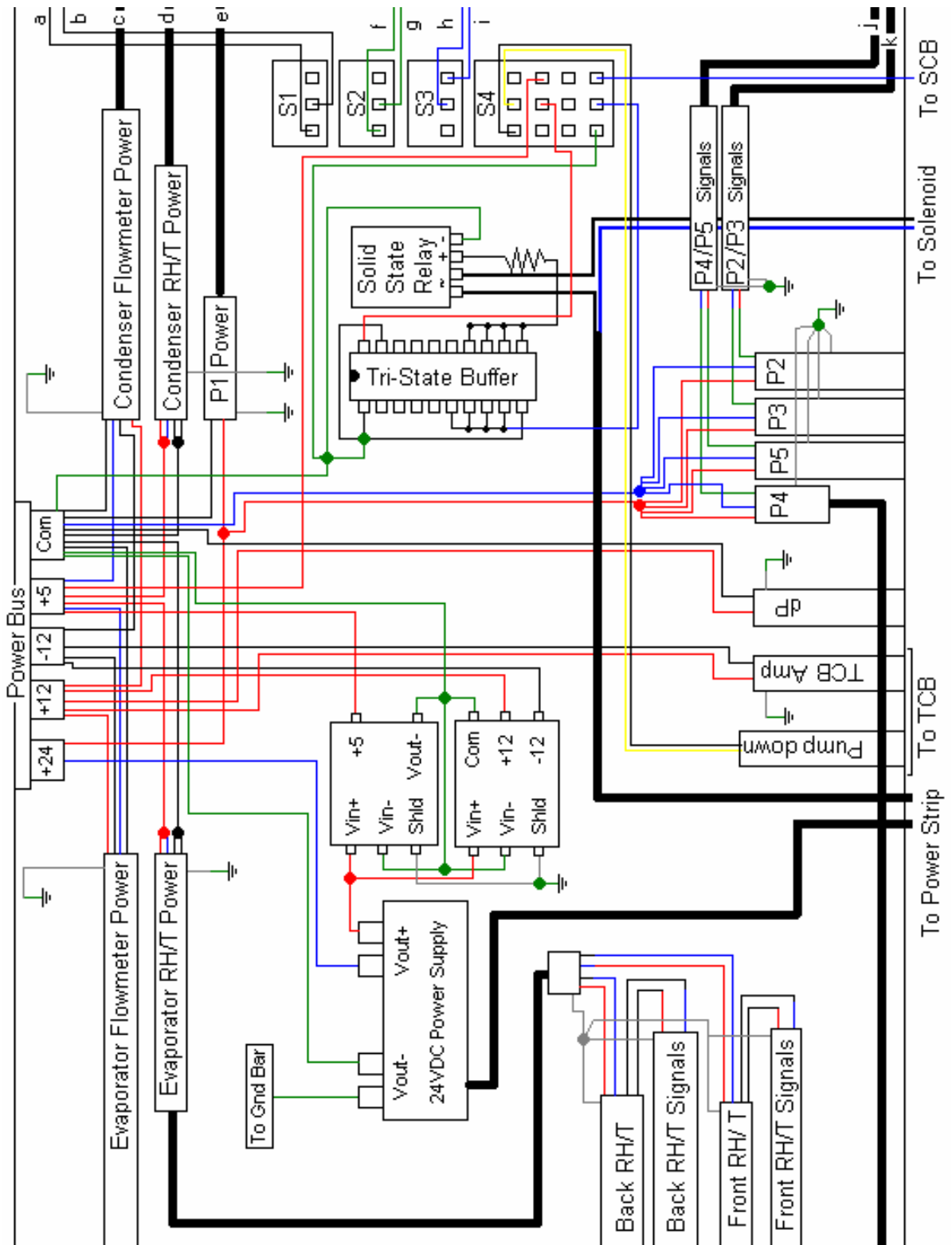
Figure D-6 Main Box Wiring Diagram (Left)

132
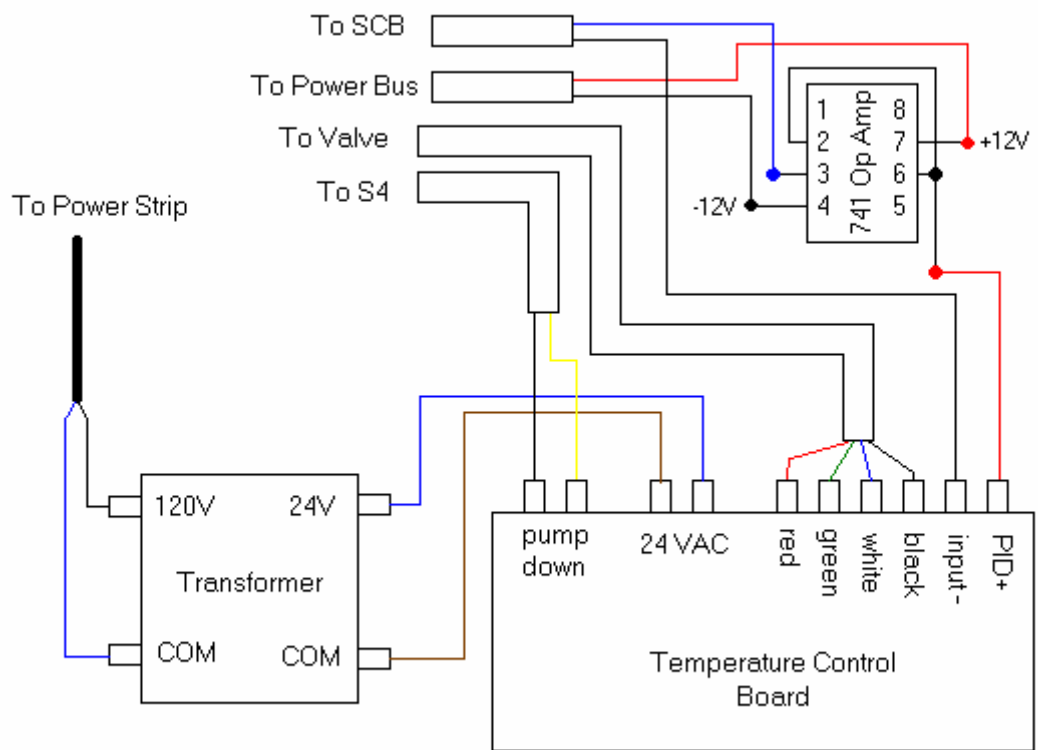
Figure D-7 Temperature Control Board Wiring Diagram
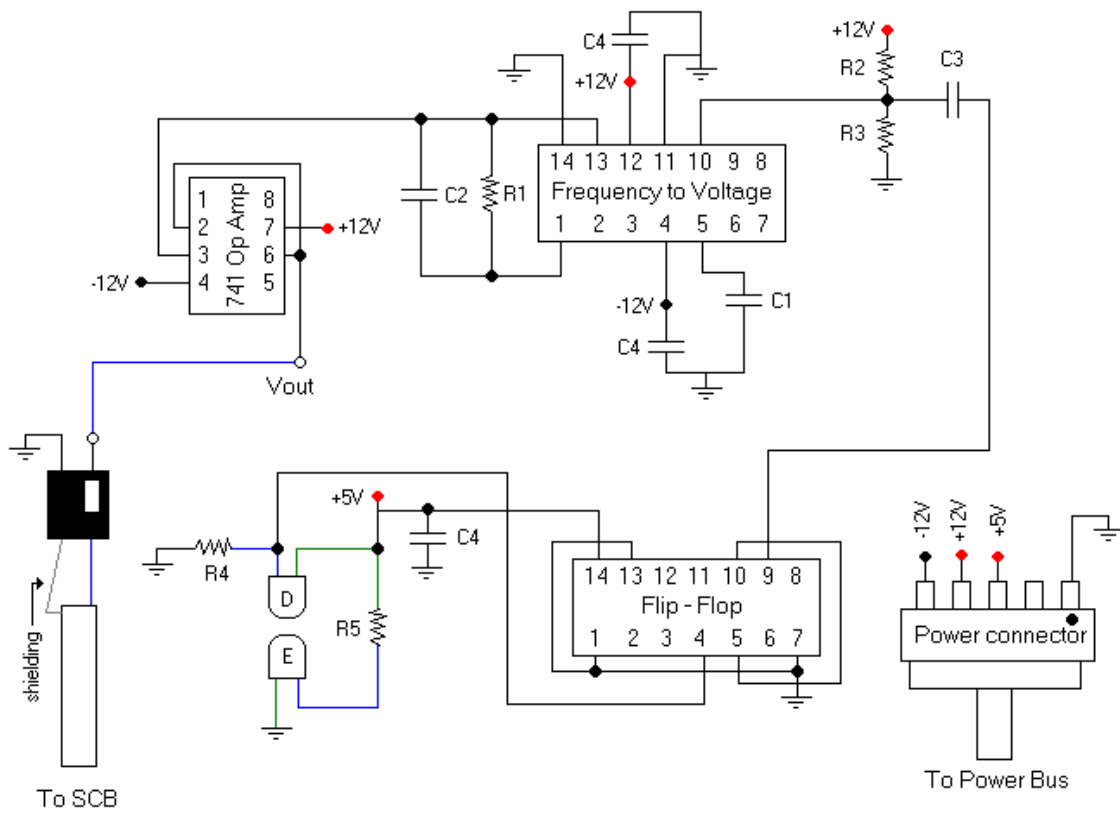
Figure D-8 Air Flow Meter Wiring Diagram

Table D.2 Air Flow Meter Key

R1	39 kΩ	R5	110 Ω	C4	1 μF
R2	10 kΩ	C1	0.1 μF	D	Detector
R3	2.2 kΩ	C2	4.7 μF	E	Emitter
R4	1 kΩ	C3	470 pF		
Notes:						
* The ground symbol represents the ground on the circuit board.						
** The voltages go to their respective buses' on the circuit board.						
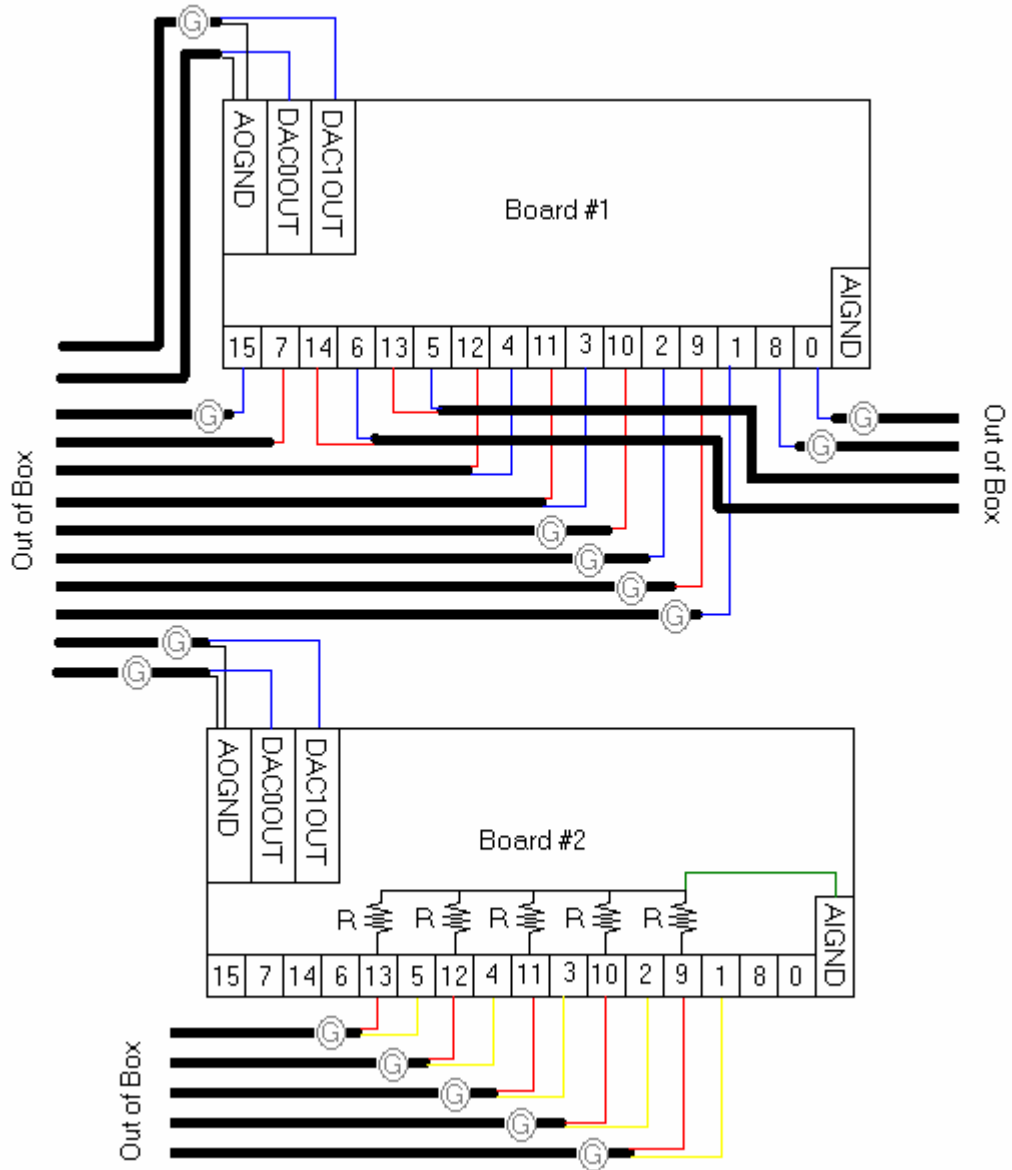
Figure D-9 Screw Terminal Board Wiring Diagram

(See Table D.3 for Key)

Table D.3 Screw Terminal Board Connections

Screw Terminal Board Connections			
Board # 1		**Board # 2**	
Channel	Signal	Channel	Signal
0	Condenser Air Flowmeter	0	Cold Junction Ref.
8	Pressure 1	8	blank
1	Pressure 2	1	Thermocouple 1 (+)
9	Pressure 3	9	Thermocouple 1 (-)
2	Pressure 4	2	Thermocouple 2 (+)
10	Pressure 5	10	Thermocouple 2 (-)
3	Evaporator Exit Humidity	3	Thermocouple 3 (+)
11	Evaporator Exit Temperature	11	Thermocouple 3 (-)
4	Evaporator Inlet Humidity	4	Thermocouple 4 (+)
12	Evaporotor Inlet Temperature	12	Thermocouple 4 (-)
5	Condenser Exit Humidity	5	Thermocouple 5 (+)
13	Condenser Exit Temperature	13	Thermocouple 5 (-)
6	Condenser Inlet Humidity	6	blank
14	Condenser Inlet Temperature	14	blank
7	Differential Pressure	7	blank
15	Evaporator Air Flowmeter	15	blank
DAC0OUT	Compressor Control	DAC0OUT	Evaporator Fan Control
DAC1OUT	Expansion Valve Control	DAC1OUT	Condenser Fan Control
* A circled G on a wire indicates that the shielding is grounded at the body of the enclosure. ** R = 1 MΩ			

LabVIEW Block Diagrams
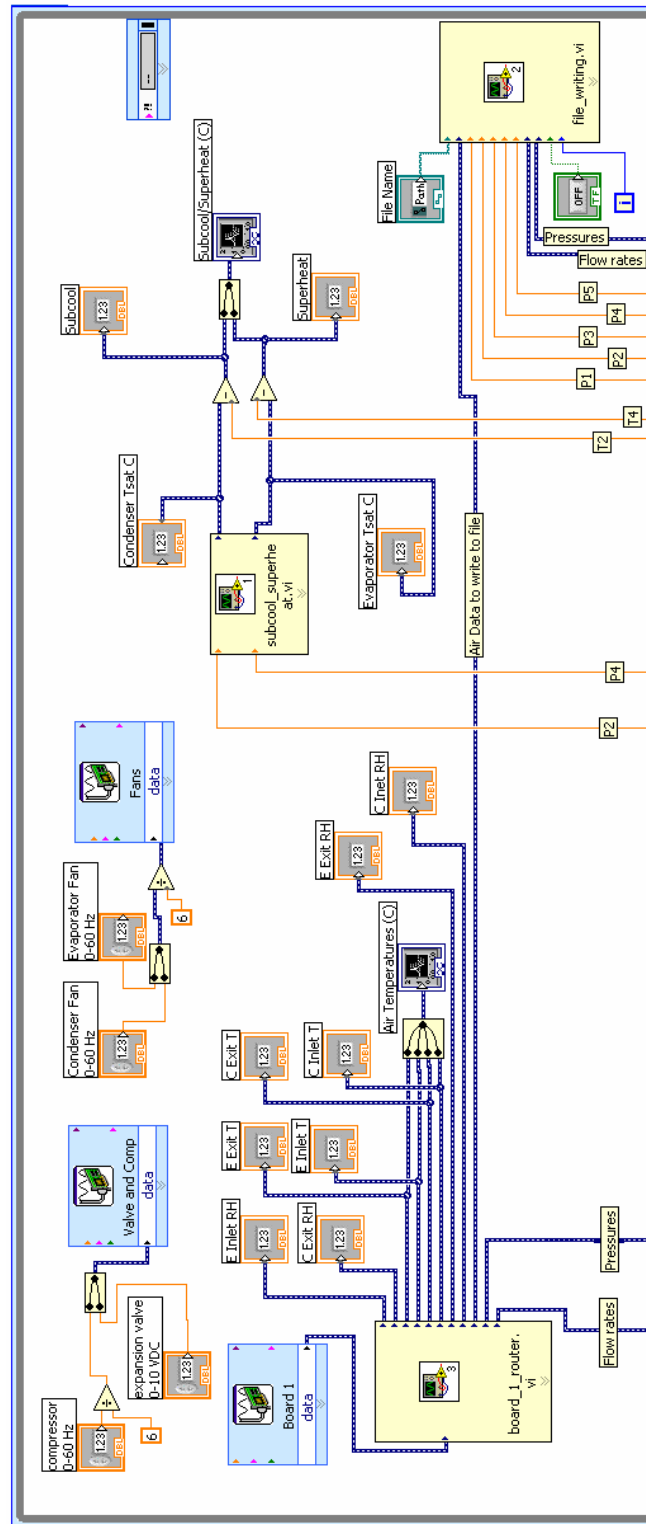
Figure D-10 Main Block Diagram (Top Half)
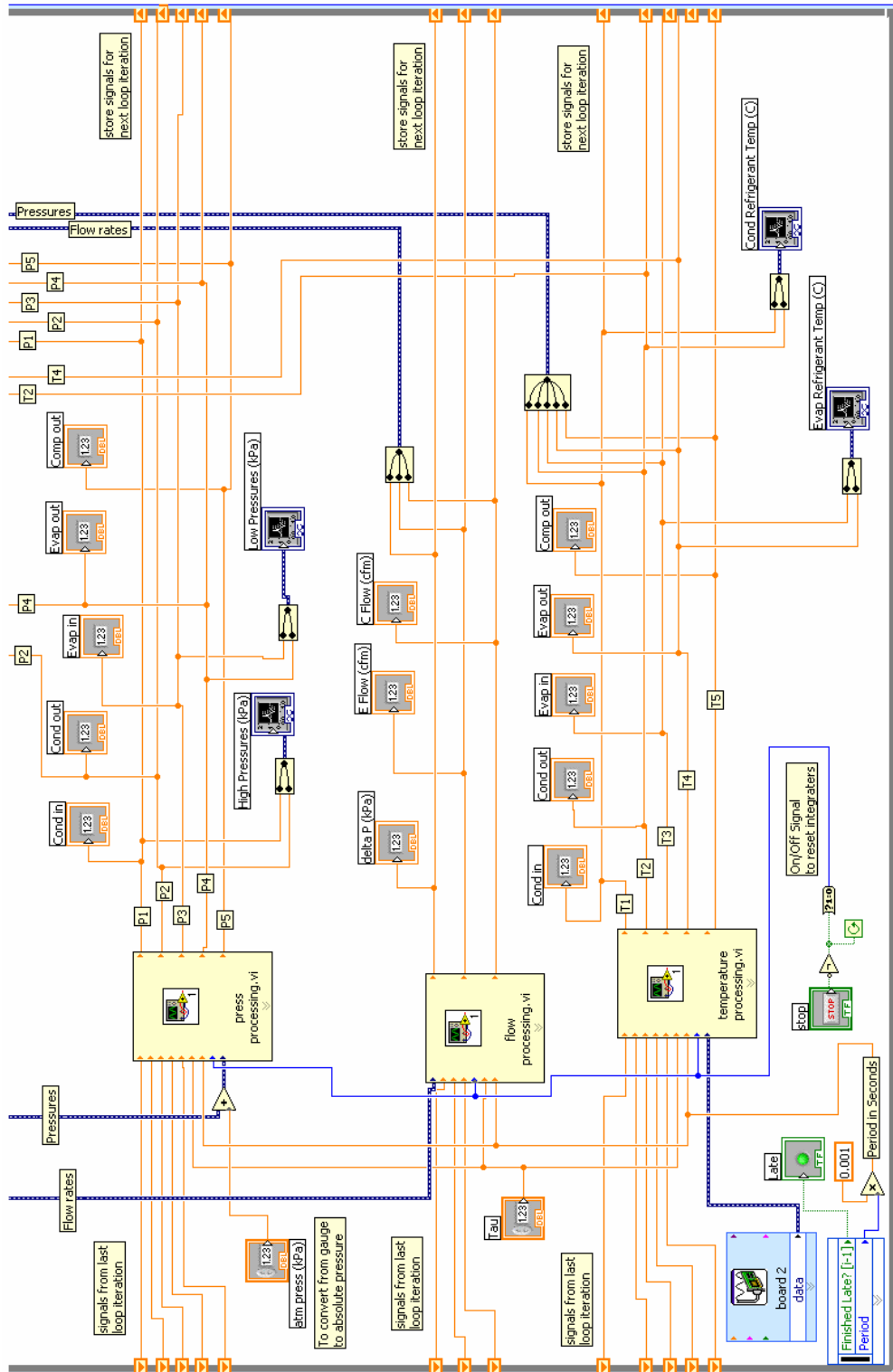
Figure D-11 Main Block Diagram (Bottom Half)

(See later figures for sub-vi's)
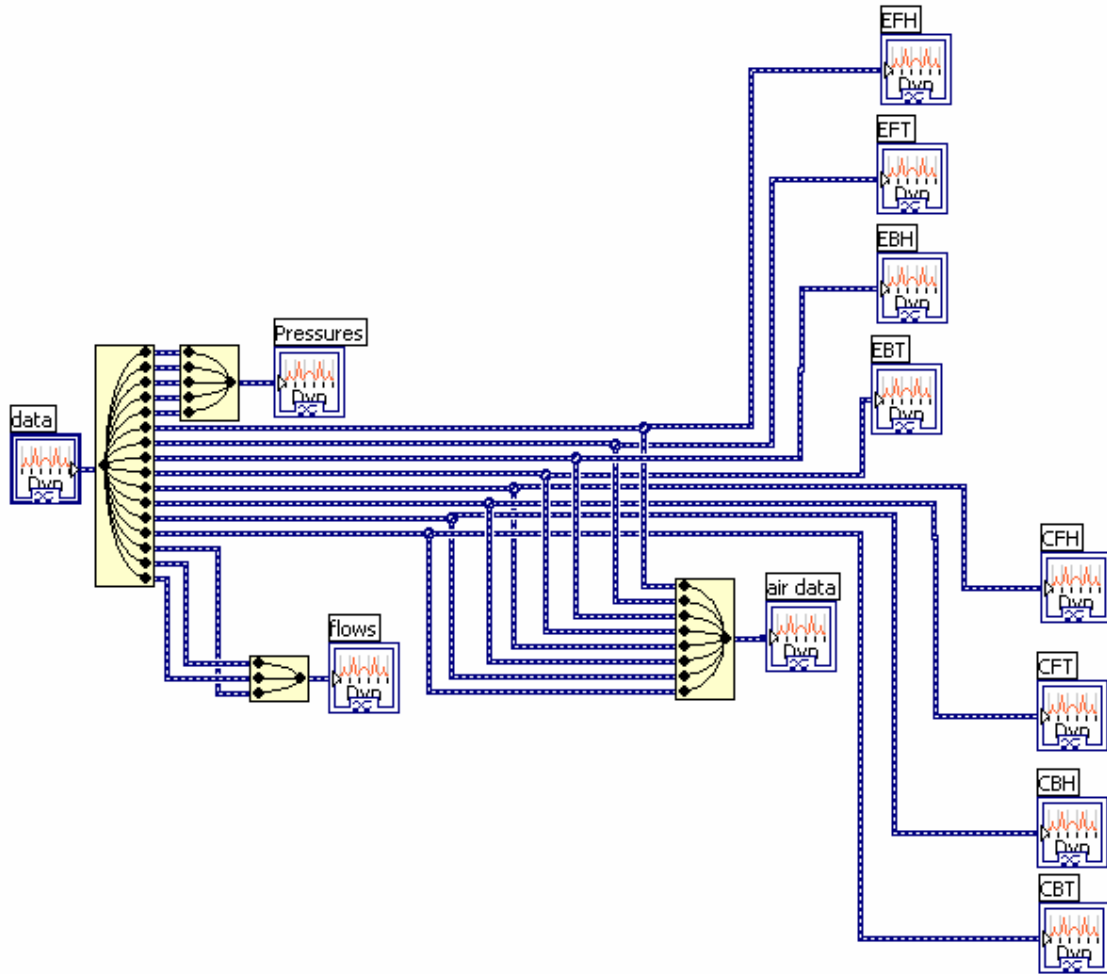
Figure D-12 board_1_router sub vi
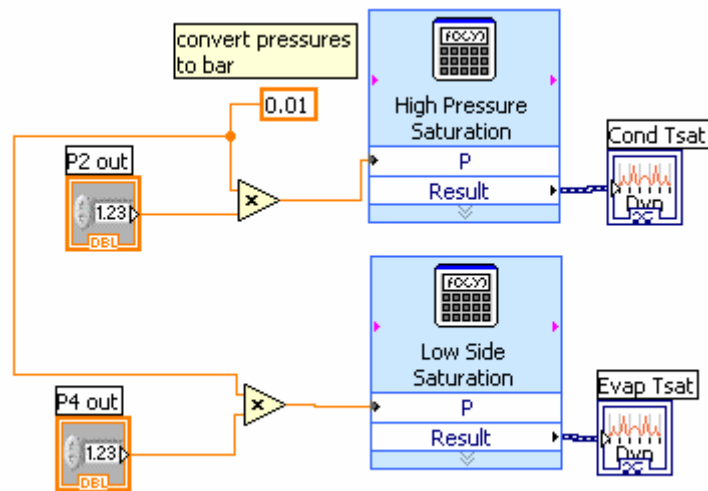
Figure D-13 sat temps sub vi
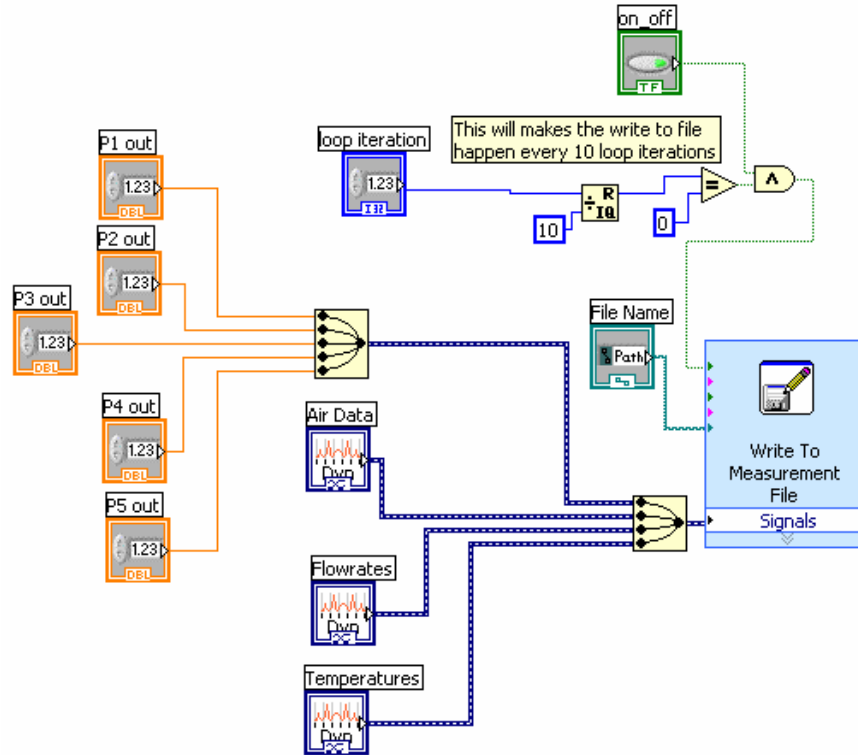
Figure D-14 file_writing sub vi
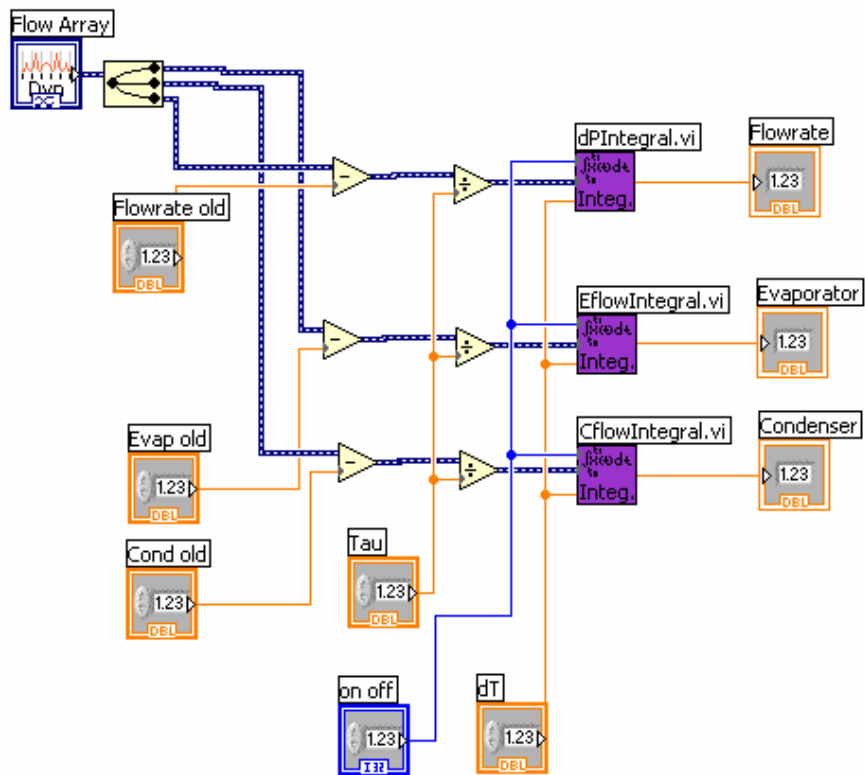
Figure D-15 flow processing sub vi
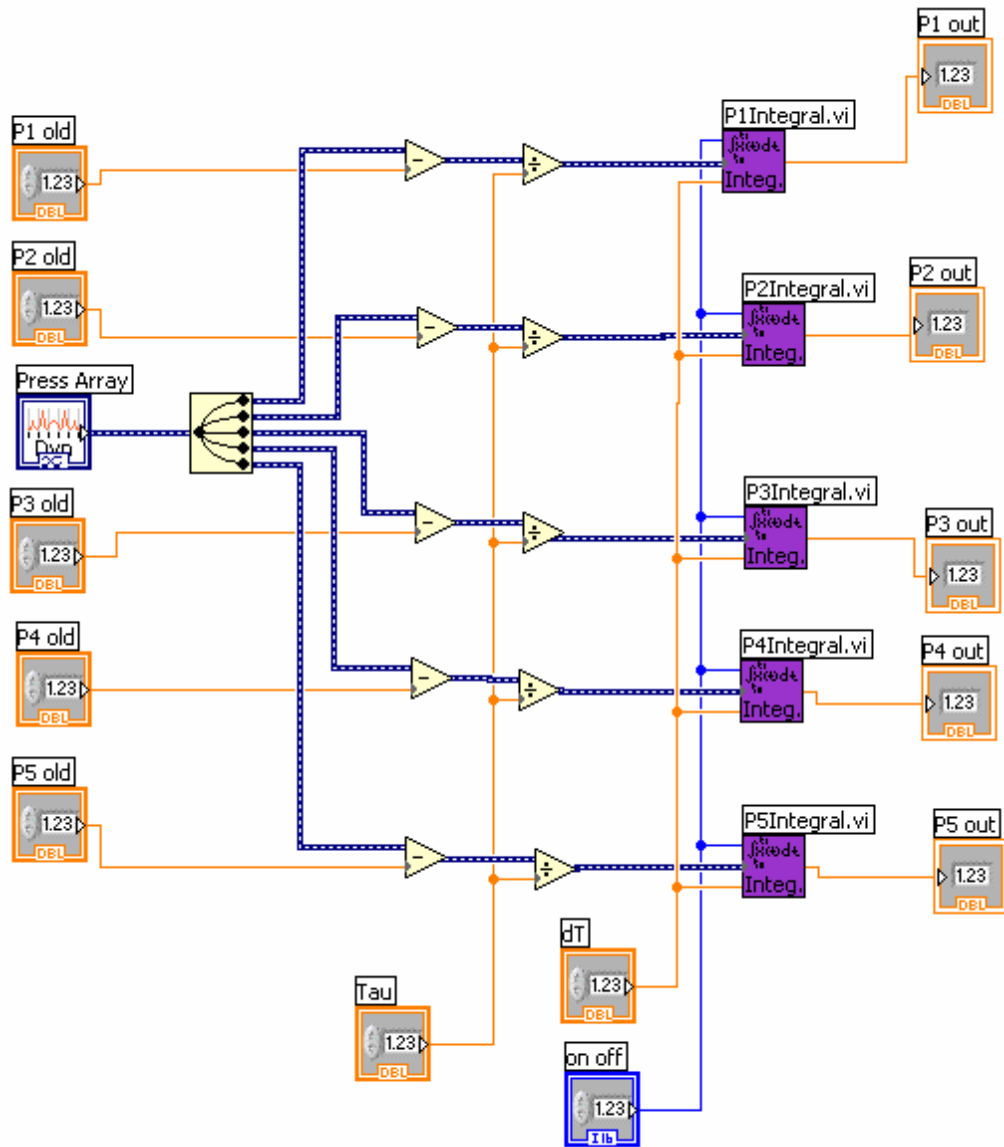
Figure D-16 press processing sub vi
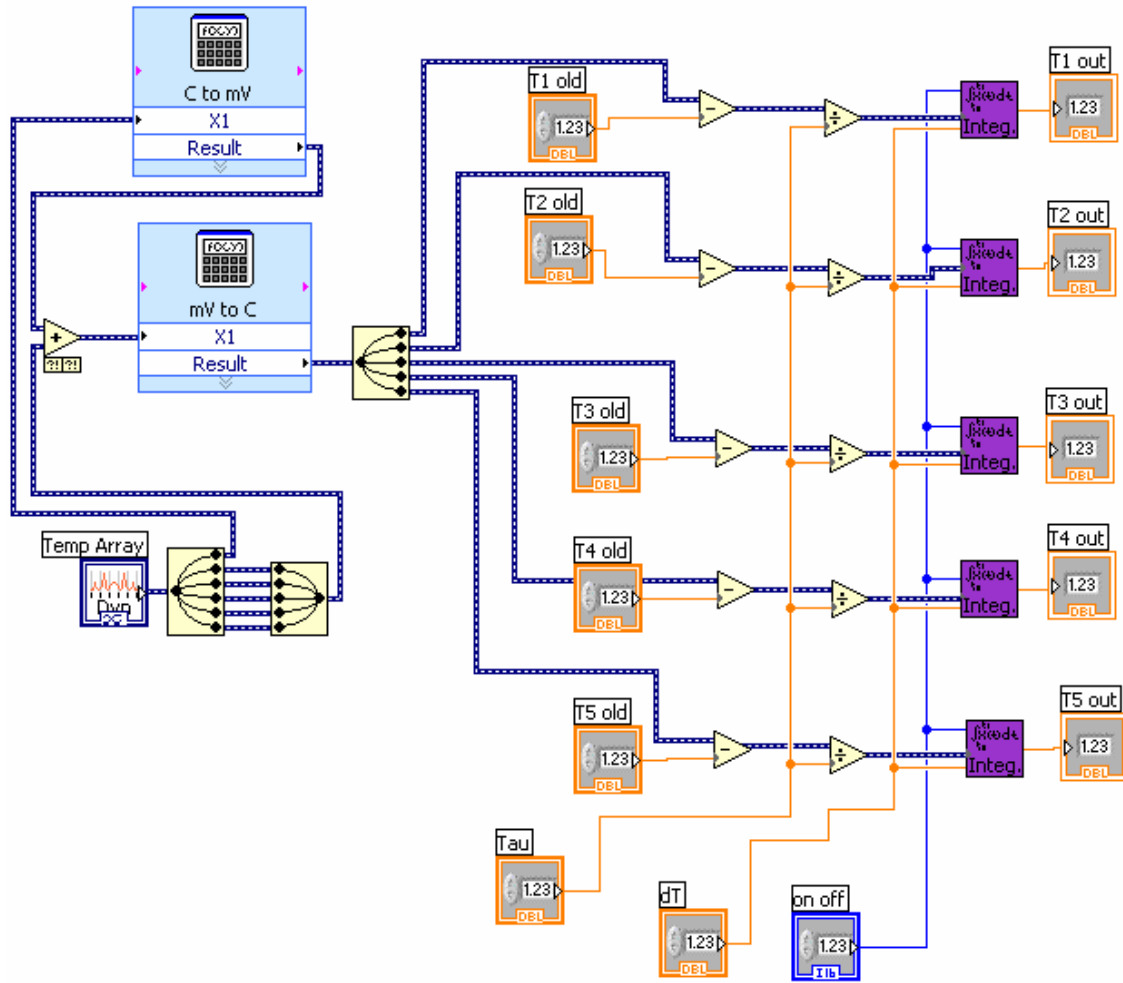
Figure D-17 temperature processing sub vi
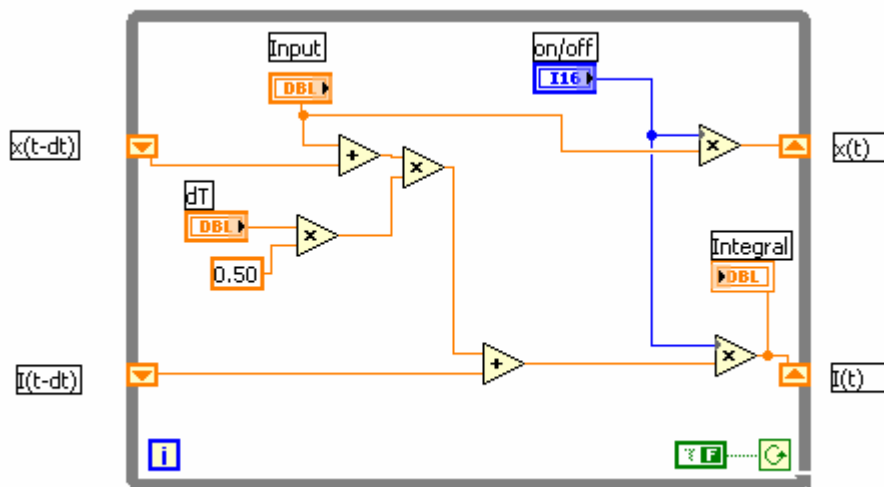
Figure D-18 Integral sub vi

Table D.4 DAQ Assistant Custom Scales

Name	Equation	Output Units	Range
DAQ Assistant Custom Scales			
Voltage-Pressure	P = (517.11)V - 517.11	kPa (gauge)	0 - 2000
Voltage-Humidity	RH = (20)V	percent	0 - 100
Voltage-Temperature	T = (26)V - 30	^{o}C	-30 - 80
pressdiff	ΔP = (4.982)V - 4.982	kPa	0 - 20
Evapflow	F = (62.4597)V + 20.862	cfm	0 - 400
Condflow	F = (64.6994)V + 10.2628	cfm	1 - 400
cjcel	T = (100)V	^{o}C	0 - 40
diffOffset	mV = (1000)V + .12	mV	-5 - 5

Table D.5 Formula Block Equations

Name	Equation	Input Units	Output Units
Formula Block Equations			
C to mV	$V = (-1.2902E-7)T^3 + (2.672E-5)T^2 + (3.9444E-2)T - 3.121E-4$	^{o}C	mV
mV to C	$T = (0.0701)V^3 + (-0.4535)V^2 + (25.352)V + 0.015$	mV	^{o}C
High Pressure Saturation	$T = (-0.1709)P^2 + (7.1201)P - 14.7079$	bar	^{o}C
Low Pressure Saturation	$T = (0.3328)P^3 + (-4.2153)P^2 + (25.5184)P - 46.9264$	bar	^{o}C

Parts Lists

Table D.6 System Components

Components				
Quantity	Device	Manufacturer	Part Number	Relevant Specifications
2	VS Mini Variable Frequency Drives	Yaskawa	GPD205 - 10P2	Supply: 115 VAC single phase, 60 Hz Output: 200-230 VAC 3 phase, 0-60 Hz Control Signal: 0-10VDC
2	AC Century Blower Motor	MagneTek	HM2H001	200-230 VAC 3 phase, 1/4 hp
1	Speedmaster Adjustable Speed AC Motor Controller	Leeson	174931	Supply: 115 VAC single phase, 60 Hz Output: 200-230 VAC 3 phase, 0-60 Hz Control Signal: 0-10VDC
1	AC Compressor Motor	Leeson	C6T17FK58A	208-230 VAC 3 phase, 3/4 hp
1	Compressor	Blissfield	CE 9910	Single Cylinder, 1/4 hp
1	Temperature Control Board	Sporlan	952660	Supply: 24VAC Control Signal: 0-10VDC
1	Stepper Expansion Valve	Sporlan	SEI - 0.5 - 10 - 8	Cooling Capacity: 0.5 ton

Table D.7 System Sensors

Sensors						
Quantity	Sensor	Manufacturer	Part Number	Supply	Output	Calibration Range
5	Pressure Transducer	Cole Parmer	07356-04	24 VDC	1-5 VDC	0-300psig
1	Type K Thermocouple Probe (grounded)	Omega	KQSS - 18U - 4	N/A	-6 - 50 mV	-200 - 1250 ^{o}C
1	Differential Pressure Meter	Rosemount	D2M22B2S1B4E5	12 VDC	1-5 VDC	0-80in water
1	V-Cone Meter	McCrometer	VT0AQC02N1	N/A	0-80in water	6-60 Liter/min
2	Air Flow meters	N/A	N/A	±12 VDC 5 VDC	0-10 VDC	50-260 cfm
4	Relative Humidity & Temperature	Precon	HS-2000V	5 VDC	1-5 VDC	0-100% -30 to 85 ^{o}C
1	Watt Meter	Triplett	460 - G	N/A	visual	0-1500W 0-750W

Table D.8 Electronic Components

Quantity	Device	Part Number	Relevant Specifications
Electronics			
1	DC Power Supply	HD24-4.8-A	Supply: 120 VAC, single phase, 60 Hz Output: 24 VDC
1	24 to 5 DC-DC Converter	PSS3-24-5	Supply: 24 VDC Ouptut: 5 VDC
1	24 to ±12 DC-DC Converter	PsSD3-24-1212	Supply: 24 VDC Output: -12 / +12 VDC
1	Transformer	TCT40-01E07AB	Input: 120V, 50/60 Hz Output: 24V @ 1.67 Amps Maximum Power: 40VA
2	Flip-Flop	74LS 74A	Supply: 5 VDC
2	Frequency to Voltage Converter	VFC32KP	Supply: ±12 VDC Output: 0-10 VDC
2	Infrared Emitter/Detector	276-142 (RadioShack)	Reverse Voltage: 5 VDC Turn on Current: 150 mA
3	741 Op-Amp	LM741CN	Supply: ±12 VDC
1	Tri-State Buffer	74HCT541N	Supply: 5 VDC
1	Solid State Relay	275-310 (RadioShack)	Control: 1.2 VDC (typ.) 20-50 mA Rated: 3A, 125 VAC

Air Flow Meter Calibration

Table D.9 Linear Regression Results

Linear Regression Results							
Measured				Calculated			
Velocity (ft/min)	Flowrate (cfm)	Evaporator Voltage (V)	Condenser Voltage (V)	Evaporator Flowrate (cfm)	Conderser Flowrate (cfm)	Evaporator Voltage (V)	Condenser Voltage (V)
543	47.4	0.40	0.55	46.2	46.1	0.42	0.57
1008	88.0	1.07	1.21	87.5	88.6	1.07	1.20
1486	129.7	1.76	1.87	130.9	131.0	1.74	1.85
2020	176.3	2.53	2.56	178.9	176.1	2.49	2.57
2515	219.5	3.16	3.24	218.4	219.6	3.18	3.23
3048	266.0	3.91	3.94	264.9	265.4	3.92	3.95

Evaporator Equations

$$V = 0.016F - 0.334$$

$$F = 62.46V + 20.87$$

Condenser Equations

$$V = 0.015F - 0.159$$

$$F = 64.70V + 10.26$$

V is the output voltage in Volts and F is the flow rate in cubic feet per minute

Table D.10 Uncertainty Results

Uncertainty Results		
Evaporator	Condenser	
Linearity Uncertainty		
0.07811	0.04467	Volts
4.879	2.890	cfm
Resolution Uncertainty		
0.0024414	0.0024414	Volts
0.152	0.158	cfm
Random Uncertainty		
0.05392	0.05462	Volts
3.368	3.534	cfm
Standard Error "+/- 1%"		
3	3	cfm
Total Uncertainty		
6.65	5.47	cfm
2.22%	1.82%	@ 300 cfm

Appendix E - Modeling Parameter Values

Table E.1 Mutual Parameter Values

Mutual				
		Direct		Indirect
Measured	A	5.95E-05 m^2	$L_{eT} = L_{cT}$	6.1 m
Measured	A_w	1.16E-05 m^2	$T_{c,air,in}$	23.4 °C
Measured	D_o	0.00952 m	$T_{c,air,out}$	31.8 °C
Measured	D_i	0.00871 m		
Tabulated	$c_{p,w}$	0.385 kJ/(kg*K)	$c_{p,air}$	1.007 kJ/(kg*K)
Tabulated	ρ_w	8933 kg/m^3	ρ_{air}	1.161 kg/m^3
Tabulated				
Calculated	mdot	0.00913 kg/s	$mdot_{c,air}$	0.186 kg/s
Calculated			$Vdot_{c,air}$	340 cfm
Calculated				
Expansion Valve and Compressor Coefficients	k11	8.56E-06 kg/(kPa*s)		
Expansion Valve and Compressor Coefficients	k12	1.75E-05 kg/(kPa*s)		
Expansion Valve and Compressor Coefficients	k13	6.06E-04 kg/(V*s)		
Expansion Valve and Compressor Coefficients	k21	-7.42E-02 kJ/(kPa*kg)		
Expansion Valve and Compressor Coefficients	k22	1.72E-02 kJ/(kPa*kg)		
Expansion Valve and Compressor Coefficients	k23	3.25E-02 unitless		
Expansion Valve and Compressor Coefficients	k31	2.30E-05 kg/(kPa*s)		
Expansion Valve and Compressor Coefficients	k32	1.20E-05 kg/(kPa*s)		
Expansion Valve and Compressor Coefficients	k33	1.43E-04 kg/(Hz*s)		

Table E.2 Evaporator Parameters

Evaporator				
	Direct		Indirect	
Measured	T_{ea}	296.7 K	P_e	348.6 kPa
			$T_{e,out}$	282.3 K
Thermodynamic Properties	h_{efg} (P_e)	194.8 kJ/kg	$c_{p,e2}$ (P_e, h_{e2})	0.9152 kJ/(kg*K)
	h_{ev} (P_e)	401.4 kJ/kg	h_{eL} (P_e)	206.6 kJ/kg
	$h_{e,out}$ (P_e, $T_{e,out}$)	405.5 kJ/kg	k_{e2} (P_e, h_{e2})	0.01207 W/(m*K)
	T_{er1} (P_e)	278.1 K	μ_{e2} (P_e, h_{e2})	1.10E-05 (N*s)/m^2
	T_{er2} (P_e, h_{e2})	280.3 K	ρ_{eg} (P_e)	17.1 kg/m^3
	ρ_{e2} (P_e, h_{e2})	16.44 kg/m^3		
	ρ_{eL} (P_e)	1278 kg/m^3		
Calculated	L_{e1}	5.71 m	C	0.0564
	L_{e2}	0.39 m	h_{e2}	403.5 kJ/kg
	T_{ew1}	281.3 K	$h_{e,in}$	250.3 kJ/kg
	T_{ew2}	290.5 K	Pr_{e2}	0.835
	α_{ei1}	2.7617 W/(m^2*K)	Re_{e2}	1.21E+05
	α_{ei2}	0.346 kW/(m^2*K)	$x_{e,in}$	0.224
	α_{eo}	0.524 kW/(m^2*K)		
	γ_e	0.952		
	ρ_{e1}	77.252 kg/m^3		
Derivatives	$d(\rho_{e1})/dP_e$	0.2336 kg/(m^3*kPa)	dh_{efg}/dP_e	-0.0663 kJ/(kg*kPa)
	$d(\rho_{eL}*h_{efg})/dP_e$	-140.52 kJ/(m^3*kPa)	$d\rho_{eL}/dP_e$	-0.2864 kg/(m^3*kPa)
	dh_{ev}/dP_e	0.049 kJ/(kg*kPa)	$\partial\alpha_{eo}/\partial Vdot$	1.118 W/(m^2*K*cfm)
	dT_{er1}/dP_e	0.0851 K/kPa	$\partial Vdot/\partial v_e$	4.25 cfm/Hz
	$\partial T_{er2}/\partial h_{e,out} = 1/c_{p,e2}$	1.09 (kg*K)/kJ		
	$\partial\alpha_{eo}/\partial v_e$	4.75E-03 kW/(m^2*K*Hz)		
	$\partial T_{er2}/\partial P_e$	0.030 K/kPa		
	$\partial\rho_{e2}/\partial h_{e,out}$	-0.096 kg^2/(m^3*kJ)		
	$\partial\rho_{e2}/\partial P_e$	0.0513 kg/(m^3*kPa)		

Table E.3 Condenser Parameter Values

		Direct		Indirect	
Measured	T_{ca}	296.7 K		P_c	1046 kPa
				$T_{c,out}$	309.1 K
				$T_{c,in}$	317.4 K
Thermodynamic Properties	$\rho_{c1}(P_c, h_{c1})$	51.03 kg/m^3		$\rho_{cv}(P_c)$	51.62 kg/m^3
	$\rho_{cL}(P_c)$	1142 kg/m^3		$\mu_{c1}(P_c, h_{c1})$	1.267E-05 (N*s)/m^2
	$h_{c,in}(P_c, T_{c,in})$	423.5 kJ/kg		$c_{p,c1}(P_c, h_{c1})$	1141 J/(kg*K)
	$h_{c,out}(P_c, T_{c,out})$	250.3 kJ/kg		$k_{c1}(P_c, h_{c1})$	0.01566 W/(m*K)
	$h_{cv}(P_c)$	419.9 kJ/kg		$\mu_{c3}(P_c, h_{c3})$	1.67E-04 (N*s)/m^2
	$h_{cL}(P_c)$	258 kJ/kg		$c_{p,c3}(P_c, h_{c3})$	1489 J/(kg*K)
	$h_{cfg}(P_c)$	161.9 kJ/kg		$k_{c3}(P_c, h_{c3})$	0.07541 W/(m*K)
	$T_{cr1}(P_c, h_{c1})$	315.8 K			
	$T_{cr2}(P_c)$	314.2 K			
Calculated	L_{c1}	0.22 m		C	0.127
	L_{c2}	5.23 m		Pr_{c1}	0.9231
	L_{c3}	0.65 m		Re_{c1}	1.05E+05
	γ_c	0.802		Pr_{c3}	3.30
	ρ_{c2}	267.8 kg/m^3		Re_{c3}	8.00E+03
	T_{cw1}	302.9 K		h_{c1}	421.7 kJ/kg
	T_{cw2}	308.5 K			
	T_{cw3}	301.17 K			
	α_{ci1}	0.421 kW/(m^2*K)			
	α_{ci2}	1.7955 kW/(m^2*K)			
	α_{ci3}	0.378 kW/(m^2*K)			
	α_{co}	0.800 kW/(m^2*K)			
	T_{cr3}	311.6 K			
	h_{c3}	254.2 kJ/kg			
Derivatives	$d(h_{cv})/dP_c$	0.0153 kJ/(kg*kPa)		$d(h_{cfg})/dP_c$	-0.0385 kJ/(kg*kPa)
	$d(h_{cL})/dP_c$	0.054 kJ/(kg*kPa)		$\partial\alpha_{co}/\partial\dot{V}$	1.118 W/(m^2*K*cfm)
	$d(\rho_{cL})/dP_c$	-0.154 kg/(m^3*kPa)		$\partial\dot{V}/\partial v_c$	4.70 cfm/Hz
	$d(\rho_{cL}*h_{cfg})/dP_c$	-68.93 kg/(m^3*kPa)			
	$\partial(\rho_{c1})/\partial P_c$	0.057 kg/(m^3*kPa)			
	$\partial(T_{cr1})/\partial P_c$	0.022 K/kPa			
	$\partial(\rho_{c1})/\partial h_{c1}$	-0.318 kg^2/(m^3*kJ)			
	$\partial(T_{cr3})/\partial h_{co}$	0.336 (kg*K)/kJ			
	$d(\rho_{c2})/dP_c$	0.104 kg/(m^3*kPa)			
	$d(T_{cr2})/dP_c$	0.036 K/kPa			
	$\partial(T_{cr3})/\partial P_c$	0.0184 K/kPa			
	$\partial(T_{cr1})/\partial h_{c1} = 1/c_{p,c1}$	0.876 (K*kg)/kJ			
	$\partial(\alpha_{co3})/\partial v_c$	5.25E-03 kW/(m^2*K*Hz)			

Table E.4 Wall Temperature Optimization Spreadsheet

	Constant Inputs	
mdot	Refrigerant Mass Flow Rate	0.00913 kg/s
D_o	Inside Tube Diameter	9.52E-03 m
D_i	Outside Tube Diameter	8.71E-03 m
$h_{e,in}$	Inlet Enthalpy	250.3 kJ/kg
h_{ev}	Saturated Vapor Enthalpy	401.4 kJ/kg
h_{eL}	Saturated Liquid Enthalpy	206.6 kJ/kg
$h_{e,out}$	Outlet Enthalpy	405.5 kJ/kg
T_{ea}	Ambient Temperature	23.5 C
T_{er1}	Temperature of Node 1 Refrigerant	4.9 C
α_{ei1}	Inside Convection Coefficient of Node 1	2.7617 kW/(m²*K)
T_{er2}	Temperature of Node 2 Refrigerant	7.14 C
α_{ei2}	Inside Convection Coefficient of Node 2	0.346 kW/(m²*K)
L_{total}	Total Heat Exchanger Length	6.1 m
	Variables	
T_{ew1}	Temperature of node 1 wall	8.10 C
T_{ew2}	Temperature of node 2 wall	17.3 C
	Calculated Variables	
L_{e1}	mdot*(h_{ev}-$h_{e,in}$) /(α_{ei1}*D_i*π(T_{ew1}-T_{er1}))	5.71 m
L_{e2}	mdot*($h_{e,out}$-h_{ev}) /(α_{ei2}*D_i*π(T_{ew2}-T_{er2}))	0.39 m
α_{eo}	mdot*(h_{ev}-$h_{e,in}$) /(π*D_o*L_{e1}*(T_{ea}-T_{ew1}))	0.524 kW/(m²*K)
L_{total}	L_{e1} + L_{e2}	6.1000 m
	Heat Transfer Values	
Q_2(meas)	mdot*($h_{e,out}$-h_{ev})	0.03741 kW
Q_2(air calc)	α_{eo}*π*D_o*L_{e2}*(T_{ea}-T_{ew2})	0.03741 kW
diff²	(Q_2(meas) - Q_2(air calc))²	4.27E-22 kW

The solver was set to vary the values of T_{ew1} and T_{ew2} to minimize the target cell that calculates the difference squared while equating the constant input total length and the calculated variable total length. The calculated variables and heat transfer values are evaluated with the given equations.

Table E.5 Recalculated Values for Modified Mass Flow Rate and Ambient Temperatures

	mdot (kg/s)		T_{ea} / T_{ca} (K)		
	"+10%"	"-10%"	75%	50%	
	0.01004	0.00821	293.5 / 298.725	290.35 / 300.08	units
α_{ei1}	2.98	2.494	no change	no change	kW/(m^2*K)
α_{ei2}	0.373	0.318	no change	no change	kW/(m^2*K)
α_{eo}	0.578	0.47	no change	no change	kW/(m^2*K)
α_{ci1}	0.454	0.387	no change	no change	kW/(m^2*K)
α_{ci2}	1.938	1.647	no change	no change	kW/(m^2*K)
α_{ci3}	0.408	0.347	no change	no change	kW/(m^2*K)
α_{co}	0.889	0.718	no change	no change	kW/(m^2*K)
T_{ew1}	281.31	281.23	281.29	281.34	K
T_{ew2}	290.55	290.45	289.25	290.55	K
T_{cw1}	302.74	303.01	303.5	304.21	K
T_{cw2}	308.35	308.55	308.35	308.25	K
T_{cw3}	301.08	301.28	302.05	303.05	K
L_{e1}	5.72	5.73	5.67	5.59	m
L_{e2}	0.38	0.37	0.42	0.51	m
L_{c1}	0.223	0.218	0.232	0.246	m
L_{c2}	5.223	5.206	5.141	5.055	m
L_{c3}	0.652	0.673	0.0725	0.797	m

	Least Squares Analysis							
		k11 *	δP_e	+ k12 *	δP_c	+ k13 *	δu_{valve}	= $\delta mdot$	$\delta mdot$ (calc)	diff^2	% diff

		k11 *	δP_e	+ k12 *	δP_c	+ k13 *	δu_{valve}	= $\delta mdot$	$\delta mdot$ (calc)	diff^2	% diff
k11	0.0308	-10.43	-8.31	-0.2	-1.173	-1.282	1.18E-02	9%
k12	0.0631	-8.96	-3.71	-0.2	-0.965	-0.946	3.57E-04	-2%
k13	2.1813	-16.93	-8.85	-0.3	-1.831	-1.734	9.34E-03	-5%
		-12.50	-4.18	-0.25	-1.056	-1.194	1.91E-02	13%
		-13.42	-8.03	-0.25	-1.559	-1.465	8.84E-03	-6%
		-21.97	45.30	0	2.126	2.182	3.12E-03	3%
		-18.32	29.78	0	1.393	1.315	6.12E-03	-6%
						sum	5.87E-02	

		k31 *	δP_e	+ k32 *	δP_c	+ k33 *	δu_{comp}	= $\delta mdot$	$\delta mdot$ (calc)	diff^2	% diff
k31	0.0828	-10.43	-8.31	0	-1.173	-1.221	2.31E-03	4%
k32	0.0431	-8.96	-3.71	0	-0.966	-0.901	4.20E-03	-7%
k33	0.5141	-16.93	-8.85	0	-1.829	-1.783	2.14E-03	-3%
		-12.50	-4.18	0	-1.054	-1.215	2.60E-02	15%
		-13.42	-8.03	0	-1.554	-1.456	9.55E-03	-6%
		-21.97	45.30	4	2.126	2.191	4.17E-03	3%
		-18.32	29.78	3	1.396	1.310	7.42E-03	-6%
						sum	5.58E-02	

		k21 *	δP_e	+ k22 *	δP_c	+ k23 *	$\delta h_{e,out}$	= $\delta h_{c,in}$	$\delta h1$ (calc)	diff^2	% diff
k21	-0.0742	-10.43	-8.31	3.8	0.9	0.75	2.11E-02	-16%
k22	0.0172	-8.96	-3.71	4.1	0.7	0.73	1.19E-03	5%
k23	0.0325	-16.93	-8.85	6.2	1.3	1.31	3.22E-05	0%
		-12.50	-4.18	5.5	1.0	1.03	1.18E-03	3%
		-13.42	-8.03	5.4	1.0	1.03	1.10E-03	3%
		-21.97	45.30	2.7	2.6	2.50	1.10E-02	-4%
		-18.32	29.78	2.1	1.8	1.94	1.93E-02	8%

Notes:
Pressures are in kPa
Mass flow rates are in kg/hr
Enthalpies are in kJ/kg
diff is the difference between measured and calcluated

sum 5.49E-02